UNIVERSITY OF OKLAHOMA

GRADUATE COLLEGE

GENES REQUIRED FOR SEDIMENT FITNESS IN *DESULFOVIBRIO DESULFURICANS* G20

A DISSERTATION

SUBMITTED TO THE GRADUATE FACULTY

In partial fulfillment of the requirements for the

degree of

Doctor of Philosophy

By

QINGWEI LUO
Norman, Oklahoma
2007

UMI Number: 3261102

ProQuest Information and Learning Company
300 North Zeeb Road
P.O. Box 1346
Ann Arbor, MI 48106-1346

GENES REQUIRED FOR SEDIMENT FITNESS IN *DESULFOVIBRIO DESULFURICANS* G20

A DISSERTATION APPROVED FOR THE
DEPARTMENT OF BOTANY AND MICROBIOLOGY

BY

Lee R. Krumholz

Joseph M. Suflita

Ralph S. Tanner

Bradley S. Stevenson

Phillip E. Klebba

Acknowledgments

With deep gratitude and appreciation I would like to give my first acknowledgment to my advisor Dr. Lee Krumholz. Dr. Krumholz gave me the opportunity to work in his lab and guided me through these years on my project. His greatness is not only shown in his scientific knowledge but also his patience on helping me improve my ability in writing manuscripts and proposals. With his help, I built up my interest in science and gained the confidence to be a good scientist. He is my role model for a scientist.

My committee also deserves my acknowledgments in many aspects. Dr. Suflita and Dr. Klebba served as my committee members throughout my entire graduate project. Dr. Tanner and Dr. Stevenson started serving as my committee when I needed them the most. All of them are great scientists and wonderful people, and they gave me scientific and career advice.

I am also grateful to work in Dr. Krumholz's lab with past and current members, especially, Dr. Jennifer Groh, Nydia Castaneda, and Dr. Mostafa Elshahed. Together with Jennifer, we developed a new technique and broke through the most difficult step of the project. With Mostafa's help, I got the chance to work on the community analysis project, which broadened my knowledge. Nydia helped me a lot when I first started in the lab and throughout the study with lots of valuable discussion.

I also want to acknowledge many members in the Department of Botany and Microbiology, for their technical support and help, especially, Dr. Scott Russell and Gregory Strout on the electron microscope project and Dr. Mary Beth Langer and Dr. Darren Smalley on the microarray operation.

I also want to thank the Department of Energy (DOE), the Natural and Accelerated Bioremediation Research (NABIR) program, for the research grant obtained by Dr. Lee Krumholz, Dr. Jimmy Ballard, Dr. Joseph Suflita, and Dr. Tyrell Conway. This grant financially supported my research and my life in Oklahoma.

Most importantly, my loving husband Dr. Bo Jin deserves many thanks. He brought me to the States and supported me all the years on my research and life. I know that my PhD journey would have been very difficult without his love.

Table of Contents

List of Tables

Chapter 4.

Appendix 1.

List of Figures

Preface

Microbes are changing our life in many aspects, however, the vast majority of the Earth's microbial life remains uncultured and unexplored, and how microbes adapt to and proliferate in their habitat is still mysterious. Molecular technologies have opened a window that provides an intimate view of associations among different microorganisms.

In this dissertation, molecular techniques were used to investigate the relationships between sulfate-reducing bacteria (SRB) and their environments to unveil what is required for sediment fitness. The sulfate-reducing bacteria are a large group of anaerobic organisms that play important roles in many biogeochemical processes. They are widely distributed in nature, and are regular components of natural and engineered systems.

To examine how these microorganisms behave and respond to stimuli in the environment, an in situ-based approach is required. Signature-tagged mutagenesis (STM) is a useful technique that was developed in 1995, and since then it has been used widely on pathogenic and commensal bacteria for identification of their virulence and/or colonization genes. This dissertation mainly describes how we modified the STM procedure and applied it to our model environmental microorganism *Desulfovibrio desulfuricans* G20 to address the role of specific genes in its environmental function. We should keep in mind that this approach would allow researchers to examine an entire set of genes required for an organism not only to survive in uncontaminated sediment but also in radionuclide-contaminated sediments and cocultures. Although this dissertation will not address the latter issues, applying our findings to the identification of genes

required for uranium reduction and hydrogen production was proposed for future projects.

With the explosion of the availability of genome sequences, SRB are currently subject to extensive genomic studies, which are yielding a new understanding of their basic biochemical mechanisms, and aiding in the development of novel techniques for the analyses of their environmental roles. The surprising number of proteins, putative and real, for which a function has yet to be described, offers a fertile area of investigation, discovery, and evolutionary understanding.

In chapter 1, I conduct the basic experiments on *D. desulfuricans* G20, which include transmission electron microscopy, growth curves and doubling times, testing antibiotic resistance, and measuring osmolarity of cultures and buffers. These data provide useful information for the following studies. This chapter was written in the style required by *Environmental Microbiology* but is not intended for publication.

In chapter 2, a modified approach for signature-tagged mutagenesis (STM) is presented, that incorporates microarray technology, making the process of screening tagged-mutant pools more streamlined when compared to other STM procedures. Together with Jennifer Groh, I have demonstrated that this system can be used to identify genes required for survival of *Desulfovibrio desulfuricans* G20 (a *δ-proteobacterium*) and *Shewanella oneidensis* MR-1 (a *γ-proteobacterium*). This system is applicable to any bacterium that can be randomly mutagenized by the mini-Tn*10* transposon employed in our study. Our mutant library can also be used on future studies of screening a variety of functional genes to address many physiological questions. This chapter was written with Jennifer L. Groh, Jimmy D. Ballard, and Lee R. Krumholz in the style required by

Applied and Environmental Microbiology. Although the primary author for the published manuscript was Jennifer L. Groh, I contributed equally in this work. Therefore, it is taken as chapter 2 in this dissertation.

In chapter 3, I present the genes that were identified by our STM method and the characterization of some functional groups. The products of identified genes belong to the various clusters of orthologous groups (COG) functional groups. The results of the characterization of amino acid biosynthesis mutants, hydrogenase mutants, and DNA repair mutants prove the importance of the specific functions for sediment fitness. These findings provide a unique view into microbial interactions with abiotic and biotic environmental factors. This chapter was written with Jennifer L. Groh, Jimmy D. Ballard, and Lee R. Krumholz in the style required by *Applied and Environmental Microbiology*.

In chapter 4, I present the proteome analysis of *Desulfovibrio desulfuricans* G20 mutants using the accurate mass and time tag (AMT) approach. This study compares the proteomes of six individual regulatory mutants to the proteome of the parent strain. These mutants were identified in the STM study that constitutes this dissertation. I show that the proteomic data are statistically reliable with the presentation of the reproducibility and the root sum square of the linear regression analysis. I also show that each regulatory gene regulates different sets of genes which may be related to sediment fitness. This chapter was written with Kim K. Hixson, Steven J. Callister, Mary S. Lipton, and Lee R. Krumholz in the style required by *Journal of Proteome Research*.

In appendix 1, I present the microbial eukaryotic community analysis of Zodletone spring (Oklahoma) using culture-independent technique. I constructed 18S

rDNA clone libraries from the spring source, mat, and crust samples and analyzed the community structures. I also show that the anaerobic fungal communities are present in the wastewater treatment sample, duck pond sample, and Ft. Lupton sample. This appendix was written with Lee R. Krumholz, Fares Z. Najar, Aaron D. Peacock, Bruce A. Roe, David C. White, and Mostafa S. Elshahed in the style required by *Applied and Environmental Microbiology*.

In appendix 2, I present the transmission electron micrograph of *Desulfovibrio desulfuricans* G20 grown under anoxic and oxic conditions. I prepared thin sections and obtained images of both samples with the transmission electron microscope. I show the distinguishing features of oxygen-exposed cells. This appendix was written with Lee R. Krumholz.

Abstract

Preliminary experiments were conducted on *Desulfovibrio desulfuricans* G20 to obtain some basic information of this bacterium. Strain G20 has a single flagellum and a doubling time of 3.2 hours at 37 °C in the lactate-sulfate medium, compared to the doubling time of 7.3 and 5.0 hours for strain Essex6 and strain ASR, respectively. G20 is resistant to several antibiotics including nalidixic acid, spectinomycin, and streptomycin.

A modified version of the signature-tagged mutagenesis (STM) procedure was developed, which incorporated microarray technology to streamline the entire screening process. A mini-Tn*10* transposon that is capable of randomly mutagenizing our model sulfate-reducing bacterium was also identified. This system can therefore be applied to other sulfate-reducing bacteria to answer questions of ecological or economical significance. This is the first study using STM to study bacterial environmental fitness.

97 genes required for sediment fitness of G20 were identified and the identification of chemotaxis genes validated our STM screening method since it would be expected to enhance sediment fitness. The growth of these sediment fitness mutants was monitored in laboratory growth media to determine whether growth rate influenced sediment fitness. Homology with other *δ-proteobacteria* was determined and the putative sediment functions of many of these genes were described. Amino acid biosynthesis mutants, hydrogenase mutants, and DNA repair mutants were characterized to prove the importance of specific functions for sediment fitness.

The proteomes of the regulatory mutants were analyzed and compared to the proteome of the parent strain. The reproducible and reliable data produced by the accurate mass and time tag approach allow us to compare protein production in the

mutants. The results showed that these regulators regulated different sets of genes which may be required for sediment survival, although the regulatory pathways remain to be elucidated. It is evident that the laboratory-adapted strain is different from sediment-adapted strain at the protein level.

Chapter 1

Preliminary Studies of *Desulfovibrio desulfuricans* G20

Summary

The gram-negative mesophilic sulfate-reducing bacteria (SRB) belonging to the genus *Desulfovibrio* are widespread in anaerobic environments. Their versatility in reducing heavy metals and oxidizing organic substrates makes them of great utilitarian and academic interest. *Desulfovibrio desulfuricans* G20 was used as a model organism for molecular and genetic studies. Preliminary studies were conducted to obtain necessary information for transposon mutagenesis. Sediment incubation experiments were carried out to determine the incubation time and inoculum size needed to establish a sediment system for screening fitness mutants. G20 was shown to have a doubling time of 3.2 hours at 37 °C and a high resistance to antibiotics including nalidixic acid, spectinomycin and streptomycin. Suitable buffers were identified for transformation experiments based on their osmolarity. These results were needed to carry out the experiments described in the following chapters.

Introduction

Sulfate-reducing bacteria (SRB) are widespread in aquatic sediments and terrestrial environments (Postgate, 1979). These microorganisms play a key role in anaerobic degradation whenever sulfate is present as a potential electron acceptor (Hansen, 1994). Under these conditions, SRB convert sulfate to sulfide and obtain their energy for growth from the oxidation of organic compounds or H_2 (Postgate, 1984). The sulfate-reducing

bacteria of the genus *Desulfovibrio* are gram-negative mesophilic anaerobes that are ubiquitous in anaerobic environments (Postgate, 1984). Their physiological activities are of profound importance for many ecological communities as they are often responsible for the terminal electron accepting processes (Widdel and Hansen, 1992). They are also capable of reducing and immobilizing metals such as chromium and uranium; toxic Cr(VI) is reduced to the much less mobile Cr(III) (Fude et al., 1994; Lovley and Phillips, 1994), while soluble U(VI) is reduced to less soluble U(IV) (Lovley et al., 1993). Recently, studies on sulfate-reducing bacteria (SRB) have mainly focused on physiology and bioremediation, and research on molecular microbiology and genetics are still at an early stage.

Signature-tagged mutagenesis (STM) was proposed to study in-situ activities of SRB at the genetic level. STM uses comparative hybridization to isolate mutants unable to survive specified environmental conditions and allows the whole genome to be screened. In STM, each insertional mutation carries a different DNA tag, which allows mutants to be differentiated from each other. STM requires the generation of an insertion mutant library and a suitable sediment model. Prior to initiating a set of experiments to develop the mutant library for genetic studies with G20, some experimental protocols including a transposon system, antibiotic markers, buffers for transformation as well as details on a selection system were needed.

Desulfovibrio species are known to have high intrinsic resistance to many antibiotics, both *in situ* (Jayaraman et al., 1999) and in the laboratory (Rapp and Wall, 1987; Argyle et al., 1992; Fu and Voordouw, 1997). Several antibiotics were tested on SRB either in pure culture or sediments and minimum inhibitory concentration (MIC)

have been reported (Postgate, 1984; Argyle et al., 1992). Because the phylogeny, as well as the physiology, of *Desulfovibrio* reflects vast diversity, it is not feasible to apply information available for other *Desulfovibrio* strains to G20. Although some antibiotic concentrations have been described for selection of G20 mutants, e.g., kanamycin and spectinomycin (Wall et al., 1996), information regarding the response of *D. desulfuricans* G20 to various antibiotics is incomplete. Experiments were conducted to obtain antibiotic resistance data prior to the molecular manipulation. In addition to various concentrations of different antibiotics tested for *D. desulfuricans* G20, we also tested some antibiotics on *D. desulfuricans* strains Essex6 and ASR for comparison.

The selection of appropriate buffers is also important for transformation experiments (Taketo, 1989; Diver et al., 1990; McDonald et al., 1995). In most circumstances, washing of cells with low salt buffer is required prior to electroporation. The ideal buffer will have a similar osmolarity to the growth medium in order to minimize damage of cells during the washing process (Eynard et al., 1992; Golzio et al., 1998). Aside from the above factors, a determination of growth rate and ideal growth conditions were required to obtain successful transformations and conjugations. Both the latter processes require controlling the recovery time, and for conjugation experiments, mating time is also determined by the doubling time. Therefore, we monitored the growth curve of G20, as well as several other strains, and reported their doubling times.

The other critical step in the development of signature-tagged mutagenesis (STM) for environmental bacteria was to develop a sediment system that could support G20 growth. The ideal system allowed surviving mutants to at least maintain population levels, while mutants with disruptions in genes required for sediment growth would be

present at a non-detectable concentration at the time of sampling. In order to characterize the response to sediment incubations, *D. desulfuricans* Essex6 was first used as a model organism. The goal was to determine the conditions necessary to allow introduced bacteria to at least maintain their population level in natural sediments. Strain G20 was then tested to validate the microcosm system as soon as we obtained G20 mutants, and details were discussed in Chapter 2.

Results and Discussion

Phylogeny and morphology of G20. *D. desulfuricans* G20 is a spontaneously nalidixic acid-resistant derivative of wild-type strain G100A (Weimer et al., 1988), which is also cured of the endogenous cryptic plasmid pBG1 (Wall et al., 1993). The 16S rRNA sequence of *D. desulfuricans* G20 has 99% similarity to *Desulfovibrio alaskensis*, and phylogenetic analysis also shows that G20 clusters with other *D. alaskensis* strains, rather than *D. desulfuricans* (Figure 1). However, the original name will be used until further DNA hybridization analysis occurs and a valid name is published. Despite the disagreement of phylogenetic position, the morphological features of G20 are in agreement with the original description (Garrity et al., 2001). A transmission electron microscopy (TEM) image of a sample prepared by negative staining shows the single flagellum on one end of the cell (Figure 2). The G20 cells are about 1 μm in diameter and 4 μm in length.

Antibiotic resistance of G20. There are three major strategies for mechanisms of bacterial resistance to antibiotics. The first strategy is inactivation of the intracellular form of the antibiotic, including enzymatic destruction of the antibiotic, as is the case for

Figure 1. Distance dendrogram based on the 16S rRNA sequences of sulfate-reducing bacteria in the GenBank database. The tree was constructed using neighbor-joining algorithm with a Jukes-Cantor correction. 16S rRNA of *Escherichia coli* K12 was used as the outgroup. Bootstrap values (in percentages) are based on 1,000 replicates and are shown for branches with more than 50% bootstrap support.

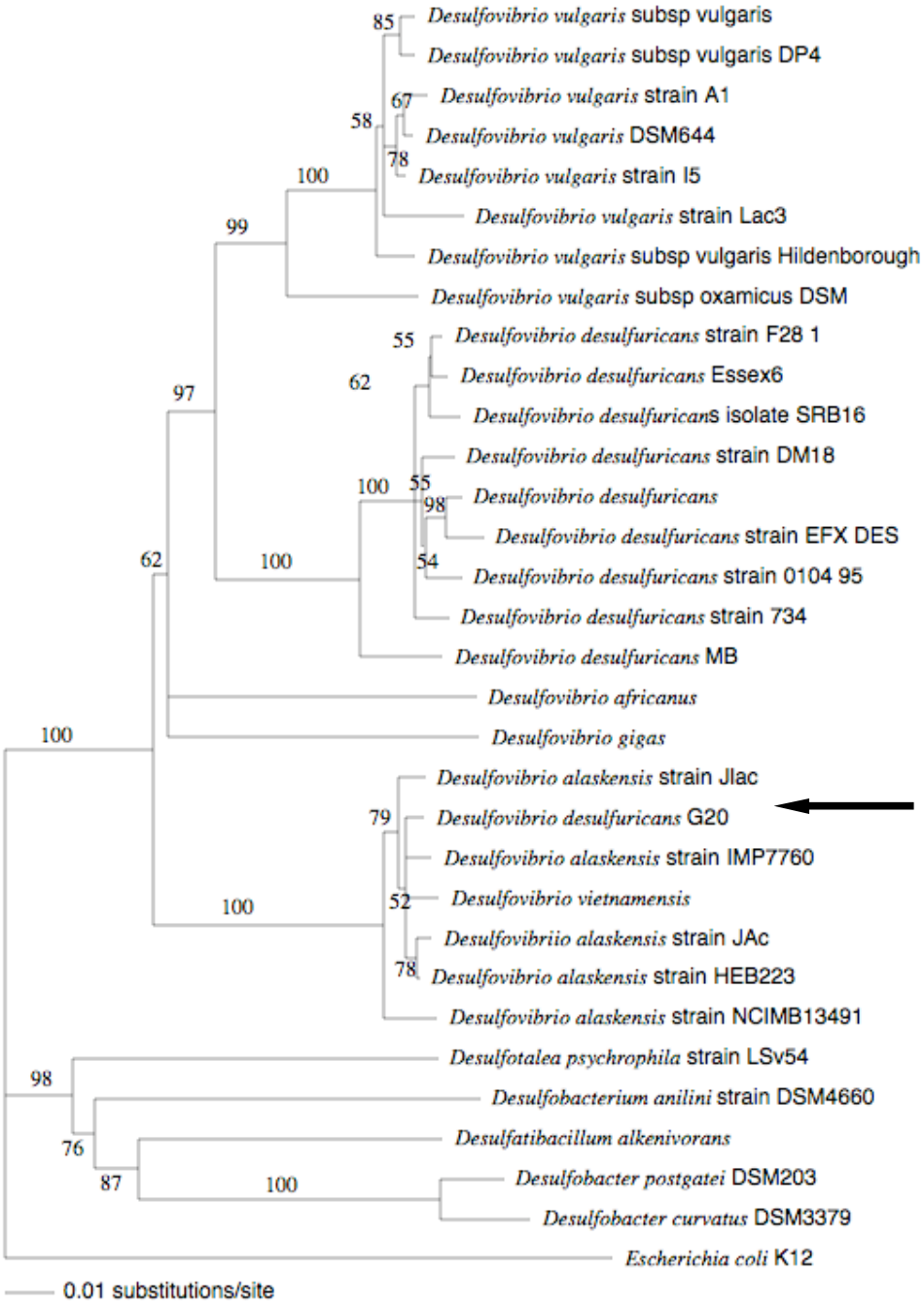
Desulfovibrio vulgaris subsp vulgaris
Desulfovibrio vulgaris subsp vulgaris DP4
Desulfovibrio vulgaris strain A1
Desulfovibrio vulgaris DSM644
Desulfovibrio vulgaris strain I5
Desulfovibrio vulgaris strain Lac3
Desulfovibrio vulgaris subsp vulgaris Hildenborough
Desulfovibrio vulgaris subsp oxamicus DSM
Desulfovibrio desulfuricans strain F28 1
Desulfovibrio desulfuricans Essex6
Desulfovibrio desulfuricans isolate SRB16
Desulfovibrio desulfuricans strain DM18
Desulfovibrio desulfuricans
Desulfovibrio desulfuricans strain EFX DES
Desulfovibrio desulfuricans strain 0104 95
Desulfovibrio desulfuricans strain 734
Desulfovibrio desulfuricans MB
Desulfovibrio africanus
Desulfovibrio gigas
Desulfovibrio alaskensis strain Jlac
Desulfovibrio desulfuricans G20
Desulfovibrio alaskensis strain IMP7760
Desulfovibrio vietnamensis
Desulfovibriio alaskensis strain JAc
Desulfovibrio alaskensis strain HEB223
Desulfovibrio alaskensis strain NCIMB13491
Desulfotalea psychrophila strain LSv54
Desulfobacterium anilini strain DSM4660
Desulfatibacillum alkenivorans
Desulfobacter postgatei DSM203
Desulfobacter curvatus DSM3379
Escherichia coli K12
0.01 substitutions/site

Figure 2. Transmission electron microscopic images of *D. desulfuricans* G20 from negatively stained sample, magnification at 42,000X; scale bar = 500 nm.

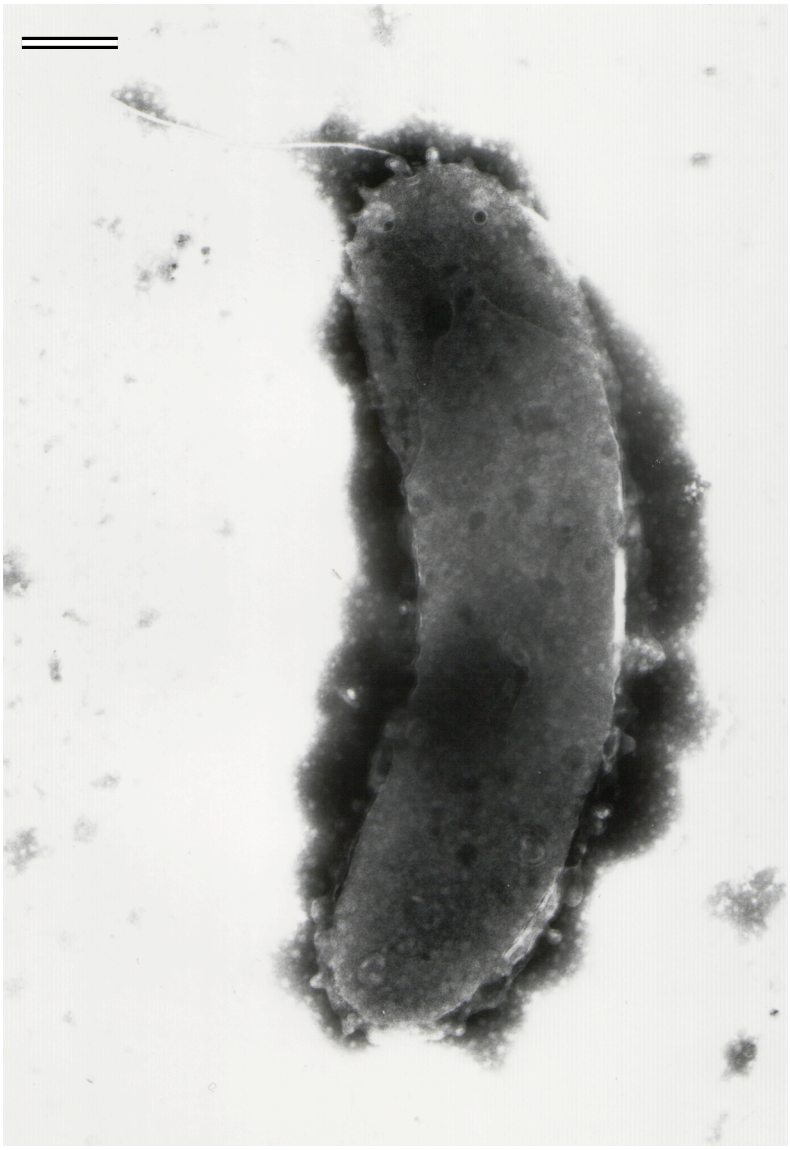

β-lactam hydrolysis, aminoglycoside modification, and fosfomycin capture by glutathione. The second strategy is to lower the ambient concentration of antibiotics inside the cells, which can be done by a combination of lowered rates of influx coupled to accelerated rates of efflux or by efflux pump alone. The third mechanism is to alter the target protein such that it still retains its physiologic function but has a lower affinity for antibiotic binding (Walsh, 2003). Representative antibiotics working on each target were tested on *D. desulfuricans* G20. The minimum inhibitory concentration (MIC) of each antibiotic was recorded and shown in Table 1. Results indicate that G20 is resistant to several types of antibiotics, especially to nalidixic acid (MIC=1.2 mg/ml) belonging to the quinolone family. Since *D. desulfuricans* G20 is a nalidixic acid resistant derivative (Wall et al., 1996), this is not surprising. Unexpectedly, other *D. desulfuricans* strains such as Essex6 and ASR are also resistant to nalidixic acid with MIC of 1 mg/ml. Strain G20 is resistant to kanamycin at levels up to 175 μg/ml, strain Essex6 is more sensitive with an MIC of 50 μg/ml, while strain ASR is more resistant with an MIC as high as 700 μg/ml. G20 is also very resistant to spectinomycin and streptomycin, which both act by targeting the 30S subunit of the bacterial ribosome. G20 also shows high resistance to ampicillin, with an MIC of 400 μg/ml in comparison to 16 μg/ml for the typical MIC breakpoint for *Enterobacteriaceae* (Paterson and Bonomo, 2005). Six metallo-β-lactamases (MBL) were annotated in the G20 genome (http://www.microbesonline.org/cgi-bin/keywordSearch.cgi?type=0&mapId=MAPID&term=1&locus=0&hit=0&disp=0&homolog=0&format=1&favorites=&byFavorites=0&taxTyping=Type+the+first+few+letters&taxSelector=207559&taxId=207559&keyword=lactamase). Further studies are

Table 1. Antibiotics tested on *D. desulfuricans* G20.

Antibiotic and site of action	MIC[a] (μg/ml)
DNA replication:	
Nalidixic acid	1200
Ribosome function:	
Kanamycin	175
Neomycin	75
Gentamicin	50
Streptomycin	1000
Spectinomycin	1600
Tetracycline	1
Erythromycin	10
Chloramphenicol	50
Cell wall biosynthesis:	
Ampicillin	400
Folate biosynthesis:	
Trimethoprim	60

[a] MIC represents minimum inhibitory concentration.

required to determine whether the chromosomally mediated MBL genes from *Desulfovibrio* species are the mechanism of resistance to β-lactam antibiotics. The observed resistance to such a wide range of antibiotics suggests that efflux may play an important role in antibiotic resistance in *Desulfovibrio*. Determining the resistance mechanisms will help us understand the development and need for antibiotic resistance mechanisms in natural systems (Groh et al., 2007), however, our goal for this study was to determine the MIC for antibiotics to be used for genetic manipulation. It was observed that for the majority of antibiotics tested, *D. desulfuricans* G20 had different MICs from strains Essex6 and ASR, and kanamycin can be a good selective marker for molecular manipulation.

Determination of growth in laboratory growth medium. Growth curves of *D. desulfuricans* G20, Essex6, and ASR were determined in duplicate incubations with optical density monitored at 600 nm wavelength (OD_{600}). The final OD_{600} reached 0.9 to 1.0, and doubling times are reported in Table 2.

Genetic manipulation in *Desulfovibrio* was optimized for conjugation experiments. In order to decrease the chance of obtaining duplicate genetic transformants, it is important to time the mating and recovery period so that cells are plated between the first and second doubling. It was observed that with the addition of tryptose to lactate-sulfate (LS) medium, the growth rate was accelerated for Essex6, from 7.3 to 5.1 hours and for ASR, from 5.0 to 4.1 hours. *Desulfovibrio* species also had a higher growth rate at 37 °C than 25 °C, exemplified by *D. vulgaris* Hildenborough, whose doubling time increased from 4.3 to 8.1 hours when temperature was decreased.

Table 2. Growth rate of *Desulfovibrio* species.

Strain	Doubling time @ 37 °C (hour)		Doubling time @ 25 °C (hour)
	Medium w/o tryptose	Medium w/ tryptose [a]	Medium w/o tryptose [a]
D. desulfuricans G20	3.2	N/A	N/A
D. deulfuricans Essex6	7.3	5.1	N/A
D. desulfuricans ASR	5.0	4.1	N/A
D. vulgaris Hildenborough	4.3	N/A	8.1

[a] N/A represents data not available.

These results indicate that we can accelerate experiments with the addition of tryptose into the growth medium or with the increase of the incubation temperature to 37 °C.

Determination of the buffers for transformation in G20. Table 3 shows the list of buffers tested in the later experiments for use in transformation experiments and their osmolarity relative to culture media. LS-marine medium has much higher osmolarity than LS medium due to the high salt content. Therefore, marine strains require higher osmolarity buffers than freshwater strains. Sucrose at 400 mM with 1 mM $CaCl_2$ or 1 mM $MgCl_2$ and 2% $NaHCO_3$ are the suitable buffers for washing freshwater strains, while 800 mM sucrose with 1 mM $MgCl_2$ is the most suitable buffer to apply to marine strains.

Establishing the sediment screening system. In order to find a suitable sediment system for screening survival mutants, we set up microcosms with subsurface landfill sediment [(Groh et al., 2005), chapter 3]. An ideal system will support growth and allow recovery of cells at the end of the incubation (Lehoux and Levesque, 2000). Results with a *D. desulfuricans* Essex6 mutant is shown in Figure 3. The initial acclimation takes 5-7 days with a rapid period of growth and with an equivalent period of decline to near initial cell concentration in non-sterile sediments. When H_2 was added as electron donor, the transient cell concentration was increased more than an order of magnitude over the no H_2 addition microcosms. This was a relatively modest change in the growth pattern, suggesting that substrate is only one of the factors controlling competition. Cells returned to concentrations near 10^5 cells/gm of sediments indicating that cell numbers are maintained at a steady state when in competition with a natural population. Autoclaved sediments showed a different trend with cell numbers increasing

Table 3. Osmolarity of media and buffers.

Solution	Osmolarity (mmol/kg)[a]
Nanopure H_2O	0
TE buffer (10 mM Tris, 1 mM EDTA, pH8.0)	13
HEPES (1 mM, pH 7.0)	4
NTA (1 mM pH 7.2)	4
Phosphate-buffered saline (PBS)	269
10% glycerol	1368
400 mM Sucrose + 1 mM $CaCl_2$	450
400 mM Sucrose + 1 mM $MgCl_2$	449
800 mM Sucrose + 1 mM $MgCl_2$	1040
400 mM Sucrose + 2 mM $MgCl_2$	450
0.7% $NaHCO_3$	218
1.4% $NaHCO_3$	311
2% $NaHCO_3$	440
3.5% $NaHCO_3$	713
7% $NaHCO_3$	1376
Lactate-sulfate (LS) medium	401
D. desulfuricans G20 culture	451
D. desulfuricans Essex6 culture	385
D. vulgaris Hildenborough	391
LS-marine medium	1090
D. desulfuricans ASR	1098
D. desulfuricans aestuarii	1093

[a] Value from average of duplicate measurements.

Figure 3. Graphs of time versus cell concentration of *D. desulfuricans* Essex6 during growth in sediments under different conditions.

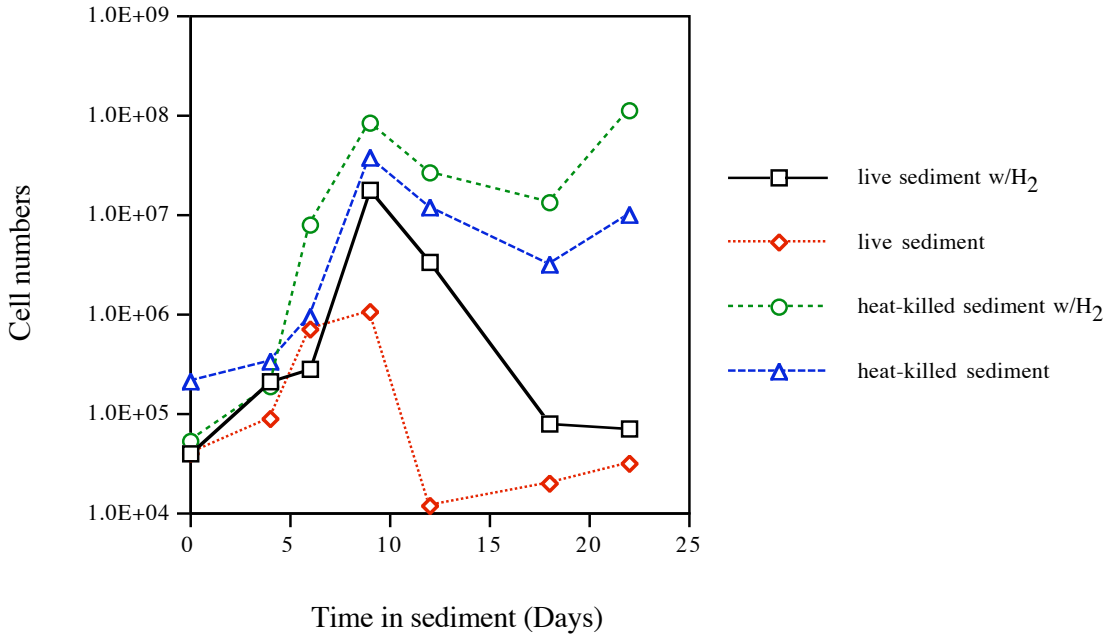

(10 times more in heat-killed sediment than non-sterile sediment) and maintenance at higher levels, suggesting that competition is critical in this system. Although we obtained more cell mass in heat-killed sediments, we preferred the use of non-sterile sediments to provide us with an opportunity to select mutants which lost the ability to compete with other bacteria. A greater than five fold increase in cell numbers provided adequate numbers of mutants for screening the tags. In order to better mimic the natural environment, we used non-sterile sediments without H_2 addition. This part of the study was performed prior to generating G20 mutants. However, after *D. desulfuricans* G20 mutants were generated, we carried out a similar experiment in non-sterile sediment system. Peak growth was observed after an 8-9 day incubation in sediments (over 10-fold increase over the inoculum was recovered) (Groh et al., 2005).

These latter experiments are noteworthy in that competition was shown to be a critical factor in maintaining population size for the different SRB. More importantly, perhaps, is that the cells able to grow a few generations and maintain themselves in the sediments can be selected for. These observations allowed us to quickly progress with STM. We were concerned that the observed phenomena (growth and decline) could have been due to one of several other factors including loss of the antibiotic resistance marker or adhesion to sediments. Two consecutive extractions from incubated microcosms were carried out to measure the recovered cells. The number of cells from the second extraction was about 10% of the number of cells from first extraction. Meanwhile, the colony-forming units (CFU) from untreated sediment extraction on plates with kanamycin were about 87% of CFU on plates without antibiotics. The CFU on plates

with kanamycin from heat-killed sediment were equivalent to the CFU on LS plate. The results ruled out both of these possibilities.

Experimental procedures

Strains and media. *D. desulfuricans* G20 was a gift from Dr. Judy Wall's laboratory, *D. desulfuricans* Essex 6 and *D. vulgaris* Hildenborough are freshwater strains from Dr. M. McInerney's laboratory, and *D. desulfuricans* subsp. aestuarii and strain ASR were marine strains from Dr. McInerney's laboratory and Dr. Bradley Tebo's laboratory, respectively. All the strains were grown in the lactate-sulfate (LS) medium prepared as described by Rapp and Wall (Rapp and Wall, 1987) under N_2. The components of LS medium included 0.1% yeast extract (Difco), 50 mM Na_2SO_4, 60 mM sodium DL-lactate, 8 mM $MgSO_4$, 20 mM NH_4Cl, 2.2 mM K_2HPO_4, 0.6 mM $CaCl_2$, 2 ml/L of vitamin solution, 12.5 ml/L of metal solution, and 25 mM HEPES (pH 7.0). Resazurin (0.62 ml/L from 0.1% stock solution) was added to indicate the reduced state of the medium. Prior to autoclaving, the pH was adjusted to 7.2. After autoclaving, cysteine and $NaHCO_3$ are added to final concentrations of 2mM and 8 mM, respectively. For growing the marine strain ASR, 30 mM $MgCl_2$ and 342 mM NaCl were also included in the medium, which was designated as LS-marine medium. The LS-tryptose medium contains all the components of the LS medium with the addition of 2% tryptose.

Growth of *D. desulfuricans* G20, Essex6 and ASR were observed by measuring the optical density (OD) at 600 nm. The inoculum was 0.5 ml of a mid-exponential phase culture for 10 ml of medium. For each microorganism, growth curves were monitored in duplicate.

Phylogenetic analysis. 16S rRNA sequences were obtained from the GenBank nucleotide database. Evolutionary distance (neighbor-joining algorithm) was determined using PAUP (version 4.01b10; Sinauer Associates, Sunderland, Mass.).

Transmission electron microscopy (TEM). Mid-log phase G20 culture was applied to TEM grids coated with formvar and carbon (FCF200-Cu, http://emsdiasum.com/microscopy/products/grids/support.aspx). Negative staining using saturated uranyl acetate solution was performed (Bozzola and Russell, 1998). Stained samples were observed in a transmission electron microscope (Zeiss 10A).

Determination of minimum inhibitory concentration. *D. desulfuricans* G20 cultures (10 ml) were grown in the LS medium, and 0.5 ml of the overnight culture was used as inoculum. For nalidixic acid, final concentrations of 200, 400, 600, 800, 1000, and 1200 μg/ml were tested. For kanamycin, final concentrations of 50, 100, 175, 350, 525, 875, and 1050 μg/ml were tested. For neomycin and gentamicin, final concentrations of 25, 50, 75, and 100 μg/ml were tested. For spectinomycin and streptomycin, final concentrations of 400, 800, 1000, 1200, 1400, and 1600 μg/ml were tested. For tetracycline, final concentrations of 0.5, 1, 2, and 5 μg/ml were tested. For erythromycin, final concentrations of 5, 10, 15, 20, and 50 μg/ml were tested. For chloramphenicol, final concentrations of 25, 50, 75, and 100 μg/ml were tested. For ampicillin, final concentrations of 100, 200, 300, 400, and 500 μg/ml were tested. For trimethoprim, final concentrations of 20, 40, 60, 80, and 100 μg/ml were tested. Cultures were examined after a one- to three-day incubation at 37°C to determine inhibition of the growth.

Measurement of osmolarity. Prior to measurement, the osmometer (Vapor Pressure Osmometer 5520, Wescor Inc.) was calibrated with a 290 mmol/kg standard solution. The osmolarities of LS medium, LS-marine medium, cultures of G20, Essex6, and ASR, $NaHCO_3$ solutions, phosphate buffered saline (PBS), sucrose solutions, 10% glycerol, 4-(2-hydroxyethyl)-1-piperazineethanesulfonic acid (HEPES) buffer, Nitrilotriacetate (NTA) buffer, and TE buffer were recorded. For each sample the measurement was performed in duplicate.

Growth in microcosms. *D. desulfuricans* Essex6 kanamycin resistant cells were grown in LS medium at 37 °C. Late-log phase cells (OD_{600} = 0.7) were harvested, washed, and diluted. Sediment microcosms were set up with 2 g of subsurface anaerobic sediment, which was collected from Norman landfill at about 2 m in depth and kept at 4 °C until use. The headspace in microcosms was flushed with 80% N_2 and 20% CO_2 gas mix. Half of the microcosms were heat killed by autoclaving. Both heat-killed sediment bottles and non-sterile sediment bottles were inoculated with about 10^5 washed cells and incubated at room temperature in the dark. Control microcosms were not inoculated. To recover cells from sediment, 4 ml of washing buffer was injected into the bottle. The washing buffer includes all the components of LS medium, with the omission of sodium lactate, sodium sulfate, vitamin solution, and yeast extract. Bottles were vigorously vortexed and shaken for about 15 minutes. One ml of sediment slurry was taken from the bottle and diluted in washing buffer. Several dilutions were plated onto LS solid medium containing kanamycin at a final concentration of 175 μg/ml. Two bottles of each treatment were sacrificed at each time point. Colony forming units (CFU) were recorded for calculating the viable kanamycin resistant cells in the sediment.

References

Argyle, J.L., Rapp-Giles, B.J., and Wall, J.D. (1992) Plasmid transfer by conjugation in *Desulfovibrio desulfuricans*. *FEMS Microbiology Letters* **94**: 255-262.

Bozzola, J.J., and Russell, L.D. (1998) *Electron Microscopy*. Sudbury, Massachusetts: Jones and Bartlett Publishers.

Diver, J.M., Bryan, L.E., and Sokol, P.A. (1990) Transformation of *Pseudomonas aeruginosa* by electroporation. *Anal Biochem* **189**: 75-79.

Eynard, N., Sixou, S., Duran, N., and Teissie, J. (1992) Fast kinetics studies of *Escherichia coli* electrotransformation. *Eur J Biochem* **209**: 431-436.

Fu, R., and Voordouw, G. (1997) Targeted gene-replacement mutagenesis of *dcrA*, encoding an oxygen sensor of the sulfate-reducing bacterium *Desulfovibrio vulgaris* Hildenborough. *Microbiology* **143 (Pt 6)**: 1815-1826.

Fude, L., Harris, B., Urrutia, M., and Beveridge, T. (1994) Reduction of Cr(VI) by a consortium of sulfate-reducing bacteria (SRB III). *Appl Environ Microbiol* **60**: 1525-1531.

Garrity, G.M., Winters, M., and Searles, D.B. (2001) *Taxonomic Outline of the Procaryotic Genera, Bergey's Manual of Systematic Bacteriology*. New York: Springer-Verlag.

Golzio, M., Mora, M.P., Raynaud, C., Delteil, C., Teissie, J., and Rols, M.P. (1998) Control by osmotic pressure of voltage-induced permeabilization and gene transfer in mammalian cells. *Biophys J* **74**: 3015-3022.

Groh, J.L., Luo, Q., Ballard, J.D., and Krumholz, L.R. (2005) A method adapting microarray technology for signature-tagged mutagenesis of *Desulfovibrio desulfuricans*

G20 and *Shewanella oneidensis* MR-1 in anaerobic sediment survival experiments. *Appl Environ Microbiol* **71**: 7064-7074.

Groh, J.L., Luo, Q., Ballard, J.D., and Krumholz, L.R. (2007) Genes that enhance the ecological fitness of *Shewanella oneidensis* MR-1 in sediments reveal the value of antibiotic resistance. *Appl Environ Microbiol* **73**: 492-498.

Hansen, T.A. (1994) Metabolism of sulfate-reducing prokaryotes. *Antonie van Leeuwenhoek* **66**: 165-185.

Jayaraman, A., Hallock, P.J., Carson, R.M., Lee, C.C., Mansfeld, F.B., and Wood, T.K. (1999) Inhibiting sulfate-reducing bacteria in biofilms on steel with antimicrobial peptides generated *in situ*. *Appl Microbiol Biotechnol* **52**: 267-275.

Lehoux, D.E., and Levesque, R.C. (2000) Detection of genes essential in specific niches by signature-tagged mutagenesis. *Current Opinion in Biotechnology* **11**: 434-439.

Lovley, D., and Phillips, E. (1994) Reduction of chromate by *Desulfovibrio vulgaris* and its c_3 cytochrome. *Appl Environ Microbiol* **60**: 726-728.

Lovley, D.R., Widman, P.K., Woodward, J.C., and Phillips, E.J. (1993) Reduction of uranium by cytochrome c3 of *Desulfovibrio vulgaris*. *Appl Environ Microbiol* **59**: 3572-3576.

McDonald, I.R., Riley, P.W., Sharp, R.J., and McCarthy, A.J. (1995) Factors affecting the electroporation of *Bacillus subtilis*. *J Appl Bacteriol* **79**: 213-218.

Paterson, D.L., and Bonomo, R.A. (2005) Extended-spectrum beta-lactamases: a clinical update. *Clin Microbiol Rev* **18**: 657-686.

Postgate, J.R. (1979) *The sulphate-reducing bacteria*. Cambridge: Cambridge University Press.

Postgate, J.R. (1984) *The sulphate-reducing bacteria*. Cambridge: Cambridge University Press.

Rapp, B.J., and Wall, J.D. (1987) Genetic transfer in *Desulfovibrio desulfuricans*. *Proc Natl Acad Sci U S A* **84**: 9128-9130.

Taketo, A. (1989) Properties of electroporation-mediated DNA transfer in *Escherichia coli*. *J Biochem (Tokyo)* **105**: 813-817.

Wall, J.D., Rapp-Giles, B.J., and Rousset, M. (1993) Characterization of a small plasmid from *Desulfovibrio desulfuricans* and its use for shuttle vector construction. *J Bacteriol* **175**: 4121-4128.

Wall, J.D., Murnan, T., Argyle, J., English, R.S., and Rapp-Giles, B.J. (1996) Transposon mutagenesis in *Desulfovibrio desulfuricans*: development of a random mutagenesis tool from Tn7. *Appl Environ Microbiol* **62**: 3762-3767.

Walsh, C. (2003) *Antibiotics -- actions, origins, resistance*. Washington, DC: ASM press.

Weimer, P.J., Van Kavelaar, M.J., Michel, C.B., and Ng, T.K. (1988) Effect of phosphate on the corrosion of carbon steel and on the composition of corrosion products in two-stage continuous cultures of *Desulfovibrio desulfuricans*. *Appl Environ Microbiol* **54**: 386-396.

Widdel, F., and Hansen, T.A. (1992) The dissimilatory sulfate- and sulfur-reducing bacteria. In *The prokaryotes*. Balows, A.T., Dworkin, H.G., Harder, M., and Shleifer, K.H. (eds). New York: Springer, pp. 583-624.

Chapter 2

A Method Adapting Microarray Technology for Signature-Tagged Mutagenesis of *Desulfovibrio desulfuricans* G20 and *Shewanella oneidensis* MR-1 in Anaerobic Sediment Survival Experiments

Abstract

Signature-tagged mutagenesis (STM) is a powerful technique that can be used to identify genes expressed by bacteria during exposure to conditions in their natural environments. To date, there have been no reports of studies in which this approach was used to study organisms of environmental, rather than pathogenic, significance. We used a mini-Tn*10* transposon-bearing plasmid, pBSL180, that efficiently and randomly mutagenized *Desulfovibrio desulfuricans* G20 in addition to *Shewanella oneidensis* MR-1. Using these organisms as model sediment-dwelling anaerobic bacteria, we developed a new screening system, modified from former STM procedures, to identify genes that are critical for sediment survival. The screening system uses microarray technology to visualize tags from input and output pools, allowing us to identify those lost during sediment incubations. While the majority of data on survival genes identified will be presented in future papers, we report here on chemotaxis-related genes identified by our STM method in both bacteria in order to validate our method. This system may be applicable to the study of numerous environmental bacteria, allowing us to identify functions and roles of survival genes in various habitats.

Introduction

Microbial survival in a habitat is subject to both biotic and abiotic influences and ultimately depends on the organism's ability to respond to prevailing environmental stresses. This response is believed to involve expression of genes that confer specific "stress response" capabilities on the cells. These functions can involve a variety of biochemical or structural features useful for the microorganism's survival. For example, sediment-dwelling microorganisms can detoxify their surroundings by reducing certain metals to less soluble forms (13, 29, 31, 53). With our current knowledge of the importance of gene expression in response to environmental factors, many essential biological events that occur in situ are most likely missed during studies of laboratory cultures. As well, there has been no way to prove that cell functions observed in the laboratory are important for the organism when it is growing in the natural environment. Recognition of this problem has been pronounced in many fields, but significant progress in addressing this issue has been made only in studies of bacterial pathogens and some commensal organisms (16). This work has allowed for studies of bacterial genes as the organisms are growing within the host. One of the most widely used techniques for identification of genes directly involved with in situ survival of the organism is signature-tagged mutagenesis (STM).

STM requires the generation of oligonucleotide-tagged mutants, the incubation of these mutants in the natural environment, and finally, identification of nonsurviving mutants by observing the loss of their corresponding tags by using a hybridization approach. The first STM study demonstrated the potential for identifying genes essential for survival of *Salmonella enterica* serovar Typhimurium in the infected host model

(mouse) (19). Since this seminal article, increasing numbers of reports of studies that have further exploited this approach for studying the in vivo survival of pathogenic microorganisms (8, 14, 16, 26, 27, 34) and commensal bacteria (18, 21) have appeared each year. Although the STM procedure has undergone many refinements during these studies (reviewed in reference (26)), all reinforce the belief that STM is a powerful approach for screening the genomes of microorganisms for genes that enable bacteria to survive in their natural habitats.

In order to adapt this technique to study bacteria of environmental significance, we chose two model organisms. These are representative of sediment-dwelling anaerobic bacteria that carry out important functions in their environments. Sulfate-reducing bacteria, such as *Desulfovibrio desulfuricans* G20, are involved in the reductive arm of the sulfur cycle and play critical roles in degrading organic compounds in sulfate- and organic-rich environments (15, 42). *Shewanella oneidensis* MR-1 is from a genus shown to be abundant in a variety of sedimentary environments, and *Shewanella* species have been used as models for studying Fe(III) (40) and radionuclide [U(VI) and Tc(VII)] transformations (13, 29). With these organisms, difficulty in achieving high efficiency and random transposition with transposon systems similar to those used in prior STM or general mutagenesis studies led us to screen a number of transposon-containing vectors. The availability of microarray technology led us to modify the screening process of the STM procedure, enabling us to mass produce microarray slides with printed tags. The microarray system also enabled us to downsize equipment necessary for carrying out hybridizations. This modified approach to STM allowed us to identify genes critical to the function of organisms of environmental significance, such as anaerobic, sediment-

dwelling bacteria.

Materials and Methods

Strains and media. A general outline of the entire STM procedure appears in Fig. 1. A list of strains and plasmids used in this study is given in Table 1. Strain G20 was grown in lactate-sulfate (LS) medium prepared as described by Rapp and Wall (44), using N_2 headspace and vitamin and metal solutions as described elsewhere (50). Prior to autoclaving, the pH was adjusted to 7.2, and after autoclaving, 8 mM bicarbonate and 0.025% cysteine were added from anaerobic stock solutions. For growth of G20 on solid media, LS agar medium (1.5% agar) was prepared, with the addition of 0.005% $PdCl_2$ (rather than cysteine), a catalyst for reduction of the medium by H_2 (contained within the anaerobic chamber). These plates were poured on the bench, and following solidification, the oxidized plates (pink from resazurin redox indicator) were dried overnight in a laminar flow hood and then moved into an anaerobic chamber and reduced overnight. *S. oneidensis* MR-1 was maintained aerobically on standard Luria broth (LB) medium and grown anaerobically with a modified LS medium [25 mM Fe(III)-citrate in place of sulfate, 50 mM lactate, no bicarbonate or cysteine, pH 7]. A minimal lactate medium was also used for aerobic growth where indicated [amended LS medium with Fe(III)-citrate omitted]. For selection of transposon mutants, 175 g/ml kanamycin was added to agar plates prepared as described above for G20 and 50 g/ml kanamycin was added to LB plates for MR-1. *Escherichia coli* strains were cultured in LB supplemented with appropriate antibiotics. Additionally, strain β-2155 required 0.05% diaminopimelic

Figure 1. Overview of STM for G20 and MR-1 sediment survival studies. Although 96 tags were originally designed and moved into *E. coli* β-2155 on pBSL180, only 60 were used for conjugation with G20 and MR-1. This model therefore shows assembly of 60 G20 and MR-1 mutants in each one of 96 "mutant pools".

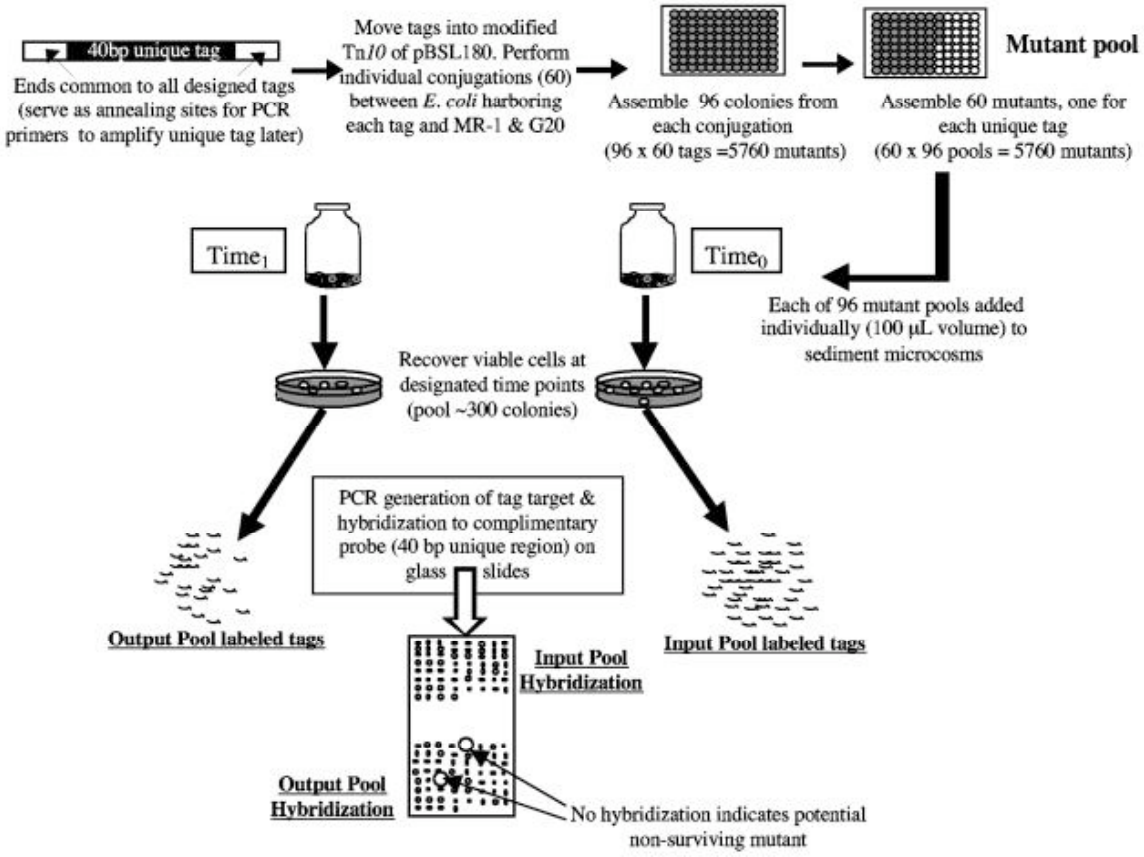

Table 1. Strains and plasmids used in this study.

Strain or plasmid	Relevant properties[a]	Source (reference)
Strains		
Desulfovibrio desulfuricans G20	Spontaneous nalidixic acid^R G100A (G200) cured of native pBG1	(55)
G20sediment	G20 passed through sediment and selected on nalidixic acid	This study
S. oneidensis MR-1	Wild-type	(38)
MR-1rif^{R}strept^R	Spontaneous Rf^R Sm^R derivative	This study
MR-1sediment	MR-1rif^{R}strept^R passed through sediments amended with iron oxyhydroxide gel and lactate and selected on streptomycin	This study
E. coli strain β2155	K-12 derivative; F'*tra*D36*lac*I^q Δ(*lac*Z)M15 *pro*A$^+$B$^+$/*thr-1004 pro thi strA hsdS* Δ(*lac*Z)M15 Δ*dapA::erm pir::*RP4(::*kan* from SM10)	(20)
Plasmids		
pRK2096	Tn*7* derivative transposon with Km^R	(54)
pRK2073	Helper plasmid with Sp^R	(24)
pRL1058a	Tn*5* transposon with Km^R	(57)
pQL1058a	CytC promotor inserted in front of Km^R gene in Tn*5* transposon of pRL1058a[b]	This study
pTnMod-RKm	Mini-Tn*5* transposon with Km^R	(10)
pTnMod-OGm	Mini-Tn*5* transposon with Gm^R	(10)
pMycoMar	Mariner-based transposon with Km^R	(45)
pBSL180	Mobilizable suicide vector; modified Tn*10* with Km^R	(2)

[a] Antibiotic abbreviations: Rf, rifampin; Sm, streptomycin; Km, kanamycin; Sp, spectinomycin; Gm, gentamicin.

[b] Two PCR primers to regions within pRL1058a transposon were synthesized, each with one half of the *cytC* promotor region from *D. vulgaris* as a tail. Following PCR (to amplify the entire pRL1058a plasmid with the *cytC* promoter inserted) using *Pfu* Turbo DNA polymerase (Stratagene), PCR products were ligated to form pQL1058a. The primers were forward primer 5'TCCCGCTTGGGAAATCCTTAACTTACCTTTGTGAAGGAGGTAGTTCGATCATGATG ATTGAACAAGATGGATT3' and reverse primer 5'TGGTATTGTGTCCGCCATGCCGTGTCAAGGAATGGAGCGGGAAAGCCTAGGCGAA ACGATCCTCATCCTG3'.

acid (DAP) for growth with LB medium. G20 and *E. coli* strains were grown at 37°C, while MR-1 was grown at 30°C. A period of 3 days was necessary for colonies of G20 to appear on solid media, while 18 h was sufficient to generate 1- to 2-mm-diameter colonies of MR-1.

For construction of our tagged-transposon mutant libraries, we used strains of G20 and MR-1 that had been adapted to sediment conditions. In order to generate these strains, G20 and MR-1 Rf^r Sm^r were incubated individually in sediment microcosms as described in greater detail below (see "Initial sediment survival experiments") and subsequently reisolated at the time of peak growth (8 to 9 days for G20 and 3 days for MR-1) based on nalidixic acid (200 g/ml) resistance for G20 and streptomycin (300 g/ml) resistance for MR-1. By utilizing such strains (now termed G20sediment and MR-1sediment) that have adjusted to sediment conditions, we hoped to avoid problems with adaptation to environmental conditions and the possibility that important functions may have been suppressed during repeated transfer in laboratory media.

Plasmids were provided by Dianne Newman (pBSL180), Judy Wall (pRK2096, pRK2073, and pRL1058a), and Gerben Zylstra (pTnMod-RKm and pTnMod-OGm).

Tag design and screening for cross hybridization among tags. Based upon tag sequences in a previously described STM system (19), we designed 96 single-stranded DNA tags, each with a 40-nucleotide (nt) variable region flanked by constant arms common to all tags: 5-CTAGGTACCTACAACCTCAAGCTT-[NK]20-AAGCTTGGTTAGAATGGGTACCATG-3, where [NK]20 represents the 40-nt variable region; N is A, C, G, or T; and K is G or T. This design prevented KpnI sites, necessary for later cloning steps, from being incorporated into the tag sequence. Following the

individual synthesis of 89-nt single-stranded tags (Integrated DNA Technologies, Inc., Coralville, Iowa), all 96 tags were individually amplified in PCRs using primers P3 and P5 (homologous to the common arms of all tags) (19), in order to create double-stranded tags for cloning into pBSL180. Primers P2 and P4 (19), internal to primers P3 and P5, were used in later steps described below to PCR amplify the unique region of tags prior to hybridization. Double-stranded tags that had been amplified by primers P3 and P5 were individually digested with KpnI (restriction sites present in the common arms) and ligated individually into KpnI-digested pBSL180. Competent cells of *E. coli* strain CC118 were transformed with the ligation product by using standard electroporation methods. Plasmid isolated with QIAprep spin miniprep kit (QIAGEN) from transformed CC118 cells was then used to electroporate *E. coli* strain β-2155.

We screened all 96 tags for cross hybridization prior to mutagenesis of strains G20sediment and MR-1sediment with each tagged form of pBSL180. Tagged pBSL180 was first isolated from individual *E. coli* β-2155 strains. We PCR amplified and then labeled tags with Cy5 dye as described in "Colony PCR" and "Target preparation" below, except that here we started with purified plasmid for PCR template and not colonies on agar medium. The 96 tags (approximately 100 ng each) were individually PCR amplified in a 96-well plate. We then pooled the well contents (6.25 μl of the 50 μl PCR mixture) from each column (8 tags per column; 12 columns) and each row (12 tags per row; 8 rows) in order to perform 20 separate labeling reactions for 20 hybridizations to microarray slides. Prior to and following the labeling reaction, DNAs from pooled columns and rows were cleaned with Amersham Microspin G-25 columns. Slides were printed with the 40-bp unique region from the 96 tags (as described below), and

hybridization of labeled tags and wash conditions were as described in "Hybridization and washing procedures" below. Based on results discussed further below, we eliminated 36 tags from the study due to cross hybridization. We continued with the 60 remaining tags (sequences of the 40-nt unique region are found in Table S1 in the supplemental material).

Generation of mutant libraries. Conjugations were carried out by picking a single colony and transferring it to either LB (strain MR-1sediment and each *E. coli* β-2155 strain containing a uniquely tagged pBSL180) or LS media (strain G20sediment). The following manipulations were carried out aerobically with MR-1 or in an anaerobic glove box (Coy Laboratory Products, Grass Lake, MI) for G20. G20 and MR-1 were grown for 10 to 20 h. *E. coli* β-2155 with one unique tag in pBSL180 was grown overnight, diluted 1:10 in LB without antibiotic selection, and grown until the optical density at 600 nm (OD_{600}) was approximately equal to that of the recipient organism (0.5 to 1.0). Volumes of *E. coli* and recipient were centrifuged together (6,000 X g, 10 min) at a 1:1 or 1:2 ratio and then resuspended in 100 μl of spent medium from the recipient strain. This mating mixture was placed onto a 0.22-μm filter in the center of an LB-DAP plate for 3 h at 30°C (for MR-1) or an LS plate for 6 h at 37°C (for G20). Cells were washed from the filter by immersion into 1 ml of the medium favored by the recipient (no DAP) in 13- by 100-mm glass tubes. Strain MR-1sediment transposon mutants were washed from the filter and then immediately plated onto LB plates supplemented with kanamycin (no DAP), while strain G20sediment transposon mutants were recovered in liquid LS medium with 200 g/ml nalidixic acid for 5 h prior to plating onto LS medium with kanamycin. Nalidixic acid was included in LS medium during the recovery in order

to kill *E. coli* β-2155, which could grow on LS medium even without addition of DAP. This conjugation procedure was repeated for each of the remaining 59 β-2155 strains harboring a uniquely tagged form of pBSL180.

For each tagged pBSL180, we picked 96 random exconjugants to a 96-well plate. With 60 unique tags, we collected 5,760 mutants in total. Mutants were then reassembled so that one mutant (of 96) from each of the original 60 plates was moved to one other plate. The procedure was repeated 96 times so that each new plate contained a pool of 60 uniquely tagged mutants. We had 96 of these mutant pools to screen in sediment per organism (Fig. 1). At this stage we also used a random sampling of mutants and standard Southern blotting procedures (3) to determine that single, random transposition events occurred in both G20 and MR-1.

Initial sediment survival experiments. Prior to creation of the transposon mutant libraries, initial sediment survival experiments were carried out for two purposes: to determine when to sacrifice sediment incubations for collection of output pools and to isolate sediment-adapted strains, as described previously. These initial sediment incubations with G20 and MR-1 Rf^r Sm^r were carried out in a manner similar to that for the mutant pool sediment incubations described below. The only differences were sacrificing replicate microcosms (two bottles per time point for G20 and three bottles per time point for MR-1) at various time points (instead of just at one time point for mutant pools) and selection of recovered cells with solid media containing nalidixic acid (G20) or streptomycin (MR-1). Sizes of inocula were approximately 10^5 to 10^6 cells for both G20 and MR-1.

With MR-1, we added 200 μmol amorphous Fe(III) oxyhydroxide, prepared as

described previously (33), in order to shift sediment from sulfate-reducing conditions to Fe(III)-reducing conditions (see "Screening of tagged mutants in natural sediments" below for a description of the sediment collected). Because previous work with STM required some growth of virulent strains in the host (8), we amended MR-1 microcosms with 20 μmol lactate in order to stimulate at least a 10-fold increase in cell numbers. In similar microcosms without addition of lactate, we were unable to achieve this amount of growth (data not shown). To assess levels of Fe(III) reduction, cells (1 ml) were first sampled from sediment incubations (as described below), and then the liquid remaining in the bottles was acidified by addition of 250 μl 6 N HCl and shaken at room temperature for 30 min. Fe(II) was measured from 0.5 ml acidified sample in each bottle, using the ferrozine assay (32, 33).

Screening of tagged mutants in natural sediments. Each mutant pool of G20 (60 uniquely tagged mutants) was grown in deep 96-well plates to late log phase (equivalent to an OD_{600} in serum tubes of 0.7) with LS medium in an anaerobic glove box. MR-1 pools were grown in shallow 96-well plates and transferred through LB, minimal lactate (aerobic), and finally modified LS medium (grown in anaerobic chamber). MR-1 pools were grown until the Fe(III)-citrate had cleared in most wells. Experiments were then continued independently for each organism but were maintained in an anaerobic glove box. The contents of all 60 wells were then pooled. Pooled cells were washed three times in modified LS anoxic minimal medium buffered with 8.3 mM bicarbonate without addition of the vitamins, trace metals, and electron donor. For G20, Na_2SO_4 was omitted but the solution contained 8.4 mM $MgSO_4$. For MR-1, Fe(III) was omitted; 7 mM NaCl and 2 mM $MgCl_2$ replaced Na_2SO_4 and $MgSO_4$, respectively (so as not to stimulate the

sulfate-reducing population); KH_2PO_4 was increased to 3.7 mM; NH_4Cl was reduced to 7.5 mM; and $CaCl_2$ was dropped to 0.34 mM to avoid precipitation. Washed cells (100 μl) were inoculated (10^5 cells) into 30-ml serum bottles containing 2 g sulfidogenic subsurface sediments from a landfill in Norman, OK, a site characterized in previous studies (4, 5). The initial water content of these sediments ranges from 10% to 25% of the total weight. Bottles were then flushed with N_2-CO_2 (4:1), as CO_2 is required to maintain a neutral pH in this system. MR-1 microcosms were amended with 200 μmol amorphous Fe(III) oxyhydroxide and 20 μmol lactate. One bottle per mutant pool was sacrificed (as described below for output pool) within 3 h for analysis of tags present in the input pool. A duplicate bottle for each mutant pool was incubated in the dark at room temperature for 8 to 9 days (G20) or 5 to 6 days (MR-1) and then sacrificed.

For extraction of cells, anoxic minimal medium buffer (4 ml) was added to the bottles and they were shaken by hand and vortexed for 15 min. Extracted cells were then diluted in the same buffer and plated onto LS plates with 175 μg/ml kanamycin in the anaerobic glove box for G20 and aerobically onto LB plates containing 100 μg/ml kanamycin for MR-1 (increased from 50 μg/ml to decrease the background of kanamycin-resistant sediment organisms). Plates were incubated as described in "Strains and media" above.

Colony PCR. Plates from the dilution series were chosen so that one to two plates containing a total of about 300 colonies were used. Colonies were scraped from plates into the same mineral medium used for inoculation of microcosms, and cells were centrifuged for 1 min (12,000 X g). The pellet from pooled colonies was resuspended in 200 μl distilled water (dH_2O). A portion (50 μl) was removed to an Eppendorf tube, and

1 ml dH_2O was added. The cells were then centrifuged for 1 min, and the supernatant was removed. Washing was repeated four times, and the final pellet was resuspended in 100 μl dH_2O. This was boiled for 5 min, placed on ice for several minutes, and then centrifuged for 2 min. The supernatant (5 μl) was used in a 50-μl PCR mixture containing 1X PCR buffer; 1.5 mM $MgCl_2$; 0.2 mM each dATP, dCTP, and dGTP; 0.12 mM dTTP; 80 M aminoallyl-dUTP (Molecular Probes); 0.1 M each of primers P2 and P4 (19); and 2.5 U Invitrogen Platinum Taq PCR parameters were 94°C for 4 min, followed by 30 cycles (G20) or 25 cycles (MR-1) of 94°C for 30 s, 50°C for 30 s, and 72°C for 30 s. All PCRs were performed using the GeneAmp PCR System 9700 (Applied Biosystems) thermal cycler. Following amplification, the reaction mixture was purified with an Amersham Microspin G-25 column according to the instructions of the manufacturer. We compared genomic DNA extracted from cell pellets by using the Invitrogen Easy DNA kit as template in tag labeling PCR to that from the boiling extract procedure described above. In every case tested, results were identical (data not shown).

Target preparation. One vial of Cy5 Mono-Reactive Dye Pack (Amersham) was dissolved in 72 μl dimethyl sulfoxide. Aliquots (4.5 μl) were distributed into amber Eppendorf tubes and dried completely in a Labconoco Centrivap (60°C, 45 min). The purified PCR product containing aminoallyl-dUTP was also dried in this manner and resuspended in 6 μl of 0.1 M Na_2CO_3 solution (pH 9). This was added to the dried Cy5 dye and incubated for 1 h at room temperature in the dark. The reaction was stopped by addition of 3 μl of sodium acetate (3 M, pH 4.5) and 41 μl water, and unbound dye was removed with Microspin G-25 columns. Dye incorporation was quantified on a DU530 Life UV/visible spectrophotometer (Beckman Instruments). The labeled PCR product

(target) was then dried completely as before and resuspended in 2.5 μl water, 50 μl Roche digoxigenin hybridization solution, and 2.5 μl salmon sperm DNA (Stratagene). Prior to hybridization, the target was heated to 65°C for 5 min and then placed on ice.

Preparation of microarray slides. The 40-nt unique region (see Table S1 in the supplemental material) and its complementary strand for each of 60 tags were synthesized separately (Invitrogen). Equivalent concentrations of the unique regions and their 40-nt complements were mixed to create 60 solutions of approximately 3.3-μg/μl final concentration in 3X SSC (1X SSC is 0.15 M NaCl plus 0.015 M sodium citrate). A small fraction of all of these solutions was spotted onto FMB Oligo Slides with poly-L-lysine surface chemistry (Full Moon BioSystems Inc.) using a Generation Array III spotter (Molecular Dynamics), creating 60 spots of approximately 100 μm in diameter (probes). On each slide, the unique tags were printed in duplicate in order to check reproducibility within the hybridization. This duplicate set was also printed on both ends of the slide, enabling us to simultaneously compare input (hybridized on one half of the slide) and output (hybridized on the other half of the slide) pools. Spotted slides were stored desiccated until ready for use within 2 months of preparation. Prior to use, slides were rehydrated briefly with steam, immediately dried on a heat block, UV cross-linked, and then blocked using a succinic anhydride blocking solution (http://omrf.ouhsc.edu/frank/M_Slide_Blocking_Protocol.html).

To demonstrate that the probes were not washed from the slides during hybridizations or washes, we compared rehydrated and UV-cross-linked slides that were stained for 5 min at room temperature with SYTO 61 red-fluorescent nucleic acid stain (Molecular Probes; 1 μl in 50 μl Tris-EDTA buffer spread over spotted probes on each

half of slides) either prior to or after the hybridization (no labeled target was applied with hybridization solution) and washing procedures described below. Slides were washed in Tris-EDTA buffer to remove the excess DNA stain, dried with 95% ethanol, and scanned at 650 nm using GenePix Pro 5.1 from Axon Instruments to compare the intensities of each stained probe before and after hybridization/washing procedures.

Hybridization and washing procedures. Each slide was placed into a Corning hybridization chamber, and 22I*25 coverslips (Erie Scientific Company) were placed over each half of the slide (one to cover the input pool and one to cover the output pool). Approximately 20 to 25 μl (100 pmol) of target was added beneath each coverslip, and hybridization units were incubated in a water bath at 37°C overnight. Prior to washing, slides were dipped in dH_2O to remove the coverslips. Following all washing procedures (see below), slides were dried under a gentle stream of nitrogen. Scanning (650 nm) and spot intensity analyses were performed using GenePix Pro 5.1 from Axon Instruments. Background was assessed locally and subtracted from each spot by using the companion software. A negative response was set at any signal below 3 times the background level. This cutoff was based on the relative variability of the background.

For washing solutions, we tested a low-stringency (high-salt) procedure and a high-stringency (low-salt) procedure to determine which one resulted in fewer cross hybridizations among the original 96 tags. Comparisons were carried out by pooling columns and rows as described in "Tag design and screening for cross hybridization among tags" above. The low-stringency wash consisted of a series of washes (10 min each at room temperature) with 2X SSC–0.1% SDS, 1X SSC–0.1% SDS, 1X SSC, and 0.5X SSC. For the high-stringency wash (from the Full Moon Oligo Slides protocol),

slides were washed in 0.2X SSC–0.2% SDS solution (prewarmed to 55°C) for 30 min on a shaker at room temperature. Slides were then removed from the first wash, dipped twice in 0.2X SSC (also prewarmed to 55°C), and then dipped three times in room temperature dH_2O. Following analysis of spot intensities, the high-stringency wash was chosen for our STM method (see Results), as fewer tags exhibited cross hybridization with this protocol.

Following analysis of these hybridizations, we attempted to decrease cross hybridizations further among 36 tags slated for elimination (out of the original 96 tags) by increasing the wash temperature of slides. Twenty pools of tags were prepared as described in "Tag design and screening for cross hybridization among tags" above. Following hybridizations, replicate slides for each of the 20 pools were washed at 55°C, 60°C, and 65°C using the high-stringency wash solutions.

Confirmation of sediment mutants. Potential nonsurviving mutants were defined as having a signal in the input pool but no signal (below 3 times the background level) in the output pool when hybridizations were analyzed. For G20 studies, mutants were confirmed by monitoring the cell number of individual mutants in sediment incubations (carried out exactly as described in "Initial sediment survival experiments" above).

MR-1 mutants were confirmed by subsequent competition experiments in sediment microcosms with parental strain MR-1sediment, as performed in previous STM studies (7, 22). These competition experiments were similar to mutant pool incubations, except that now only one transposon mutant and strain MR-1sediment were inoculated together in a 100-μl volume (~10^3 cells each) of the anoxic minimal medium buffer described above. The inoculum size was lowered from that used in mutant pools (10^5 total cells) to

reflect the approximate concentration of one tagged mutant among 59 other tagged mutants. Following extraction of replicate microcosms (in duplicate bottles) with anoxic minimal medium buffer at 0 and 5 days, surviving cells were plated onto LB plus kanamycin (100 μg/ml) and LB plus streptomycin (300 μg/ml). The transposon mutant was enumerated by colony counts on kanamycin plates, while the number of recovered strain MR-1sediment CFU was the difference between kanamycin (mutant) and streptomycin (total) plate counts. These numbers were used to calculate a competitive index (CI), a measure of output ratio of mutant to parent strain/input ratio of mutant to parent strain (7, 22). Where deemed necessary, a CI was also determined in anoxic Fe(III)-citrate laboratory medium for growth of individual potential nonsurvivors competing with strain MR-1sediment (inoculated with 106 to 107 cells each, from separate, mid-log-phase aerobic lactate medium cultures). The output ratio in this case was determined by total cell count taken when the brown coloration of Fe(III)-citrate medium was beginning to clear. In previous growth experiments, we monitored cell number (by plating onto LB medium) and Fe(II) accumulation (ferrozine assay described above) in this medium and determined that clearing occurred near the mid-log phase of growth and as a result of Fe(III) reduction to Fe(II) (data not shown).

Arbitrary PCR and identification of interrupted genes. Arbitrary PCR was used to determine the DNA sequences of the sites of transposon insertion in confirmed sediment-impaired mutants and was modified from previous procedures (36, 41). Approximately 3 ml of overnight mutant culture was centrifuged and washed, and DNA was extracted using the colony PCR protocol described above. In all PCRs, the Expand Long Template PCR system (Roche) was used according to the manufacturer's

instructions. For the first round of PCR (25-μl reaction mixture), 5 μl supernatant from the prepared pellet was used with primers Tn10ext (5'GTGTTCCGCTTCCTTTAGCAGC3') and Arb1 (41). Parameters were (i) 95°C for 5 min; (ii) 15 cycles of 95°C for 45 s, 40°C for 45 s, and 68°C for 1 min; and (iii) 20 cycles of 95°C for 45 s, 45°C for 45 s, and 68°C for 1 min. For the second round of PCR (50-μl reaction mixture), 2 μl of first-round product was used with primers Tn10seq (5'GTCGACGGTATCGATAAGCTTG3') and Arb2 (41). Parameters were (i) 95°C for 5 min; (ii) 15 cycles of 95°C for 45 s, 45°C for 45 s, and 68°C for 1 min; and (iii) 15 cycles of 95°C for 45 s, 50°C for 45 s, and 68°C for 1 min. The resultant PCR product was purified with the PCR purification kit from QIAGEN and sequenced directly using the Tn10seq primer. For identification of the interrupted gene, sequence obtained from arbitrary PCR was compared to the NCBI database by using blastn. The genome sequence for MR-1 has been published (17), while annotation completed to date for G20 is available at http://www.ncbi.nlm.nih.gov/genomes/framik.cgi?db genome&gi 5163.

Results

Transposition system for G20 and MR-1. Wall et al. (54) described several vectors suitable for transposon mutagenesis in *D. desulfuricans* G20. We mutagenized strain G20 and other strains of *Desulfovibrio* with several of these vectors, using both conjugation and electroporation procedures. Although we observed efficient transformation (Table 2) using the Tn7-based pRK2096, transposon insertion (as determined by Southern blot hybridization) was not random (data not shown). Subsequent electroporation experiments using Tn5-based pRL1058a resulted in low

transformation efficiency (four transformants/μg DNA). Additionally, Southern blot analysis of mutant chromosomal DNA showed only two different insertion patterns (among 10 mutants tested) (data not shown). We attempted to improve the efficiency of pRL1058a transposition by inserting the *Desulfovibrio vulgaris* cytochrome c promoter in front of the kanamycin resistance gene of the Tn5 transposon. This promoter has been used to express different genes in *Desulfovibrio* and *E. coli* (6, 52). Although the transformation efficiency did increase slightly, this modification (plasmid designated pQL1058a) did not result in random insertions. This was possibly due to transposon instability, since the transposase gene was encoded on the transposon (11).

We also tested the ability of several other vectors to mutagenize G20, using both electroporation and conjugation. These included pTnMod-RKm and pTnMod-OGm, two mini- Tn5 plasmids that have transposase encoded outside the transposon (10), and pMycoMar, with a mariner transposon (1). In all cases, no transposon mutants were obtained with G20. One commercially available kit with Tn5 and transposase mix (Epicenter) was also used for electroporation into G20, but the transformation efficiency was very low (Table 2).

For transposon mutagenesis of MR-1, we obtained a mini-Tn10 plasmid, pBSL180 (Table 1), whose features include a relatively small size (6.3 kb), an R6K origin of replication (requires the π protein for replication), a kanamycin resistance gene (*npt*II), and the multiple cloning site of pBluescriptII within the Tn10, as well as a mutant ATS Tn10 transposase gene encoded outside the transposon (2). The R6K origin of replication is critical for use in transposon mutagenesis of MR-1, as many plasmids, including those with origins such as p15A and pMB1, are capable of replicating in *Shewanella* (37); our

results; D. Lies, personal communication). The importance of the mutant ATS Tn10 transposase is that it displays a lower degree of insertion specificity than the wild-type Tn10 transposase, which is known to insert into hot spots (25).

Fortuitously, by conjugating *E. coli* strain β-2155 harboring pBSL180 with G20, we found that the frequency of conjugation was sufficient (Table 2) for us to create STM mutant libraries with this mutagenesis system in both G20 and MR-1. Southern blot analysis confirmed that mutations occurred randomly in the strain G20 chromosome (Fig. 2). Random transposition was previously shown for MR-1 (40) and through Southern blotting performed in our study (data not shown).

Probe preparation for spotting. Complementary oligonucleotide pairs of the unique region for each tag served as the probe (40 bp). In initial experiments, we tested the effect on the hybridization signal of the concentration of probe DNA (10 ng/μl, 300 ng/μl, 670 ng/μl, or 3.3 μg/μl) used in spotting. Spots with 3.3 μg/μl of 40-bp DNA produced the strongest hybridization signal. Spot intensities for the remaining concentrations were 2%, 5%, and 32%, respectively, relative to 3.3 μg/μl.

We then compared spotted slides that were incubated with SYTO 61 red-fluorescent nucleic acid stain added either before or after hybridization/washing procedures. We observed that fluorescence from the DNA stain did not change during the hybridization and washing steps (data not shown), indicating that the majority of spotted DNA remained bound to our slides. This also indicated that 3X SSC, commonly used in microarray spotting at the time (47), was sufficient for spotting our double-stranded probes to the glass slide.

Hybridization and washing conditions. Prior to hybridization, blocking of slides

Table 2. Frequency of conjugation and efficiency of electroporation with *Desulfovibrio desulfuricans* G20.

Plasmid	Transposon	DNA transfer method[b]	Frequency or efficiency[c]
pRL1058a	Tn*5*	Electroporation	4 transformants / 1μg DNA
pQL1058a	Tn*5*	Electroporation	6 transformants / 1μg DNA
pRK2096	Tn*7*	Conjugation	10^{-6}—10^{-5}
pTnMod-OGm	Mini-Tn*5*	Electroporation	0
pTnMod-RKm	Mini-Tn*5*	Electroporation	3 transformants / 1μg DNA
EZ::TN[a]	Tn*5*	Electroporation	18 transformants / 1μg DNA
pMycoMar	Mariner	Electroporation	0
pBSL180	Mini-Tn*10*	Conjugation	10^{-6}—10^{-5}

[a] Kit from Epicentre containing a transposon-transposase mixture (not a plasmid).

[b] Electroporation was carried out as previously described (49) with the following modifications. Cells were harvested at late-log phase with OD_{600} of 0.6-0.7. To maintain osmolarity similar to G20, 400 mM sucrose with 1 mM $MgCl_2$ was used as both washing and electroporation buffers. Electroporation was performed in the anaerobic glove box, after which cells were immediately recovered in 400 μl of LS medium.

[c] Frequency represents the number of antibiotic-resistant CFUs divided by the number of recipient CFUs in conjugation experiments. Efficiency represents transformants per μg DNA used in electroporation experiments.

Figure 2. Southern blot analysis of G20 mutants transformed with pBSL180 Tn*10* transposon. pBSL180 was used as a probe. Lane 1 and 25, 1 Kb DNA ladder; lane 2 to 4, pBSL180 HindIII-digested fragments; lane 5 to 24 and 26 to 47, HindIII digest of chromosomal DNAs from independent G20 mutants (two bands are expected from Tn*10*); lane 48, HindIII digest of chromosomal DNA of untransformed G20.

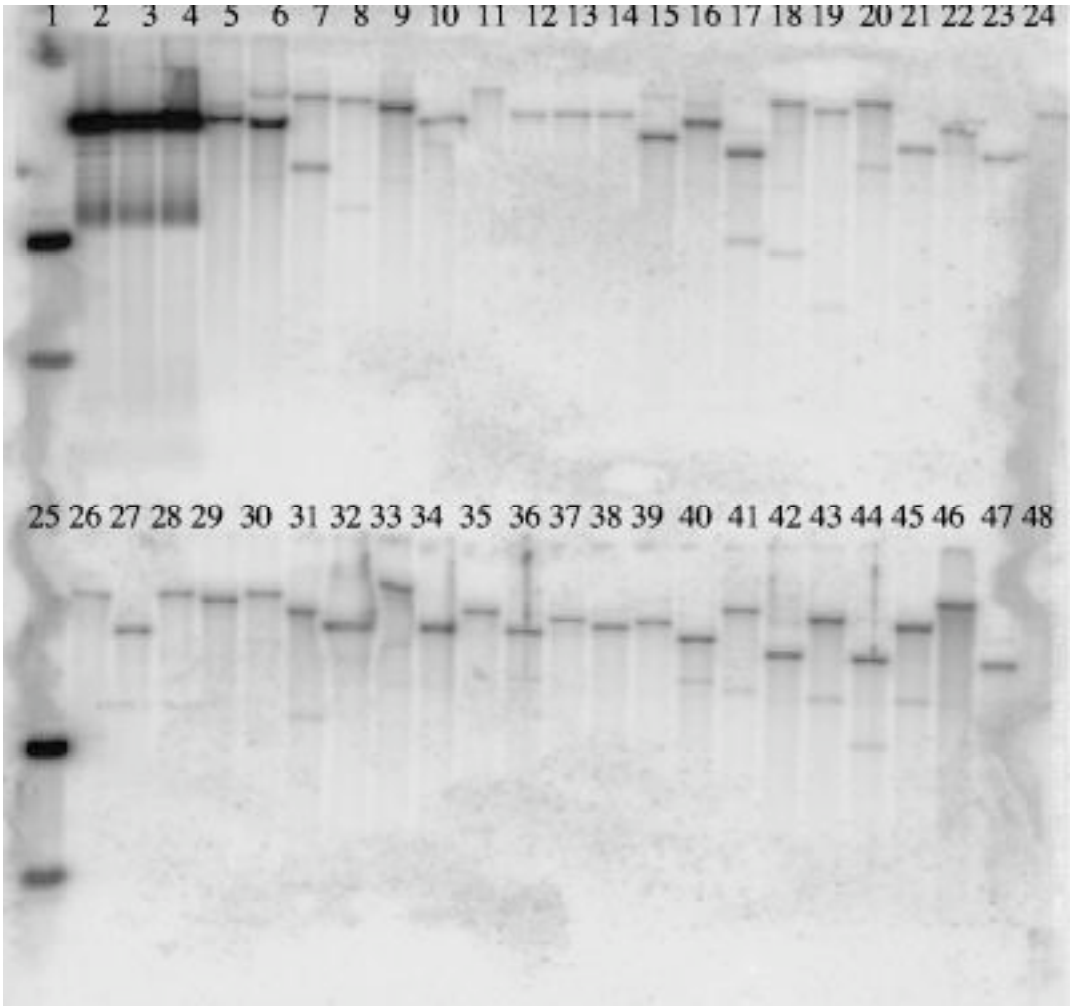

was found to be essential to achieve reproducible results, as it allowed for even spreading of target across the spotted slide surface. Comparison of two washing protocols showed that the high-stringency wash yielded the strongest signal with minimal cross hybridization (Fig. 3).

With this chosen washing condition, we investigated whether increasing the washing temperature above room temperature could eliminate the cross hybridization of 36 tags slated for elimination. We found that the chosen increases in wash temperature failed to reduce cross hybridizations and actually decreased spot intensities of all specific hybridizations (Table 3). These 36 tags were eliminated based on these results and those from the cross hybridization screen (by columns and rows as described in Materials and Methods). Sixty of the original 96 synthesized tags remained for mutagenesis of G20 and MR-1 (see Table S1 in the supplemental material for tag sequences).

Initial sediment survival experiments. Initial sediment survival tests were performed to determine how long incubations should proceed before extraction of surviving mutants. From initial sediment survival tests of G20, we found that peak growth (approximately 20-fold over the initial inoculum level) was reached after 8 to 9 days of incubation at room temperature (Fig. 4a). As we believed that this amount of growth would be sufficient to select nonsurvivors from survivors, STM screens were carried out at this time point for G20. From initial survival tests of MR-1, we found that it was necessary to supply sediments with lactate in order for MR-1 to grow at least 10-fold and to remain at concentrations above the initial inoculum concentration for at least 7 days (Fig. 4b). We then chose to sacrifice MR-1 STM microcosms [amended with Fe(III) oxyhydroxide and lactate] at 5 to 6 days, a time point at which Fe(III) reduction

Figure 3. Comparison of (a) high-salt (low-stringency) and (b) low-stringency) wash conditions following hybridization of row and column pools (20) for 96 tags. The results shown represent one pooled column (eight tags from eight PCRs in one column of a 96-well plate). The remaining 7 columns and 12 rows were also individually labeled for 19 separate hybridizations with the microarray (spotted with the 96 original tags), but those data are not shown here. The portion of the array displayed is from a region containing the eight complimentary probes for the eight labeled tags used in this example (spots 1 to 4, 7, 8, 13 and 14), in addition to eight other spotted probes (5, 6, 9 to 12, 15, and 16) that are not complimentary to the eight labeled tags added in the hybridization solution. In all 20 hybridizations, cross hybridization of targets to nonspecific probes over the whole array occurred less often for high-stringency conditions (b) than for low-stringency conditions (a). In the example shown in this figure, circles are placed over probes to which nonspecific target has annealed under low-stringency conditions only.

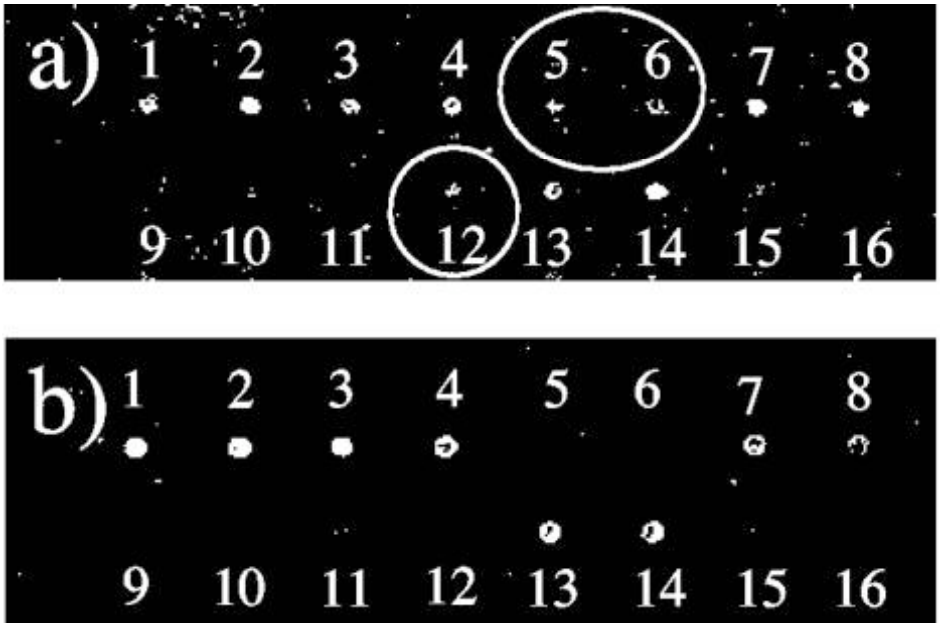

Table 3. Signal intensities of eight tags (from one row of 12 columns and 8 rows tested) bound to their respective complimentary probe as a function of increasing wash temperature.

Temperature		**Relative Signal Intensity[a] of tag:**							
Preheat	Wash	Tag A1	Tag B1	Tag C1	Tag D1	Tag E1	Tag F1	Tag G1	Tag H1
55°C	RT	1	1	1	1	1	1	1	1
55°C	55°C	0.51	0.44	0.31	0.41	0.34	0.12	0.07	0.07
60°C	60°C	0.26	0.25	0.25	0.13	0.17	0.02	0.08	0.1
65°C	65°C	0.19	0.21	0.16	0.15	0.03	0.06	0.11	0.12

[a] The number given is the fraction of the observed signal intensity relative to that for the 55°C-preheated wash solution with room temperature washing. For generation of these data, one slide spotted with duplicate arrays was used. The signal was averaged from these two arrays.

Figure 4. Growth curves in subsurface sediments of (a) G20 (data represent averages for two microcosms) and (b) MR-1 (data represent averages for three microcosms). For MR-1, squares represent CFU, open circles represent soluble Fe(II) detected from the same microcosms as CFU, and closed circles represent Fe(II) detected in identical, sterile microcosms. Error bars show standard deviations, but these are too small to appear in most cases.

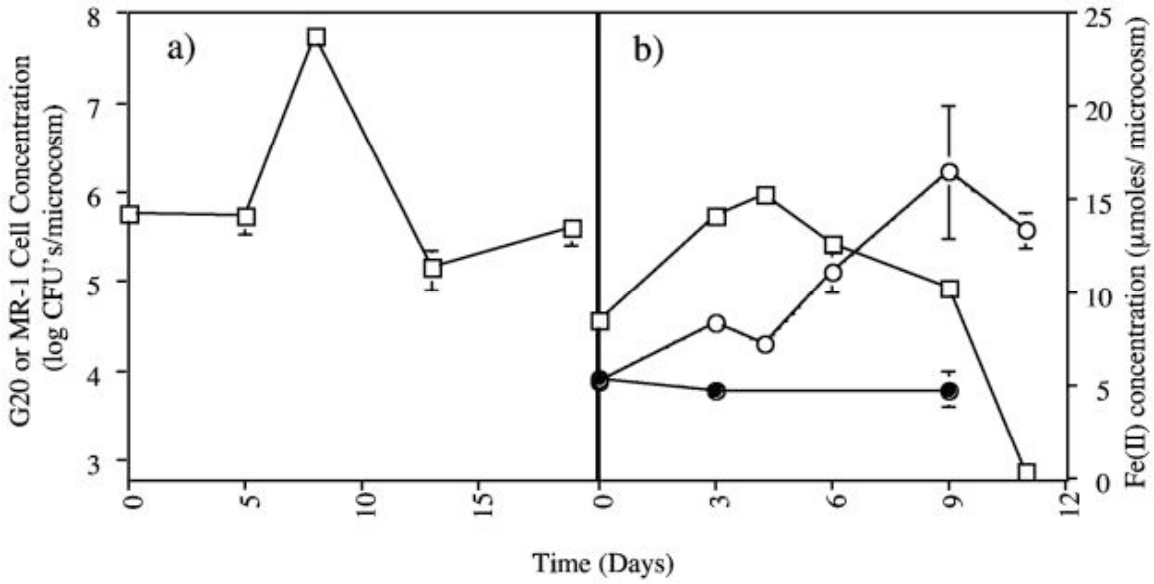

was occurring, as evidenced by Fe(II) accumulation in initial sediment survival experiments (Fig. 4b).

Screening of tagged mutants in natural sediments. To investigate recovery of tags from the input and output pools, we initially varied the number of colonies pooled for production of labeled target. In these early trials, we compared collections of 300, 700, and 3,500 colonies and found that pooled target from these resulted in similar hybridizations for some mutant pools but that on occasion, pooled target from more than 300 colonies could contribute to weak hybridization signals for mutants that might actually have been impaired in sediment survival. To ensure that we would not miss potentially impaired mutants, we elected to use approximately 300 colonies for recovery in subsequent sediment screens.

With regard to optimization of the number of PCR cycles, we observed that 30 PCR cycles with wild-type MR-1 genomic DNA as the template generated an unknown labeled target that hybridized weakly to some probe sequences spotted on the glass slide. We cannot explain why this occurred, because wild-type MR-1 does not contain any of the 60 tags and therefore should not generate target that hybridizes with our array, but we did find that using only 25 PCR cycles eliminated this background hybridization.

To test the reproducibility of our STM screening procedure, several mutant pools were run through independent replicate sediment microcosms. Target was labeled from 300 colonies collected from each independent microcosm, and hybridizations on separate slides were performed. In all cases, hybridizations identified the same potentially impaired sediment mutants, and the same survivors appeared among all replicates (data not shown). On account of this and the fact that we performed a confirmation step for

each potential nonsurvivor to ensure that we had correctly identified mutants impaired in sediment survival, we hybridized DNA from a single microcosm for each of the 96 mutant pools of each organism.

A total of 96 mutant pools (of both G20 and MR-1), containing 60 uniquely tagged mutants in each pool, were grown as described in Materials and Methods, washed, and inoculated into sulfidogenic subsurface sediment microcosms [amended with Fe(III) and lactate for MR-1]. Potential nonsurviving mutants, defined as producing essentially no signal (below 3 times the background level) when hybridized slides were analyzed (a sample input versus output pool hybridization is shown in Fig. 5), were confirmed by subsequent competition experiments. In general, cell numbers for truly impaired MR-1 mutants were 20 to 30% of those for the parent strain when both were recovered after 5 days of incubation in competition sediment microcosms (data not shown). For G20, cell numbers of impaired mutants decreased to 0 to 9% of the initial inoculum. As a comparison, G20 mutants that survived in sediment had individual recoveries above 500% of the inoculum concentration. Of 208 potential sediment-impaired mutants for G20 identified during the first screening, 117 were confirmed by independent reinoculation of each into sediment. Of 86 potential sediment-impaired mutants for MR-1, 56 were confirmed by competition experiments, but 8 of these were also impaired in Fe(III)-citrate growth.

Validation of the methods described herein. In order to validate our method, we present chemotaxis genes that our STM study identified in both G20 and MR-1. For MR-1, the interrupted gene SO2323 had a CI in sediment of 0.1 ± 0.02, confirming its impaired status in sediment. The CI for Fe(III)-citrate growth was not determined for this

Figure 5. Hybridization results from one mutant pool, comparing (a) input pool hybridization with (b) output pool hybridization following sediment incubation. Circles have been placed around those tags present in the input pool and absent from the output pool. The 60 tags are positioned in four rows and eight columns, and all 60 tags are spotted in duplicate. For the slide shown, 10 tags did not fluoresce in both the input and output pools. As a result of being absent from the input pool, these 10 were not considered impaired mutants in this mutant pool.

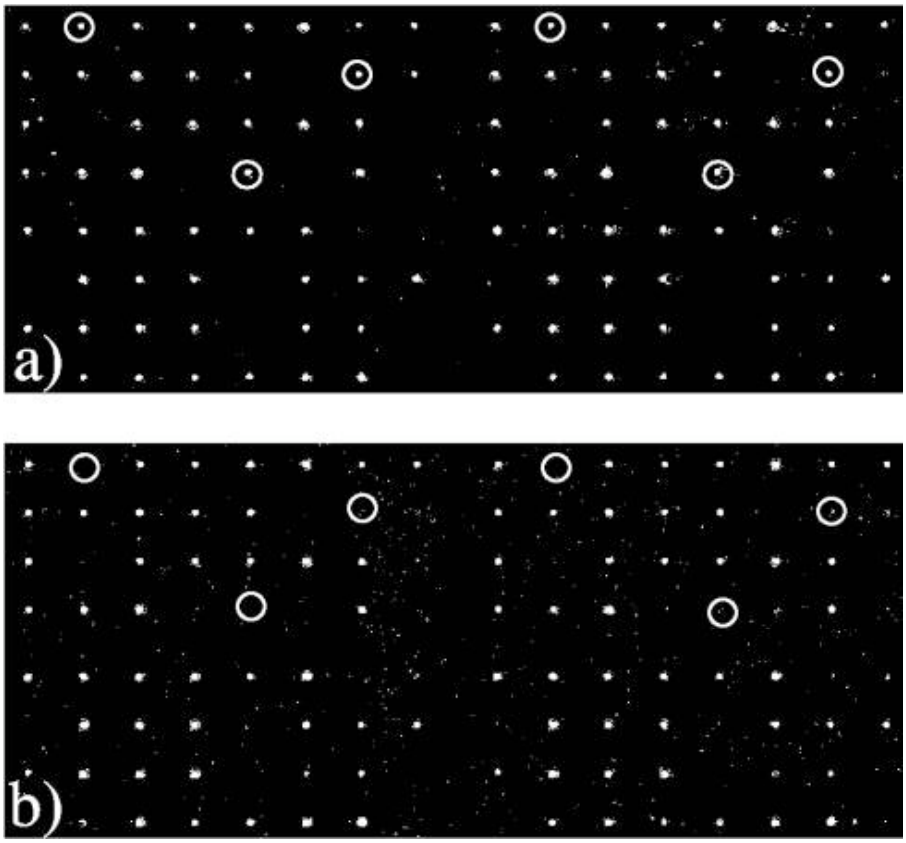

mutant, as its growth in this medium appeared similar to growth observed for the parent strain prior to inoculation of these strains together in sediment competition experiments. SO2323 encodes a putative methyl-accepting chemotaxis protein (MCP) and starts a multicistronic operon of five genes putatively involved in chemotaxis functions. Similar genes may also be present in other environmental bacteria, as evidenced by protein sequence similarities across entire putative MCPs present in *Magnetococcus* sp. strain MC-1 and *D. vulgaris* Hildenborough (37 and 32% identity, respectively), while similarity to other bacterial proteins is restricted to the conserved C-terminal half of the protein.

A G20 transposon mutant with a similar gene (VIMMS392990) interrupted was recovered at 4% of the original inoculum concentration when inoculated back into sediment microcosms on its own. This gene is a monocistronic operon. Best similarity to other environmental organisms exists with sequences for MCPs in the NCBI protein database for *D. vulgaris* (designated DcrH) and *Geobacter sulfurreducens* PCA (41 and 44% similarity, respectively), as well as 42% similarity to one protein of *Geobacter metallireducens*. Similarity to protein sequences from these *δ-Proteobacteria* occurs mainly within the C-terminal region of the protein. Interestingly, this protein is orthologous to an MCP of *Vibrio cholerae* and *Shewanella oneidensis* MR-1 across the entire protein, but with a lower degree of homology. The vast number of genes identified in both organisms cannot be discussed thoroughly in this paper, which focuses on development of a novel STM method for environmental bacteria. We will present our genes, confirmation of the genes (through competition experiments or inoculation of individual mutants back into sediment), and discussions of their potential function in

sediment survival in future papers for each organism.

Discussion

This paper is the first report on the use of the STM method with environmental microorganisms. Before we could successfully apply STM to detect genes essential for survival of G20 and MR-1 in their specific niches, we had to satisfy three key requirements of STM: a mutagenesis procedure that provides efficient and random transposition, a model to represent in-situ conditions, and a system to screen for transposon mutants impaired in in-situ survival. We tried several available transposon systems, including vectors previously described as suitable for transposon mutagenesis in *D. desulfuricans* G20 (54), but found that of all vectors we tested, only the mini-Tn*10* transposon system provided both efficient and random transposition for generation of mutant libraries in both *Desulfovibrio* strain G20 and *Shewanella oneidensis* MR-1 (5,760 mutants each). While this number of mutants did not constitute a saturating screen of either organism's genome (G20 has 3,862 open reading frames [http://img.jgi.doe.gov/pub/main.cgi?page taxonDetail&taxon_oid400040000], and MR-1 had 4,758 open reading frames when the sequence was published (17)), we expected 5,760 mutants to reveal many genes necessary for sediment survival. In former STM studies, many genes required for survival were identified, whereas fewer mutants had been screened for bacteria with genome sizes comparable to those of MR-1 and G20 (34).

Just as optimization of the animal host model was important for studying pathogens by STM (reviewed in reference (8)), a model sediment system for our environmental microbes had to be optimized, considering parameters such as pool complexity, inoculum

concentration, time course for incubations, and recovery of surviving mutants. The simultaneous use of 60 tagged mutants in our study, a number falling between the 48 (7) and 96 (35) tagged mutants used in pathogenic studies with reusable tags, did not present a pool complexity problem, a condition described in reference (8) in relation to STM pathogen studies. By repeating incubation and hybridization of several pools early into development of our method, we found that the same mutants were consistently identified as impaired. An inoculum size similar to that used in prior STM studies (19, 35) was found to be suitable for our study. The time point at which each organism's mutant pool was extracted was determined from preliminary sediment incubations and occurred following growth of cells, a condition necessary in pathogen STM studies to select virulent strains from avirulent strains (8).

The optimized procedure that we have developed samples fewer colonies from sediment than prior STM studies have used for the host (19, 35). Screening this smaller number ensured that we would not miss potentially impaired mutants, but we had to contend with more false negatives (mutants exhibiting no hybridization signal in the output pool that were subsequently shown to survive in confirmation experiments). The purpose of the secondary screen (competition experiments or inoculation of individual mutants back into sediment) was to identify those mutants that were truly attenuated in sediment survival. Competition experiments with MR-1 showed that impaired mutant cell numbers at 5 days were 20 to 30% of cell numbers for the parent strain. Since 300 colonies would give each tag the chance of being represented five times (if all 60 tagged mutants grew equally and had the same chance of being picked for the 300-colony pool), collection of more colonies could have masked these mutants.

To help reduce the frequency of false negatives and confirmation experiments, at least duplicate replications of microcosms and microarrays would need to be incorporated into the experimental design. Replicates may also alleviate some problems associated with inherent factors of the STM protocol (e.g., soil heterogeneity and technical issues with PCR and microarrays) that may influence whether or not mutant tags are observed.

Despite the breakthrough made by the original STM method in identification of virulence-related genes in pathogenesis studies, the use of standard dot blotting techniques for pool analysis does not allow for efficient screening of mutants (19). In this respect, the technique was subsequently improved with a PCR-based STM (28). This system uses 12 tags designed and synthesized for specific and optimal PCR detection. Using this method, 12 libraries (one for each unique tag) are obtained, and single mutants from each library are picked to form pools comprised of 12 different mutants. The screening process consists of a separate PCR for each of the 12 tags. Agarose gels obviate the need for hybridizations by showing whether a PCR product is amplified with each tag as a primer paired with a universal primer within the kanamycin resistance gene of the transposon (28). Recently more tags have been designed for use in this PCR-based STM (43), increasing the number of mutants that can be screened at once to 72. This involves the use of additional tags as well as three different miniTn5 vectors. Groups of mutants are screened in a similar manner as when there were only 12 tags, but by using multiplex PCR. The disadvantage of this system is that more than one mutagenesis vector may not be available for organisms in which genetic systems are not fully developed (as with many environmentally relevant bacteria). The alternative is to increase the number of PCRs, increasing the cost and the labor involved. For the

procedure described in this paper, the addition of more tag sequences to one vector used to create mutant pools achieves the same result as using multiple vectors to increase the number of uniquely tagged mutants.

A separate method that aimed at more efficient screening of mutants applied high-density oligonucleotide array technology, as developed by Affymetrix (30), to screen double-tagged transposon mutants (22). This technology involves synthesis of oligonucleotides directly on the array by using a combination of photolithography and oligonucleotide chemistry, while the method described here utilizes mechanical microspotting (for a more detailed comparison, see reference (46)). At present, the advantage of our approach is affordability, because STM requires the screening of a large number of mutant pools, dependent on the number of unique tags employed, by individual hybridizations. Furthermore, our method uses only one array per pool, as each slide is spotted with the set of 60 probes on both ends, allowing simultaneous analysis of input and output pools. While the photolithographic approach may provide quantitative fitness data (48, 56), our approach satisfies the original intent of STM and currently does so at lower costs. For STM, quantitative data relevant to survival can also be assessed through studies of each individual impaired mutant that was identified by the screening process, rather than in the screen itself.

A final advantage of our method is that there is no need to digest and purify the 18-bp conserved arms from the labeled tag targets prior to hybridization, because only the 40-bp variable region is immobilized on the array as the probe. The early STM studies required an additional step to remove the invariable arms from the labeled probes ("target" in microarray terminology) prior to blot hybridization with colonies or plasmids

containing the tagged transposons (19, 35).

Sequencing of interrupted genes in confirmed mutants from each organism identified MCPs as critical for sediment survival of both G20 and MR-1. While sequence similarity to these chemotaxis proteins exists with other proteins within MR-1 and G20, this similarity is confined mainly to C-terminal regions that are conserved across diverse MCPs and not to the variable N-terminal region comprising the periplasmic domain that is involved in recognition of specific attractants and repellants (51). Finding these genes validates our screen in that we expect chemotaxis response proteins to be necessary for bacteria to react to attractants and repellents encountered in their environment in order to compete with surrounding microorganisms. An earlier study has shown that a chemotactic strain of *Pseudomonas fluorescens* survived significantly better in sediment than a nonmotile strain, while the strains had equivalent growth rates in liquid media (23).

At this time we do not know the specific environmental stimuli for the chemotaxis proteins in our survival studies, but both *Desulfovibrio* and *Shewanella* have demonstrated chemotaxis in previous studies. MR-1 displayed chemotaxis to certain electron acceptors, while there was no tactic response to ferric citrate and Mn(IV) oxide (39). In addition, besides a weak response for formate, MR-1 did not display a tactic response to other carbon sources tested (39). Another study on chemotaxis in *Geobacter metallireducens* reported that MR-1 is not motile when grown with Fe(III) oxide in motility plate assays (9). *D. vulgaris* has shown a chemotactic response to oxygen concentration or redox potential of the environment, and chemotaxis may help the cells find an optimal anaerobic environment (12).

In summary, adapting microarray technology to STM enabled us to mass produce microarray slides spotted with our tags as probes and to downsize the equipment necessary for carrying out hybridizations. We created tagged vectors which we demonstrated were suitable for mutagenizing environmentally significant members of the *δ*- and *γ*-*Proteobacteria*. This system may be applicable to a variety of environmental bacteria, creating many possibilities for future research areas regarding in situ activities of these bacteria, as in bioremediation and geomicrobiological processes.

References

1. **Akerley, B. J., E. J. Rubin, A. Camilli, D. J. Lampe, H. M. Robertson, and J. J. Mekalanos.** 1998. Systematic identification of essential genes by in vitro mariner mutagenesis. Proc. Natl. Acad. Sci. USA **95:**8927-32.
2. **Alexeyev, M. F., and I. N. Shokolenko.** 1995. Mini-Tn*10* transposon derivatives for insertion mutagenesis and gene delivery into the chromosome of Gram-negative bacteria. Gene **160:**59-62.
3. **Ausubel, F. M., R. Brent, R. E. Kingston, D. D. Moore, J. G. Seidman, J. A. Smith, and K. Struhl.** 1987. Current protocols in molecular biology. Green Publishing Associates, New York.
4. **Beeman, R. E., and J. M. Suflita.** 1990. Environmental factors influencing methanogenesis in a shallow anoxic aquifer: a field and laboratory study. J. Ind. Microbiol. **5:**45-58.
5. **Beeman, R. E., and J. M. Suflita.** 1987. Microbial ecology of a shallow unconfined ground water aquifer polluted by municipal landfill leachate. Microb. Ecol. **14:**39-54.
6. **Cannac, V., M. S. Caffrey, G. Voordouw, and M. A. Cusanovich.** 1991. Expression of the gene encoding cytochrome c3 from the sulfate-reducing bacterium *Desulfovibrio vulgaris* in the purple photosynthetic bacterium *Rhodobacter sphaeroides*. Arch. Biochem. Biophys. **286:**629-32.
7. **Chiang, S. L., and J. J. Mekalanos.** 1998. Use of signature-tagged transposon mutagenesis to identify *Vibrio cholerae* genes critical for colonization. Mol. Microbiol. **27:**797-805.

8. **Chiang, S. L., J. J. Mekalanos, and D. W. Holden.** 1999. In vivo genetic analysis of bacterial virulence. Annu. Rev. Microbiol. **53:**129-154.

9. **Childers, S. E., S. Ciufo, and D. R. Lovley.** 2002. *Geobacter metallireducens* accesses insoluble Fe(iii) oxide by chemotaxis. Nature **416:**767-769.

10. **Dennis, J. J., and G. J. Zylstra.** 1998. Plasposons: modular self-cloning minitransposon derivatives for rapid genetic analysis of gram-negative bacterial genomes. Appl. Environ. Microbiol. **64:**2710-5.

11. **Dyson, P. J.** 1999. Isolation and development of transposons. Methods Microbiol. **29:**133-167.

12. **Fu, R., J. D. Wall, and G. Voordouw.** 1994. DcrA, a c-type heme-containing methyl-accepting protein from *Desulfovibrio vulgaris* Hildenborough, senses the oxygen concentration or redox potential of the environment. J. Bacteriol. **176:**344-50.

13. **Ganesh, R., K. G. Robinson, G. D. Reed, and G. S. Sayler.** 1997. Reduction of hexavalent uranium from organic complexes by sulfate- and iron-reducing bacteria. Appl. Environ. Microbiol. **63:**4385-4391.

14. **Handfield, M., and R. C. Levesque.** 1999. Strategies for isolation of in vivo expressed genes from bacteria. FEMS Microbiol. Rev. **23:**69-91.

15. **Hansen, T. A.** 1994. Metabolism of sulfate-reducing prokaryotes. Antonie Leeuwenhoek **66:**165-85.

16. **Hayes, F.** 2003. Transposon-based strategies for microbial functional genomics and proteomics. Annu. Rev. Genet. **37:**3-29.

17. **Heidelberg, J. F., I. T. Paulsen, K. E. Nelson, E. J. Gaidos, W. C. Nelson, T. D. Read, J. A. Eisen, R. Seshadri, N. Ward, B. Methe, R. A. Clayton, T. Meyer, A. Tsapin, J. Scott, M. Beanan, L. Brinkac, S. Daugherty, R. T. DeBoy, R. J. Dodson, A. S. Durkin, D. H. Haft, J. F. Kolonay, R. Madupu, J. D. Peterson, L. A. Umayam, O. White, A. M. Wolf, J. Vamathevan, J. Weidman, M. Impraim, K. Lee, K. Berry, C. Lee, J. Mueller, H. Khouri, J. Gill, T. R. Utterback, L. A. McDonald, T. V. Feldblyum, H. O. Smith, J. C. Venter, K. H. Nealson, and C. M. Fraser.** 2002. Genome sequence of the dissimilatory metal ion-reducing bacterium *Shewanella oneidensis*. Nat. Biotechnol. **20:**1118-1123.

18. **Hendrixson, D. R., and V. J. DiRita.** 2004. Identification of *Campylobacter jejuni* genes involved in commensal colonization of the chick gastrointestinal tract. Mol. Microbiol. **52:**471-484.

19. **Hensel, M., J. E. Shea, C. Gleeson, M. D. Jones, E. Dalton, and D. W. Holden.** 1995. Simultaneous identification of bacterial virulence genes by negative selection. Science **269:**400-3.

20. **Herz, K., S. Vimont, E. Padan, and P. Berche.** 2003. Roles of NhaA, NhaB, and NhaD Na+/H+ antiporters in survival of *Vibrio cholerae* in a saline environment. J. Bacteriol. **185:**1236-1244.

21. **Heungens, K., C. E. Cowles, and H. Goodrich-Blair.** 2002. Identification of *Xenorhabdus nematophila* genes required for mutualistic colonization of *Steinernema carpocapsae* nematodes. Mol. Microbiol. **45:**1337-1353.

22. **Karlyshev, A. V., P. C. F. Oyston, K. Williams, G. C. Clark, R. W. Titball, E. A. Winzeler, and B. W. Wren.** 2001. Application of high-density array-based signature-tagged mutagenesis to discover novel *Yersinia* virulence-associated genes. Infect. Immun. **69:**7810-7819.

23. **Kennedy, M. J., and J. G. Lawless.** 1985. Role of chemotaxis in the ecology of denitrifiers. Appl. Environ. Microbiol. **49:**109-14.

24. **Kim, C. H., D. R. Helinski, and G. Ditta.** 1986. Overlapping transcription of the *nif*A regulatory gene in *Rhizobium meliloti*. Gene **50:**141-8.

25. **Kleckner, N., J. Bender, and S. Gottesman.** 1991. Uses of transposons with emphasis on Tn*10*. Methods Enzymol. **204:**139-80.

26. **Lehoux, D. E., and R. C. Levesque.** 2000. Detection of genes essential in specific niches by signature-tagged mutagenesis. Curr. Opin. Biotechnol. **11:**434-439.

27. **Lehoux, D. E., F. Sanschagrin, I. Kukavica-Ibrulj, E. Potvin, and R. C. Levesque.** 2004. Identification of novel pathogenicity genes by PCR signature-tagged mutagenesis and related technologies, p. 289-304. *In* N. Woodford and A. P. Johnson (ed.), Genomics, Proteomics, and Clinical Bacteriology, vol. 266. Humana Press, Totowa.

28. **Lehoux, D. E., F. Sanschagrin, and R. C. Levesque.** 1999. Defined oligonucleotide tag pools and PCR screening in signature-tagged mutagenesis of essential genes from bacteria. Biotechniques **26:**473-480.

29. **Lloyd, J. R., J. Chesnes, S. Glasauer, D. J. Bunker, F. R. Livens, and D. R. Lovley.** 2002. Reduction of actinides and fission products by Fe(III)-reducing bacteria. Geomicrobiol. J. **19:**103-120.

30. **Lockhart, D. J., H. Dong, M. C. Byrne, M. T. Follettie, M. V. Gallo, M. S. Chee, M. Mittmann, C. Wang, M. Kobayashi, H. Horton, and E. L. Brown.** 1996. Expression monitoring by hybridization to high-density oligonucleotide arrays. Nat. Biotechnol. **14:**1675-1680.

31. **Lovley, D. R., D. E. Holmes, and K. P. Nevin.** 2004. Dissimilatory Fe(III) and Mn(IV) reduction. Adv. Microb. Physiol. **49:**219-86.

32. **Lovley, D. R., and E. J. P. Phillips.** 1986. Availability of trivalent iron for microbial reduction in bottom sediments of the freshwater tidal Potomac River. Appl. Environ. Microbiol. **52:**751-7.

33. **Lovley, D. R., and E. J. P. Phillips.** 1986. Organic matter mineralization with reduction of ferric iron in anaerobic sediments. Appl. Environ. Microbiol. **51:**683-9.

34. **Mecsas, J.** 2002. Use of signature-tagged mutagenesis in pathogenesis studies. Curr. Opin. Microbiol. **5:**33-37.

35. **Mei, J.-M., F. Nourbakhsh, C. W. Ford, and D. W. Holden.** 1997. Identification of *Staphylococcus aureus* virulence genes in a murine model of bacteremia using signature-tagged mutagenesis. Mol. Microbiol. **26:**399-407.

36. **Merrell, D. S., D. L. Hava, and A. Camilli.** 2002. Identification of novel factors involved in colonization and acid tolerance of *Vibrio cholerae*. Mol. Microbiol. **43:**1471-1491.

37. **Myers, C. R., and J. M. Myers.** 1997. Replication of plasmids with the p15A origin in *Shewanella putrefaciens* MR-1. Lett. Appl. Microbiol. **24:**221-225.

38. **Myers, C. R., and K. H. Nealson.** 1988. Bacterial manganese reduction and growth with manganese oxide as the sole electron acceptor. Science **240:**1319-21.

39. **Nealson, K. H., D. P. Moser, and D. A. Saffarini.** 1995. Anaerobic electron acceptor chemotaxis in *Shewanella putrefaciens*. Appl. Environ. Microbiol. **61:**1551-4.

40. **Newman, D. K., and R. Kolter.** 2000. A role for excreted quinones in extracellular electron transfer. Nature **405:**94-97.

41. **O'Toole, G. A., and R. Kolter.** 1998. Initiation of biofilm formation in *Pseudomonas fluorescens* WCS365 proceeds via multiple, convergent signalling pathways: a genetic analysis. Mol. Microbiol. **28:**449-61.

42. **Postgate, J. R.** 1984. The sulfate reducing bacteria, 2nd ed. Cambridge University Press, Cambridge.

43. **Potvin, E., D. E. Lehoux, I. Kukavica-Ibrulj, K. L. Richard, F. Sanschagrin, G. W. Lau, and R. C. Levesque.** 2003. In vivo functional genomics of *Pseudomonas aeruginosa* for high-throughput screening of new virulence factors and antibacterial targets. Environ. Microbiol. **5:**1294-1308.

44. **Rapp, B. J., and J. D. Wall.** 1987. Genetic transfer in *Desulfovibrio desulfuricans*. Proc. Natl. Acad. Sci. USA **84:**9128-30.

45. **Rubin, E. J., B. J. Akerley, V. N. Novik, D. J. Lampe, R. N. Husson, and J. J. Mekalanos.** 1999. In vivo transposition of mariner-based elements in enteric bacteria and mycobacteria. Proc. Natl. Acad. Sci. USA **96:**1645-50.

46. **Schena, M., R. A. Heller, T. P. Theriault, K. Konrad, E. Lachenmeier, and R. W. Davis.** 1998. Microarrays: biotechnology's discovery platform for functional genomics. Trends Biotechnol. **16:**301-306.

47. **Shalon, D., S. J. Smith, and P. O. Brown.** 1996. A DNA microarray system for analyzing complex DNA samples using two-color fluorescent probe hybridization. Genome Res. **6:**639-45.

48. **Shoemaker, D. D., D. A. Lashkari, D. Morris, M. Mittmann, and R. W. Davis.** 1996. Quantitative phenotypic analysis of yeast deletion mutants using a highly parallel molecular bar-coding strategy. Nat. Genet. **14:**450-456.

49. **Smidt, H., J. Van der Oost, and W. M. De Vos.** 2001. Development of a gene cloning and inactivation system for halorespiring *Desulfitobacterium dehalogenans*. Appl. Environ. Microbiol. **67:**591-597.

50. **Steger, J. L., C. Vincent, J. D. Ballard, and L. R. Krumholz.** 2002. *Desulfovibrio* sp. genes involved in the metabolism of hydrogen and lactate. Appl. Environ. Microbiol. **68:**1932-1937.

51. **Stewart, R. C., and F. W. Dahlquist.** 1987. Molecular components of bacterial chemotaxis. Chem. Rev. **87:**997-1025.

52. **Voordouw, G., and S. Brenner.** 1986. Cloning and sequencing of the gene encoding cytochrome c3 from *Desulfovibrio vulgaris* (Hildenborough). European J. Biochem. **159:**347-51.

53. **Wall, J. D., C. L. Hemme, B. Rapp-Giles, J. A. Ringbauer, L. Casalot, and T. Giblin.** 2003. Genes and genetic manipulations of *Desulfovibrio*, p. 85-98. *In* M.

W. Adams, J. G. Ferry, L. L. Barton, M. K. Johnson, and L. G. Ljungdahl (ed.), Biochemistry and Physiology of Anaerobic Bacteria. Springer, New York.

54. **Wall, J. D., T. Murnan, J. Argyle, R. S. English, and B. J. Rapp-Giles.** 1996. Transposon mutagenesis in *Desulfovibrio desulfuricans*: development of a random mutagenesis tool from Tn7. Appl. Environ. Microbiol. **62:**3762-7.

55. **Wall, J. D., B. J. Rapp-Giles, and M. Rousset.** 1993. Characterization of a small plasmid from *Desulfovibrio desulfuricans* and its use for shuttle vector construction. J. Bacteriol. **175:**4121-8.

56. **Winzeler, E. A., D. D. Shoemaker, A. Astromoff, H. Liang, K. Anderson, B. Andre, R. Bangham, R. Benito, J. D. Boeke, H. Bussey, A. M. Chu, C. Connelly, K. Davis, F. Dietrich, S. W. Dow, M. El Bakkoury, F. Foury, S. H. Friend, E. Gentalen, G. Giaever, J. H. Hegemann, T. Jones, M. Laub, H. Liao, N. Liebundguth, D. J. Lockhart, A. Lucau-Danila, M. Lussier, N. M'Rabet, P. Menard, M. Mittmann, C. Pai, C. Rebischung, J. L. Revuelta, L. Riles, C. J. Roberts, P. Ross-MacDonald, B. Scherens, M. Snyder, S. Sookhai-Mahadeo, R. K. Storms, S. Veronneau, M. Voet, G. Volckaert, T. R. Ward, R. Wysocki, G. S. Yen, K. Yu, K. Zimmermann, P. Philippsen, M. Johnston, and R. W. Davis.** 1999. Functional characterization of the *S. cerevisiae* genome by gene deletion and parallel analysis. Science **285:**901-906.

57. **Wolk, C. P., Y. Cai, and J. M. Panoff.** 1991. Use of a transposon with luciferase as a reporter to identify environmentally responsive genes in a cyanobacterium. Proc. Natl. Acad. Sci. USA **88:**5355-5359.

Supplementary Table 1. Sequences for 40 nt unique region of each tag.

Tag name	Sequence (5' to 3')
A1	ATGTCGTTCGATTGCGAGCTTTCGTGAGCTATATCGCTAG
A2	TGCTATAGCTATTGCGCGTTCGTTGGGTCGTGGCTGAGAG
A3	TTAGCTGGTGAGAGATCTAGACTAGTTGAGCTGGCTATCG
A4	GGATTTCGGGCTTGCTATGGAGCTATGGCTTGCGTTAGCT
A5	GTAGCTTGCGCTAGCGTTCTGGCTTGCGTGAGTTCTAGTG
A6	GGCTTGCGTTCGAGCTTTGGATCTTGAGCTCTAGTTCTCG
A7	GTGGCTAGTTATCGTTAGCGATCTTGATCGAGTTAGTTGG
A8	GGTGCTATTGGGTTATGTGTCGATTGGGTTGGATGTGTGG
A9	GTCGTTAGCGTGCTTGAGCTGTTGGTTGGTAGATTGTGCG
A10	GGCTGGATTGCTAGTTCGTTAGGTCTAGGTTGCTAGGTCG
A12	GTCTAGCTTTGGCTAGGGTGATCGTTGGTTCGTGATTGAG
B1	GGCTGGAGTGCTTGCTTGATGGCTTGAGTTCGCGTTGGGT
B2	TGCTTGATCGGTTGCTAGCTCTCTGGTTCGGTTCTAGCTG
B4	TGCTCGTTGTCGATTGAGCTGGCTTGCGCGGTCTCGATTT
B7	GTCGATCGTGATGTCTGGTGATCGATTTCGATAGCTAGTG
B8	TGGTCTAGCTCGATCTAGCGTTGTATCGAGCTAGCTAGCG
B9	GTATATCTAGATTGCTCTATCGTGATAGCGATCGCTAGTG
B10	TTAGATCTCTGGCTATCGAGATGGCTAGCTAGTGTGGTTT
B11	GGAGCTTTATCGTGATGTCGTTGGATATGGGTCTGTCGAG
B12	TTCGATGTCTAGTTATCTGGCGTTGGATCTCGAGCTTGCT
C5	AGATAGTTCGCTCTTGATCGGGAGCTAGCTATTTATTTAG
C6	ATCGTGATCGATAGTTGGATCGGTCGCTATTTAGTGCGTT
C7	CTTGAGCTATCTATGGGTCTAGCTCTAGGTCGAGTTCGAT
C8	CGTTAGCGCTCTAGATATCGAGTTTGATAGCTAGATCTCT
C10	TTCTTGAGCTCTAGATAGATGTAGCTATGGATCTAGCTCT
C12	CTAGCGATAGGTAGGTCTTTAGATCGGTCTATCGTGCGCT
D2	ATTGCTTTAGCGGTGTATTTCGAGTTCTAGCGTGCTATAG
D3	AGAGATATCGTTAGCGATCTAGCTAGCTCGATCGGTATCG
D4	CTAGATCGTTCGTTAGGTCGTGCTATGGCTATCGTGCTAT
D5	ATTGCTTGAGCTAGAGCTATCGCTATAGCTAGCTATAGCG
D6	CTGTAGGCGGTTATCGATCGCTCGGTAGGTATCGCTTGAT
D7	TTCGTTCTATTGGGATCGTGCTCGCTTTAGCGAGCTAGCT
D8	TTCGATCTAGGGAGTTCGTTAGCGATGTCGATCTAGCGGT
D10	CTTGATTGAGCTCTGTAGCTAGCTCGATCTGTCTAGTGCT
D11	ATCTGTAGCTTTAGCGATCTATCGCTCTAGCGATATGTGT
D12	CGATCTGTCGGTCTAGATCGTTCGATCTAGCGGTCTATCG
E1	CTCTATCGTTGGCGCTATCTAGCGTTCTATCGTTCTATCG
E2	CGGTCTATCGATAGTTATCTCGCTAGGGTTCTAGCGTTAG
E10	GTCGTTAGTTAGGTCGCTGGCGATATCGCGTTCGCTTGCT
E11	TTATCGTTAGGTATCGTTCTAGATATCGGTAGGTATAGCG
E12	AGCTCGTTCGGTAGCGATCGATAGTTCTCGAGTTAGCGAT
F2	CTTTGTGGATCGGGTGGGTTGTCTATTTGTATGTCTATAT
G1	CGCTCGCGGGAGATATCGATAGCGGGATATAGAGCGGGTT

G2	ATTTCTTTGTTTGGGGAGGGTGGGTTGGATAGGGATTGGT
G4	GTTTGTTTCGGGCGGGCTTTATATATGGCGCGCGTTATAG
G5	CGCTTTCTTTAGGGAGGGCGCGCGCTATTTATTTAGAGAG
G6	AGATATATTTAGCGCGCGGGTTTTCGCGCTCTTTATATAG
G7	TGTGTGTTGGAGGGCTTTCTATAGAGCGATAGCTAGAGCT
G8	GGTTGGTTATATATATCTTTATTTCGCGCGGGATTTGGTT
G9	TTTTGGGGAGAGATATCTATCTCTCTTTGGTTGGTTAGAG
G10	GGTTGGTTGTGTATATAGGGATTTCGCGCGGGTTATATCG
G11	TTTGATATCGCGCGATTTCTTTGGTTGGTTAGAGAGATAT
G12	GGGTGGTTATATTTCGTTGGTTAGAGAGGGTTTTAGAGAT
H4	GTTGGTTGAGAGAGATCTCTCTGGTTATTTATTTGTGTTG
H5	ATTTGTTTCTTTCTCTCTATATAGAGAGATTTCTCTGTGT
H6	TTGGTTGGATATGTCGGGCGGGCTCTCTATTTGGGGTTGG
H7	TTGGAGAGATATTTTGGGTTCTTTCTGTTGTGATAGAGAG
H8	GGGGAGGGCGGGTGGGCGGGGGGGTTTTATATGGCGCTCT
H9	CGCTCGCTCGCTATATAGAGAGGGATTTCGCGGGCGATAG
H10	GTGTGGCGCGCTTTATCTATCTAGAGATATATTTGTTTCT

Chapter 3

Identification of Genes that Confer Sediment Fitness to *Desulfovibrio desulfuricans* G20

Abstract

We used *Desulfovibrio desulfuricans* G20 as a model environmental microorganism to identify genes required for fitness in aquifer sediments. A library of 5760 signature-tagged-mutants was screened and 97 genes representing 108 mutants were identified to be crucial for sediment fitness. The fitness genes belong to a variety of functional categories including signal transduction, binding and transport, membrane biosynthesis, central metabolism, and insertion elements. The majority of the genes have orthologs in other sequenced δ-*Proteobacteria*, suggesting a general role for these genes during growth in aquifer sediments. The sediment fitness mutants were shown to grow similarly to parent strains in lactate-sulfate medium. Several mutants were characterized to determine whether the predicted function of the identified gene was lost in those mutants. This includes mutations in genes encoding proteins involved in amino acid biosynthesis, hydrogenase activity and the SOS response. These results provide direct evidence that the abilities to synthesize certain amino acids, to grow with H_2 and to respond to DNA damage are sediment fitness characteristics for *Desulfovibrio*. This study also sheds light on our understanding of how environmental microorganisms adapt to their niches at the genetic level.

Introduction

Sulfate-reducing bacteria play important roles in a variety of anaerobic environments and have the potential to be used for bioremediation of metals and hydrocarbons (31, 47, 49). The vast majority of past studies have focused on growth in laboratory media. Yet with our current knowledge of the importance of changes in gene expression in response to environmental factors (21) and recent developments demonstrating the utility of in-situ microbial studies (25, 41), the limitations of studying microbial processes in the laboratory have become evident. Sediments provide unique habitats for microorganisms (19) and environmental bacteria must therefore contend with nutrient limitation, competition, different osmotic pressures, changes in the redox potential, and other factors. Bacteria growing in sediments likely possess characteristics distinct from those grown in laboratory, pure culture conditions (4). Sediment growth has been shown to occur in discrete steps: surface attachment and multiplication, microcolony formation, and differentiation during growth (17). The differences between sediment growth and laboratory batch culture have led to the hypothesis that some physiological functions are only displayed during exposure to the natural environment.

There have been limited efforts to prove that cellular functions observed in the laboratory are important for microorganisms growing in the natural environment. In order to address these issues, a modified signature-tagged mutagenesis (STM) technique was adopted and *Desulfovibrio desulfuricans* G20 and *Shewanella oneidensis* MR-1 were used as model environmental bacteria for studying functions for *in situ* growth (15). *S. oneidensis* MR-1 belongs to *γ-Proteobacteria* and is a facultative iron-reducing bacterium, while *D. desulfuricans* G20 belongs to *δ-Proteobacteria* and is a strictly anaerobic sulfate-reducing bacterium. Using *S. oneidensis* MR-1 as a model organism,

47 genes were identified that enhanced sediment fitness and further demonstrated that antibiotic efflux was a required process for bacteria in sediment (16). In this study, we describe the identification of *D. desulfuricans* G20 genes apparently necessary for fitness in aquifer sediments and further characterized several of them.

Materials and Methods

Strains and Media. *Desulfovibrio desulfuricans* G20 was grown in lactate-sulfate (LS) medium prepared as described by Rapp and Wall (42), using N_2 headspace and vitamin and metal solutions as described elsewhere (5, 50). The medium contained 50 mM sodium sulfate, 66 mM sodium lactate, 0.1% yeast extract, vitamins and minerals. Prior to autoclaving, the pH was adjusted to 7.2, and after autoclaving, 8 mM bicarbonate and 2mM cysteine were added from anaerobic stock solutions. For growth of G20 on solid media, LS agar medium (1.5% agar) was prepared as described by Groh, et al. (15). H_2 (contained within the anaerobic chamber) was used as reducing agent and 0.005% $PdCl_2$ was used as a catalyst for reduction of the agar plates.

A mineral medium, prepared as described by Castaneda-Carrion (5) with a few modifications, was also used. The mineral medium contained 10 mM sodium sulfate, 25 mM sodium lactate, 0.05% yeast extract, vitamins and minerals. Mixed gas (N_2:CO_2=4:1) was used for the headspace. Prior to autoclaving, the pH was adjusted to 7.2, and after autoclaving, 8 mM bicarbonate and 1.6 mM of Na_2S were added from anaerobic stock solutions. For experiments testing H_2 as electron donor, sodium lactate was omitted, and 10 mM of sodium acetate and 10 ml of H_2 was added to the cultures. For experiments testing the yeast extract requirement of mutants, the yeast extract

concentration was modified. A strain of $G20_{sediment}$ (15), which had been adapted to sediment conditions, was used as a parent strain for construction of our tagged-transposon mutant library. Details on the generation of a mutant library was described in a previous study (15). For growing transposon mutants, 175 μg/ml kanamycin was added to the agar plates and 1050 μg/ml kanamycin was added to the liquid medium.

Identification of sediment fitness mutants. A total of 5760 signature-tagged Tn*10* transposon mutants were collected, grown in lactate-sulfate (LS) liquid medium and assembled into 96 pools, each containing 60 differently tagged mutants. Pools were then washed and about 10^5 cells were inoculated into 25-ml serum bottles containing 2 g of untreated (not sterile) sediment from the aquifer underlying the Norman, Oklahoma landfill. Landfill sediments were collected at a depth of approximately 2 m within the anoxic zone using a hand auger as previously described (45). Sediments were collected into sterile jars and transported to the lab where they were flushed with N_2 and refrigerated prior to use. Screening experiments were performed as previously described (15). Mutants unable to grow in sediment or unable to compete with native microorganisms were originally selected based on the fact that the oligonucleotide tag within the chromosome of the mutant was not recovered from sediments after the 8-day incubation period. A microarray-based hybridization was used to quantify tag recovery. Putative fitness mutants were rescreened in sediment microcosms individually to confirm their inability to survive. The recovery rate from sediment was defined as the recovered cell number from sediment after the incubation relative to the initial cell number (both determined by plating cells on lactate sulfate medium) (15). Southern hybridization was carried out on 42 randomly selected mutants and it was shown that the transposon had

inserted randomly and in a single location within the genome (data not shown).

Identification of interrupted genes. In order to identify genes interrupted by insertion of the transposon within the genome, the transposon insertion sites were amplified using a random/specific primer set followed by a second round of PCR, as described previously (15). Genomic DNA from the G20 wild-type strain served as negative control in all reactions. The PCR products were purified and DNA sequencing was performed at the Oklahoma Medical Research Foundation (Oklahoma City, OK). Sequence similarity searches were carried out using the NCBI database (http://www.ncbi.nlm.nih.gov/sutils/genom_table.cgi) and by employing the BLASTN and BLASTP algorithms (1). All DNA sequences were also compared with genome sequences in the Virtual Institute for Microbial Stress and Survival database (http://www.microbesonline.org/).

Growth curve determination. All sediment fitness mutants were collected from original libraries and assembled into two (1-ml/well) 96-well plates (Beckman Instruments, Inc., #BK267007). For storage, all mutants were frozen at –80 °C in LS medium containing 25% glycerol (v/v). Overnight cultures (0.1 ml) were used to inoculate serum tubes containing LS medium. Their growth was monitored during incubations at 37 °C by measuring optical density at 600 nm (OD_{600}). Duplicate tubes for each mutant were used and strain $G20_{sediment}$ was used as control.

Three mutants [C10(pG11), C10(pB6), and C8(pE11)] with transposon insertions in genes annotated to be involved in energy metabolism (Table 1) were individually cultured in LS medium to test for their abilities to grow with H_2 as an electron donor. Cultures were inoculated into the mineral medium with lactate as electron donor. The

growing culture (OD_{600} about 0.4) was used as inoculum (0.1 ml) for cultures incubated with the addition of H_2 or lactate as electron donor. H_2 containing cultures were shaken and OD_{600} values were recorded. Duplicate tubes were used for each mutant, and strains $G20_{wildtype}$ and $G20_{sediment}$ as controls.

Three mutants [G12(pD6), B12(pE4), and A2(pE11)] with a transposon insertion within genes involved in amino acid biosynthesis (Table 1) were individually cultured in LS medium and 0.1 ml was transferred into mineral medium with lactate as electron donor. Log phase culture (OD_{600} 0.4) was then used as inoculum into mineral media containing 0, 0.05%, 0.01%, and 0.005% yeast extract. Duplicate tubes were used for each mutant, and strain $G20_{sediment}$ was used as control. OD_{600} were recorded.

Determination of survival after UV treatment. Mutants with the transposon inserted in the *umuC* and *ruvB* genes (Table 1) were individually cultured in LS medium to an OD_{600} of 0.5-0.7. Cells (2 ml) were added to 18 ml of LS medium in a Petri dish and then exposed to UV light at 254 nm at the distance of 10 centimeter for 10 seconds, 30 seconds, 1 min, 3 min, and 5 min. After UV exposure, serial dilutions were made into 2-ml 96-well plates (Beckman Instruments, Inc., #BK609681) for 3-well most probable number (MPN) counts. Growth was recorded after two-day incubation at 37 °C.

Results

Identification of genes needed for growth of *D. desulfuricans* G20 in anoxic sediments. *D. desulfuricans* G20 increased in number roughly 5-fold while growing in sediment during the 8-day incubation period (data not shown). Fitness mutants were chosen if cell numbers were less than 10% of the inoculum concentration after the 8-day

Table 1. List of mutants characterized in this study.

Mutant	Locus [d]	Predicted Product	Sediment Recovery (%)	Similarity to (%)		
				D. vu[a]	*G. me*[b]	*G. su*[c]
Energy metabolism						
C10(pG11)	Dde_2134*	Hydrogenase (NiFe) small subunit (HydA)	0.5	77	37	38
C10(pB6)	Dde_3282*	Formate C-acetyltransferase	0.3	35	28	33
C8(pE11)	Dde_0081*	Fe-only hydrogenase	0.3	73	27	28
Amino acid biosynthesis						
G12(pD6)	Dde_1081[L]	Arginine biosynthesis bifunctional protein ArgJ	0.3	65	50	48
B12(pE4)	Dde_3487*	Chorismate mutase/prephenate dehydratase	0	72	43	41
A2(pE11)	Dde_0079	Tryptophan synthase, beta subunit	0.5	81	62	32
DNA replication, recombination and repair						
A8(pF7)	Dde_2322*	Holliday junction DNA helicase RuvB	0.3	84	62	63
B12(pF11)	Dde_2973[L]	DNA-directed DNA polymerase UmuC	0.5	54	26	25

[a] *D. vu* represents *Desulfovibrio vulgaris* Hildenborough.

[b] *G. me* represents *Geobacter metallireducens*.

[c] *G. su* represents *Geobacter sulfurreducens* PCA.

/ represents homologs to *Desulfovibrio desulfuricans* G20 proteins were not found.

[d] * labeled loci are the genes within the operon, [L] labeled loci are the last gene of the operon.

sediment incubation. A total of 108 fitness mutants were identified. An overview of their recovery rates from sediment and their homologs to other *δ-Proteobacteria* whose genomes were sequenced is shown in Table 2.

These mutants represent transposition events into 97 open reading frames (ORFs) whose predicted products fall into a wide variety of functional categories (Table 2). The positions of ORFs with transposon insertions were identified and their locations on the chromosome were not biased, as indicated by the gene locus number. It is noted that these genes were distributed throughout the chromosome and this result is consistent with previous pathogenesis studies for growth and viability *in vivo* (35, 40). Nine genes were identified twice (Dde_2334, Dde_3478, Dde_3635, Dde_2001, Dde_1551, Dde_1682, Dde_0339, Dde_3047, and Dde_0618) and one gene (Dde_3016) was identified three times by different tagged-transposons in different locations within the gene. Bioinformatics analysis indicated that proteins from all the functional category groups [based on clusters of orthologous groups (COG) analysis] were identified, except cell division genes (Figure 1), which are likely to be essential not only for *in situ* growth, but for growth in general. Such mutants would not be present in the library, as they would have been eliminated during the initial selection on LS plates (27, 33).

The mutants have been organized into COG functional categories (Table 2 and Figure 1). In order to better understand the importance of each of these COG in sediment fitness, the relative number of mutants from each COG category is presented as a percent of the total number of fitness mutants (108 mutants) and as a percent of the total number of genes annotated to be within that COG category (Figure 1). Both of these numbers provide us with an indication of the importance of that COG in sediment fitness. Based

Table 2. Attenuated *D. desulfuricans* G20 mutants identified by screening in sulfidogenic sediment.

Mutant	Locus[d]	Predicted Product	Sediment Recovery (%)	Similarity to (%)		
				D. vu[a]	*G. me*[b]	*G. su*[c]
Energy metabolism						
G7(pH10)	Dde_0043*	Iron-sulfur cluster-binding protein	0.3	75	46	52
G9(pC1)	Dde_0044*	Pyruvate flavodoxin/ferredoxin oxidoreductase, thiamine diP-binding domain protein	3.5	77	57	53
G11(pH5)	Dde_0410[L]	Glycerol kinase	0	84	65	63
C10(pG11)	Dde_2134*	Hydrogenase (NiFe) small subunit (HydA)	0.5	77	37	38
A3(pH11)	Dde_2334[L]	Succinyl-CoA synthetase, alpha subunit	0	65	46	49
D5(pB3)	Dde_2334[L]	Succinyl-CoA synthetase, alpha subunit	1.1	65	46	49
C10(pB6)	Dde_3282*	Formate C-acetyltransferase	0.3	35	28	33
A8(pF3)	Dde_3709*	Ferredoxin, 4Fe-4S, putative	7.2	81	24	23
C8(pE11)	Dde_0081*	Fe-only hydrogenase	0.3	73	27	28
Amino acid biosynthesis						
A2(pE11)	Dde_0079	Tryptophan synthase, beta subunit	0.5	81	62	32
G12(pD6)	Dde_1081[L]	Arginine biosynthesis bifunctional protein ArgJ	0.3	65	50	48
C10(pF5)	Dde_3111	L-Serine dehydratase	1.6	42	/	/
A5(pA9)	Dde_3130*	Acetolactate synthase, small subunit	0.3	64	34	33
E2(pG11)	Dde_0104	Glutamine synthetase	0	85	51	49
B12(pE4)	Dde_3487*	Chorismate mutase/prephenate dehydratase	0	72	43	41
C6(pF6)	Dde_3487*	Chorismate mutase/prephenate dehydratase	0	72	43	41
A5(pB6)	Dde_3635[L]	Glutamate synthase (NADPH), homotetrameric	0	75	33	53
A9(pC7)	Dde_3635[L]	Glutamate synthase (NADPH), homotetrameric	0.5	75	33	53
Nucleotide metabolism						
A1(pA10)	Dde_0113*	Ribonucleoside-diphosphate reductase	0.3	79	54	54
A4(pE7)	Dde_3016*	Anaerobic ribonucleoside-triphosphate reductase, putative	0	83	/	/
C12(pB6)	Dde_3016*	Anaerobic ribonucleoside-triphosphate reductase, putative	0	83	/	/
H7(pG4)	Dde_3016*	Anaerobic ribonucleoside-triphosphate reductase, putative	0	83	/	/

Carbohydrate metabolism						
C10(pE3)	Dde_0415[L]	Alpha amylase domain protein	3.5	/	44	/
E1(pF11)	Dde_1178	Glycerone kinase	0.8	86	/	/
H8(pG2)	Dde_1424	Alpha-glucan phosphorylase	1.3	73	49	49
Coenzyme metabolism						
G2(pA11)	Dde_1379	Thiamine-phosphate pyrophosphorylase	0.4	62	45	45
H8(pF5)	Dde_2713[L]	Lipoate-protein ligase B	1.3	69	41	40
H10(pG10)	Dde_3495*	Cobinamide kinase and cobinamide phosphate guanylyltransferase	0.3	30	33	32
Lipid metabolism						
G9(pB10)	Dde_2001	Phospholipid/glycerol acyltransferase	0.3	58	27	28
H4(pD3)	Dde_2001	Phospholipid/glycerol acyltransferase	0	58	27	28
Cell envelope						
A1(pG11)	Dde_0428[L]	Glycosyltransferase-like	0.3	49	/	/
A9(pC4)	Dde_0438*	UDP-N-acetylglucosamine pyrophosphorylase related protein	0	/	/	/
A6(pA2)	Dde_1370*	N-Acetylmuramoyl-L-alanine amidase	5.6	41	38	37
D8(pA12)[S]	Dde_1437*	Carboxyl-terminal protease	0.1	63	46	45
B2(pF1)	Dde_1551	D-Alanyl-D-alanine dipeptidase	3.7	/	/	/
D2(pE11)	Dde_1551	D-Alanyl-D-alanine dipeptidase	0.8	/	/	/
A3(pF6)	Dde_1682	Uncharacterized protein involved in outer membrane biogenesis-like	0	33	/	21
B1(pF7)	Dde_1682	Uncharacterized protein involved in outer membrane biogenesis-like	0.8	33	/	21
H6(pH11)	Dde_3043*	D-Alanine-D-alanine ligase and related ATP-grasp enzymes-like	1.1	/	26	/
B8(pC6)	Dde_3694*	Glucose-1-phosphate cytidylyl-transferase	0	76	27	27
E2(pG5)	Dde_3138*	Membrane protein	0	/	/	/
A4(pH9)	Dde_3102	Membrane protein, putative	0.3	60	/	/
Transport and binding protein						
G5(pB9)	Dde_0495*	Heavy metal translocating P-type ATPase	0.5	45	36	37
E11(pD9)	Dde_3504	Chloride channel family protein	0.3	71	29	30
C10(pG3)	Dde_3725*	Phosphonate uptake transporter	0.3	83	/	/
A9(pG2)	Dde_0208	Conserved hypothetical protein (domain: Na+/H+ antiporter)	1.6	28	/	/
D8(pH9)	Dde_2476	Na+/H+ antiporter family protein	0	63	/	/
E2(pB11)	Dde_0371*	Dipeptide ABC transporter substrate-binding protein	1.0	26	27	26
G2(pG2)	Dde_0396[L]	Amino acid ABC transporter, permease protein, 3-TM region, His/Glu/Gln/Arg/opine	7.2	42	/	39
G9(pB1)	Dde_1386	Amino acid ABC transporter,	4.0	70	/	37

		permease protein, 3-TM region, His/Glu/Gln/Arg/opine				
C7(pE7)	Dde_0339	Outer membrane protein, OMPP1/FadL/TodX family	0.3	54	/	/
G11(pG11)	Dde_0339	Outer membrane protein, OMPP1/FadL/TodX family	0	54	/	/
A3(pE2)	Dde_0132	Permease, putative	9.1	53	22	22
A6(pH4)	Dde_0630*	Sodium:solute symporter family protein	0.3	34	34	32
G9(pB4)	Dde_1335[L]	ABC transporter, permease protein	0	58	28	25
Signal transduction						
H9(pF8)	Dde_0602*	Multi-sensor signal transduction histidine kinase	0	28	38	40
G5(pA9)	Dde_1945	Putative PAS/PAC sensor protein	0.3	29	35	38
D12(pB8)	Dde_3715[L]	Multi-sensor signal transduction histidine kinase	0	69	27	39
C8(pC10)[S]	Dde_1569[L]	Metal dependent phosphohydrolase	0	71	58	52
B12(pG11)	Dde_3047[L]	Serine phosphatase	0.3	31	26	33
B8(pB6)	Dde_3047[L]	Serine phosphatase	0	31	26	33
G9(pD12)	Dde_3096*	Putative PAS/PAC sensor protein	1.5	28	25	25
A4(pG11)	Dde_2734	Methyl-accepting chemotaxis sensory transducer	0	41	28	32
D5(pD2)	Dde_0458	Methyl-accepting chemotaxis sensory transducer	3.7	41	42	44
D12(pC8)	Dde_1755	Methyl-accepting chemotaxis sensory transducer	0.3	35	31	27
B2(pG1)	Dde_3212[L]	CheD, stimulates methylation of MCP proteins	2.9	52	44	47
DNA replication, recombination and repair						
E12(pC12)	Dde_0534	Putative transposase protein	0.5	/	/	/
B4(pB9)	Dde_0618	ISxcd1 transposase	0	50	36	24
G9(pG3)	Dde_0618	ISxcd1 transposase	1.6	50	36	24
D5(pC2)	Dde_3364[L]	ISxcd1 transposase	2.4	50	36	24
A8(pF7)	Dde_2322*	Holliday junction DNA helicase RuvB	0.3	84	62	63
A12(pF10)	Dde_2872	Transposase-like	0.3	/	/	30
B12(pF11)	Dde_2973[L]	DNA-directed DNA polymerase UmuC	0.5	54	26	25
D12(pF8)	Dde_3099	Methylated-DNA--protein-cysteine methyltransferase	0	/	/	/
Ribosomal structure and biogenesis						
C6(pB7)	Dde_0389*	Dihydrouridine synthase family protein	0.3	65	41	41
G9(pH3)	Dde_1432[L]	Ribosomal protein L11 methyltransferase, putative	3.2	63	37	37
Transcription regulatory functions						

C6(pB5)	Dde_0247*	DNA-directed RNA polymerase, omega subunit	0	84	61	59
D12(pE9)	Dde_1614*	Regulatory protein GntR, HTH	0.3	58	/	49
G2(pC4)	Dde_3684*	Hypothetical protein (domain: HTH-ARSR)	0.5	/	/	/
A1(pD3)	Dde_0289	Putative transcriptional regulator, Fis family	0	45	42	39
Posttranslational modification						
B10(pF9)	Dde_0278*	Radical SAM domain protein	0	58	/	/
G6(pH7)	Dde_1002[L]	Peptide methionine sulfoxide reductase	0.8	41	61	42
B8(pF6)	Dde_1203*	Thioredoxin reductase	0	56	34	36
B10(pF3)	Dde_2313	Thiol peroxidase	0.8	82	66	63
H8(pE2)	Dde_3318*	Hypothetical protein (domain: trans-aconitate methyltransferase)	7.2	/	29	/
Others						
C8(pA7)	Dde_0151*	Metallo-beta-lactamase family protein	0.3	73	/	/
D11(pC10)	Dde_0266	Acetyltransferases-like	0.3	/	/	/
A9(pB11)	Dde_0966	Metal dependent phosphohydrolase	0.8	/	/	/
B11(pC2)[S]	Dde_1652*	Metal dependent phosphohydrolase	0	55	35	34
C6(pG11)	Dde_3164*	DHH family protein	0.5	53	36	34
A4(pH11)	Dde_3451*	Conserved hypothetical protein (domain: Predicted SAM-dependent methyltransferases)	0.3	60	43	44
B11(pF2)[S]	Dde_1729*	Protein of unknown function DUF34	0	46	30	28
G9(pF3)	Dde_2698*	ATP synthase protein I	1.3	57	/	38
D11(pF11)	Dde_3374*	Phage putative head morphogenesis protein, SPP1 gp7	0.3	56	/	/
C12(pG2)	Dde_3386*	Phage tail tape measure protein TP901, core region	1.3	30	/	/
E2(pA10)	Dde_0833*	ATPase	0.3	54	49	45
C10(pF3)	Dde_2869*	Type I restriction-modification system, S subunit	7.7	/	/	/
Hypothetical and conserved hypothetical proteins						
B9(pF11)	Dde_0728[L]	Conserved hypothetical protein	0.3	/	/	/
C6(pF11)	Dde_0222*	Conserved hypothetical protein	0	61	/	/
B8(pA10)	Dde_0229*	Conserved hypothetical protein	0.3	65	49	49
G11(pA11)	Dde_0983*	Hypothetical protein	0.3	65	39	38
B12(pC10)	Dde_1127*	Hypothetical protein	0.3	67	51	50
D5(pF5)	Dde_2572	Hypothetical protein	6.1	32	/	/
B8(pG6)	Dde_2586	Hypothetical protein	0.8	/	/	/
G9(pF5)	Dde_3771	Hypothetical protein	2.4	/	/	/
H8(pC4)	Dde_3760	Hypothetical protein	0	/	/	/
G7(pE11)	Dde_0940	Hypothetical protein	0.5	/	/	/

[a] *D. vu* represents *Desulfovibrio vulgaris* Hildenborough.

[b] *G. me* represents *Geobacter metallireducens*.

[c] *G. su* represents *Geobacter sulfurreducens* PCA.

/ represents homologs to *Desulfovibrio desulfuricans* G20 proteins were not found.

[d] * labeled loci are the genes within the operon, [L] labeled loci are the last gene of the operon.

[ς] labeled mutants had slower growth in LS medium than the parent strain.

Figure 1. The fraction of identified genes in each category relative to total identified genes compared with the percentage of the total predicted gene products in each category relative to total gene products from *D. desulfuricans* G20 genome. The gene products are grouped in their corresponding functional categories according to the NCBI annotation (http://www.ncbi.nlm.nih.gov/sutils/coxik.cgi?gi=18914).

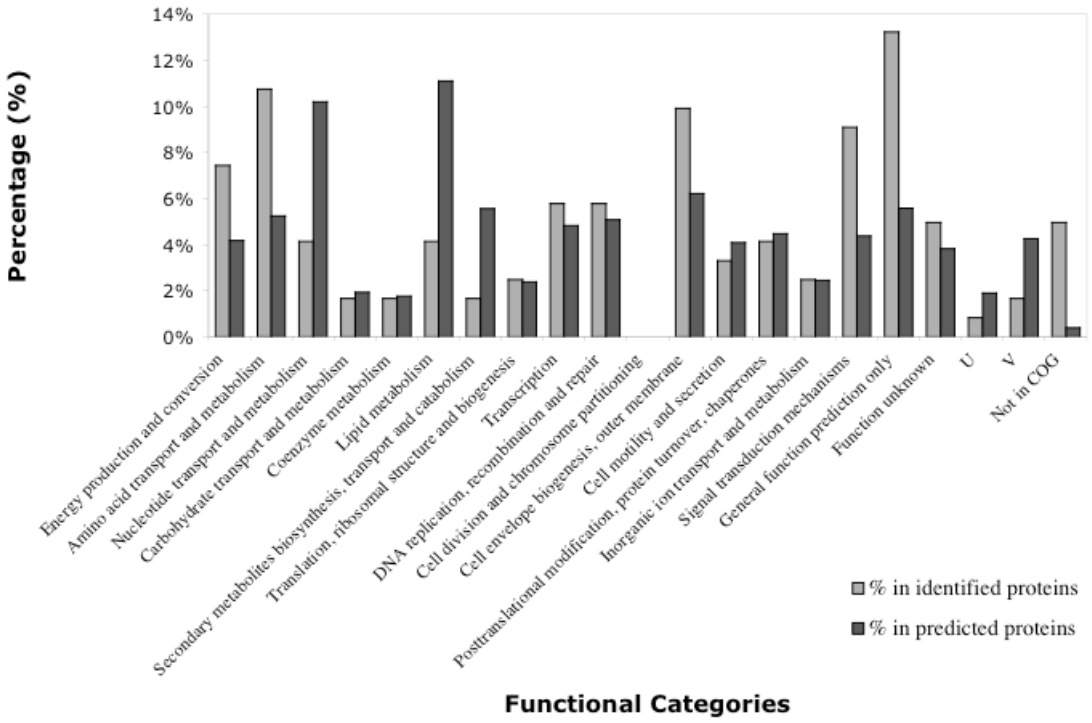

on this analysis, the most important COGs for sediment fitness include those for energy production and conversion, amino acid transport and metabolism, cell envelope biogenesis, signal transduction mechanisms, nucleotide transport and metabolism, and lipid metabolism.

All sediment fitness mutants were able to grow in lactate-sulfate medium. The majority of mutants had identical growth rates to strain $G20_{sediment}$, with only four growing more slowly than $G20_{sediment}$ (indicated in Table 2). During the pooled incubation in sediment, it is possible that these slow growing mutants were unable to grow or compete with native bacteria or other mutants in the sediment due to a lower level of inoculum (caused by slower growth in the inoculum tubes). However, these mutants were then grown and inoculated into sediment individually and shown to be unable to survive, confirming that the functions of these interrupted genes were also needed for sediment survival.

Three methyl-accepting chemotaxis proteins (MCP) (Dde_2734, Dde_0458 and Dde_1755) were identified. One of the genes identified and annotated as an MCP (Dde_2734), has 34% identity to the only characterized MCP in *D. vulgaris*, DcrA, which is thought to sense the oxygen concentration or the redox potential of the environment (13). In other STM studies, with *Campylobacter jejuni* in the chick gastrointestinal tract (18) and *S. oneidensis* MR-1 in sediment (16), MCP proteins were found to play important roles of colonization or survival as well.

Outer membrane components have been found necessary for virulence and colonization by pathogenic microorganisms through STM studies (11, 22, 34, 35). The screen revealed mutations within Dde_0428, Dde_1370, and Dde_3043, whose homologs

in *Escherichia coli* and *Listeria monocytogenes* have functions during peptidoglycan and lipopolysaccharide synthesis (8, 36). Two other individual mutants had insertions at different positions of one gene (Dde_1551) encoding D-alanyl-D-alanine dipeptidase, whose homologs in *E. coli* are involved in reprogramming cell-wall biosynthesis for better survival under starvation conditions (28). A similar function in strain G20 seems possible.

Other interesting findings include the importance of a gene coding for a protein annotated to be in the metallo-β-lactamase family. These enzymes are known for their ability to catalyze hydrolysis of the β-lactam ring of antibiotics including penicillins and cephalosporins (24). Based on this information, it seems possible that the ability to deal with β-lactam antibiotics confers sediment fitness on the bacteria. Similarly, a multidrug resistance pump conferring resistance to chloramphenicol and tetracycline was shown to increase sediment fitness in *S. oneidensis* MR-1 (16). A mutant of Dde_3016 encoding anaerobic ribonucleoside-triphosphate reductase was independently isolated multiple times as a fitness mutant. Anaerobic ribonucleoside-triphosphate reductase was also found to be important for intestinal colonization of *E. coli* (55); however, the mechanism has not yet been elucidated.

Growth of strains with transposon insertion in amino acid biosynthesis genes. Among all sediment fitness mutants, there is a group of mutants with disruptions in amino acids biosynthesis genes. Three mutants G12(pD6), B12(pE4), and A2(pE11) with recoveries of 0.27%, 0, and 0.53%, respectively, from sediment are listed in Table 1. The interruption in mutant G12(pD6) is in the gene encoding N-acetylglutamate synthase (ArgJ), which catalyzes two activities in the cyclic version of arginine biosynthesis: the

synthesis of acetylglutamate from glutamate and acetyl-CoA, and of ornithine by transacetylation between acetylornithine and glutamate (43). This protein has 37% similarity to the *E. coli* arginine biosynthesis bifunctional protein ArgJ. The transposon insertion in mutant B12(pE4) is located in the gene encoding chorismate mutase / prephenate dehydratase. This enzyme is a cytoplasmic protein with 31% similarity to *E. coli* chorismate mutase / prephenate dehydratase. Chorismate mutase catalyses the conversion of chorismate to prephenate in the tyrosine and phenylalanine biosynthesis pathways (59). Prephenate dehydratase (PDT) catalyses the decarboxylation of prephenate into phenylpyruvate, which is involved in the terminal part of the phenylalanine biosynthesis pathway. In some bacteria, PDT is a monofunctional enzyme; while in G20, it was predicted to be bifunctional. The interruption in mutant A2(pE11) occurs in the gene encoding the tryptophan synthase (TrpB), beta subunit. The enzyme is responsible for the final step of L-tryptophan biosynthesis. It has very high homology to TrpB in other bacteria including *E. coli* (55%), *D. vulgaris* (81.15%), *Geobacter metallireducens* (68.25%), and *Geobacter sulfurreducens PCA* (31.71%). This protein also has a paralog in G20, with 57% identity.

In order to be certain that the loss in sediment fitness for these mutants was due to the loss of the ability to synthesize amino acids. Growth was assessed with different concentrations of yeast extract. Yeast extract provides the complex nutrients for cell growth (53), which includes trace amount of amino acids. Figure 2 shows growth curves in decreasing yeast extract concentrations with lactate as electron donor. Without yeast extract in the medium, all of these mutants had impaired growth; mutant A2(pE11) had decreased growth rate, but still reached the same final OD_{600} as the parent strain, while

Figure 2. Growth of *D. desulfuricans* $G20_{sediment}$ and the mutants G12(pD6), B12(pE4), and A2(pE11) in mineral medium with yeast extract at concentrations of 0.05% (A), 0.01% (B), 0.005% (C), and 0% (D). Data shown represent the average of duplicate cultures. Error bars represent standard deviations.

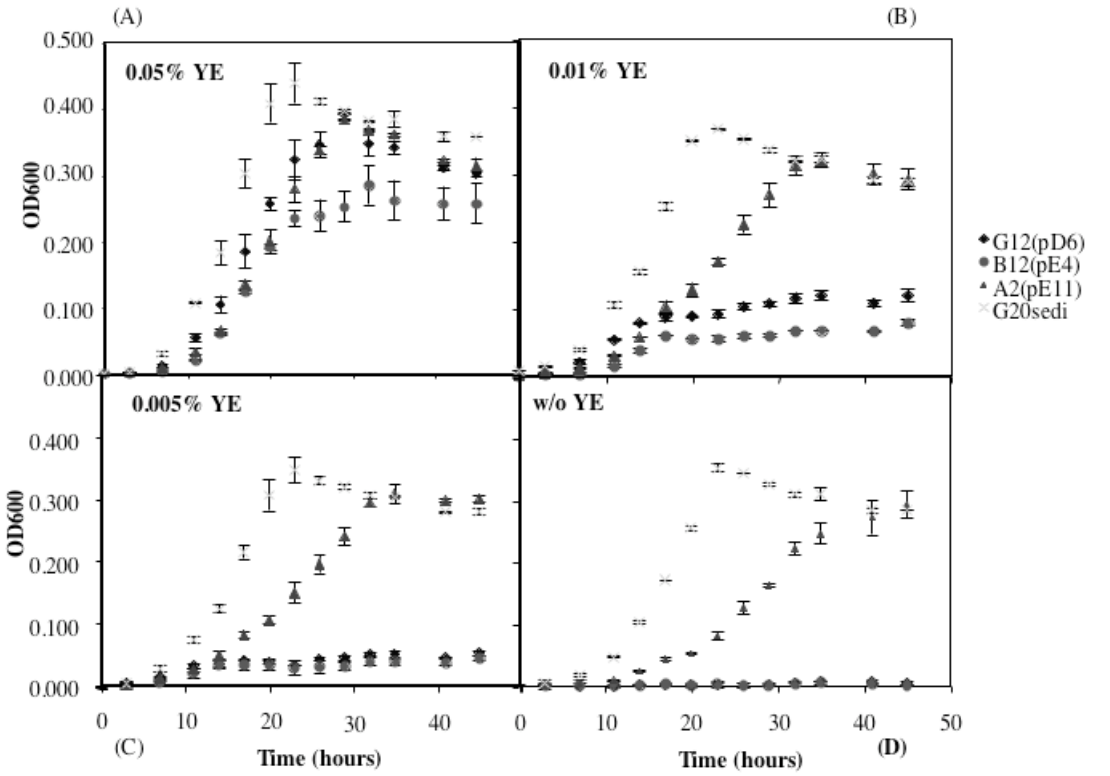

mutants B12(pE4) and G12(pD6) did not show detectable growth. These results indicate the *D. desulfuricans* G20 has ability to synthesize all the necessary amino acids when growing in mineral medium. The mutants G12(pD6) and B12(pE4) lost the ability to grow without added amino acids, a function apparently needed to grow in sediments. The slower growth of mutant A2(pE11) suggests to us that the paralog of TrpB is functional, but perhaps less efficient than the mutant TrpB, apparently conferring a growth disadvantage in sediments and liquid cultures.

Growth of strains with UV treatment. Mutants B12(pF11) and A8(pF7) had transposon insertions in genes encoding UmuC and RuvB. UV and many chemicals appear to cause mutagenesis by a process of translesion synthesis that requires DNA polymerase III and the SOS-regulated proteins UmuD, UmuC and RecA. This machinery allows replication to continue through DNA lesions, therefore avoiding lethal interruption of DNA replication after DNA damage (48). The UmuC is a well-conserved protein in prokaryotes and is present in all kingdoms of life (52). UmuC in G20 has an ortholog in *E. coli* with 41.67% identity and it is also conserved within the *δ-Proteobacteria* (Table 2).

RuvB forms the complex of RuvABC which are involved in Holliday junction resolution. During DNA replication, recombination and repair processes, Holliday junctions are formed (9). RuvA forms a helicase complex with RuvB, mediating the Holliday junction migration by localized denaturation and re-annealing (10).

To test whether interruptions in these genes affect cell survival ability after DNA damage, we compared mutants survival after exposing cells to UV light (254 nm wavelength) for different periods of time. The survival rate of each mutant is shown in

Table 3, calculated based on MPN counts. Both mutants had at least 10-fold lower survival rates than the parent strain after exposure to UV providing strong evidence for a role of the interrupted genes in the response to mutagens.

Growth of strains with transposon insertion in energy production genes. Three mutants with interruptions in genes involved in generation of energy were further studied and are listed in Table 1. Comparative growth studies with different electron donors were performed for a preliminary characterization of the mutant phenotype. Mutant C10(pB6) had an interrupted gene encoding formate C-acetyltransferase. Formate C-acetyltransferase (also known as pyruvate formate-lyase) is a key enzyme of anaerobic glucose metabolism, converting Coenzyme A and pyruvate to acetyl-CoA and formate (32). In *E. coli,* it uses a radical mechanism to reversibly cleave the C1-C2 bond of pyruvate (2). Previous studies have shown that pyruvate-formate lyase was required when carbon-starved *E. coli* entered stationary phase (37). This enzyme in G20 has 33.5% homology to formate C-acetyltransferase in *E. coli*, and conserved in *Streptococcus* species. Finding the ortholog for G20 during the sediment selection suggests that G20 may be similarly experiencing carbon limitation. The similar growth relative to the parent strain in both LS medium (66 mM lactate) and mineral medium (25 mM lactate) (Figure 3) indicated that with adequate carbon in the form of lactate, the mutant was able to grow as well as the parent strain.

Mutant C10(pG11) had a transposon insertion in a gene encoding the NiFe hydrogenase small subunit (HydA). NiFe hydrogenase is a periplasmic protein, composed of a large and a small subunit, and is believed to be involved in H_2 uptake (56). The NiFe Hydrogenase small subunit in G20 has 77.0% homology to hydrogenase

Table 3. Comparison of the survival rates after UV treatment based on MPN counts.

Mutant	Survival ratio[a] after UV exposure				
	10 seconds	30 seconds	1 minute	3 minutes	5 minutes
A8(pF7)	$2.3*10^{-2}$	$1.3*10^{-3}$	$1.0*10^{-5}$	$4.2*10^{-8}$	$1.79*10^{-8}$
B12(pF11)	$0.6*10^{-2}$	$1.0*10^{-3}$	$2.77*10^{-7}$	$5.5*10^{-8}$	$2.29*10^{-8}$
$G20_{sediment}$	$1.05*10^{-1}$	$1.2*10^{-2}$	$7.69*10^{-4}$	$6.5*10^{-7}$	$6.5*10^{-7}$

[a] survival ratio was calculated from survived cell numbers after UV exposure divided by original cell numbers.

Figure 3. Growth of *D. desulfuricans* $G20_{sediment}$ strain and the mutants C10(pG11), C10(pB6), and C8(pE11) in mineral medium using lactate (A) and H_2 (B) as electron donor. Cultures were incubated at 37 °C, with shaking for H_2 tubes and without shaking for lactate tubes. Data shown represent the average of duplicate cultures. Error bars represent standard deviations.

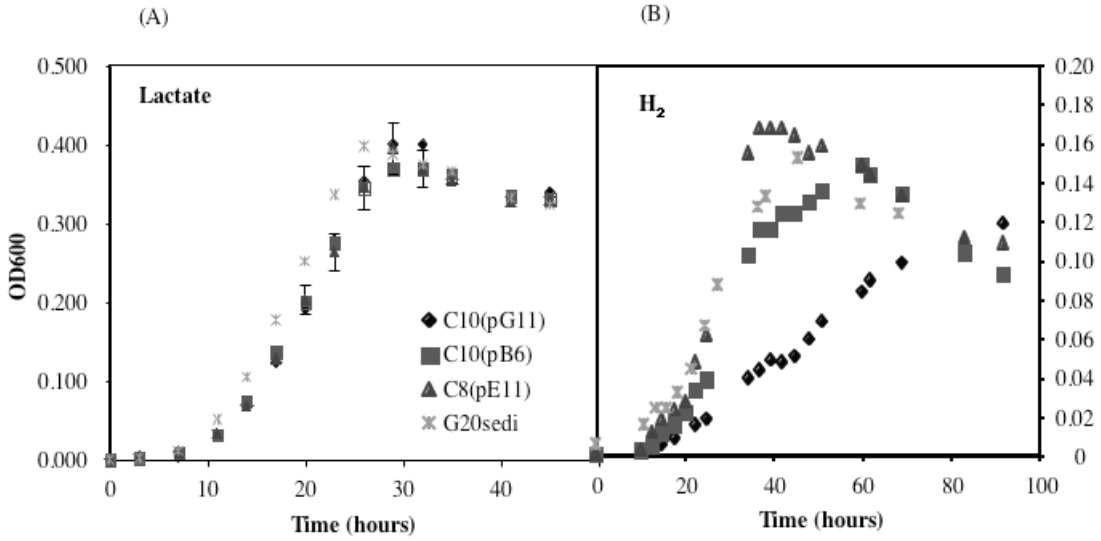

(HydA) in *Desulfovibrio vulgaris*, 38.19% homology to hydrogenase in *Geobacter sulfurreducens* PCA, and 37.11% homology to hydrogenase in *Geobacter metallireducens*. This enzyme has two paralogs (HynB-1 and HynB-2) in G20. The deletion mutant of its ortholog in *D. vulgaris* Hildenborough was found to grow similarly during exponential phase and quickly die during stationary growth phase (14).

Mutant C8(pE11) has a transposon insertion in the gene encoding the Fe-only hydrogenase. Fe-only hydrogenase, which contains 4Fe-4S clusters, is composed of two subunits and is present in the periplasmic space. Cytochrome c3 is likely the physiological electron carrier for the enzyme. However, the role of the Fe-only hydrogenase as an uptake or production (39, 54) hydrogenase is still being debated.

Both the parent strain and mutants grew similarly in lactate mineral medium (Figure 3). However, only the NiFe hydrogenase mutant C10(pG11) grew more slowly with H_2 than $G20_{sediment}$ strain (Figure 3). These results confirm a role of the NiFe hydrogenase in H_2 uptake.

Discussion

This paper reports results obtained with the modified STM technique (15) for identifying sediment fitness genes in sulfate-reducing bacteria. The screen resulted in the identification of 97 genes in strain G20 with the proportion of fitness genes (~3%) within the range of other STM findings with pathogens (33), and higher than with another environmental bacterium (*S. oneidensis* MR-1) (16) (1% of total genes). It is perhaps not surprising that MR-1 had less genes involved in sediment survival, as it is likely there is greater redundancy within the MR-1 genome as a result of the larger size.

Among the fitness genes identified, chemotaxis proteins validate our screen as we would predict that chemotaxis proteins would be mainly required for the response to attractants and repellents encountered in the environment and would be needed to compete with surrounding microorganisms (23). Although MCPs have conserved transmembrane domains, their extracellular ligand-binding domains vary, allowing bacteria to sense different physicochemical stimuli, to amplify and process resultant signals, and to trigger adaptive responses to the stimuli (60). *D. desulfuricans* G20 has 55 total genes annotated to be involved in chemotaxis, a number that is among the largest in all sequenced bacterial genomes. Among the putative chemotaxis genes, 35 paralogs of MCPs share 21-35% identity. The large number of MCPs make the G20 chemotaxis system much more complex than *E. coli* and *B. subtilis* models. One chemotaxis protein in G20 was found to be important for sediment fitness and its ortholog in *D. vulgaris* is thought to sense the redox potential in lab medium (13). A possible function of this chemotaxis protein in G20 could be in sensing redox potential in sediments.

The broad range of potential functions of our genes and their homologs in other bacteria indicates that many of these genes are likely important for sediment fitness in many environmental bacteria. The similarities of the genes to orthologs in other sequenced *δ-Proteobacteria* e.g., *D. vulgaris* Hildenborough, *G. metallireducens*, and *G. sulfurreducens* PCA were obtained from the Virtual Institute for Microbial Stress and Survival database (http://www.microbesonline.org/) and data are shown in Table 2. These *δ-Proteobacteria* are anaerobic environmental bacteria also thought to be important in aquifer systems (7, 29, 38). A high similarity to orthologs in these microorganisms (20-85%) may indicate that these genes play similar roles during

sediment growth in a variety of bacteria. Although the cellular function of genes from one species cannot always be determined based on database searches, similar functions of proteins, originally identified through homolog analysis, have been subsequently proven (16, 51). Thus, genes that have been identified as critical for G20 sediment fitness might have similar functions to their homologs in other microorganisms. It is important to note that transposon insertions located in an operon would likely influence expression of downstream genes and the observed phenotype may be attributed to this (polar) effect. Our results only identify the transposon-inserted gene and whether the gene is located within an operon or as the terminal ORF of an operon. The latter type of insertion is less likely to have a polar effect.

In this study, we did some preliminary characterization of energy production, amino acid biosynthesis, and DNA repair genes. Identical growth characteristics in both LS medium and lactate mineral medium for the selected mutants and the parent strain provide strong evidence that these genes are specifically involved in sediment fitness.

Growth experiments with mutants G12(pD6) and B12(pE4) suggested that they have lost the ability to synthesize arginine or phenylalanine for growth. Given that free amino acids are likely present at very low levels in sediments, the inability to generate all of the needed amino acids likely influenced the ability to survive. Pathogens and commensal microorganisms on the other hand, do not likely undergo similar constraints (18). Others have shown that amino acid biosynthesis can be elevated in response to nutrient limitation, stress or amino acids restriction (57), perhaps having an indirect effect on fitness under those conditions. Studies with pure cultures have shown that a salvage pathway for amino acid biosynthesis is often found in bacteria (44). Results presented

here suggest a role for the salvage pathway during in-situ growth.

H_2 is a common intermediate in natural environments and SRB are capable of using it as an energy source (30). The interruption of the NiFe hydrogenase gene, encoding for a well-studied protein thought to be involved in uptake of H_2 during growth (56), decreased its H_2 dependent growth rate. Our experiments with another mutant C8(pE11) encoding the Fe-only hydrogenase showed no growth effect with H_2 as electron donor, suggesting an alternative role for this protein during sediment growth. H_2 is a key intermediate in aquatic sediments and it influences the function and population structure of microbial ecosystems (20). In anoxic sediments, H_2 partial pressures are strictly maintained at low, steady-state levels by H_2-consuming organisms (30). As H_2 levels drop below 10 nM, sulfate-reducing bacteria are known to outcompete methanogens and acetogens for H_2 as demonstrated in sediment (20) and pure culture (26) systems. The selection of the uptake hydrogenase in the assay for loss of sediment fitness provides direct evidence for a role in sediment H_2 uptake by *Desulfovibrio*.

Published analyses of sediments have clearly demonstrated the presence of mutagens, which can threaten the viability of aquatic biota (6). DNA damaging agents range from UV light to fungal metabolites to reactive oxygen species (52). Although the role of specific DNA repair pathways have not been studied in natural systems, both error-free (RuvABC) (46) and error-prone (UmuDC) (48) pathways are universally present in environmental bacteria (3, 12, 58). Previous studies have shown that DNA repair mechanisms (specifically RecA) are induced upon exposure of pure cultures living in natural environments to UV light (3) or chemical mutagens (12). Results presented here showing the importance of *umuC* and *ruvB* genes in sediment survival clearly

demonstrate a role for DNA repair systems in sediment dwelling bacteria in dealing with in-situ concentrations of mutagens.

Although much work remains in understanding specific roles for identified genes during sediment growth, our limited studies demonstrated several functions needed by G20 during growth in sediment. Identification of all 97 genes important for growth/fitness gives us an idea of the variety of proteins required by environmental microbes to adapt to their niches. Based on the fact that more than 70% of the identified gene products have homologs in *D. vulgaris* Hildenborough, *G. metallireducens*, and *G. sulfurreducens* PCA, it is likely that many of these genes have universally required properties.

References

1. **Altschul, S. F., W. Gish, W. Miller, E. W. Myers, and D. J. Lipman.** 1990. Basic local alignment search tool. J. Mol. Biol. **215:**403-10.
2. **Becker, A., K. Fritz-Wolf, W. Kabsch, J. Knappe, S. Schultz, and A. F. Volker Wagner.** 1999. Structure and mechanism of the glycyl radical enzyme pyruvate formate-lyase. Nat. Struct. Biol. **6:**969-75.
3. **Booth, M. G., W. H. Jeffrey, and R. V. Miller.** 2001. RecA expression in response to solar UVR in the marine bacterium *Vibrio natriegens*. Microb. Ecol. **42:**531-539.
4. **Brune, A., P. Frenzel, and H. Cypionka.** 2000. Life at the oxic-anoxic interface: microbial activities and adaptations. FEMS Microbiol. Rev. **24:**691-710.
5. **Castaneda-Carrion, I. N.** 2001. Isolation and genetic characterization of subsurface microorganisms. Master thesis. University of Oklahoma, Norman, OK.
6. **Chen, G., and P. A. White.** 2004. The mutagenic hazards of aquatic sediments: a review. Mutat. Res. **567:**151-225.
7. **Coates, J. D., E. J. Phillips, D. J. Lonergan, H. Jenter, and D. R. Lovley.** 1996. Isolation of *Geobacter* species from diverse sedimentary environments. Appl. Environ. Microbiol. **62:**1531-6.
8. **Deng, M., and R. Misra.** 1996. Examination of AsmA and its effect on the assembly of *Escherichia coli* outer membrane proteins. Mol. Microbiol. **21:**605-12.

9. **Dickman, M. J., S. M. Ingleston, S. E. Sedelnikova, J. B. Rafferty, R. G. Lloyd, J. A. Grasby, and D. P. Hornby.** 2002. The RuvABC resolvasome. Eur. J. Biochem. **269:**5492-501.

10. **Donaldson, J. R., C. T. Courcelle, and J. Courcelle.** 2006. RuvABC is required to resolve Holliday junctions that accumulate following replication on damaged templates in *Escherichia coli*. J. Biol. Chem. **281:**28811-21.

11. **Dziva, F., P. M. van Diemen, M. P. Stevens, A. J. Smith, and T. S. Wallis.** 2004. Identification of *Escherichia coli* O157:H7 genes influencing colonization of the bovine gastrointestinal tract using signature-tagged mutagenesis. Microbiology **150:**3631-3645.

12. **Elasri, M. O., T. Reid, S. Hutchens, and R. V. Miller.** 2000. Response of a *Pseudomonas aeruginosa* biofilm community to DNA-damaging chemical agents. FEMS Microbiol Ecol **33:**21-25.

13. **Fu, R., J. D. Wall, and G. Voordouw.** 1994. DcrA, a c-type heme-containing methyl-accepting protein from *Desulfovibrio vulgaris* Hildenborough, senses the oxygen concentration or redox potential of the environment. J. Bacteriol. **176:**344-50.

14. **Goenka, A., J. K. Voordouw, W. Lubitz, W. Gartner, and G. Voordouw.** 2005. Construction of a [NiFe]-hydrogenase deletion mutant of *Desulfovibrio vulgaris* Hildenborough. Biochem. Soc. Trans. **33:**59-60.

15. **Groh, J. L., Q. Luo, J. D. Ballard, and L. R. Krumholz.** 2005. A method adapting microarray technology for signature-tagged mutagenesis of

Desulfovibrio desulfuricans G20 and *Shewanella oneidensis* MR-1 in anaerobic sediment survival experiments. Appl. Environ. Microbiol. **71:**7064-74.

16. **Groh, J. L., Q. Luo, J. D. Ballard, and L. R. Krumholz.** 2007. Genes that enhance the ecological fitness of *Shewanella oneidensis* MR-1 in sediments reveal the value of antibiotic resistance. Appl. Environ. Microbiol. **73:**492-8.

17. **Hamilton, W. A.** 1985. Sulfate-reducing bacteria and anaerobic corrosion. Annu. Rev. Microbiol. **39:**195-217.

18. **Hendrixson, D. R., and V. J. DiRita.** 2004. Identification of *Campylobacter jejuni* genes involved in commensal colonization of the chick gastrointestinal tract. Mol. Microbiol. **52:**471-84.

19. **Hewson, I., G. A. Vargo, and J. A. Fuhrman.** 2003. Bacterial diversity in shallow oligotrophic marine benthos and overlying waters: effects of virus infection, containment, and nutrient enrichment. Microb. Ecol. **46:**322-36.

20. **Hoehler, T. M., D. B. Albert, M. J. Alperin, B. M. Bebout, C. S. Martens, and D. J. Des Marais.** 2002. Comparative ecology of H_2 cycling in sedimentary and phototrophic ecosystems. Antonie Van Leeuwenhoek **81:**575-85.

21. **Holmes, D. E., K. P. Nevin, and D. R. Lovley.** 2004. *In situ* expression of *nifD* in *Geobacteraceae* in subsurface sediments. Appl. Environ. Microbiol. **70:**7251-7259.

22. **Karlyshev, A. V., P. C. F. Oyston, K. Williams, G. C. Clark, R. W. Titball, E. A. Winzeler, and B. W. Wren.** 2001. Application of high-density array-based signature-tagged mutagenesis to discover novel *Yersinia* virulence-associated genes. Infect. Immun. **69:**7810-7819.

23. **Kennedy, M. J., and J. G. Lawless.** 1985. Role of chemotaxis in the ecology of Denitrifiers. Appl. Environ. Microbiol. **49:**109-114.

24. **Knox, J. R., and P. C. Moews.** 1991. Beta-lactamase of *Bacillus licheniformis* 749/C. Refinement at 2 A resolution and analysis of hydration. J. Mol. Biol. **220:**435-55.

25. **Krumholz, L. R., D. A. Elias, and J. M. Suflita.** 2003. Immobilization of cobalt by sulfate-reducing bacteria in subsurface sediments. Geomicrobiol J **20:**61-72.

26. **Krumholz, L. R., S. H. Harris, S. T. Tay, and J. M. Suflita.** 1999. Characterization of two subsurface H_2-utilizing bacteria, *Desulfomicrobium hypogeium* sp. nov. and *Acetobacterium psammolithicum* sp. nov., and their ecological roles. Appl. Environ. Microbiol. **65:**2300-6.

27. **Lehoux, D. E., and R. C. Levesque.** 2002. Polymerase chain reaction-based signature-tagged mutagenesis. Methods Mol. Biol. **182:**127-137.

28. **Lessard, I. A., and C. T. Walsh.** 1999. VanX, a bacterial D-alanyl-D-alanine dipeptidase: resistance, immunity, or survival function? Proc. Natl. Acad. Sci. U. S. A. **96:**11028-32.

29. **Lloyd, J. R., V. A. Sole, C. V. Van Praagh, and D. R. Lovley.** 2000. Direct and Fe(II)-mediated reduction of technetium by Fe(III)-reducing bacteria. Appl. Environ. Microbiol. **66:**3743-9.

30. **Lovley, D. R., and S. Goodwin.** 1988. Hydrogen concentrations as an indicator of the predominant terminal electron-accepting reactions in aquatic sediments. Geochimica et Cosmochimica Acta **52:**2993-3003.

31. **Lovley, D. R., P. K. Widman, J. C. Woodward, and E. J. Phillips.** 1993. Reduction of uranium by cytochrome c3 of *Desulfovibrio vulgaris*. Appl. Environ. Microbiol. **59:**3572-6.

32. **Matheron, C., A. M. Delort, G. Gaudet, and E. Forano.** 1997. Re-investigation of glucose metabolism in *Fibrobacter succinogenes*, using NMR spectroscopy and enzymatic assays. Evidence for pentose phosphates phosphoketolase and pyruvate formate lyase activities. Biochim. Biophys. Acta **1355:**50-60.

33. **Mecsas, J.** 2002. Use of signature-tagged mutagenesis in pathogenesis studies. Curr. Opin. Microbiol. **5:**33-37.

34. **Mei, J.-M., F. Nourbakhsh, C. W. Ford, and D. W. Holden.** 1997. Identification of *Staphylococcus aureus* virulence genes in a murine model of bacteremia using signature-tagged mutagenesis. Mol. Microbiol. **26:**399-407.

35. **Merrell, D. S., D. L. Hava, and A. Camilli.** 2002. Identification of novel factors involved in colonization and acid tolerance of *Vibrio cholerae*. Mol. Microbiol. **43:**1471-1491.

36. **Navarre, W. W., and O. Schneewind.** 1999. Surface proteins of gram-positive bacteria and mechanisms of their targeting to the cell wall envelope. Microbiol. Mol. Biol. Rev. **63:**174-229.

37. **Nystrom, T.** 2004. Stationary-phase physiology. Annu. Rev. Microbiol. **58:**161-81.

38. **Phelps, T. J., and J. G. Zeikus.** 1985. Effect of fall turnover on terminal carbon metabolism in Lake Mendota sediments. Appl. Environ. Microbiol. **50:**1285-1291.

39. **Pohorelic, B. K., J. K. Voordouw, E. Lojou, A. Dolla, J. Harder, and G. Voordouw.** 2002. Effects of deletion of genes encoding Fe-only hydrogenase of *Desulfovibrio vulgaris* Hildenborough on hydrogen and lactate metabolism. J. Bacteriol. **184:**679-86.

40. **Potvin, E., D. E. Lehoux, I. Kukavica-Ibrulj, K. L. Richard, F. Sanschagrin, G. W. Lau, and R. C. Levesque.** 2003. *In vivo* functional genomics of *Pseudomonas aeruginosa* for high-throughput screening of new virulence factors and antibacterial targets. Environ Microbiol **5:**1294-1308.

41. **Purdy, K. J., T. M. Embley, and D. B. Nedwell.** 2002. The distribution and activity of sulphate reducing bacteria in estuarine and coastal marine sediments. Antonie Leeuwenhoek **81:**181-187.

42. **Rapp, B. J., and J. D. Wall.** 1987. Genetic transfer in *Desulfovibrio desulfuricans*. Proc. Natl. Acad. Sci. U. S. A. **84:**9128-30.

43. **Sakanyan, V., D. Charlier, C. Legrain, A. Kochikyan, I. Mett, A. Pierard, and N. Glansdorff.** 1993. Primary structure, partial purification and regulation of key enzymes of the acetyl cycle of arginine biosynthesis in *Bacillus stearothermophilus*: dual function of ornithine acetyltransferase. J. Gen. Microbiol. **139:**393-402.

44. **Sekowska, A., V. Denervaud, H. Ashida, K. Michoud, D. Haas, A. Yokota, and A. Danchin.** 2004. Bacterial variations on the methionine salvage pathway. BMC Microbiol **4:**9.

45. **Senko, J. M., J. D. Istok, J. M. Suflita, and L. R. Krumholz.** 2002. In-situ evidence for uranium immobilization and remobilization. Environ Sci Technol **36:**1491-6.

46. **Shinagawa, H., K. Makino, M. Amemura, S. Kimura, H. Iwasaki, and A. Nakata.** 1988. Structure and regulation of the *Escherichia coli* ruv operon involved in DNA repair and recombination. J. Bacteriol. **170:**4322-9.

47. **Sierra-Alvarez, R., S. Karri, S. Freeman, and J. A. Field.** 2006. Biological treatment of heavy metals in acid mine drainage using sulfate reducing bioreactors. Water Sci Technol **54:**179-85.

48. **Smith, B. T., and G. C. Walker.** 1998. Mutagenesis and more: *umuDC* and the *Escherichia coli* SOS response. Genetics **148:**1599-610.

49. **So, C. M., C. D. Phelps, and L. Y. Young.** 2003. Anaerobic transformation of alkanes to fatty acids by a sulfate-reducing bacterium, strain Hxd3. Appl. Environ. Microbiol. **69:**3892-900.

50. **Steger, J. L., C. Vincent, J. D. Ballard, and L. R. Krumholz.** 2002. *Desulfovibrio* sp. genes involved in the respiration of sulfate during metabolism of hydrogen and lactate. Appl. Environ. Microbiol. **68:**1932-1937.

51. **Sung, H. M., G. Yeamans, C. A. Ross, and R. E. Yasbin.** 2003. Roles of YqjH and YqjW, homologs of the *Escherichia coli* UmuC/DinB or Y superfamily of DNA polymerases, in stationary-phase mutagenesis and UV-induced mutagenesis of *Bacillus subtilis*. J. Bacteriol. **185:**2153-60.

52. **Sutton, M. D., B. T. Smith, V. G. Godoy, and G. C. Walker.** 2000. The SOS response: recent insights into *umuDC*-dependent mutagenesis and DNA damage tolerance. Annu. Rev. Genet. **34:**479-497.

53. **Tanner, R. S.** 1997. Cultivation of bacteria and fungi, p. 52-60. *In* C. J. Hurst, Knudsen, G. R., McInerney, M. J., Stetzenbach, L. D., and Walter, M. V. (ed.), Manual of environmental microbiology. ASM press, Washington, D.C.

54. **van den Berg, W. A., W. M. van Dongen, and C. Veeger.** 1991. Reduction of the amount of periplasmic hydrogenase in *Desulfovibrio vulgaris* (Hildenborough) with antisense RNA: direct evidence for an important role of this hydrogenase in lactate metabolism. J. Bacteriol. **173:**3688-94.

55. **Van Diemen, P. M., F. Dziva, M. P. Stevens, and T. S. Wallis.** 2005. Identification of enterohemorrhagic *Escherichia coli* O26:H- genes required for intestinal colonization in calves. Infect. Immun. **73:**1735-1743.

56. **Voordouw, G., V. Niviere, F. G. Ferris, P. M. Fedorak, and D. W. Westlake.** 1990. Distribution of hydrogenase genes in *Desulfovibrio* spp. and their use in identification of species from the oil field environment. Appl. Environ. Microbiol. **56:**3748-3754.

57. **Weerasinghe, J. P., T. Dong, M. R. Schertzberg, M. G. Kirchhof, Y. Sun, and H. E. Schellhorn.** 2006. Stationary phase expression of the arginine biosynthetic operon *argCBH* in *Escherichia coli*. BMC Microbiol **6:**14.

58. **Wilson, C., T. M. Caton, J. A. Buchheim, M. A. Buchheim, M. A. Schneegurt, and R. V. Miller.** 2004. DNA-repair potential of *Halomonas* spp. from the Salt Plains Microbial Observatory of Oklahoma. Microb. Ecol. **48:**541-9.

59. **Zhang, S., G. Pohnert, P. Kongsaeree, D. B. Wilson, J. Clardy, and B. Ganem.** 1998. Chorismate mutase-prephenate dehydratase from *Escherichia coli*. Study of catalytic and regulatory domains using genetically engineered proteins. J. Biol. Chem. **273:**6248-53.

60. **Zhulin, I. B., A. N. Nikolskaya, and M. Y. Galperin.** 2003. Common extracellular sensory domains in transmembrane receptors for diverse signal transduction pathways in bacteria and archaea. J. Bacteriol. **185:**285-294.

Chapter 4

Proteome Analysis of *Desulfovibrio desulfuricans* G20 Mutants Using the Accurate Mass and Time (AMT) Tag Approach

Abstract

Abundance values obtained from direct LC-MS analyses were used to compare the proteomes of six transposon-insertion mutants of *Desulfovibrio desulfuricans* G20, the lab strain ($G20_{lab}$) and a sediment-adapted strain ($G20_{sediment}$). Three mutations were in the signal transduction histidine kinases, and three mutations were in the regulatory proteins. The high-throughput accurate mass and time (AMT) tag proteomic approach was utilized to analyze the proteomes. A total of 1318 proteins were identified with high confidence, approximately 35% of all predicted proteins in the *D. desulfuricans* G20 genome. Proteins from all functional categories were identified. Significant differences in the abundance of 30 proteins were detected between the $G20_{lab}$ strain and the $G20_{sediment}$ strain. Abundances of proteins for energy metabolism, ribosomal synthesis, membrane biosynthesis, transport, and flagellar synthesis were affected in the mutants. Specific examples of proteins down-regulated in mutants include a putative tungstate transport system substrate-binding protein and several proteins related to energy production, e.g., 2-oxoacid:acceptor oxidoreductase, cytochrome c-553, formate acetyltransferase. In addition, several signal transduction mechanism proteins were regulated in one mutant, and the abundances of ferritin and hybrid cluster protein were reduced in another mutant. However, the similar abundance of universal stress proteins, heat shock proteins and chemotaxis proteins in the mutants revealed that regulation of chemotactic behavior and

stress regulation might not be observed under our growth conditions. This study provides the first proteomic overview of several sediment fitness mutants of G20, and the evidence of the difference between lab strains and sediment-adapted strains at the protein level.

Introduction

Sulfate-reducing bacteria (SRB), which use sulfate as a terminal electron acceptor to oxidize both organic and inorganic compounds, are ubiquitous in soils and sediments [1]. Since *Desulfovibrio* species were found to be capable of immobilizing uranium [2] and other heavy metals [3, 4] natural environments, their physiology and molecular genetics have been extensively studied in the laboratory [5, 6]. SRB have also been broadly studied *in situ* and often show different physiological characteristics in the environment. For example, actively sulfate reducing *Desulfovibrio* species were present in the photooxic zone [7], while the laboratory pure cultures of *Desulfovibrio* species can only be grown under anaerobic conditions. Therefore, it is clear that SRB exhibit a differentiated set of reactions to adapt to different conditions. It has also been observed that sediment adapted strains have different physiological features from their corresponding well-adapted lab strains [8]; however, there is no study that compares the protein production between the two types of strains.

D. desulfuricans G20, originally isolated from a petroleum producing well, serves as a model organism for the study of sediment survival and molecular genetics in SRB. The genome of *D. desulfuricans* G20 is available from the National Center for Biotechnology Information (NCBI) database and the bacterium is easy to cultivate for biochemical studies. The genome information provides an opportunity to obtain further

insights into the metabolism of this organism by applying whole-genome approaches to the study of transcriptional and translational responses of *D. desulfuricans* G20 in lab medium and in sediment. Furthermore, more than 5000 transposon-insertion mutants were generated during our previous study [9]. About 100 genes were identified as important genes related to sediment survival [10]. Among them, several mutations occurred within general regulatory genes and these mutants were unable to survive in sediment. These include genes for histidine kinases belonging to the two-component regulatory systems (TCSs), which mediate responses to a variety of environmental signals. To adapt to and survive complex environmental changes in nature, it may be especially important that different TCSs form regulatory networks. However, little is known about whether functional interactions between different TCSs form signaling networks in *D. desulfuricans* G20. In addition, little information is available on the expression of these regulatory genes, or on which pathways they regulate.

Studies using microarray technology greatly increased our knowledge of global transcriptomic regulation within *Desulfovibrio* species under different stresses, including salt [11], heat [12], and nitrite [13] stress. These studies allowed an identification of energy metabolism pathways and genes related to stress adaptation and have shown us the versatility of this microorganism's metabolism and its ability to adapt to various stresses. Previous work has mainly focused on comparing growth phases [14], electron donors [15], and stressors, at the mRNA level. However, mRNA abundance is not always correlated with protein abundance [16]; furthermore, information of post-transcriptional and post-translational modification processes is not available from the transcriptomic analyses. With the development of capillary liquid chromatography and tandem mass spectrometry

technology, high throughput proteomic analysis has been applied to many organisms [17-19] to identify and compare protein abundance under different growth conditions.

The goals of this investigation were to elucidate proteome abundance information for *D. desulfuricans* G20 strains, to examine the proteins involved in sediment survival, and to identify possible regulatory pathways involved in these TCSs. To accomplish this, the AMT tag approach [19, 20] was used which allows peptides to be identified quantitatively with high confidence and high throughput. We analyzed the proteomes of *D. desulfuricans* $G20_{lab}$ and $G20_{sediment}$ strains, as well as several transposon mutants that did not survive in sediment. The AMT abundance values were used as a quantitative measurement of relative protein abundances within individual samples. Normalized z-scores were used to quantify the relative protein abundances. Z-score differences between samples of at least 1.5 or greater were considered significant.

Materials and Methods

Strains, media, and culture conditions. *D. desulfuricans* G20, a spontaneous nalidixic acid resistant strain, was obtained from Dr. Judy Wall at the University of Missouri-Columbia. Cultures were grown in lactate-sulfate (LS) medium, prepared as described by Rapp and Wall [21], with N_2 in the headspace. The medium contained 50 mM sulfate and 66 mM lactate, and vitamin and metal solutions as described elsewhere [22]. Prior to autoclaving, the pH was adjusted to 7.2. After autoclaving, 8 mM bicarbonate and 0.025% cysteine were added from anaerobic stock solutions. The lab strain has been cultured in this medium for several years. To generate a sediment-adapted strain, approximately 10^5 cells of the lab strain were inoculated into a microcosm with 2 g of

sulfidogenic subsurface sediment and incubated in the dark at room temperature for one week. Inoculum-free microcosms were set up as controls. Cells were extracted from the sediment and plated onto LS solid medium with 200 μg/ml nalidixic acid. Colonies were obtained from the plates and inoculated into LS liquid medium. Glycerol stocks were prepared after a 24-hour incubation period. This strain was designated as $G20_{sediment}$, as mentioned previously [9]. No colonies were obtained from uninoculated microcosms. Strain $G20_{sediment}$ was used as a parent strain for conjugation experiments to obtain transposon-insertion mutants as described previously [9]. Six mutants obtained during our previous work were used for this study. Details on the mutants are available in Table 1.

All of these strains were cultivated from glycerol stocks and grown in LS medium to mid-log phase (OD_{600} = 0.5). Cells were harvested anaerobically by centrifugation at 8,000 rpm for 10 minutes at 4°C, supernatants were decanted, and pellets were resuspended in 1 ml of washing buffer [9]. Cell pellets were placed into liquid N_2 immediately, and stored at –80°C until shipment. The cells were shipped to Pacific Northwest National Laboratory (PNNL) on dry ice.

Peptide preparation. The cell pellets were resuspended in two pellet volumes of 50 mM ammonium bicarbonate, pH 7.8. The cell suspensions were lysed by bead beating the mixture with 0.1 mm zirconia/silica beads in a mini-beadbeater (Biospec, Bartlesville OK) for 3 min. at 4,500 rpm. Lysates were collected and placed immediately on ice to inhibit proteolysis. The protein solutions were digested with trypsin and the digested peptides were desalted using Supelco (St. Louis, MO) Supelclean C-18 tubes as described elsewhere [23]. Peptide concentrations were determined by BCA assay (Pierce, Rockford IL) using a bovine serum albumin standard.

Table 1. List of G20 mutants used for proteomic analysis.

Mutant	Sediment Recovery (%) [10]	Interrupted Gene Locus	Protein Description	Contained Domain	Potential Function
A1(pD3)	0	Dde_0289 (633 aa)	Transcriptional regulator, Fis family	RocR (~500 aa)	Activates rRNA transcription, regulation of virulence factors, inhibition of the initiation of DNA replication
B8(pB6)	0	Dde_3047 (397 aa)	Serine phosphatase RsbU, regulator of sigma subunit		Regulates important virulence factors, influences the survival ability
D12(pE9)	0.3	Dde_1614 (224 aa)	Regulatory protein GntR, HTH	FadR (~215 aa)	Regulates various biological processes, repressor for uxuRBA operon
H9(pF8)	0	Dde_0602 (711 aa)	Multi-sensor signal transduction histidine kinase	BaeS (~330 aa)	Involved in two-component regulatory system, domain found in heat shock protein Hsp90
D12(pB8)	0	Dde_3715 (653 aa)	Multi-sensor signal transduction histidine kinase	BaeS (~250 aa)	Involved in two-component regulatory system, domain found in heat shock protein Hsp90
G5(pA9)	0.3	Dde_1945 (676 aa)	Putative PAS/PAC sensor protein	AtoS (~125 aa)	Associated with a histidine kinase or a sensor protein, involved in lesion formation, swarming and production of extracellular protease

Capillary LC separations. All peptide mixtures from the whole cell lysate, as well as off-line strong cation exchange (SCX) fractions of the same lysate, were then separated by an automated in-house designed HPLC system as described elsewhere [23, 24]. The separated samples were fractionated into as many as 100 and as few as 25 fractions [25]. Fractions were concentrated to about 1 μg/μL for direct analysis by LC-MS/MS.

MS/MS acquisition. Eluate from the HPLC was directly transferred into an ion trap MS (LCQ, ThermoFinnigan, San Jose, CA) using electrospray ionization (ESI). For the MS/MS detection, a total of 10 μg (1 μg/μL) of total peptide were loaded onto the reversed phase column for each analysis. The mass spectrometer operated in a data-dependent MS/MS mode over a series of seven smaller segmented *m/z* ranges (400-700, 700-900, 900-1100, 1100-1300, 1300-1500, 1500-1700, 1700-2000), and in a 400-2000 m/z range for several SCX fractions obtained from many cultures and growths of *D. desulfuricans* G20. The details for the generation of initial mass and time tag database are described elsewhere [26]. This database serves as a "look up" table for subsequent high-resolution experiments. The MS/MS spectra were analyzed using the peptide identification software SEQUEST [27] in conjunction with the annotated protein translations from the genome sequence of *D. desulfuricans* G20. Filtered identifications were based on peptide identification that had minimum Xcorr values of 1.9, 2.2, and 3.5 for charge states of 1+, 2+ and 3+ respectively if detected at least twice in all the analyses. For fully, partially, and non-tryptic terminal peptides only detected once, filtered identifications were based on peptide values that had a minimum Xcorr value of 1.9, 2.2, and 3.75 for charge states of 1+, 2+, and 3+ respectively. Additionally, all peptides had to have a minimum δCN value of 0.1.

Accurate mass and time (AMT) tag validation. Using 5 μg (0.5 μg/μL) of total peptide from each of the same samples, intact peptide mass data were obtained using the same HPLC system, but using an FTICR mass spectrometer for MS detection. A mass calibration mixture was infused at the end of each analysis, and the masses of the compounds in the mixture were used to calibrate all of the spectra within the analyses. The mass tags identified from the tandem mass spectrometry analysis were stored in the mass tag database and were matched against unique peptides detected with the FTICR, as described previously [20]. Search tolerances for peptide peak matching were ±6 ppm for the mass and ±2% of the total analysis time for the elution time. Those PMT tags that matched the closest with the FTICR and elution time data were validated as AMT tags.

Data analysis. The acquired AMT peptide data were further filtered, by setting the SLiC score > 0.5 as a cutoff, to increase the confidence levels of peptide identification. In order to minimize false positives, the peptides detected in only one of the three separate LC-FTICR MS measurements were excluded from the analyses. The relative protein abundances were estimated by averaging the abundances of multiple peptides for a given protein, and only those peptides whose intensities were ≥ 33% of the most abundant peptide for the given protein were chosen. Z-scores were calculated for each protein from the $\log_2$ of the abundance and were used to compare these estimated abundances across all the strains and then were clustered by using the hierarchical clustering algorithms available in Spotfire ® (Spotfire Inc., Cambridge, MA, USA).

For the calculation of the "Codon Adaptation Index" (CAI), a measure of the expressivity of a given gene based on its codon usage, 3775 gene sequences of *D. desulfuricans* G20 were downloaded from the NCBI database. CAI calculation required

a determination of relative adaptiveness value ω for *D. desulfuricans* G20, which were obtained from the University of Maryland, Baltimore County (UMBC, http://www.evolvingcode.net/codon/cai/cai.php). CAI values for each ORF of total proteins of G20 and 1318 identified proteins from this study were computed using a calculator available from the same website.

Results and Discussion

1. Reproducibility of LC-FTICR analyses:

We chose a single growth condition for this study and analyzed the protein profiles of $G20_{sediment}$, $G20_{lab}$, and six insertion mutants that were deficient in sediment fitness. One of our goals was to provide global protein diversity information for *D. desulfuricans* G20 using the high-throughput AMT tag approach. To address these issues, protein abundance value profiles were generated using the mass analyses obtained from the LC-FTICR MS runs. We identified about 1300 proteins from eight samples and more than 600 common proteins were identified.

The reproducibility of LC-FTICR MS analyses was focused on evaluating protein abundance values by comparing triplicate analyses of the same biological sample. The analysis of triplicate protein abundance values from LC-FTICR MS measurements of peptides from one $G20_{sediment}$ sample was shown as an example in Figure 1. Plots of protein abundance values across different independent measurements showed strongly linear patterns, indicating high measurement reproducibility. Linear regression of these data demonstrated reproducibility and root sum square (R^2) values were near or above 0.9.

Figure 1. Scatter plot of protein abundance of $G20_{sediment}$ samples. Abundance values were shown in log_2 form. (A)-(C). Comparison of protein abundances between three independent LC-FTICR measurements of $G20_{sediment}$ sample1. Each spot represents one protein and the abundance was averaged from detected peptides of that run. (D). Comparison of protein abundances between two biological replicates. Each spot represents one protein and the abundance was averaged from detected peptides of three independent runs. Root sum square (R^2) values for each pair of comparison were shown inside the plots.

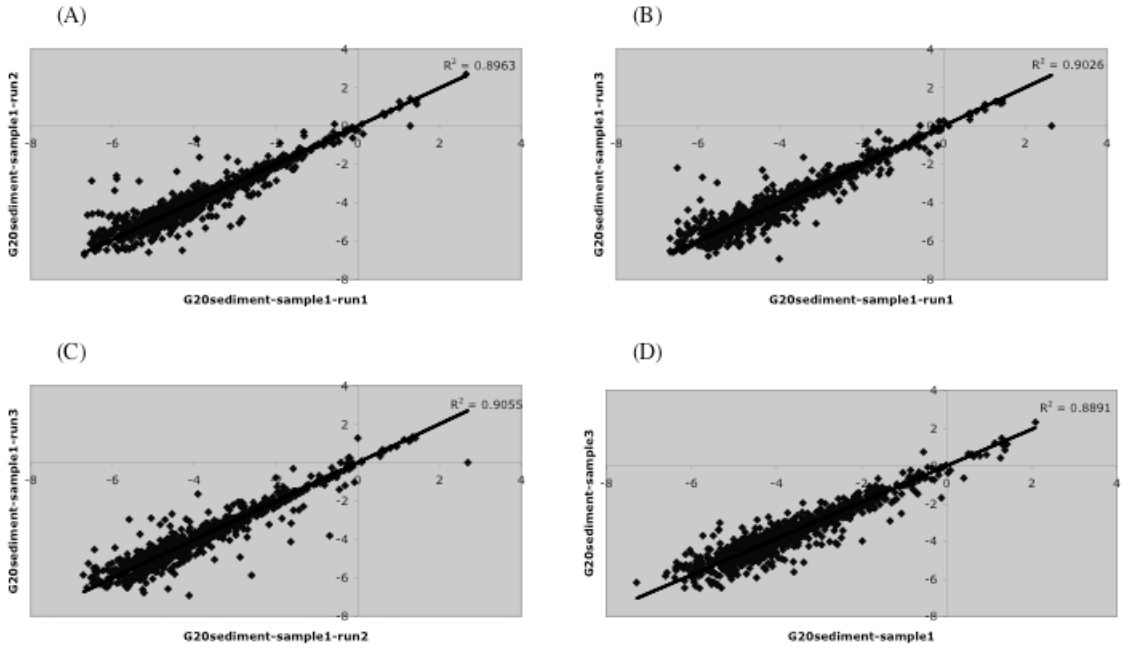

The reproducibility of the LC-FTICR data was also evaluated by comparing results from two biological replicates of $G20_{sediment}$ samples, prepared independently from mid-log phase cells. In this case, the average AMT abundance from three measurements per sample was used for comparison. A total of 1054 proteins were identified among all runs and replicates in $G20_{sediment}$ samples. Statistical analyses showed good reproducibility between biological replicates (R^2=0.9).

The same evaluations were performed on all the samples, and the R^2 values for both replicate runs and replicate biological samples were around 0.9 (data not shown).

2. Overview of proteomic analyses:

With the AMT tag approach, a total of 1318 proteins were identified, representing 35% of the predicted gene products encoded in *D. desulfuricans* G20 genome. For the majority (98%) of the proteins, two or more unique peptides were detected per protein. With the high confidence of the identification of peptides, proteins identified by only one unique peptide were considered valid, due to the fact that some proteins only have one detectable tryptic peptide when using a mass spectrometer. These identified proteins have been predicted to be involved in all functional categories (Figure 2). A large number of identified proteins also fell into the category of proteins with unknown functions, including the hypothetical, conserved hypothetical, and unassigned functional proteins. This finding is consistent with previous work [18, 28] on the importance of "hypothetical proteins" in cell function.

A codon usage-based approach, the Codon Adaptation Index (CAI) was used to determine whether the detection of proteins was biased towards those that were more highly expressed. The CAI index uses a set of highly expressed genes from a species as

Figure 2. Functional classes of proteins detected by AMT approach. Each bar represents the average number of proteins detected in all samples, and the average percentage of each functional category is shown next to each bar. Error bar represents the range of detected proteins in different samples. The proteins are grouped in their functional categories according to the NCBI annotation (http://www.ncbi.nlm.nih.gov/entrez/query.fcgi?db=genome&cmd=Retrieve&dopt=Protein+Table&list_uids=18914).

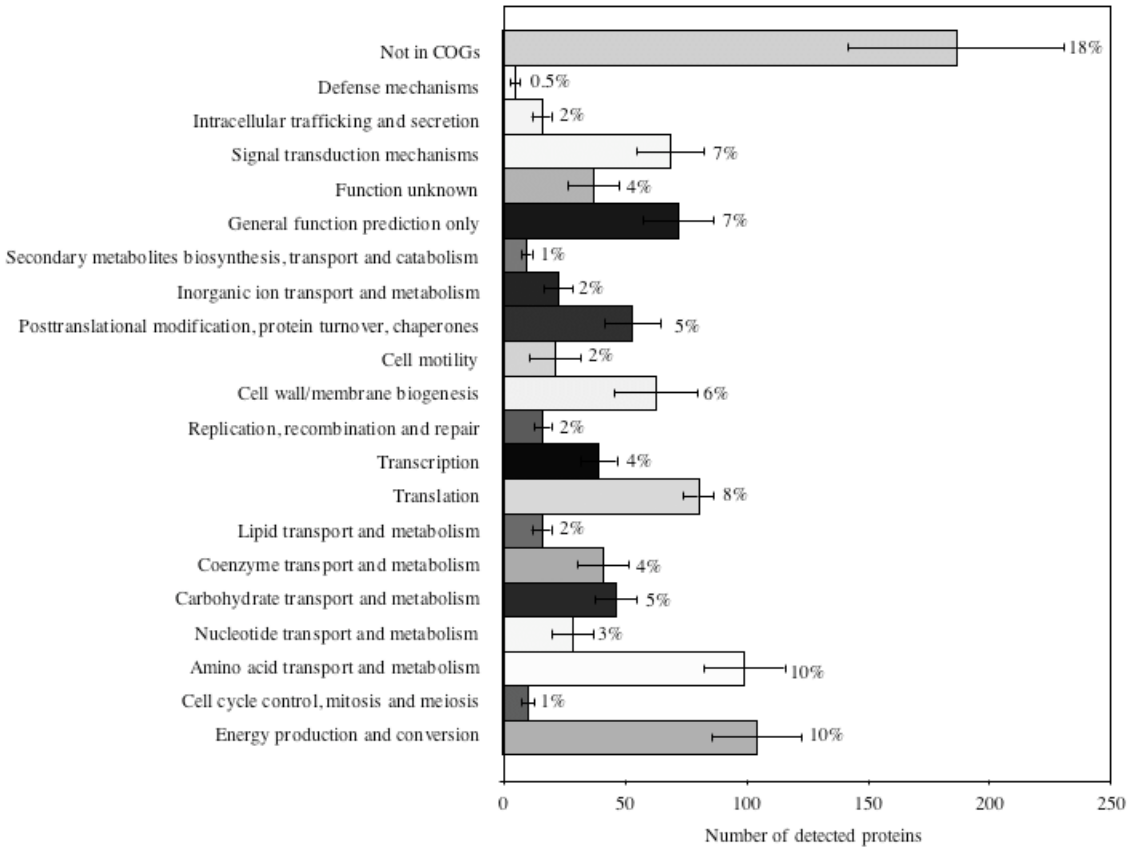

references to assess the relative merits of each codon, and a score for a gene sequence is calculated from the frequency of use of all codons in that gene sequence. The index is useful for predicting the level of expression of a gene, and gives an approximate indication of the likely success of heterologous gene expression [29]. CAI values range from about 0.1 to close to 1.0 with higher values representing more highly expressed proteins. The CAI for all genomic proteins was determined and compared to CAI values for those that were measured in cell extracts (Figure 3). Kolmogorov-Smirnov tests ($P<0.0001$) indicated that these two distributions were different. The results showed that 60% of the identified proteins had CAI values larger than 0.7 and only 3% had CAI values smaller than 0.6. This suggests that, although the LC-FTICR MS demonstrated the ability to detect relatively low abundance proteins, the majority of proteins identified in this study still represent relatively abundant proteins in *D. desulfuricans* G20.

For the systematic analyses, the proteomic profiles of six insertion mutants and two controls of G20 were generated using the AMT tag approach with a z-score normalization to compare relative protein abundance. There are many sources of systematic variation in the LC-MS-based proteomic experiments that affect protein abundance measurement. These sources include variations in sample preparation, LC separation, electrospray ionization efficiency, and mass spectrometer performance. Normalization is the term used to describe the process of removing or correcting for such variations [19]. Protein abundance values with $\log_2$ ratios of $|z| > 1.5$ were considered significant [14, 18]. All of the enzymes required for the metabolism of sulfate (ATP sulfurylase, inorganic pyrophosphatase, adenylyl sulfate (APS) reductase, and bisulfite reductase) were detected in all of the samples with relatively high abundance

Figure 3. Distribution of CAI values for all encoding genes in the *D. desulfuricans* G20 genome and for genes encoding proteins identified by this study.

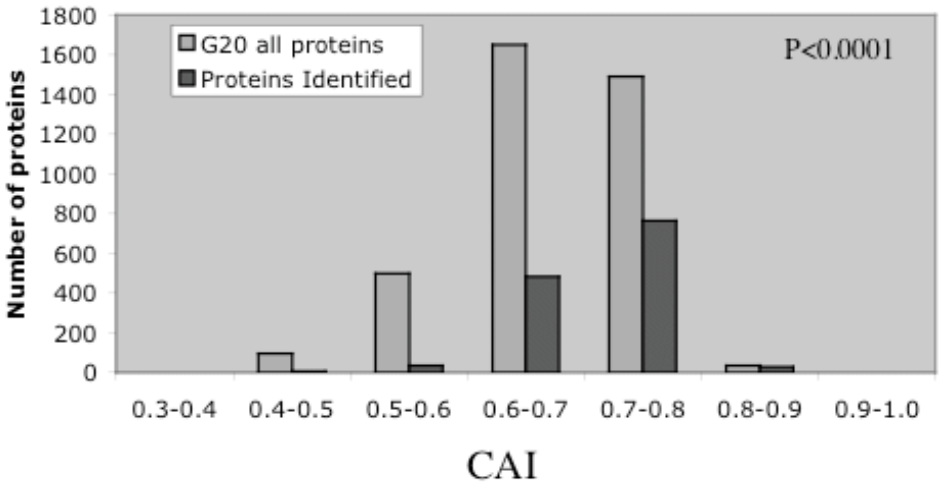

(Supplementary Table 1). No significant differences were observed between samples. Similar abundance values for all of the samples may explain why the strains grew similarly in lactate-sulfate medium. It also indicates that these mutated genes do not regulate sulfate reduction in G20.

3. $G20_{sediment}$ versus $G20_{lab}$ strains:

The second goal of this investigation was to compare the protein profiles of *D. desulfuricans* $G20_{sediment}$ to the $G20_{lab}$ strain. It is clear that all bacterial cultures undergo genetic change in the laboratory, although perhaps it is not immediately obvious from the phenotype [8]. However, several researchers have proposed the idea of returning frequently to the natural environment to obtain samples of bacteria that have not been separated from their evolutionarily important selective pressures [30]. It seems that there is a tradeoff between having long-term, well-characterized cultures and recent cultures that probably reflect the natural environment more accurately. However, we are not aware of any studies that show the difference between these two types of pure cultures. In this study, we compared the proteomes of the well-adapted lab strain and the same strain conditioned to grow in sediments, in order to look at significant global protein abundances.

Among the 1097 and 995 proteins detected in the $G20_{sediment}$ and $G20_{lab}$ samples respectively, 955 proteins were detected in both samples. Proteins with significant changes are listed in Table 2. One of the eight proteins with lower abundance in $G20_{sediment}$, is a pyruvate ferredoxin/flavodoxin oxidoreductase (Dde_0046), although its abundance value (0.27) was relatively high when compared to other proteins found in both samples. Pyruvate ferredoxin oxidoreductase (POR) catalyzes the oxidation of

Table 2. Proteins with significant changes in $G20_{sediment}$ strain.

Locus	Protein Description	Functional Category	Changes in $G20_{sediment}$ [a]
Dde_0046	Pyruvate ferredoxin/flavodoxin oxidoreductase family protein	C	-1.62
Dde_1359	Elongator protein 3/MiaB/NifB	C	*1.94*
Dde_3055	Formate acetyltransferase 2	C	*2.54*
Dde_2744	Aminotransferase, class V	E	2.52
Dde_2852	Sodium:alanine symporter	E	**-2.96**
Dde_2285	1,4-alpha-glucan branching enzyme	G	*2.09*
Dde_3685	HPCH/HPAI aldolase family protein	G	4.89
Dde_2839	Valyl-tRNA synthetase, class Ia	J	-1.66
Dde_2844	Queuine/other tRNA-ribosyltransferase:Queuine tRNA-ribosyltransferase	J	**-3.45**
Dde_0553	Hypothetical protein	K	*2.52*
Dde_0047	Elongator protein 3/MiaB/NifB	L	*3.55*
Dde_0542	Formamidopyrimidine-DNA glycolase	L	*1.76*
Dde_3571	ATP-dependent DNA helicase, UvrD/REP family	L	**-3.26**
Dde_0367	3-deoxy-D-manno-octulosonic-acid transferase, putative	M	*1.50*
Dde_0426	Glycosyl transferase, group 1/2 family protein	M	*2.50*
Dde_0831	Chain length determinant family protein	M	*3.62*
Dde_1711	Flagellar hook protein FlgE	N	*1.81*
Dde_2099	ATPase	O	*1.80*
Dde_3546	Conserved hypothetical protein	O	*1.94*
Dde_1189	Conserved hypothetical protein	P	3.39
Dde_1774	Conserved hypothetical protein	R	*1.94*
Dde_2055	GatB/Yqey family protein	S	-1.90
Dde_3139	Conserved hypothetical protein	S	*1.73*
Dde_0160	ATP-binding region, ATPase-like	T	*2.78*
Dde_2716	HD domain protein	T	*2.02*
Dde_2213	Hypothetical protein		**-2.62**
Dde_2284	Asparaginase family protein		*2.26*
Dde_2886	Methyltransferase FkbM		*1.83*
Dde_3026	Hypothetical protein		**-2.53**
Dde_3515	Formate dehydrogenase formation protein FdhE, putative		*1.77*

[a] Represents the difference in Z-score between the $G20_{sediment}$ and $G20_{lab}$. Number in italic means the protein was detected in $G20_{sediment}$ sample only, number in bold means the protein was detected in $G20_{lab}$ sample only.

pyruvate to acetyl-CoA in the cytoplasm and has been purified from *Desulfovibrio africanus* [31]. Its low abundance in our $G20_{sediment}$ strain may reflect the fact that pyruvate is not the primary electron donor in the sediment. Three ribosomal proteins queuine/other tRNA-ribosyltransferase (Dde_2844), valyl-tRNA synthetase (Dde_2839), and GatB/Yqey family protein (Dde_2055) were also observed in low abundance in the $G20_{sediment}$. The valyl-tRNA synthetase in *Escherichia coli* plays an important role in correcting misactivation and misacylation errors by regulating a tRNA (Val)-dependent editing reaction [32]. GatB is the B subunit of a glutamyl-tRNA amidotransferase protein, which in *Bacillus subtilis,* controls the formation of correctly charged Gln-$tRNA^{Gln}$ through the transamidation of misacylated Glu-$tRNA^{Gln}$ [33].

Several proteins (22) were more abundant in the $G20_{sediment}$, e.g., two different elongator proteins 3/MiaB/NifB (Dde_1359 & Dde_0047), methyltransferase (Dde_2886) and aminotransferase (Dde_2744). Most aminotransferases play multiple functions in different pathways and exemplify the class of enzymes with ambiguous substrates [34]; while some aminotransferases are unique catalysts for a particular reaction, for example, in *E. coli,* mutations in ilvE, hisC, or bioA lead to auxotrophic requirements for isoleucine, histidine, or biotin, respectively [35-37]. Since no elevated levels of gene products of ilvE, hisC, or bioA were observed in the strain $G20_{sediment}$, the elevated abundance level of this aminotransferase (Dde_2744) suggests that this protein plays general functions in transamination reactions in G20. Methyltransferases may acts as methylating agents modifying DNA and may produce lethal and mutagenic lesions. Using methyltransferases is one of the mechanisms to correct modified DNA strands and repair potentially lethal lesions [38]. MiaB protein is a bifunctional radical-S-

adenosylmethionine enzyme involved in thiolation and methylation of tRNA in bacteria [39]. Elevated flagellar hook protein (Dde_1711) abundances in the $G20_{sediment}$ were expected since there are potential benefits to cell motility including increased nutrient acquisition, toxic substance avoidance, and the ability to migrate to optimal colonization sites [40]. Formate dehydrogenase formation protein (FdhE) also showed elevated abundance levels in the $G20_{sediment}$ sample. FdhE has been found to be involved in the formation of respiratory formate dehydrogenase in *E. coli* [41].

4. Possible gene regulation in G20 mutants:

The third goal of this investigation was to identify possible regulatory roles of the mutated gene products. That is to understand why these mutants were unable to survive in sediment, while there was no obvious change of growth characteristics in LS medium, indicated by the similar doubling time relative to $G20_{lab}$ (data not shown).

Three mutants had insertion mutations in open reading frames annotated as signal transduction histidine kinases (HKs). HKs usually belong to two-component systems (TCSs), which are required for innumerable adaptive responses in bacteria. TCSs are widespread and exist not only in prokaryotes, but also in eukaryotes [42]. A typical TCS includes a HK and a partner response regulator (RR). The HK acts as a sensor and is autophosphorylated in response to an input signal and the histidine-to-aspartate phosphotransfer to the RR results in a cellular output response.

The *D. desulfuricans* G20 genome encodes 44 HK proteins, 42 RR proteins, and 8 hybrid HK proteins (containing both HK and RR domains). In at least ten cases, pairs of HK and RR proteins are encoded by adjacent or nearby genes that are often arranged in operons. However, some are encoded by genes that appear to be separated on the

chromosome. The interrupted HK gene in the mutant D12(pB8) is located in a nine-gene operon that includes a HK, a RR, a nitrogen regulation protein, a universal stress protein, three transmembrane proteins, and two conserved hypothetical proteins. In mutant H9(pF8), the HK gene (locus Dde_0602) is located in an operon that includes the periplasmic component of an ABC-type phosphate/phosphonate transport system and a nitrogen regulation protein. While in mutant G5(pA9), the HK gene (locus Dde_1945) is a single gene, with the corresponding RR perhaps located in a separate part of the genome.

Interestingly, we found that the abundances of several proteins were affected by the deletion of more than one TCS. For example, high abundance values for the glutamyl-tRNA^{Gln} amidotransferase A subunit (Dde_1020) were observed in mutant D12(pB8), H9(pF8), and G5(pA9). Glutamyl-tRNA amidotransferase converts Glu-tRNA^{gln} to Gln-tRNA^{gln} in bacteria not able to form Gln-tRNA directly from glutamine [33]. High abundance of methyltransferase GidB was observed only in mutant H9(pF8) and G5(pA9), but not in mutant D12(pB8). GidB is a family of bacterial glucose inhibited division proteins involved in the regulation of cell division [43]. Fifteen other common proteins with lower abundance were observed in mutants G5(pA9), H9(pF8), and D12(pB8) (data not shown), indicating that many TCSs may have common physiological roles in *Desulfovibrio* [44].

The histidine kinase in two mutants H9(pF8) and D12(pB8) have BaeS domains. BaeS sensor kinase and BaeR RR, control the expression of the *spy* gene in response to envelope stress in *E. coli* [45]. The BaeS/BaeR system is also thought to control genes for an efflux pump (*mdtABC)* in *E. coli* [46, 47]. The *E. coli baeSR* mutants showed increased

sensitivity to myricetin, gallic acid, nickel chloride, and especially sodium tungstate [48]. A putative tungstate transport system substrate-binding protein was in low abundance in mutant H9(pF8). This protein may be involved in tungstate efflux, thus its low abundance could cause the mutant to be more sensitive to tungstate, or an analog in sediment. These two interrupted histidine kinases have a 27% identity in amino acid sequence, and they down-regulated 18 proteins in common. However, the up-regulated proteins were very different in these mutants (see Table 3 & 4). In mutant H9(pF8), two cell envelope biogenesis proteins, methyltransferase GidB (Dde_2293) and glycosyltransferase (Dde_2890), constituted a large percentage of the proteins identified. This is consistent with the previous finding that the BaeS/BaeR system controls an envelope stress pathway [45]. While in mutant D12(pB8), several proteins involved in energy production were highly abundant, e.g., alcohol dehydrogenase (Dde_3523), flavodoxin (Dde_3667), and Ni-Fe hydrogenase, small subunit (Dde_2137). It is uncertain whether this sensor protein also senses electron status in the cell. The differentially regulated proteins imply that several different sets of genes are controlled by different networks of TCSs [49].

The mutated signal transduction histidine kinase in mutant G5(pA9) has an AtoS domain. AtoS-AtoC also belongs to a TCS family and AtoS functions both as a transcriptional and post-translational regulator [50]. In a typical AtoS-AtoC system, the atoS gene coding for a sensor kinase, is located just upstream of atoC. AtoS/AtoC deletion mutants of *E. coli* showed increased use of glucuronamide as a carbon source [48]. The *ato*SC mutants also showed increased sensitivity to sodium chloride, and were more susceptible to changes in osmolarity, some membrane active agents, aminoglycosides,

Table 3. Proteins with significant changes in mutant D12(pB8).

Locus	Protein Description	Functional Category[a]	Changes in mutant D12(pB8)
Dde_3523	Alcohol dehydrogenase, iron-containing	C	2.95
Dde_1359	Elongator protein 3/MiaB/NifB	C	-1.95
Dde_3667	Flavodoxin, short chain	C	1.59
Dde_3055	Formate acetyltransferase 2	C	-2.55
Dde_2137	Ni-Fe hydrogenase, small subunit:Twin-arginine translocation pathway signal	C	2.42
Dde_2744	Aminotransferase, class V	E	-2.63
Dde_2664	Diaminopimelate decarboxylase	E	1.67
Dde_1305	Peptidase, M24 family	E	-2.62
Dde_2353	Alpha amylase, catalytic subdomain	G	4.29
Dde_0801	Precorrin-4 C11-methyltransferase region	H	-1.73
Dde_2982	Ribosomal protein L31	J	-1.87
Dde_2289	Sua5/YciO/YrdC/YwlC	J	-2.42
Dde_0553	Hypothetical protein	K	-2.53
Dde_0349	Transcriptional regulator, LysR family	K	-2.65
Dde_2457	HDIG	KT	1.55
Dde_0367	3-deoxy-D-manno-octulosonic-acid transferase, putative	M	-1.52
Dde_0426	Glycosyl transferase, group 1/2 family protein	M	-2.51
Dde_0431	Similar to Putative glycosyl/glycerophosphate transferases involved in teichoic acid biosynthesis TagF/TagB/EpsJ/RodC	M	-2.62
Dde_2099	ATPase	O	-1.81
Dde_1189	Conserved hypothetical protein	P	-3.49
Dde_0799	Conserved hypothetical protein	R	-2.67
Dde_3468	Tyrosine protein kinase:Serine/threonine protein kinase	RTKL	-2.71
Dde_3139	Conserved hypothetical protein	S	-1.74
Dde_1497	Conserved hypothetical protein	S	2.61
Dde_0160	ATP-binding region, ATPase-like	T	-2.80
Dde_3535	ATP-binding region, ATPase-like:Histidine kinase A, N-terminal	T	-3.09
Dde_2716	HD domain protein	T	-2.04
Dde_1016	Helix-turn-helix, Fis-type	T	-2.20
Dde_0695	Response regulator receiver	T	2.50
Dde_2284	Asparaginase family protein	-	-2.28
Dde_0807	Conserved hypothetical protein	-	-1.63
Dde_2038	Conserved hypothetical protein	-	-2.58
Dde_0194	Conserved hypothetical protein	-	-3.56
Dde_2610	Conserved hypothetical protein	-	1.64
Dde_3430	Excisionase/Xis, DNA-binding	-	2.17
Dde_3515	Formate dehydrogenase formation protein FdhE, putative	-	-1.79
Dde_1020	Glutamyl-tRNA(Gln) amidotransferase A subunit	-	1.77
Dde_0409	Glycerol uptake facilitator protein KO: K02440 glycerol uptake facilitator protein	-	-1.60
Dde_0877	Hypothetical protein	-	2.32
Dde_2224	Hypothetical protein	-	2.28

Dde_2270	Hypothetical protein	-	3.40
Dde_3184	Hypothetical protein	-	2.36

[a] – represents function uncategorized.

Table 4. Proteins with significant changes in mutant H9(pF8).

Locus	Protein Description	Functional Category[a]	Changes in mutant H9(pF8)
Dde_1793	2-oxoacid:acceptor oxidoreductase, beta subunit, pyruvate/2-ketoisovalerate	C	-1.68
Dde_1821	Cytochrome c-553	C	-1.96
Dde_3055	Formate acetyltransferase 2	C	-2.47
Dde_2744	Aminotransferase, class V	E	-2.47
Dde_0234	ABC transporter, periplasmic substrate-binding protein, putative tungstate transport system substrate-binding protein	H	-1.72
Dde_0801	Precorrin-4 C11-methyltransferase region	H	-1.65
Dde_2722	Protein of unknown function UPF0004	J	-1.56
Dde_2289	Sua5/YciO/YrdC/YwlC	J	-2.34
Dde_0553	Hypothetical protein	K	-2.45
Dde_3426	Hypothetical protein	K	-2.10
Dde_0349	Transcriptional regulator, LysR family	K	-2.57
Dde_0047	Elongator protein 3/MiaB/NifB	L	-3.48
Dde_1491	Endonuclease III/Nth	L	-2.27
Dde_0542	Formamidopyrimidine-DNA glycolase	L	-1.69
Dde_0426	Glycosyl transferase, group 1/2 family protein	M	-2.43
Dde_2293	Methyltransferase GidB	M	2.45
Dde_2890	Similar to Glycosyltransferase	M	1.52
Dde_0431	Similar to Putative glycosyl/glycerophosphate transferases involved in teichoic acid biosynthesis TagF/TagB/EpsJ/RodC	M	-2.54
Dde_2892	Hypothetical protein	M/S	1.96
Dde_2148	Chemotaxis protein CheZ, putative	NT	-1.68
Dde_0305	AhpC/TSA family protein	O	-1.56
Dde_2099	ATPase	O	-1.63
Dde_1774	Conserved hypothetical protein	R	-1.88
Dde_0799	Conserved hypothetical protein	R	-2.59
Dde_0793	RNA-binding region RNP-1 (RNA recognition motif)	R	2.23
Dde_3139	Conserved hypothetical protein	S	-1.66
Dde_3214	Conserved hypothetical protein	S	1.65
Dde_0773	Conserved hypothetical protein	S	1.56
Dde_2303	Hypothetical protein	S	-2.80
Dde_0160	ATP-binding region, ATPase-like	T	-2.72
Dde_3535	ATP-binding region, ATPase-like:Histidine kinase A, N-terminal	T	-1.90
Dde_1016	Helix-turn-helix, Fis-type	T	-2.12
Dde_2284	Asparaginase family protein	-	-2.20
Dde_2038	Conserved hypothetical protein	-	-2.50
Dde_0194	Conserved hypothetical protein	-	-3.57
Dde_1384	Conserved hypothetical protein	-	1.74
Dde_3430	Excisionase/Xis, DNA-binding	-	2.54
Dde_3515	Formate dehydrogenase formation protein FdhE, putative	-	-1.71
Dde_1020	Glutamyl-tRNA(Gln) amidotransferase A subunit	-	1.85

Dde_2641	Hybrid cluster protein	-	-1.71
Dde_0877	Hypothetical protein	-	1.91
Dde_2224	Hypothetical protein	-	2.47
Dde_3014	Hypothetical protein	-	-2.73
Dde_0447	TonB dependent receptor domain protein	-	4.36

[a] – represents function uncategorized.

and a respiratory inhibitor [48]. A recent transcriptome analysis of the *E. coli* two-component systems revealed that possible roles of the AtoS-AtoC system included flagellar synthesis and chemotactic behavior [48]. This histidine kinase gene in G20 is a single gene, which does not form a typical *ato*SC operon. Proteins with significant changes in mutant G5(pA9) are shown in Table 5. Several proteins with decreased abundance in this mutant were related to energy production, e.g., 2-oxoacid:acceptor oxidoreductase (Dde_1793), cytochrome c-553 (Dde_1821), formate acetyltransferase (Dde_3055), ethanolamine utilization protein eutM precursor (Dde_3270). Cytochrome c-553 from sulfate-reducing bacteria is a low-oxidoreduction-potential cytochrome that lacks the of primary sequence homology to other cytochromes c [51]. The redox potential of this protein is abnormally low (+20 mV) when compared with a normal range of approximately 200-450 mV for the cytochrome c family [51]. Low abundances of cytochrome c-553 in mutants may explain why these mutants were not competitive in sediment.

The insertion in mutant A1(pD3) was within Dde_0289, encoding a protein that contains a RocR domain. RocR is a member of the NtrC/NifA family of regulators and a member of a family of prokaryotic enhancer-binding proteins that act together with sigma 54 factors. In *Bacillus subtilis*, the positive regulatory protein RocR is required for the expression of both *rocABC* and *rocDEF*, two operons involved in arginine and ornithine catabolism [52]. However, our data set did not further elucidate the regulation in this pathway. Instead, we found three signal transduction mechanism proteins (with loci: Dde_2148, Dde_0160, and Dde_2716) with low abundance and three signal transduction mechanism proteins (with loci: Dde_1399, Dde_2457, and Dde_1697) with high

Table 5. Proteins with significant changes in mutant G5(pA9).

Locus	Protein Description	Functional Category[a]	Changes in mutant G5(pA9)
Dde_1793	2-oxoacid:acceptor oxidoreductase, beta subunit, pyruvate/2-ketoisovalerate	C	-1.51
Dde_1821	Cytochrome c-553	C	-1.59
Dde_3055	Formate acetyltransferase 2	C	-2.50
Dde_2642	Iron-sulfur cluster-binding protein	C	-1.50
Dde_0086	Oxygen-insensitive NAD(P)H nitroreductase	C	2.09
Dde_2744	Aminotransferase, class V	E	-2.40
Dde_3552	Aspartate ammonia-lyase, putative	E	1.72
Dde_0801	Precorrin-4 C11-methyltransferase region	H	-1.68
Dde_2722	Protein of unknown function UPF0004	J	-1.59
Dde_2289	Sua5/YciO/YrdC/YwlC	J	-2.37
Dde_0553	Hypothetical protein	K	-2.48
Dde_3426	Hypothetical protein	K	-2.13
Dde_0047	Elongator protein 3/MiaB/NifB	L	-3.51
Dde_1491	Endonuclease III/Nth	L	-2.31
Dde_0542	Formamidopyrimidine-DNA glycolase	L	-1.72
Dde_0426	Glycosyl transferase, group 1/2 family protein	M	-2.46
Dde_1433	Heptosyltransferase family protein	M	2.76
Dde_2293	Methyltransferase GidB	M	2.35
Dde_2203	Peptidase, M23/M37 family	M	1.75
Dde_0431	Similar to Putative glycosyl/glycerophosphate transferases involved in teichoic acid biosynthesis TagF/TagB/EpsJ/RodC	M	-2.57
Dde_2892	Hypothetical protein	M/S	1.96
Dde_0305	AhpC/TSA family protein	O	-1.60
Dde_2099	ATPase	O	-1.76
Dde_3270	Ethanolamine utilization protein eutM precursor	QC	-1.71
Dde_1774	Conserved hypothetical protein	R	-1.91
Dde_0799	Conserved hypothetical protein	R	-2.62
Dde_3139	Conserved hypothetical protein	S	-1.70
Dde_0773	Conserved hypothetical protein	S	1.83
Dde_2303	Hypothetical protein	S	-1.87
Dde_3535	ATP-binding region, ATPase-like:Histidine kinase A, N-terminal	T	-3.04
Dde_1016	Helix-turn-helix, Fis-type	T	-2.16
Dde_0560	Cell division transporter substrate-binding protein FtsY	U	1.51
Dde_2284	Asparaginase family protein	-	-2.23
Dde_0194	Conserved hypothetical protein	-	-3.55
Dde_1621	Conserved hypothetical protein	-	-3.27
Dde_2610	Conserved hypothetical protein	-	2.26
Dde_3430	Excisionase/Xis, DNA-binding	-	1.99
Dde_3515	Formate dehydrogenase formation protein FdhE, putative	-	-1.74
Dde_1020	Glutamyl-tRNA(Gln) amidotransferase A subunit	-	1.75

Dde_2641	Hybrid cluster protein	-	-1.53
Dde_0446	Hypothetical protein	-	2.02
Dde_0877	Hypothetical protein	-	1.96
Dde_2224	Hypothetical protein	-	2.47
Dde_3026	Hypothetical protein	-	3.16

[a] – represents function uncategorized.

abundance in this mutant. This may suggest that this transcriptional regulator is involved in the regulation of a signal transduction network. The complete list of proteins with significant abundance changes are shown in Table 6. One probable rubredoxin (Dde_2749) was also found to be in low abundance in this mutant. Rubredoxin in *Desulfovibrio* species plays an important role, not only in electron transport, but also in the protection from oxidative stress [53]. It has been shown that during periods of oxidative stress, rubredoxin could divert electron flow from the electron transport chain of *D. vulgaris* to rubrerythrin and superoxide reductase, thereby simultaneously protecting autooxidizable redox enzymes and lowering intracellular hydrogen peroxide and superoxide levels [53]. It is possible that this protein plays similar roles in strain G20.

Mutant B8(pB6) has a mutation in Dde_3047 serine phosphatase RsbU, a regulator of the sigma subunit. RsbU is thought to play a role in activating SigB but may also play some unknown additional roles [54]. Both RsbU and SigB were found to regulate important virulence factors in *Staphylococcus aureus*, thereby contributing significantly to the outcome of staphylococcal infection [54, 55]. Previous experiments suggested that SigB or RsbU influences the ability of *S. aureus* to survive in the bloodstream and reach the joints, rather than the ability to multiply in the joint and cause inflammation[54]. In addition, RsbU and SigB are also involved in the regulation of virulence determinant production. Many virulence proteins are part of cell envelopes [56, 57]. We therefore expected to find a lowered abundance of cell envelope biogenesis related proteins in this mutant. Three proteins with significant changes include a conserved hypothetical membrane protein (Dde_2565), glycosyl transferase (Dde_0426), and

Table 6. Proteins with significant changes in mutant A1(pD3).

Locus	Protein Description	Functional Category[a]	Changes in mutant A1(pD3)
Dde_1359	Elongator protein 3/MiaB/NifB	C	-2.03
Dde_2749	Probable rubredoxin	C	-3.00
Dde_2285	1,4-alpha-glucan branching enzyme	G	-2.18
Dde_2378	Protein of unknown function UPF0004:tRNA-i(6)A37 modification enzyme MiaB	J	-1.52
Dde_0553	Hypothetical protein	K	-2.61
Dde_1399	ATPase	KT	1.78
Dde_2457	HDIG	KT	1.54
Dde_1491	Endonuclease III/Nth	L	-2.43
Dde_0542	Formamidopyrimidine-DNA glycolase	L	-1.85
Dde_0367	3-deoxy-D-manno-octulosonic-acid transferase, putative	M	-1.59
Dde_0831	Chain length determinant family protein	M	-2.91
Dde_2565	Conserved hypothetical membrane protein	M	-2.14
Dde_2148	Chemotaxis protein CheZ, putative	NT	-1.50
Dde_2099	ATPase	O	-1.89
Dde_1189	Conserved hypothetical protein	P	-3.34
Dde_1774	Conserved hypothetical protein	R	-2.03
Dde_0793	RNA-binding region RNP-1 (RNA recognition motif)	R	2.00
Dde_0160	ATP-binding region, ATPase-like	T	-2.87
Dde_2716	HD domain protein	T	-2.11
Dde_1697	Response regulator receiver:ATP-binding region, ATPase-like:Histidine kinase A, N-terminal	T	1.67
Dde_2284	Asparaginase family protein	-	-2.35
Dde_0409	Glycerol uptake facilitator protein KO: K02440 glycerol uptake facilitator protein	-	-1.68
Dde_3026	Hypothetical protein	-	2.50
Dde_2315	Hypothetical protein	-	-1.67

[a] – represents function uncategorized.

glycosyl/glycerophosphate transferase (Dde_0431) that may be involved in teichoic acid biosynthesis. Significant changes in proteins of this mutant are shown in Table 7.

Mutant D12(pE9) has a mutation in a transcriptional regulator (Dde_1614) with an FadR domain. The FadR regulon is globally connected to the universal stress response of *E. coli*, an important function in bacteria. Global regulator FadR is required for specific alterations in the membrane lipid-fatty acid composition for survival of the cell during fluctuating environmental conditions. FadR, in conjuction with a long-chain fatty acyl-CoA, long-chain acyl-ACP, ppGpp and cAMP, are key players in regulating the activities of enzymes and expression of genes involved in fatty acid and phospholipid metabolism in dividing and ageing *E. coli* cells [58]. Mutations in FadR result in an aseptate morphology during rapid growth, accumulation of cardiolipin, cell lysis, and poor stasis survival. However, no universal stress proteins or phospholipid metabolism-related proteins were observed to undergo significant changes in this mutant. Interestingly, the abundances of ferritin (Dde_1791) and hybrid cluster protein (Dde_2641) were reduced in this mutant. Ferritins are widespread in all domains of life, including aerobic and anaerobic organisms. Ferritins function by detoxifying iron or protecting against O_2 and its radical products [59]. Hybrid cluster proteins (HCPs) contain two types of Fe-S clusters and a novel type of hybrid cluster. The first HCPs were isolated from sulfate-reducing bacteria. Subsequent studies found that they were present in a wide range of organisms, including aerobic, anaerobic, and facultative cells from all domains of life [60]. Studies conducted with *E. coli* show that transcription of HCP was induced by hydrogen peroxide, and this induction was regulated by the redox-sensitive transcriptional activator, OxyR. The *E. coli oxyR* mutant exhibited higher sensitivity to

Table 7. Proteins with significant changes in mutant B8(pB6).

Locus	Protein Description	Functional Category[a]	Changes in mutant B8(pB6)
Dde_3523	Alcohol dehydrogenase, iron-containing	C	3.99
Dde_2137	Ni-Fe hydrogenase, small subunit:Twin-arginine translocation pathway signal	C	2.40
Dde_2744	Aminotransferase, class V	E	-2.64
Dde_2664	Diaminopimelate decarboxylase	E	1.59
Dde_2282	Hydantoinase/oxoprolinase family protein	EQ	-1.76
Dde_3685	HPCH/HPAI aldolase family protein	G	-5.45
Dde_2289	Sua5/YciO/YrdC/YwlC	J	-2.34
Dde_0553	Hypothetical protein	K	-2.45
Dde_0349	Transcriptional regulator, LysR family	K	-2.58
Dde_0047	Elongator protein 3/MiaB/NifB	L	-3.49
Dde_1491	Endonuclease III/Nth	L	-2.28
Dde_2565	Conserved hypothetical membrane protein	M	-1.62
Dde_0426	Glycosyl transferase, group 1/2 family protein	M	-2.43
Dde_0431	Similar to Putative glycosyl/glycerophosphate transferases involved in teichoic acid biosynthesis TagF/TagB/EpsJ/RodC	M	-2.55
Dde_2892	Hypothetical protein	M/S	2.29
Dde_0305	AhpC/TSA family protein	O	-1.57
Dde_2099	ATPase	O	-1.53
Dde_1189	Conserved hypothetical protein	P	-3.38
Dde_3248	Rhodanese-like	P	4.50
Dde_0799	Conserved hypothetical protein	R	-2.59
Dde_3139	Conserved hypothetical protein	S	-1.67
Dde_2716	HD domain protein	T	-1.96
Dde_2284	Asparaginase family protein	-	-2.20
Dde_2627	Conserved hypothetical protein	-	2.03
Dde_2038	Conserved hypothetical protein	-	-2.51
Dde_0807	Conserved hypothetical protein	-	-1.66
Dde_2610	Conserved hypothetical protein	-	1.87
Dde_0194	Conserved hypothetical protein	-	-3.52
Dde_3515	Formate dehydrogenase formation protein FdhE, putative	-	-1.71
Dde_1020	Glutamyl-tRNA(Gln) amidotransferase A subunit	-	1.75
Dde_2752	Histone-like bacterial DNA-binding protein	-	-1.72
Dde_0877	Hypothetical protein	-	1.70
Dde_2224	Hypothetical protein	-	2.61
Dde_3026	Hypothetical protein	-	2.82

[a] – represents function uncategorized.

hydrogen peroxide [60]. These results may indicate that HCP is involved in oxidative stress protection. Significant changes including 17 proteins with high abundance values and 35 proteins with low abundance values in this mutant are shown in Table 8.

5. Other proteins:

Proteins involved in energy metabolism. Seventy-four proteins detected in the samples were involved in energy production and conversion. Key proteins involved in energy metabolism were detected and are listed in Supplementary Table 2. The majority of proteins observed showed no significant changes, and the consistent protein levels in these mutants indicate that they are not regulated by these regulatory genes. Three hydrogenases (Dde_1213, Dde_2138, and Dde_2281) were detected in all the strains, at similar abundance levels. Major components of an ATP synthase were also identified and comparative analysis showed that ATP synthase proteins had similar abundance value in mutants, indicating that the interrupted genes in our mutants do not regulate ATP synthesis in G20. Several nitroreductases were detected, suggesting that nitrate reduction is an inherent feature of strain G20. There was no indication that the H_2 cycle, CO cycle, or the formate cycle had any differential impact on sediment survival within these mutants.

Stress proteins. We suspected that some of the regulated proteins would be universal stress proteins and heat shock proteins, due to their functions related to the stress response. Universal stress proteins were found to be important for the protection of cells under salt, oxygen, heat, or osmolarity stresses [61, 62]. The production of these protein were found to be stimulated by a large variety of conditions, such as stationary phase, and carbon starvation [61, 63]. Heat shock proteins (HSPs) also play important roles in the

Table 8. Proteins with significant changes in mutant D12(pE9).

Locus	Protein Description	Functional Category[a]	Changes in mutant D12(pE9)
Dde_1793	2-oxoacid:acceptor oxidoreductase, beta subunit, pyruvate/2-ketoisovalerate	C	-1.61
Dde_1359	Elongator protein 3/MiaB/NifB	C	-1.78
Dde_3775	Ferredoxin I	C	2.56
Dde_2642	Iron-sulfur cluster-binding protein	C	-1.56
Dde_0086	Oxygen-insensitive NAD(P)H nitroreductase	C	2.29
Dde_1792	Pyruvate ferredoxin oxidoreductase, alpha subunit	C	-1.53
Dde_0046	Pyruvate ferredoxin/flavodoxin oxidoreductase family protein	C	1.66
Dde_2744	Aminotransferase, class V	E	-2.46
Dde_2282	Hydantoinase/oxoprolinase family protein	EQ	-1.67
Dde_2285	1,4-alpha-glucan branching enzyme	G	-1.93
Dde_3736	Glyceraldehyde-3-phosphate dehydrogenase, type I	G	-1.69
Dde_3685	HPCH/HPAI aldolase family protein	G	-5.20
Dde_0801	Precorrin-4 C11-methyltransferase region	H	-1.56
Dde_2844	Queuine/other tRNA-ribosyltransferase:Queuine tRNA-ribosyltransferase	J	4.43
Dde_2289	Sua5/YciO/YrdC/YwlC	J	-2.25
Dde_0349	Transcriptional regulator, LysR family	K	-2.49
Dde_2457	HDIG	KT	1.58
Dde_3571	ATP-dependent DNA helicase, UvrD/REP family	L	3.10
Dde_0542	Formamidopyrimidine-DNA glycolase	L	-1.60
Dde_0831	Chain length determinant family protein	M	-2.26
Dde_0426	Glycosyl transferase, group 1/2 family protein	M	-2.34
Dde_2734	Bacterial chemotaxis sensory transducer	NT	-1.79
Dde_2560	Alkyl hydroperoxide reductase	O	-2.09
Dde_2099	ATPase	O	-1.64
Dde_3546	Conserved hypothetical protein	O	-1.78
Dde_2946	HflK	O	1.51
Dde_2068	Peptidase M22, glycoprotease	O	1.58
Dde_1189	Conserved hypothetical protein	P	-3.28
Dde_1791	Ferritin	P	-1.53
Dde_1774	Conserved hypothetical protein	R	-1.79
Dde_0793	RNA-binding region RNP-1 (RNA recognition motif)	R	2.32
Dde_1822	Similar to Uncharacterized protein SCO1/SenC/PrrC involved in biogenesis of respiratory and photosynthetic systems	R	1.79
Dde_3468	Tyrosine protein kinase:Serine/threonine protein kinase	RTKL	-2.54
Dde_2303	Hypothetical protein	S	-2.71
Dde_1116	MJ0042 finger-like region	S	2.40
Dde_0160	ATP-binding region, ATPase-like	T	-2.63
Dde_3535	ATP-binding region, ATPase-like:Histidine kinase A, N-terminal	T	-1.52
Dde_2716	HD domain protein	T	-1.87
Dde_1016	Helix-turn-helix, Fis-type	T	-2.03

Dde_2519	Zn-finger, prokaryotic DksA/TraR C4 type	T	1.92
Dde_2284	Asparaginase family protein	-	-2.11
Dde_2627	Conserved hypothetical protein	-	2.36
Dde_2038	Conserved hypothetical protein	-	-2.41
Dde_2169	Conserved hypothetical protein	-	-2.05
Dde_2610	Conserved hypothetical protein	-	2.30
Dde_1811	Conserved hypothetical protein	-	-1.60
Dde_3515	Formate dehydrogenase formation protein FdhE, putative	-	-1.62
Dde_2641	Hybrid cluster protein	-	-2.64
Dde_2224	Hypothetical protein	-	2.48
Dde_3026	Hypothetical protein	-	3.34
Dde_2315	Hypothetical protein	-	-2.12
Dde_2886	Methyltransferase FkbM	-	1.64

[a] – represents function uncategorized.

responses to the different environmental onslaughts, not only heat. In some cases, HSPs are also linked to resistance to DNA-damaging agents and to respiratory uncouplers [12, 62, 64]. Both the specific protection against an acute emerging stress, as well as the non-specific, prospective protection against future stress, are adaptive functions crucial for surviving stress and low-nutrient conditions in nature.

Recent transcriptomic analyses in *D. vulgaris* showed that many genes have augmented expression levels under salt stress, nitrite stress, and heat stress [11-13]. Stress proteins are known to play important roles in protecting cells from sudden environmental changes. Several universal stress proteins and heat shock proteins were detected in the proteome (Supplementary Table 3). No significant changes in stress proteins were observed in our proteomic data. This may indicate that, under our growth condition, the cells are not experiencing sudden changes, thus stress proteins cannot be revealed in this study. This result also indicates that during exponential phase cells did not encounter similar significant stresses as cells that enter stationary phase [65, 66].

Ribosomal proteins. Ribosomal proteins were predicted to be the most abundant proteins in the bacterial cells during the exponential phase and were expected to be present in high numbers. In agreement with this prediction, we identified 50 ribosomal proteins (see Supplementary Table 4), representing 91% of the total number of predicted ribosomal proteins. Ribosomal protein synthesis consumes more than 50% of the cells total energy [67]. However, we are not aware of any study that proposes a role for ribosomal proteins in sediment growth or adaptation. Indeed, ribosomal proteins exist in certain ratios when forming ribosomes [68], with most ribosomal proteins being present in a single copy. Therefore, you would expect that all of the ribosomal proteins should be

present in similar amounts in the cell. However, our proteomic data do not support this idea, as some ribosomal proteins are more abundant than others. The $G20_{sediment}$ strain had similar abundance values for ribosomal proteins when compared to the $G20_{lab}$ strain. On the other hand, the mutants had a few ribosomal proteins at either higher or lower abundance. It is unknown whether synthesizing ribosomal proteins at the different ratio is a disadvantage when cells are growing in the sediment. In addition, ribosomal-associated proteins, e.g., amino-acyl-tRNA synthetases, and translational elongation factors, were also detected in this study. A total of 32 genes encoding putative amino-acyl-tRNA synthetase have been found in the *D. desulfuricans* G20 genome, and 21 of their proteins were detected in this study (see Supplementary Table 4). Amino-acyl-tRNA synthetases are essential proteins for ensuring the fidelity of transfer of genetic information from the DNA into the protein [69]. Their similar abundances in exponential phase samples from all mutants may explain the similar growth rate in laboratory media.

Conclusions

Our proteomic profiles of $G20_{sediment}$ and $G20_{lab}$ provide us with the direct evidence that, at the protein level, well-adapted lab strains have different features from less adapted sediment strains.

Proteomic analyses of sediment fitness mutants provide the opportunity to look at the global regulation of genes involved in many biological processes, although the observed phenomena may not always be a direct consequence of interruption of each TCS. Indeed, single protein changes may reflect complex shifts in cellular physiology. However, further studies to identify the nature of the suggested functional interactions

between TCSs should shed light on the TCS networks in G20. The limitation of this study is that we only used one growth phase and one growth condition for culturing and comparing the different mutants. Many TCSs, operating under specific growth conditions, may not have been strongly induced under the growth condition we used. In general, no attempt was made to ascertain whether these differences were attributable to the loss of the two-component system *per se,* or to the loss of the function of a nearby gene(s). Further studies may elucidate specific functions.

The AMT tag approach is a powerful tool that may help identify the regulatory networks of signal transduction systems since growth condition changes and their corresponding effects can be monitored over a high number of proteins over a large dynamic range.

References

1. Postgate, J. R., *The sulfate reducing bacteria*. 2nd Edition ed.; Cambridge University Press: Cambridge, 1984.

2. Lovley, D. R.; Phillips, E. J., Reduction of uranium by *Desulfovibrio desulfuricans*. *Appl Environ Microbiol* **1992,** 58, (3), 850-6.

3. Lloyd, J. R.; Ridley, J.; Khizniak, T.; Lyalikova, N. N.; Macaskie, L. E., Reduction of technetium by *Desulfovibrio desulfuricans*: biocatalyst characterization and use in a flowthrough bioreactor. *Appl Environ Microbiol* **1999,** 65, (6), 2691-6.

4. Tucker, M. D.; Barton, L. L.; Thomson, B. M., Removal of U and Mo from water by immobilized *Desulfovibrio desulfuricans* in column reactors. *Biotechnol Bioeng* **1998,** 60, (1), 88-96.

5. Rapp-Giles, B. J.; Casalot, L.; English, R. S.; Ringbauer, J. A., Jr.; Dolla, A.; Wall, J. D., Cytochrome c(3) mutants of *Desulfovibrio desulfuricans*. *Appl Environ Microbiol* **2000,** 66, (2), 671-7.

6. Pollock, W. B.; Voordouw, G., Molecular biology of c-type cytochromes from *Desulfovibrio vulgaris* Hildenborough. *Biochimie* **1994,** 76, (6), 554-60.

7. Risatti, J. B.; Capman, W. C.; Stahl, D. A., Community structure of a microbial mat: the phylogenetic dimension. *Proc Natl Acad Sci U S A* **1994,** 91, (21), 10173-7.

8. Dykhuizen, D. E.; Hartl, D. L., Selection in chemostats. *Microbiol Rev* **1983,** 47, (2), 150-68.

9. Groh, J. L.; Luo, Q.; Ballard, J. D.; Krumholz, L. R., A method adapting microarray technology for signature-tagged mutagenesis of *Desulfovibrio desulfuricans*

G20 and *Shewanella oneidensis* MR-1 in anaerobic sediment survival experiments. *Appl Environ Microbiol* **2005,** 71, (11), 7064-74.

10. Luo, Q.; Groh, J. L.; Ballard, J. D.; Krumholz, L. R., Identification of *Desulfovibrio desulfuricans* G20 genes that confer sediment fitness using signature-tagged mutagenesis. *Environmental Microbiology* **submit**.

11. Mukhopadhyay, A.; He, Z.; Alm, E. J.; Arkin, A. P.; Baidoo, E. E.; Borglin, S. C.; Chen, W.; Hazen, T. C.; He, Q.; Holman, H. Y.; Huang, K.; Huang, R.; Joyner, D. C.; Katz, N.; Keller, M.; Oeller, P.; Redding, A.; Sun, J.; Wall, J.; Wei, J.; Yang, Z.; Yen, H. C.; Zhou, J.; Keasling, J. D., Salt stress in *Desulfovibrio vulgaris* Hildenborough: an integrated genomics approach. *J Bacteriol* **2006,** 188, (11), 4068-78.

12. Chhabra, S. R.; He, Q.; Huang, K. H.; Gaucher, S. P.; Alm, E. J.; He, Z.; Hadi, M. Z.; Hazen, T. C.; Wall, J. D.; Zhou, J.; Arkin, A. P.; Singh, A. K., Global analysis of heat shock response in *Desulfovibrio vulgaris* Hildenborough. *J Bacteriol* **2006,** 188, (5), 1817-28.

13. He, Q.; Huang, K. H.; He, Z.; Alm, E. J.; Fields, M. W.; Hazen, T. C.; Arkin, A. P.; Wall, J. D.; Zhou, J., Energetic consequences of nitrite stress in *Desulfovibrio vulgaris* Hildenborough, inferred from global transcriptional analysis. *Appl Environ Microbiol* **2006,** 72, (6), 4370-81.

14. Clark, M. E.; He, Q.; He, Z.; Huang, K. H.; Alm, E. J.; Wan, X. F.; Hazen, T. C.; Arkin, A. P.; Wall, J. D.; Zhou, J. Z.; Fields, M. W., Temporal Transcriptomic Analysis as *Desulfovibrio vulgaris* Hildenborough Transitions into Stationary Phase during Electron Donor Depletion. *Appl Environ Microbiol* **2006,** 72, (8), 5578-88.

15. Zhang, W.; Culley, D. E.; Scholten, J. C.; Hogan, M.; Vitiritti, L.; Brockman, F. J., Global transcriptomic analysis of *Desulfovibrio vulgaris* on different electron donors. *Antonie Van Leeuwenhoek* **2006,** 89, (2), 221-37.

16. Nie, L.; Wu, G.; Zhang, W., Correlation between mRNA and protein abundance in *Desulfovibrio vulgaris*: a multiple regression to identify sources of variations. *Biochem Biophys Res Commun* **2006,** 339, (2), 603-10.

17. Zhang, W.; Gritsenko, M. A.; Moore, R. J.; Culley, D. E.; Nie, L.; Petritis, K.; Strittmatter, E. F.; Camp, D. G., 2nd; Smith, R. D.; Brockman, F. J., A proteomic view of *Desulfovibrio vulgaris* metabolism as determined by liquid chromatography coupled with tandem mass spectrometry. *Proteomics* **2006**.

18. Ding, Y. H.; Hixson, K. K.; Giometti, C. S.; Stanley, A.; Esteve-Nunez, A.; Khare, T.; Tollaksen, S. L.; Zhu, W.; Adkins, J. N.; Lipton, M. S.; Smith, R. D.; Mester, T.; Lovley, D. R., The proteome of dissimilatory metal-reducing microorganism *Geobacter sulfurreducens* under various growth conditions. *Biochim Biophys Acta* **2006,** 1764, (7), 1198-206.

19. Fang, R.; Elias, D. A.; Monroe, M. E.; Shen, Y.; McIntosh, M.; Wang, P.; Goddard, C. D.; Callister, S. J.; Moore, R. J.; Gorby, Y. A.; Adkins, J. N.; Fredrickson, J. K.; Lipton, M. S.; Smith, R. D., Differential label-free quantitative proteomic analysis of *Shewanella oneidensis* cultured under aerobic and suboxic conditions by accurate mass and time tag approach. *Mol Cell Proteomics* **2006,** 5, (4), 714-25.

20. Smith, R. D.; Anderson, G. A.; Lipton, M. S.; Pasa-Tolic, L.; Shen, Y.; Conrads, T. P.; Veenstra, T. D.; Udseth, H. R., An accurate mass tag strategy for quantitative and high-throughput proteome measurements. *Proteomics* **2002,** 2, (5), 513-23.

21. Rapp, B. J.; Wall, J. D., Genetic transfer in *Desulfovibrio desulfuricans*. *Proc Natl Acad Sci U S A* **1987,** 84, (24), 9128-30.

22. Steger, J. L.; Vincent, C.; Ballard, J. D.; Krumholz, L. R., *Desulfovibrio* sp. genes involved in the respiration of sulfate during metabolism of hydrogen and lactate. *Appl Environ Microbiol* **2002,** 68, (4), 1932-1937.

23. Masselon, C.; Pasa-Tolic, L.; Tolic, N.; Anderson, G. A.; Bogdanov, B.; Vilkov, A. N.; Shen, Y.; Zhao, R.; Qian, W. J.; Lipton, M. S.; Camp, D. G., 2nd; Smith, R. D., Targeted comparative proteomics by liquid chromatography-tandem fourier ion cyclotron resonance mass spectrometry. *Anal Chem* **2005,** 77, (2), 400-6.

24. Shen, Y.; Tolic, N.; Zhao, R.; Pasa-Tolic, L.; Li, L.; Berger, S. J.; Harkewicz, R.; Anderson, G. A.; Belov, M. E.; Smith, R. D., High-throughput proteomics using high-efficiency multiple-capillary liquid chromatography with on-line high-performance ESI FTICR mass spectrometry. *Anal Chem* **2001,** 73, (13), 3011-21.

25. Qian, W. J.; Liu, T.; Monroe, M. E.; Strittmatter, E. F.; Jacobs, J. M.; Kangas, L. J.; Petritis, K.; Camp, D. G., 2nd; Smith, R. D., Probability-based evaluation of peptide and protein identifications from tandem mass spectrometry and SEQUEST analysis: the human proteome. *J Proteome Res* **2005,** 4, (1), 53-62.

26. Fujiki, Y.; Hubbard, A. L.; Fowler, S.; Lazarow, P. B., Isolation of intracellular membranes by means of sodium carbonate treatment: application to endoplasmic reticulum. *J Cell Biol* **1982,** 93, (1), 97-102.

27. Strittmatter, E. F.; Kangas, L. J.; Petritis, K.; Mottaz, H. M.; Anderson, G. A.; Shen, Y.; Jacobs, J. M.; Camp, D. G., 2nd; Smith, R. D., Application of peptide LC

retention time information in a discriminant function for peptide identification by tandem mass spectrometry. *J Proteome Res* **2004,** 3, (4), 760-9.

28. Elias, D. A.; Monroe, M. E.; Marshall, M. J.; Romine, M. F.; Belieav, A. S.; Fredrickson, J. K.; Anderson, G. A.; Smith, R. D.; Lipton, M. S., Global detection and characterization of hypothetical proteins in *Shewanella oneidensis* MR-1 using LC-MS based proteomics. *Proteomics* **2005,** 5, (12), 3120-30.

29. Sharp, P. M.; Li, W. H., The codon Adaptation Index--a measure of directional synonymous codon usage bias, and its potential applications. *Nucleic Acids Res* **1987,** 15, (3), 1281-95.

30. Smith, D. W., *Ecological actions of sulfate-reducing bacteria*. Springer-Verlag: New York, 1993.

31. Pieulle, L.; Guigliarelli, B.; Asso, M.; Dole, F.; Bernadac, A.; Hatchikian, E. C., Isolation and characterization of the pyruvate-ferredoxin oxidoreductase from the sulfate-reducing bacterium *Desulfovibrio africanus. Biochim Biophys Acta* **1995,** 1250, (1), 49-59.

32. Tardif, K. D.; Horowitz, J., Functional group recognition at the aminoacylation and editing sites of *E. coli* valyl-tRNA synthetase. *Rna* **2004,** 10, (3), 493-503.

33. Curnow, A. W.; Hong, K.; Yuan, R.; Kim, S.; Martins, O.; Winkler, W.; Henkin, T. M.; Soll, D., Glu-tRNAGln amidotransferase: a novel heterotrimeric enzyme required for correct decoding of glutamine codons during translation. *Proc Natl Acad Sci U S A* **1997,** 94, (22), 11819-26.

34. Jensen, R. A.; Calhoun, D. H., Intracellular roles of microbial aminotransferases: overlap enzymes across different biochemical pathways. *Crit Rev Microbiol* **1981,** 8, (3), 229-66.

35. Umbarger, H. E.; Mueller, J. H., Isoleucine and valine metabolism of *Escherichia coli*. I. Growth studies on amino acid-deficient mutants. *J Biol Chem* **1951,** 189, (1), 277-85.

36. Garrick-Silversmith, L.; Hartman, P. E., Histidine-requiring mutants of *Escherichia coli* K12. *Genetics* **1970,** 66, (2), 231-44.

37. Stoner, G. L.; Eisenberg, M. A., Purification and properties of 7, 8-diaminopelargonic acid aminotransferase. *J Biol Chem* **1975,** 250, (11), 4029-36.

38. Sedgwick, B., Repairing DNA-methylation damage. *Nat Rev Mol Cell Biol* **2004,** 5, (2), 148-57.

39. Pierrel, F.; Douki, T.; Fontecave, M.; Atta, M., MiaB protein is a bifunctional radical-S-adenosylmethionine enzyme involved in thiolation and methylation of tRNA. *J Biol Chem* **2004,** 279, (46), 47555-63.

40. Ottemann, K. M.; Miller, J. F., Roles for motility in bacterial-host interactions. *Mol Microbiol* **1997,** 24, (6), 1109-17.

41. Schlindwein, C.; Giordano, G.; Santini, C. L.; Mandrand, M. A., Identification and expression of the *Escherichia coli* fdhD and fdhE genes, which are involved in the formation of respiratory formate dehydrogenase. *J Bacteriol* **1990,** 172, (10), 6112-21.

42. West, A. H.; Stock, A. M., Histidine kinases and response regulator proteins in two-component signaling systems. *Trends Biochem Sci* **2001,** 26, (6), 369-76.

43. Gal-Mor, O.; Borovok, I.; Av-Gay, Y.; Cohen, G.; Aharonowitz, Y., Gene organization in the trxA/B-oriC region of the Streptomyces coelicolor chromosome and comparison with other eubacteria. *Gene* **1998,** 217, (1-2), 83-90.

44. Oshima, T.; Aiba, H.; Masuda, Y.; Kanaya, S.; Sugiura, M.; Wanner, B. L.; Mori, H.; Mizuno, T., Transcriptome analysis of all two-component regulatory system mutants of *Escherichia coli* K-12. *Mol Microbiol* **2002,** 46, (1), 281-91.

45. Raffa, R. G.; Raivio, T. L., A third envelope stress signal transduction pathway in *Escherichia coli*. *Mol Microbiol* **2002,** 45, (6), 1599-611.

46. Baranova, N.; Nikaido, H., The baeSR two-component regulatory system activates transcription of the yegMNOB (mdtABCD) transporter gene cluster in *Escherichia coli* and increases its resistance to novobiocin and deoxycholate. *J Bacteriol* **2002,** 184, (15), 4168-76.

47. Nagakubo, S.; Nishino, K.; Hirata, T.; Yamaguchi, A., The putative response regulator BaeR stimulates multidrug resistance of *Escherichia coli* via a novel multidrug exporter system, MdtABC. *J Bacteriol* **2002,** 184, (15), 4161-7.

48. Zhou, L.; Lei, X. H.; Bochner, B. R.; Wanner, B. L., Phenotype microarray analysis of *Escherichia coli* K-12 mutants with deletions of all two-component systems. *J Bacteriol* **2003,** 185, (16), 4956-72.

49. Winfield, M. D.; Groisman, E. A., Phenotypic differences between *Salmonella* and *Escherichia coli* resulting from the disparate regulation of homologous genes. *Proc Natl Acad Sci U S A* **2004,** 101, (49), 17162-7.

50. Lioliou, E. E.; Kyriakidis, D. A., The role of bacterial antizyme: From an inhibitory protein to AtoC transcriptional regulator. *Microb Cell Fact* **2004,** 3, (1), 8.

51. Blackledge, M. J.; Guerlesquin, F.; Marion, D., Comparison of low oxidoreduction potential cytochrome c553 from *Desulfovibrio vulgaris* with the class I cytochrome c family. *Proteins* **1996,** 24, (2), 178-94.

52. Gardan, R.; Rapoport, G.; Debarbouille, M., Role of the transcriptional activator RocR in the arginine-degradation pathway of *Bacillus subtilis*. *Mol Microbiol* **1997,** 24, (4), 825-37.

53. Coulter, E. D.; Kurtz, D. M., Jr., A role for rubredoxin in oxidative stress protection in *Desulfovibrio vulgaris*: catalytic electron transfer to rubrerythrin and two-iron superoxide reductase. *Arch Biochem Biophys* **2001,** 394, (1), 76-86.

54. Jonsson, I. M.; Arvidson, S.; Foster, S.; Tarkowski, A., Sigma factor B and RsbU are required for virulence in *Staphylococcus aureus*-induced arthritis and sepsis. *Infect Immun* **2004,** 72, (10), 6106-11.

55. Knobloch, J. K.; Jager, S.; Horstkotte, M. A.; Rohde, H.; Mack, D., RsbU-dependent regulation of *Staphylococcus epidermidis* biofilm formation is mediated via the alternative sigma factor sigmaB by repression of the negative regulator gene icaR. *Infect Immun* **2004,** 72, (7), 3838-48.

56. Walters, S. B.; Dubnau, E.; Kolesnikova, I.; Laval, F.; Daffe, M.; Smith, I., The *Mycobacterium tuberculosis* PhoPR two-component system regulates genes essential for virulence and complex lipid biosynthesis. *Mol Microbiol* **2006,** 60, (2), 312-30.

57. Marraffini, L. A.; Dedent, A. C.; Schneewind, O., Sortases and the art of anchoring proteins to the envelopes of gram-positive bacteria. *Microbiol Mol Biol Rev* **2006,** 70, (1), 192-221.

58. DiRusso, C. C.; Nystrom, T., The fats of *Escherichia coli* during infancy and old age: regulation by global regulators, alarmones and lipid intermediates. *Mol Microbiol* **1998,** 27, (1), 1-8.

59. Carrondo, M. A., Ferritins, iron uptake and storage from the bacterioferritin viewpoint. *Embo J* **2003,** 22, (9), 1959-68.

60. Almeida, C. C.; Romao, C. V.; Lindley, P. F.; Teixeira, M.; Saraiva, L. M., The role of the hybrid-cluster protein in oxidative stress defense. *J Biol Chem* **2006**.

61. Kvint, K.; Nachin, L.; Diez, A.; Nystrom, T., The bacterial universal stress protein: function and regulation. *Curr Opin Microbiol* **2003,** 6, (2), 140-5.

62. Hecker, M.; Volker, U., General stress response of *Bacillus subtilis* and other bacteria. *Adv Microb Physiol* **2001,** 44, 35-91.

63. Siegele, D. A., Universal stress proteins in *Escherichia coli. J Bacteriol* **2005,** 187, (18), 6253-4.

64. Schumann, W., The *Bacillus subtilis* heat shock stimulon. *Cell Stress Chaperones* **2003,** 8, (3), 207-17.

65. Cohen, D. P.; Renes, J.; Bouwman, F. G.; Zoetendal, E. G.; Mariman, E.; de Vos, W. M.; Vaughan, E. E., Proteomic analysis of log to stationary growth phase *Lactobacillus plantarum* cells and a 2-DE database. *Proteomics* **2006**.

66. Beyer-Sehlmeyer, G.; Kreikemeyer, B.; Horster, A.; Podbielski, A., Analysis of the growth phase-associated transcriptome of *Streptococcus pyogenes*. *Int J Med Microbiol* **2005,** 295, (3), 161-77.

67. Madina Iskakova, S. R. C., Knud H. Nierhaus, *Regulation of ribosome biosynthesis in Escherichia coli*. Wiley-Vch Verlag Gmbh & Co.. KGaA: Weinheim, Germany, 2004; p 429-448.

68. Lewin, B., *Ribosomes provide a translation factory*. Oxford University Press: USA, 1995; Vol. V.

69. Szymanski, M.; Deniziak, M.; Barciszewski, J., The new aspects of aminoacyl-tRNA synthetases. *Acta Biochim Pol* **2000,** 47, (3), 821-34.

Supplementary Table 1. Abundances of sulfate reduction-related proteins in different mutants.

Locus	Protein Description	Abundance value in:							
		A1(pD3)	B8(pB6)	D12(pB8)	D12(pE9)	G5(pA9)	H9(pF8)	G20sedi	G20lab
Dde_2265	ATP-sulfurylase	3.49	3.67	3.48	3.72	3.62	3.58	3.34	3.47
Dde_1778	Inorganic pyrophosphatase, manganese-dependent	3.47	3.52	3.28	4.08	3.63	3.55	3.27	3.31
Dde_1110	Adenylylsulfate reductase, alpha subunit	3.42	3.68	3.56	3.88	3.69	3.60	3.22	3.41
Dde_1109	Adenylylsulfate reductase, beta subunit	3.83	3.88	3.83	4.42	4.17	3.91	3.77	3.69
Dde_0526	Sulfite reductase, dissimilatory-type alpha subunit	2.82	2.81	2.72	3.24	3.22	3.06	2.77	2.70
Dde_0527	Sulfite reductase, dissimilatory-type beta subunit	3.07	3.08	2.84	3.35	3.03	2.86	2.88	2.93
Dde_0528	Dissimilatory sulfite reductase B	2.55	2.65	2.83	3.65	2.52	2.54	2.45	3.45
Dde_0762	Dissimilatory sulfite reductase, gamma subunit	3.81	3.62	3.48	4.22	3.89	3.56	3.62	3.70

Supplementary Table 2. Proteins involved in energy metabolism.

Locus	Protein Description	Change in abuncance at [a]:						
		A1(pD3)	B8(pB6)	D12(pB8)	D12(pE9)	G5(pA9)	H9(pF8)	G20lab
Dde_1690	2-oxoglutarate dehydrogenase, E3 component, lipoamide dehydrogenase	0.28	0.15	0.02	0.17	0.24	0.13	0.25
Dde_3222	3-isopropylmalate dehydrogenase	-0.57	0.79	0.49	-1.02	-0.15	-0.22	0.20
Dde_3242	Acetate kinase	0.04	-0.05	0.01	0.39	0.29	0.21	-0.03
Dde_0050	Alcohol dehydrogenase, iron-containing	-0.65	-0.69	-0.61	-0.90	-0.76	-0.78	0.00
Dde_1164	Alcohol dehydrogenase, iron-containing	-0.41	-0.19	-0.60	-0.97	-0.74	-0.61	0.13
Dde_3539	Aldehyde oxidoreductase	0.02	-0.08	0.00	-0.50	-0.33	-0.30	-0.05
Dde_2460	Aldehyde:ferredoxin oxidoreductase, tungsten-containing	0.40	-0.52	-0.30	0.01	0.09	-0.23	0.64
Dde_0990	ATP synthase F0, B' subunit, putative	0.88	0.28	0.95	-0.07	0.49	0.48	0.10
Dde_0989	ATP synthase F0, subunit B	0.70	0.55	0.99	0.27	0.56	0.66	0.21
Dde_0987	ATP synthase F1, alpha subunit	0.49	0.56	0.14	0.64	0.55	0.33	0.12
Dde_0985	ATP synthase F1, beta subunit	0.33	0.37	0.25	0.69	0.55	0.48	0.03
Dde_3244	Conserved hypothetical protein	0.13	0.20	-0.32	0.61	0.53	0.35	-0.94
Dde_1842	Cysteine-rich domain protein	-0.43	0.35	0.34	0.39	0.22	0.02	-0.01
Dde_1821	Cytochrome c-553	-0.83	-0.33	-0.32	-1.34	**-1.59**	**-1.96**	0.31
Dde_0750	Dehydrogenase, FMN-dependent family	-0.48	-0.68	-0.74	-0.91	-0.69	-0.80	0.30
Dde_0057	Dihydroorotate dehydrogenase, electron transfer subunit	0.07	0.66	0.18	0.44	0.46	0.08	0.08
Dde_0581	Electron transport complex protein RnfC, putative	0.85	0.00	0.21	0.68	0.69	0.91	0.66
Dde_0583	Electron transport complex, RnfABCDGE type, G subunit	-0.20	0.41	0.29	-0.06	0.31	0.24	-0.13
Dde_3709	Ferredoxin, 4Fe-4S, putative	0.15	-0.20	-0.13	-0.45	-0.27	-0.75	-0.11
Dde_3078	Fe-S cluster assembly protein NifU	-0.28	0.31	0.26	-0.30	0.00	0.10	0.00
Dde_0410	Glycerol kinase	-0.34	-0.50	-0.64	-0.44	-0.46	-0.57	-0.08
Dde_3239	Glycolate oxidase, subunit GlcD	0.31	0.18	0.06	0.34	0.10	0.14	0.16
Dde_0988	H+-transporting two-sector ATPase, delta (OSCP) subunit	0.83	0.46	0.40	-0.54	0.26	0.35	0.29
Dde_0986	H+-transporting two-sector ATPase, gamma subunit	0.38	0.63	0.54	0.29	0.62	0.73	0.40
Dde_1208	Heterodisulfide reductase, B subunit	-0.13	0.09	0.15	0.49	0.42	0.50	-0.45
Dde_1207	Heterodisulfide reductase, C subunit	0.24	0.08	0.18	0.18	0.08	0.02	0.04
Dde_1112	Heterodisulfide reductase, iron-sulfur-binding subunit, putative	0.20	0.28	0.22	0.70	0.54	0.46	0.17
Dde_1111	Heterodisulfide reductase, putative	0.23	0.01	0.10	0.26	0.30	0.48	0.25
Dde_1113	Heterodisulfide reductase, transmembrane subunit, putative	0.36	0.20	0.26	-0.18	-0.06	0.05	0.53
Dde_0648	Hmc operon protein 6	0.21	0.35	0.26	0.75	0.71	0.68	0.29
Dde_1213	Hydrogenase, putative	0.04	-0.17	0.05	0.05	0.09	0.00	0.00
Dde_2146	Iron-sulfur cluster-binding protein	0.06	0.05	0.12	0.39	0.03	0.19	0.37
Dde_3240	Iron-sulfur cluster-binding protein	0.60	0.25	0.45	0.58	0.57	0.60	0.22
Dde_3245	Iron-sulfur cluster-binding protein	0.54	0.28	0.30	0.52	0.59	0.72	0.19
Dde_3200	Iron-sulfur cluster-binding/ATPase domain protein	0.22	0.27	0.01	-0.27	-0.47	-0.03	0.02

Dde_3201	Iron-sulfur cluster-binding/ATPase domain protein	-0.06	-0.26	-0.04	-0.81	-0.38	-0.24	0.02
Dde_3476	Isocitrate dehydrogenase, NADP-dependent	0.14	0.31	-0.04	0.26	0.24	0.23	0.07
Dde_2934	Molybdopterin oxidoreductase, iron-sulfur cluster-binding subunit, putative	0.67	0.61	0.58	0.32	0.25	0.59	0.33
Dde_3637	NADP-dependent malic enzyme-related protein	-0.03	-0.16	-0.04	0.01	0.14	0.06	-0.01
Dde_3337	Nigerythrin	-1.06	-0.45	-0.65	-1.44	-1.10	-1.11	-0.14
Dde_2271	Nitrate reductase, gamma subunit, putative	0.67	0.90	1.02	0.33	0.61	0.87	0.15
Dde_1195	Nitroreductase family protein	0.36	0.47	0.56	0.52	0.39	1.01	-0.12
Dde_3604	Oxidoreductase, FAD/iron-sulfur cluster-binding domain protein	-0.18	-0.29	-0.58	-1.44	-0.97	-0.93	-0.05
Dde_3636	Oxidoreductase, NAD-binding, putative	-0.08	-0.29	-0.16	-0.04	0.02	-0.09	-0.06
Dde_1572	PBS lyase HEAT-like repeat	0.24	0.22	0.02	0.56	0.18	0.09	0.32
Dde_2281	Periplasmic [Fe] hydrogenase, large subunit	0.57	0.38	0.51	0.84	0.89	1.02	0.07
Dde_2138	Periplasmic [NiFe] hydrogenase, large subunit, isozyme 1	-0.32	-0.23	-0.29	-1.10	-0.83	-0.93	0.13
Dde_3241	Phosphate acetyltransferase	0.10	-0.06	-0.08	0.05	0.07	0.10	-0.15
Dde_0054	Proline dehydrogenase/delta-1-pyrroline-5-carboxylate dehydrogenase	-0.05	0.02	-0.03	0.12	0.22	0.06	-0.61
Dde_1406	Putative aconitate hydratase	-0.07	-0.31	-0.21	-0.09	-0.01	-0.28	0.06
Dde_2081	Pyruvate carboxylase, putative	0.41	0.12	0.35	0.09	-0.02	0.29	0.00
Dde_1639	Pyruvate ferredoxin oxidoreductase, alpha subunit, putative	0.40	0.06	0.06	-0.35	-0.41	-0.13	0.19
Dde_1637	Pyruvate ferredoxin oxidoreductase, gamma subunit, putative	0.43	-0.45	-0.25	-0.82	-0.81	-0.57	-0.09
Dde_0046	Pyruvate ferredoxin/flavodoxin oxidoreductase family protein	0.22	0.22	0.09	**1.66**	0.17	0.31	**1.62**
Dde_0467	Pyruvate ferredoxin/flavodoxin oxidoreductase family protein	0.32	0.21	0.41	0.26	0.26	0.32	0.02
Dde_0045	Pyruvate ferredoxin/flavodoxin oxidoreductase, beta subunit, putative	0.05	-0.85	0.03	-0.09	0.20	0.24	-1.01
Dde_0044	Pyruvate flavodoxin/ferredoxin oxidoreductase, thiamine diP-binding domain protein	0.16	0.00	0.02	0.03	0.16	0.32	0.12
Dde_3237	Pyruvate:ferredoxin (flavodoxin) oxidoreductase	0.31	0.27	0.43	0.40	0.17	0.34	0.11
Dde_2272	Reductase, iron-sulfur binding subunit, putative	0.46	0.09	0.07	0.38	0.24	0.27	0.02
Dde_2524	Related to nitroreductase	-0.77	-0.51	-0.89	-1.32	-1.25	-1.33	-0.02
Dde_3195	Rubredoxin-oxygen oxidoreductase	-0.28	-0.29	-0.26	-0.41	-0.27	-0.46	-0.01
Dde_1222	Rubrerythrin	-0.13	0.08	0.09	0.07	-0.14	-0.02	-0.38
Dde_1320	Rubrerythrin, putative	-0.11	0.47	0.43	0.29	-0.13	0.18	-0.14
Dde_1079	Sulfite reductase, assimilatory-type	0.92	0.44	0.05	0.78	0.80	0.91	1.01
Dde_2067	Thioredoxin	0.00	0.55	0.05	0.74	-0.28	-0.18	0.52
Dde_0685	Tungsten formylmethanofuran dehydrogenase family protein/molybdopterin binding protein	0.07	-0.30	-0.35	-0.20	-0.35	-0.24	0.09
Dde_0652	Twin-arginine translocation pathway signal	0.26	0.29	0.48	0.59	0.68	0.69	0.14
Dde_2274	Twin-arginine translocation pathway signal	0.50	0.30	0.30	0.42	0.30	0.28	0.26
Dde_2933	Twin-arginine translocation pathway signal	0.53	0.24	0.40	0.07	-0.05	0.30	0.44

[a] Proteins whose change in abundance was at least 1.50 or –1.50 are indicated in bold.

Supplementary Table 3. Abundance changes of detected stress proteins in all samples.

Locus	Protein Description	Changes in mutant [a]:						
		A1(pD3)	B8(pB6)	D12(pB8)	D12(pE9)	G5(pA9)	H9(pF8)	G20sedi[b]
Dde_1454	Universal stress protein family	-0.48	-0.32	-0.18	-0.74	-0.39	-0.42	0.01
Dde_0589	Universal stress protein family	-0.40	-0.20	-0.23	-0.80	-0.61	-0.59	-0.16
Dde_2727	Universal stress protein family	-1.05	-0.06	-0.24	-0.84	-0.40	-0.93	0.52
Dde_3712	Universal stress protein family	-0.35	0.00	0.17	-0.77	-0.40	-0.34	-0.14
Dde_0098	Universal stress protein family	-0.47	0.09	-0.17	-1.15	-1.02	-1.01	-0.03
Dde_2643	Universal stress protein UspA-like protein	-0.29	-0.13	0.19	-0.04	0.24	0.63	0.20
Dde_0227	Carbon starvation protein A, putative	0.71	1.00	0.99	-1.30	-0.17	-0.25	-0.48
Dde_0248	Heat shock protein DnaJ	0.32	0.39	0.49	0.08	0.43	0.73	-0.31
Dde_1659	Heat shock protein DnaJ, N-terminal	0.04	0.64	0.63	0.15	0.20	0.37	-0.08
Dde_1025	Heat shock protein GrpE	-0.32	0.06	0.34	0.15	0.43	0.45	0.17
Dde_2014	Heat shock protein HslU	0.30	0.50	0.56	0.33	0.60	0.74	-0.08
Dde_1023	Heat shock protein Hsp70	-0.27	0.19	0.27	0.05	0.19	0.19	0.19
Dde_1147	Heat shock protein HtpG (Hsp90)	-0.28	-0.02	0.09	-0.43	0.00	-0.05	-0.02
Dde_1343	Heat shock protein, Hsp20 family	-0.33	0.68	0.64	-0.96	0.05	0.05	0.39
Dde_1344	Heat shock protein, Hsp20 family	-0.25	0.76	0.93	-0.78	0.03	0.40	-0.22
Dde_3092	Heat shock protein, Hsp20 family	-0.43	-0.16	0.01	-0.16	-0.01	-0.07	0.32
Dde_3412	Small HspC2 heat shock protein	-0.46	0.19	0.03	-1.01	-0.82	-0.70	-0.19

[a] $\log_2$(ratio) of abundance value for mutant to G20sediment.

[b] $\log_2$(ratio) of abundance value for G20sediment to G20lab.

Supplementary Table 4. Ribosomal proteins and ribosomal-associated proteins detected in this study.

Locus	Protein Description	A1(pD3)	B8(pB6)	D12(pB8)	D12(pE9)	G2(pC4)	G5(pA9)	G9(pD12)	H9(pF8)	G20sedi
Dde_2374	Alanyl-tRNA synthetase, class IIc	0.08	0.22	0.30	0.43	-0.05	0.45	0.52	0.51	-0.15
Dde_2295	Arginyl-tRNA synthetase, class Ic	-0.13	-0.73	-0.55	-0.45	-0.57	-0.37	-0.41	-0.51	0.03
Dde_0099	Asparaginyl-tRNA synthetase, class IIb	-0.03	0.09	0.01	0.15	-0.07	-0.03	0.22	0.00	-0.13
Dde_0012	Aspartyl-tRNA synthetase bacterial/mitochondrial type	0.39	0.21	0.37	0.56	-0.08	0.64	0.77	0.64	-0.10
Dde_2634	Bacterial phenylalanyl-tRNA synthetase, beta subunit	0.58	0.49	0.58	0.76	0.33	0.67	0.88	0.71	-0.02
Dde_2121	Cysteinyl-tRNA synthetase, class Ia	-0.11	-0.17	-0.14	-0.10	-0.21	0.01	0.06	-0.12	0.00
Dde_0626	Glutaminyl-tRNA synthetase	-0.30	-0.32	-0.16	0.10	-0.23	0.13	0.20	-0.19	0.11
Dde_2648	Glutamyl-tRNA synthetase bacterial/mitochondrial	0.16	-0.09	-0.12	-0.04	-0.26	0.20	0.33	0.17	-0.06
Dde_2034	Glycyl-tRNA synthetase, alpha subunit	-0.14	-0.24	-0.31	-0.12	-0.12	0.03	-0.04	-0.31	-0.31
Dde_2033	Glycyl-tRNA synthetase, beta subunit	0.59	-0.01	0.39	0.17	-0.11	0.08	-0.02	-0.04	-0.62
Dde_0011	Histidyl-tRNA synthetase, class IIa	0.05	0.23	0.06	0.11	0.28	0.32	0.41	0.46	-0.05
Dde_2142	Isoleucyl-tRNA synthetase, class Ia	0.17	0.11	0.20	0.37	0.24	0.43	0.58	0.43	-0.16
Dde_2439	Leucyl-tRNA synthetase bacterial/mitochondrial, class Ia	0.36	0.17	0.06	0.35	0.07	0.22	0.34	0.13	-0.03
Dde_1365	Lysyl-tRNA synthetase, class-2	0.44	0.15	0.37	0.48	0.06	0.75	0.88	0.60	-0.02
Dde_1594	Methionyl-tRNA synthetase, class Ia:Methionyl-tRNA synthetase, beta subunit, C-terminal	0.37	0.05	0.00	0.24	-0.08	0.15	0.25	0.14	0.01
Dde_2635	Phenylalanyl-tRNA synthetase, alpha subunit	0.52	0.24	0.22	0.55	-0.13	0.56	0.77	0.63	-0.20
Dde_0196	Seryl-tRNA synthetase, class IIa	0.25	0.29	0.25	0.30	0.14	0.61	0.75	0.52	-0.02
Dde_2639	Threonyl-tRNA synthetase, class Iia	0.31	0.15	0.23	0.48	0.07	0.57	0.47	0.40	-0.10
Dde_3607	Tryptophanyl-tRNA synthetase, class Ib	0.04	-0.26	-0.18	-0.32	-0.66	0.02	0.15	-0.17	0.20
Dde_0228	Tyrosyl-tRNA synthetase, class Ib	0.34	0.32	0.36	0.15	0.10	0.34	0.52	0.50	0.04
Dde_2839	Valyl-tRNA synthetase, class Ia	1.44	0.04	0.10	0.34	-0.12	0.39	0.41	0.39	**-1.66**
Dde_2251	Bacterial ribosomal protein S3	0.21	0.16	0.21	0.27	0.14	0.34	0.50	0.50	0.07
Dde_2993	Ribosomal protein L1, bacterial and chloroplast form	0.27	0.19	0.07	0.28	0.33	0.39	0.42	0.41	-0.16
Dde_2994	Ribosomal protein L10	0.21	0.41	0.55	0.36	0.49	0.53	0.70	0.58	-0.13
Dde_2992	Ribosomal protein L11, bacterial	0.45	0.54	0.19	0.40	0.73	0.30	0.60	0.57	-0.35
Dde_2607	Ribosomal protein L13, bacterial and organelle form	0.48	-0.01	0.21	0.09	0.07	0.26	0.38	0.36	0.00
Dde_2247	Ribosomal protein L14, bacterial and organelle form	0.91	0.89	0.82	1.16	1.25	1.08	1.29	1.30	-0.64
Dde_2238	Ribosomal protein L15, bacterial form	0.44	0.40	0.35	0.31	0.25	0.61	0.59	0.55	-0.10
Dde_2250	Ribosomal protein L16	0.39	0.33	0.29	0.21	0.64	0.32	0.49	0.62	-0.18
Dde_2230	Ribosomal protein L17	0.78	0.95	0.48	0.70	1.01	0.70	0.99	0.89	-0.31
Dde_2241	Ribosomal protein L18	0.30	0.27	0.18	-0.10	-0.59	-0.09	0.40	0.95	0.16
Dde_1095	Ribosomal protein L19	0.46	0.42	0.18	0.56	0.68	0.46	0.77	0.62	-0.08
Dde_2254	Ribosomal protein L2, bacterial and organelle form	0.47	0.37	0.10	0.63	1.03	0.40	0.57	0.50	-0.22
Dde_2636	Ribosomal protein L20, bacterial and organelle form	0.37	0.13	0.08	0.24	0.36	0.46	0.98	0.50	-0.01

Dde_2692	Ribosomal protein L21	0.38	0.32	0.17	0.14	0.08	0.46	0.58	0.57	0.05
Dde_2252	Ribosomal protein L22, bacterial and organelle form	0.37	0.37	0.45	0.66	0.88	0.59	0.70	0.68	0.14
Dde_2255	Ribosomal protein L23	0.51	0.67	0.42	0.48	0.74	0.66	0.79	0.65	-0.23
Dde_2246	Ribosomal protein L24	1.23	1.20	0.46	1.24	1.49	0.59	**1.56**	0.94	-0.32
Dde_2127	Ribosomal protein L25	0.34	0.09	0.00	0.56	0.64	0.17	0.36	0.32	-0.01
Dde_2691	Ribosomal protein L27	0.65	0.49	0.33	0.64	0.71	0.66	0.91	0.74	-0.20
Dde_2425	Ribosomal protein L28	0.23	0.14	0.31	-0.04	0.02	0.43	0.56	0.69	-0.04
Dde_2249	Ribosomal protein L29	0.28	0.24	0.07	0.65	0.88	0.44	0.58	0.51	-0.01
Dde_2257	Ribosomal protein L3	0.43	0.25	0.25	0.28	0.66	0.44	0.57	0.48	-0.12
Dde_2239	Ribosomal protein L30, bacterial	0.48	0.63	0.66	0.29	0.50	0.77	0.97	0.90	-0.19
Dde_2982	Ribosomal protein L31	0.34	0.45	**-1.87**	0.43	0.02	0.41	0.93	0.83	0.19
Dde_2637	Ribosomal protein L35	0.55	0.34	0.53	0.31	0.49	0.53	0.65	0.91	-0.18
Dde_2256	Ribosomal protein L4	0.25	0.29	0.15	0.50	0.86	0.55	0.70	0.64	-0.01
Dde_2245	Ribosomal protein L5	0.45	0.73	0.59	0.48	0.72	0.56	0.92	0.65	-0.35
Dde_2242	Ribosomal protein L6	0.39	0.25	0.19	0.32	0.16	0.39	0.43	0.48	-0.18
Dde_2995	Ribosomal protein L7/L12	-0.42	-1.33	-0.76	0.46	-0.14	-0.16	-0.32	-0.37	0.56
Dde_1410	Ribosomal protein L9	0.10	-0.01	0.00	0.71	0.36	0.43	0.46	0.42	-0.05
Dde_0507	Ribosomal protein S1	0.02	-0.04	0.08	0.54	0.35	0.57	0.49	0.34	0.04
Dde_2258	Ribosomal protein S10, bacterial form	0.29	0.56	0.38	0.47	0.48	0.46	0.65	0.64	-0.24
Dde_2233	Ribosomal protein S11	0.41	0.34	0.22	0.53	0.89	0.21	0.46	0.27	-0.18
Dde_2263	Ribosomal protein S12, bacterial and chloroplast form	0.51	0.66	0.54	0.49	1.04	0.71	0.86	0.88	-0.29
Dde_2234	Ribosomal protein S13	0.17	0.38	0.42	0.41	0.56	0.54	0.58	0.58	-0.09
Dde_2244	Ribosomal protein S14	0.61	0.42	0.24	-0.95	-0.78	0.41	0.84	1.18	-0.32
Dde_3166	Ribosomal protein S15, bacterial chloroplast and mitochondrial type	0.28	0.31	0.41	1.22	**1.82**	0.45	0.47	0.45	-0.18
Dde_1099	Ribosomal protein S16	-0.45	0.38	0.43	0.26	0.65	0.70	0.66	0.35	0.48
Dde_2248	Ribosomal protein S17	0.32	0.71	0.51	0.86	0.87	0.74	0.89	0.73	-0.01
Dde_1411	Ribosomal protein S18	0.22	0.51	0.40	0.43	0.46	0.79	0.85	0.76	0.10
Dde_2253	Ribosomal protein S19, bacterial and organelle form	0.69	0.46	0.03	0.47	0.68	0.29	0.52	0.43	-0.30
Dde_1133	Ribosomal protein S2, bacterial and organelle form	0.54	0.29	0.23	0.32	0.17	0.42	0.66	0.44	0.12
Dde_2031	Ribosomal protein S20p	0.39	0.51	0.45	0.25	-0.19	0.55	0.53	0.89	0.16
Dde_2056	Ribosomal protein S21	0.57	0.40	0.41	0.30	0.99	0.46	0.67	0.86	-0.50
Dde_2232	Ribosomal protein S4, bacterial and organelle form	0.41	0.43	0.35	0.45	0.69	0.53	0.66	0.69	0.02
Dde_2240	Ribosomal protein S5, bacterial and organelle form	0.74	0.33	0.44	-0.10	0.42	0.01	0.33	0.25	-0.37
Dde_1412	Ribosomal protein S6	0.24	0.06	-0.06	0.65	0.52	0.36	0.44	0.31	0.04
Dde_2262	Ribosomal protein S7, bacterial and organelle form	0.33	0.71	0.60	0.46	0.97	0.66	0.72	0.53	0.11
Dde_2243	Ribosomal protein S8	0.55	0.32	0.32	-0.12	-0.27	0.21	0.45	0.38	-0.05
Dde_2608	Ribosomal protein S9	0.48	0.23	0.47	0.20	0.45	0.57	0.77	0.81	-0.23
Dde_1432	Ribosomal protein L11 methyltransferase, putative	0.09	0.11	0.07	0.34	0.41	0.64	0.44	0.46	-0.21
Dde_2011	RNA binding S1	-0.06	-0.41	-0.30	-0.03	-0.44	-0.14	-0.01	-0.10	-0.02
Dde_3167	RNA binding S1:KH	0.29	0.03	0.06	0.27	0.16	0.35	0.51	0.48	-0.02
Dde_3581	RNA methyltransferase TrmH, group 3	0.40	0.36	0.39	0.21	0.28	0.35	0.46	0.61	-0.18
Dde_0974	RNA methyltransferase, TrmH	-0.15	-0.27	-0.61	-0.68	-0.95	-1.23	-1.21	-1.20	0.36

	family									
Dde_0400	RND efflux system, outer membrane lipoprotein, NodT	0.56	0.49	0.49	0.49	0.39	0.39	0.31	0.69	-0.27
Dde_1772	Sigma 54 modulation protein/ribosomal protein S30EA	-0.48	0.13	0.06	-1.19	-0.92	-0.71	-1.06	-0.61	-0.08
Dde_2741	Small GTP-binding protein domain	-0.47	-0.25	-0.28	-1.39	-1.26	-0.97	-1.36	-0.91	-0.07
Dde_2289	Sua5/YciO/YrdC/YwlC	-0.01	**-2.34**	**-2.42**	**-2.25**	**-2.08**	**-2.37**	**-2.35**	**-2.34**	0.10
Dde_2063	Translation elongation factor G:Small GTP-binding protein domain	0.29	0.36	0.06	-0.12	0.05	0.25	0.60	0.38	-0.24
Dde_2261	Translation elongation factor G:Small GTP-binding protein domain	0.24	0.25	0.33	0.76	0.60	0.59	0.80	0.56	-0.12
Dde_2989	Translation elongation factor Tu:Small GTP-binding protein domain	0.19	0.24	-0.13	0.87	0.78	0.52	0.65	0.45	-0.16
Dde_3614	Translation initiation factor IF-1	0.26	0.13	0.15	0.37	0.27	0.73	0.85	0.80	-0.20
Dde_3769	Translation initiation factor IF-1	-0.06	0.15	0.13	0.24	0.41	0.22	0.15	0.59	0.03
Dde_1484	tRNA (guanosine-2'-O-)-methyltransferase	0.67	0.08	0.07	0.24	0.41	-0.09	0.58	0.15	-0.08
Dde_3165	tRNA pseudouridine synthase B	0.40	0.27	-0.04	0.26	0.18	0.17	0.83	0.88	-0.27
Dde_1415	Type I secretion outer membrane protein, TolC	0.23	0.28	0.36	-0.05	-0.41	0.11	-0.03	0.37	-0.09
Dde_0809	YjgF-like protein	-0.21	0.17	0.20	0.51	0.94	0.00	-0.01	0.03	-0.08
Dde_2372	Conserved hypothetical protein	-1.01	-0.53	-0.93	0.32	-0.60	0.08	-0.06	0.15	0.92
Dde_1698	Conserved hypothetical protein 92	0.27	0.17	0.12	0.75	0.06	0.67	0.74	0.51	-0.21
Dde_1953	Elongation factor P	-0.36	-0.67	-0.51	-0.04	-0.44	0.18	0.01	-0.34	0.33
Dde_1422	Gid protein	-0.01	0.15	0.07	0.24	0.41	0.12	0.62	0.24	-0.08
Dde_2615	Glutamyl-tRNA(Gln) amidotransferase B subunit	-0.18	-0.07	-0.09	-0.04	-0.15	0.22	0.15	0.19	0.04
Dde_1021	Glutamyl-tRNA(Gln) amidotransferase C subunit	-0.34	0.31	-0.84	0.46	-0.53	-0.01	0.34	-0.05	-0.01
Dde_2966	HD domain protein	0.07	-0.79	-0.46	-0.54	-1.07	-0.38	-0.38	-0.46	-0.07
Dde_0152	Helicase, C-terminal:DEAD/DEAH box helicase, N-terminal	0.26	-0.53	-0.08	-0.07	-0.30	0.19	0.26	0.10	0.16
Dde_0341	Helicase, C-terminal:DEAD/DEAH box helicase, N-terminal	0.09	-0.13	0.33	-1.27	-1.06	0.44	0.38	0.52	1.16
Dde_3162	Initiation factor 2:Small GTP-binding protein domain	0.26	0.26	0.30	0.04	0.04	0.36	0.54	0.46	-0.10
Dde_2638	Initiation factor 3	-0.51	-0.37	-0.60	-0.45	-0.34	-0.32	-0.32	-0.22	-0.51
Dde_1781	Metallo-beta-lactamase family protein	0.12	-0.05	-0.09	-0.32	-0.24	-0.27	-0.36	-0.24	-0.11
Dde_0014	Methionyl-tRNA formyltransferase	0.12	0.43	0.17	0.35	0.37	0.21	0.35	0.40	0.25
Dde_3627	Outer membrane efflux protein	0.35	-0.15	-0.25	-0.04	-0.39	-0.20	-0.65	-0.23	-0.02
Dde_2236	Peptidase M24A, methionine aminopeptidase, subfamily 1	0.85	0.80	0.43	0.93	0.80	0.67	1.13	0.74	-0.29
Dde_2984	Peptide chain release factor 1	-0.06	-0.19	-0.10	0.02	-0.26	0.18	0.23	0.32	-0.07
Dde_1805	Peptide chain release factor 2	-0.01	0.15	0.07	0.24	0.41	-0.14	0.15	0.15	-0.08
Dde_2206	Prolyl-tRNA synthetase, bacterial	0.50	0.16	0.17	0.36	0.17	0.38	0.56	0.33	-0.16
Dde_2722	Protein of unknown function UPF0004	-0.16	0.00	0.00	-0.43	-1.30	**-1.59**	**-1.56**	**-1.56**	0.16
Dde_0506	Protein of unknown function UPF0004:Conserved hypothetical protein	0.17	0.15	0.07	0.24	0.41	0.12	0.15	0.15	-0.08
Dde_2378	Protein of unknown function UPF0004:tRNA-i(6)A37 modification enzyme MiaB	**-1.52**	-1.37	0.83	-1.27	0.01	-1.39	-1.37	-1.36	1.43
Dde_0539	Protein-L-isoaspartate methyltransferase homolog	0.37	0.79	0.45	0.63	0.54	0.65	0.95	0.73	-0.16

Dde_0076	Putative translation initiation factor, aIF-2BI:Initiation factor 2B alpha/beta/delta	-0.16	-0.25	-0.32	-0.45	-0.42	-0.41	-0.36	-0.23	0.02
Dde_2844	Queuine/other tRNA-ribosyltransferase:Queuine tRNA-ribosyltransferase	0.01	0.15	0.07	**4.43**	0.41	0.12	0.28	0.15	**-3.45**
Dde_0537	Ribonuclease E and G	0.48	0.13	0.22	-0.03	0.09	-0.03	0.15	0.36	-0.23

Appendix 1

Diversity of the Microeukaryotic Community in Sulfide-Rich Zodletone Spring (Oklahoma)

Abstract

The microeukaryotic community in Zodletone Spring, a predominantly anaerobic sulfide and sulfur-rich spring, was examined using an 18S rRNA gene cloning and sequencing approach. The majority of the 288 clones sequenced from three different locations at Zodletone Spring belonged to the *Stramenopiles*, *Alveolata*, and *Fungi*, with members of the phylum *Cercozoa*, order *Diplomonadida*, and family *Jakobidae* representing a minor fraction of the clone library. No sequences suggesting the presence of novel kingdom level diversity were detected in any of the three libraries. A large fraction of stramenopile clones encountered were monophyletic with either members of the genus *Cafeteria* (order *Bicosoecida*) or members of the order *Labyrinthulida* (slime nets), both of which have so far been encountered mainly in marine habitats. The majority of the observed fungal clone sequences belonged to the ascomycetous yeasts (order *Saccharomycetales*), were closely related to yeast genera within the *Hymenobasidiomycetes* (phylum *Basidiomycetes*), or formed a novel fungal lineage with several previously published or database-deposited clones. To determine whether the unexpected abundance of fungal sequences in Zodletone Spring clone libraries represents a general pattern in anaerobic habitats, we generated three clone libraries from three different anaerobic settings (anaerobic sewage digester, pond sediment, and hydrocarbon-exposed aquifer sediments) and partially sequenced 210 of these clones. Phylogenetic

analysis indicated that clone sequences belonging to the kingdom *Fungi* represent a significant fraction of all three clone libraries, an observation confirmed by phospholipid fatty acid and ergosterol analysis. Overall, this work reveals an unexpected abundance of *Fungi* in anaerobic habitats, describes a novel, yet-uncultured group of *Fungi* that appears to be widespread in anaerobic habitats, and indicates that several of the previously considered marine protists could also occur in nonmarine habitats.

Introduction

The utilization of culture-independent approaches for describing microbial assemblages in various ecosystems has altered our view on the breadth of prokaryotic diversity. For example, by extensive 16S rRNA gene-based analysis of various marine and terrestrial ecosystems, the number of bacterial divisions and candidate divisions has increased from 12 in 1987 (68) to at least 52 (53). Similarly, numerous novel archaeal lineages, many of which have a global distribution, have been detected in both marine (11) and terrestrial (7) ecosystems.

Recently, a similar approach utilizing small subunit (SSU) rRNA gene amplification, cloning, and sequencing has been applied to study eukaryotic diversity. The few available studies primarily examined the microeukaryotic community in different marine environments, including the photic and aphotic zones of pelagic oceans (12, 13, 25, 39, 43, 61), anoxic marine salt marsh sediments (60), and hydrothermal vents (17, 38). Collectively, these studies suggest an unexpected level of diversity with the detection of sequences representing potential novel lineages within known eukaryotic groups, as well as sequences suggesting the presence of novel kingdom level diversity

within the microeukaryotic community. The use of 18S rRNA gene-based analysis to study freshwater anaerobic communities has received relatively less attention than marine surveys. However, the work of Dawson and Pace (10) suggests the presence of a similar broad diversity at the kingdom level within freshwater lake sediments.

An argument has recently been presented stating that SSU rRNA surveys overestimate the level of eukaryotic diversity at the megaevolution level (6, 9). The reasoning is that there is an inadequate number of available 18S rRNA gene sequences representing some of these novel fast-evolving groups, chimeric sequences have been incorporated into phylogenetic analysis, long branch attraction artifacts may have occurred, and there are a relatively high number of described eukaryotic taxa with no available sequence data (6).

The present work examines the microeukaryotic communities in Zodletone Spring in southwestern Oklahoma. Zodletone Spring has a high dissolved sulfide concentration in the emergent water (8 to 10 mM) and maintains hypoxic conditions in the water and anoxia in the underlying sediments throughout the course of the spring. Another important characteristic of the spring is the continuous bubbling of short-chain alkanes (methane, ethane, and propane) from the source of the spring, resulting in high hydrocarbon levels, especially in the source area. Recent surveys of the bacterial and archaeal communities in Zodletone Spring revealed an extremely diverse microbial community with several novel bacterial and archaeal lineages (18, 19). The study of the microeukaryotic community in the spring will add to our knowledge regarding microeukaryotes that can thrive under anaerobic conditions in general and under extreme conditions of high sulfide concentrations and hydrocarbon exposure in particular. The

resulting increase in the 18S rRNA gene sequences in databases will lead to better phylogenetic resolution for both known and novel eukaryotic lineages that suffer from low sampling. Also, extensive 18S rRNA gene sampling in Zodletone Spring will allow us to practically test the two previously outlined hypotheses regarding the level of eukaryotic diversity at the kingdom level. Finally, comparing the overall patterns of eukaryotic diversity in Zodletone Spring with patterns observed in other anaerobic environments examined in this and other studies will contribute to our understanding of the global patterns of microeukaryotic diversity within anaerobic habitats. Our results support the view that the number of novel high-level eukaryotic lineages is much lower than previously inferred from other SSU rRNA surveys, and we document the presence of several eukaryotic groups previously thought to be restricted to marine environments. We also show an unexpected abundance of fungi in all studied ecosystems and suggest a wide distribution of a novel fungal lineage in anaerobic environments.

Materials and Methods

Site description. Zodletone Spring emerges near Zodletone Mountain in the Anadarko basin in southwestern Oklahoma. Water emerges at the spring source at a rate of 8 liters/s and flows for about 20 m before discharging at a neighboring creek (Stinking Creek). The source is mainly an anaerobic area of sulfide-saturated sediments which approximately 50 cm of water overlies. As a result of light exposure and constant high sulfide concentrations, microbial mats of differing structures are visible throughout the spring. It has been shown that due to phototrophically driven sulfide oxidation mediated by the spring microbial community, barite and calcite are formed throughout the spring

and as mineral crusts located on the bank of an adjacent creek (55). These crusts appear to precipitate from sulfide-laden groundwater that percolates out of the creek banks.

Sampling. Eukaryotic diversity was examined in three locations in Zodletone Spring: the sulfide-saturated, hydrocarbon-exposed spring source; the microbial mat community; and the bacterial crust formations on the banks of the creek. Samples were collected using a sterile spatula and frozen immediately on dry ice. They were transferred to the laboratory within 3 h of sampling, where they where stored at 20°C. In addition to samples obtained in Zodletone Spring, samples were also obtained from three different anaerobic locations: an anaerobic sewage digester from a sewage treatment plant in Norman, OK (clone library ww), anaerobic sediments from a gas-condensate-contaminated site near Ft. Lupton, CO (clone library ftlp), and anoxic sediment (5 cm deep) from a freshwater pond (duck pond) in Norman, OK (clone library dp). All samples were collected in August 2003, frozen immediately, and stored at 20°C for a maximum of 1 week prior to DNA extraction. Subsurface sediment used for constructing the fl library was collected in June 2001 and stored frozen for 2 years.

DNA extraction, PCR amplification, cloning, and sequencing. DNA isolation was carried out using a lysis-bead-beating protocol (15). The custom primers (Invitrogen Corp., Carlsbad, CA) used for amplifying the 18S rRNA gene were 82f and 1520r (10). We checked the primers for specificity by confirming the length of the amplification product using agarose gel electrophoresis. As well, all sequences obtained from the cloning procedure were 18S rRNA gene sequences. 18S rRNA genes were amplified from the bulk community DNA in a 50-μl reaction mixture containing (final concentration): 2 l of 1:100 dilution of extracted DNA, 1X PCR buffer (Invitrogen), 1.5

mM $MgSO_4$, 0.2 mM (each) deoxynucleoside triphosphate mixture, 2.5 U of platinum Taq DNA polymerase (Invitrogen), and 10 μM (each) forward and reverse primers. PCR amplification was carried out on a Gene Amp PCR system 9700 thermocycler according to the following protocol: denaturation for 5 min at 94°C, 30 cycles of 94°C for 30 s, 55°C for 15 s, and 72°C for 2 min, followed by a final extension at 72°C for 10 min. PCR products were cloned into a TOPO-TA cloning vector and sequenced as previously described (19).

Phylogenetic analysis. Shannon-Weiner Index, species evenness, average nucleotide diversity (θ), and percentage of coverage were determined according to previously described procedures (32, 42). For phylogenetic placement, sequences initially were compared to the GenBank nr database and checked using BLAST (1). Sequences with more than 98% similarity were considered to be of the same operational taxonomic unit (OTU). The generation of chimeric sequences during PCR-based diversity studies has been frequently observed (36), and several studies have demonstrated the accumulation of chimeric bacterial, archaeal (31), and eukaryotic (6) rRNA gene sequences in the databases. The presence of chimeric sequences in our data set was checked by screening all sequences with the CHECK-CHIMERA program, available through the ribosomal database website (40). Also, sequences with low (92%) database similarity were manually inspected to detect the presence of universally conserved regions. In addition, we used a partial treeing analysis approach (31), in which trees were generated using various segments of the 18S rRNA gene sequence and the resulting tree topologies were compared to each other and to the full-length tree. An example of partial treeing analysis for the fungal data set is provided as supplementary

material (see Fig. S1a-c in the supplemental material). Overall, 12 chimeric sequences (10 from Zeuk and 1 each from the dp and ftlp clone libraries) were detected and removed from the data set. Zodletone sequences and GenBank-downloaded sequences were aligned using the ClustalX program (63). The program ModelTest (52) was used to choose the optimum model of DNA substitution for each data set. Phylogenetic trees were constructed using representatives of closely related reference sequences to highlight the phyogenetic affiliation of clones obtained in this study. Evolutionary distance (neighbor-joining algorithm) and maximum-parsimony trees were constructed using PAUP (version 4.01b10; Sinauer Associates, Sunderland, Mass.). Bayesian analysis for the fungal data set were performed with MrBayes version 3.0b4 (30), using the GTRG model of evolution with 500,000 generations run and 5,000 trees sampled. The first 100 trees were discarded, and the consensus tree was computed from the remaining trees using PAUP 4.01b. All phylogenetic trees show the frequencies of occurrence of specific OTUs in the source, mat, and crust clone libraries in parentheses from Zodletone samples (designated Zeuk), as well as in ww, dp, or ftlp libraries.

Phospholipid fatty acid (PLFA) and ergosterol analysis. Sediment or solids were extracted with the single-phase chloroform-methanol buffer system of Bligh and Dyer (8) as modified by White et al. (67). The total lipid extract was fractionated into neutral lipids, glycolipids, and polar lipids by silicic acid column chromatography (28). The neutral lipids (sterols) were saponified and then derivatized with *N,O*-bis(trimethylsilyl)trifluoroacetamide (BSTFA) (46), while the polar lipids were transesterified to the fatty acid methyl esters by a mild alkaline methanolysis (28).

Ergosterol and PLFA methyl esters were analyzed by gas chromatography/ mass

spectroscopy using a Hewlett-Packard 6890 series gas chromatograph interfaced to a Hewlett-Packard 5973 mass selective detector using a 50-m DB-1 column (0.1-mm inner diameter, 0.1-m film thickness). The injector and detector were maintained at 290°C and 300°C, respectively. The column temperature was programmed at 60°C for 1 min, then ramped at 20°C min1 to 150°C, held for 4 min, then ramped at 7°C min1 to 230°C, held for 2 min, and finally ramped at 10°C min1 to 300°C and held for 3 min. Mass spectra were determined by electron impact at 70 eV. Methyl nonadecanonate was used as the internal standard, and the PLFA and ergosterol were expressed as the equivalent peak response to the internal standard.

Nucleotide sequence accession numbers. Sequences obtained in this study were deposited in GenBank under accession numbers AY916560 through AY916665.

Results

Composition and comparative diversity of Zodletone source, mat, and crust clone libraries. A library of 108, 95, and 85 clones was constructed and sequenced from the source, mat, and crust clone libraries, respectively. Figure 1 summarizes the group level affiliation of clone sequences. Clone sequences belonging to the *Stramenopiles*, *Fungi*, and *Alveolata* collectively represented 97, 94, and 93% of the source, mat, and crust clone libraries, respectively, while those belonging to the *Cercozoa*, *Diplomonadida*, and *Jakobidae* represented a minor fraction of the clone libraries. In spite of sequencing a total of 288 clones from Zodletone Spring, no novel kingdom level diversity was detected. Selection for a few dominant species was evident, as five OTUs belonging to the orders *Bicosoecida*, *Labyrinthulida*, and *Bacillariophyceae* made up

Figure 1. Distribution of Zodletone source (black columns), mat (white columns), and crust (gray columns) clones among various eukaryotic groups.

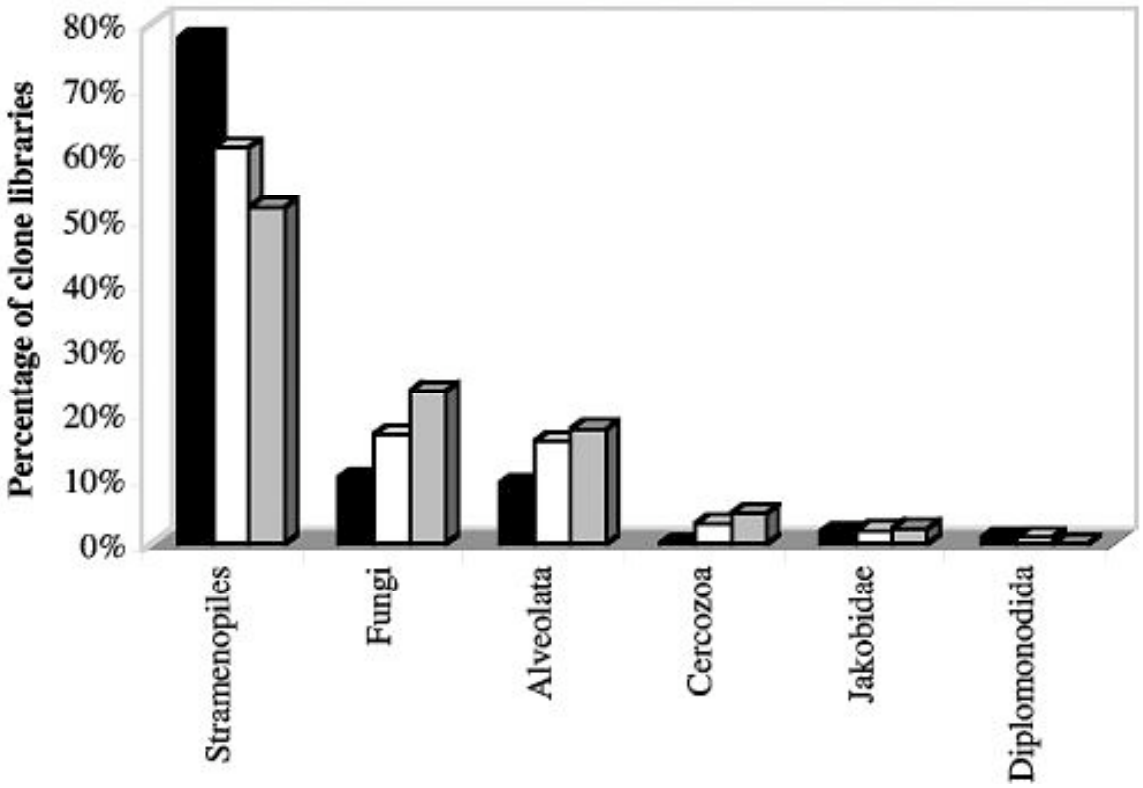

54% of the total number of clones sequenced. Various diversity indices (see Table S1 in the supplemental material) suggested a lower level of diversity within the source clone library, compared to the mat and crust clone libraries. This lower diversity is probably a reflection of the harsher conditions (higher sulfide and hydrocarbon concentration) at the spring source.

Phylogenetic placement. (i) Stramenopiles. Within the three Zodletone clone libraries, *Stramenopiles* clone sequences belonged to four different groups: the pinnate diatoms (class *Bacillariophyceae*), golden algae (class *Chrysophyceae*), order *Bicosoecida*, and slime nets (order *Labyrinthulida*) (Fig. 2). *Bicosoecida* clones (2 OTUs, 81 clones) were monophyletic, with strong bootstrap support, to members of the genus *Cafeteria*. All currently known *Cafeteria* spp. had been obtained from marine sources such as marine plankton and hydrothermal vents (2, 5, 23, 34). *Labyrinthulida* clone sequences (2 OTUs, 11 clones) were only 93% similar to their closest relatives (*Aplanochytrium kerguelense*) (Fig. 2). Similar to *Cafeteria*, all members of the *Labyrinthulida* have so far been isolated from marine and estuarine environments (51), and culture-independent studies have often encountered this group in anaerobic, marine habitats (17, 39, 43, 61) Therefore, this work shows that this group of microeukaryotes could also occur in other aquatic habitats.

(ii) Fungi. Fungal clones represented a significant fraction of the clone libraries in Zodletone Spring (16% of the total number of clones) (Fig. 1). Fungal sequences are often observed (10) in clone libraries during surveys of eukaryotes from anaerobic environments (10, 17, 60, 61) but are rarely discussed. In Zodletone clone libraries, most fungal clones belonged to four main groups (Fig. 3). (i) Several clone sequences (3

Figure 2. Distance dendrogram based on the 18S sequences of stramenopile OTUs encountered in Zodletone source, mat, and crust clone libraries. The tree was constructed using a general time reversible substitution model, with a proportion of invariable site value of 0.13128 and a variable site gamma distribution shape parameter at 0.3493. *Hexamita inflata* (L07836) was used as the outgroup. Bootstrap values (in percentages) are based on 1,000 replicates and are shown for branches with more than 50% bootstrap support. Numbers in parentheses represent the frequencies of occurrence of a specific OTU in the source, mat, and crust clone libraries, respectively.

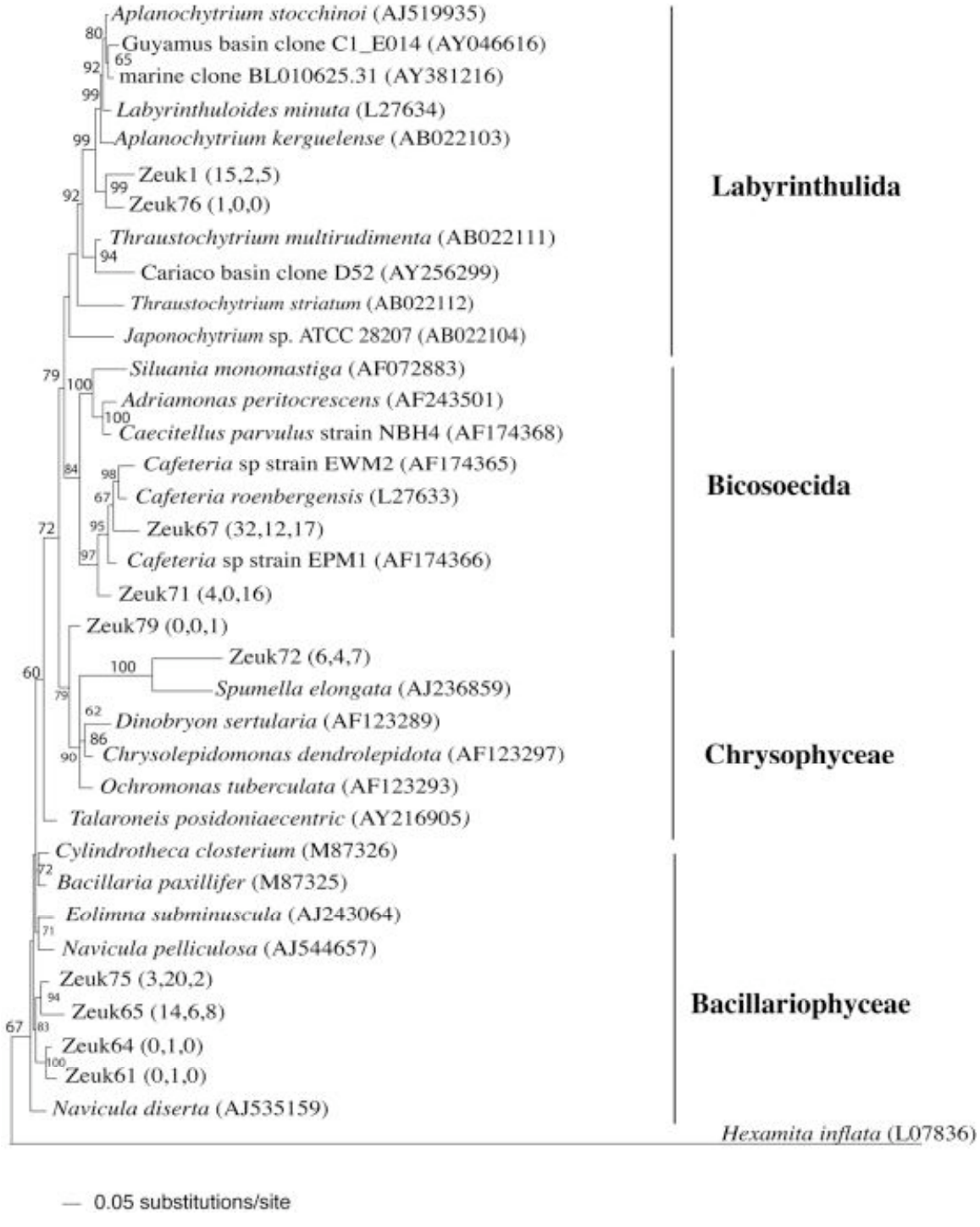
Aplanochytrium stocchinoi (AJ519935)
Guyamus basin clone C1_E014 (AY046616)
marine clone BL010625.31 (AY381216)
Labyrinthuloides minuta (L27634)
Aplanochytrium kerguelense (AB022103)
Zeuk1 (15,2,5)
Zeuk76 (1,0,0)
Thraustochytrium multirudimenta (AB022111)
Cariaco basin clone D52 (AY256299)
Thraustochytrium striatum (AB022112)
Japonochytrium sp. ATCC 28207 (AB022104)
Labyrinthulida
Siluania monomastiga (AF072883)
Adriamonas peritocrescens (AF243501)
Caecitellus parvulus strain NBH4 (AF174368)
Cafeteria sp strain EWM2 (AF174365)
Cafeteria roenbergensis (L27633)
Zeuk67 (32,12,17)
Cafeteria sp strain EPM1 (AF174366)
Zeuk71 (4,0,16)
Zeuk79 (0,0,1)
Bicosoecida
Zeuk72 (6,4,7)
Spumella elongata (AJ236859)
Dinobryon sertularia (AF123289)
Chrysolepidomonas dendrolepidota (AF123297)
Ochromonas tuberculata (AF123293)
Talaroneis posidoniaecentric (AY216905)
Chrysophyceae
Cylindrotheca closterium (M87326)
Bacillaria paxillifer (M87325)
Eolimna subminuscula (AJ243064)
Navicula pelliculosa (AJ544657)
Zeuk75 (3,20,2)
Zeuk65 (14,6,8)
Zeuk64 (0,1,0)
Zeuk61 (0,1,0)
Navicula diserta (AJ535159)
Bacillariophyceae
Hexamita inflata (L07836)
0.05 substitutions/site

Figure 3. Distance dendrogram based on the 18S sequences of fungal OTUs encountered in Zodletone source, mat, and crust clone libraries as well as in ww, ftlp, and dp clone libraries. The tree was constructed using a Tamura-Nei substitution model, with a proportion of invariable site value of 0.1218 and a variable site gamma distribution shape parameter at 0.4114. *Cafeteria roenbergensis* was used as the outgroup. Bootstrap values (in percentages) are based on 1,000 replicates and are shown for branches with more than 50% bootstrap support. Numbers in parentheses represent the frequencies of occurrence of a specific OTU in the source, mat, and crust clone libraries, respectively.

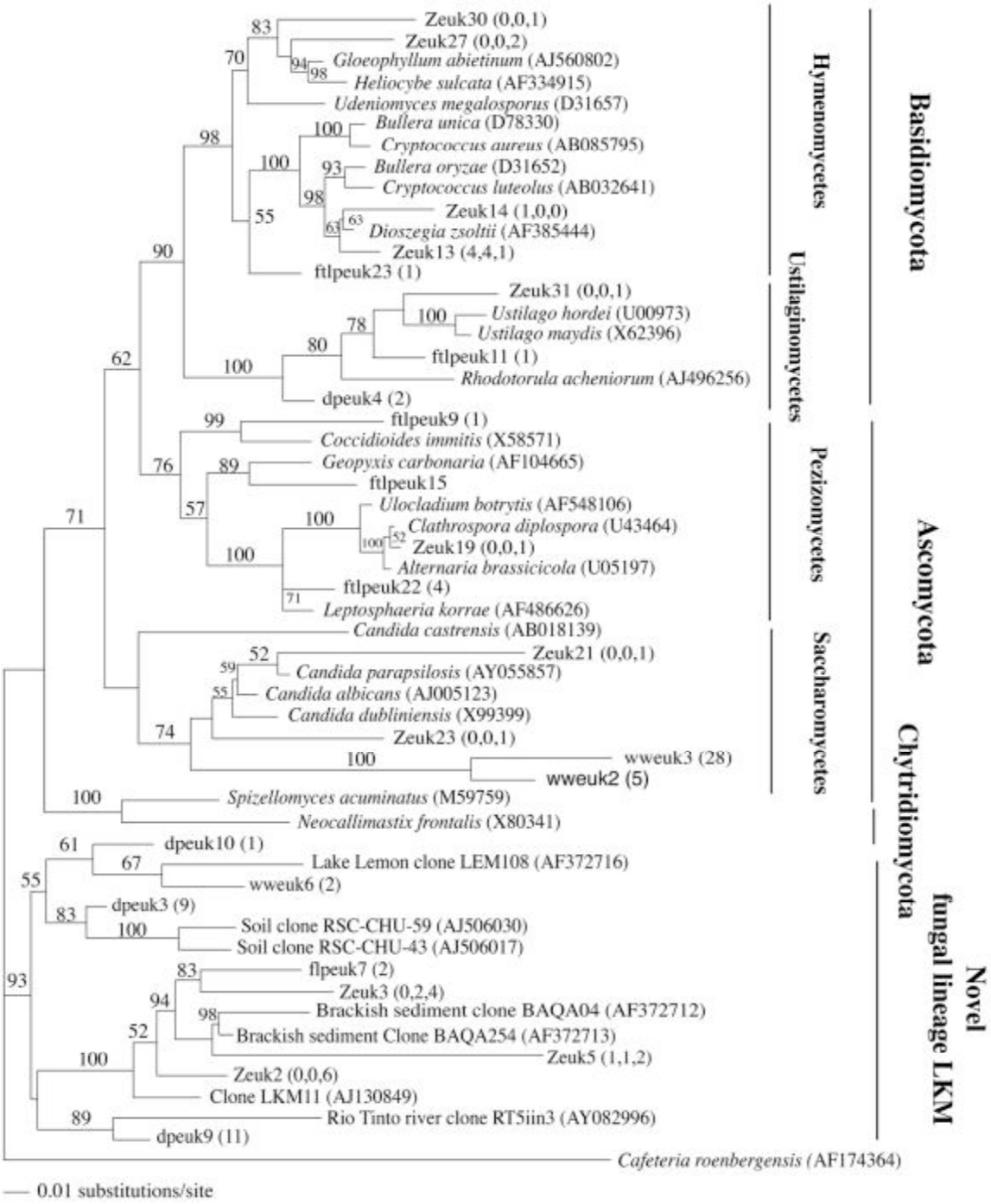
Zeuk30 (0,0,1)
Zeuk27 (0,0,2)
Gloeophyllum abietinum (AJ560802)
Heliocybe sulcata (AF334915)
Udeniomyces megalosporus (D31657)
Bullera unica (D78330)
Cryptococcus aureus (AB085795)
Bullera oryzae (D31652)
Cryptococcus luteolus (AB032641)
Zeuk14 (1,0,0)
Dioszegia zsoltii (AF385444)
Zeuk13 (4,4,1)
ftlpeuk23 (1)
Zeuk31 (0,0,1)
Ustilago hordei (U00973)
Ustilago maydis (X62396)
ftlpeuk11 (1)
Rhodotorula acheniorum (AJ496256)
dpeuk4 (2)
ftlpeuk9 (1)
Coccidioides immitis (X58571)
Geopyxis carbonaria (AF104665)
ftlpeuk15
Ulocladium botrytis (AF548106)
Clathrospora diplospora (U43464)
Zeuk19 (0,0,1)
Alternaria brassicicola (U05197)
ftlpeuk22 (4)
Leptosphaeria korrae (AF486626)
Candida castrensis (AB018139)
Zeuk21 (0,0,1)
Candida parapsilosis (AY055857)
Candida albicans (AJ005123)
Candida dubliniensis (X99399)
Zeuk23 (0,0,1)
wweuk3 (28)
wweuk2 (5)
Spizellomyces acuminatus (M59759)
Neocallimastix frontalis (X80341)
dpeuk10 (1)
Lake Lemon clone LEM108 (AF372716)
wweuk6 (2)
dpeuk3 (9)
Soil clone RSC-CHU-59 (AJ506030)
Soil clone RSC-CHU-43 (AJ506017)
flpeuk7 (2)
Zeuk3 (0,2,4)
Brackish sediment clone BAQA04 (AF372712)
Brackish sediment Clone BAQA254 (AF372713)
Zeuk5 (1,1,2)
Zeuk2 (0,0,6)
Clone LKM11 (AJ130849)
Rio Tinto river clone RT5iin3 (AY082996)
dpeuk9 (11)
Cafeteria roenbergensis (AF174364)
0.01 substitutions/site
Hymenomycetes
Ustilaginomycetes
Pezizomycetes
Saccharomycetes
Basidiomycota
Ascomycota
Chytridiomycota
Novel fungal lineage LKM

OTUs, 16 clones) had no affiliation with any of the known fungal phyla and, together with several published or database-deposited clones (10, 65), form a novel lineage, which we named novel fungal lineage LKM, after clone LKM11 (AJ130849), the first published sequence belonging to this group (65). (ii) Members of the tremallales clade within the *Hymenomycetes* (phylum *Basidiomycetes*), with their closest relatives being members of known yeast genera, e.g., *Bullera*, *Fellomyces*, and *Kockovaella*. (iii) Members of the plant pathogenic class *Ustilaginomycetes* within the *Basidiomycetes* with close (99%) similarity to the smut fungi *Ustilago hordei* and *Ustilago maydis*. (iv) Members of the class *Saccharomycetes* within the *Ascomycota*. The source clone library had a high percentage (55% of the total fungal clones) of *Hymenobasidiomycetes*, clone sequences related to yeast genera. In contrast, the majority of the fungal clone sequences in the mat and crust clone libraries belonged to the novel LKM group.

(iii) Alveolates. All alveolates from Zodletone belonged to the class *Ciliophora* (ciliates), the presence of which has long been established in anaerobic environmments (22). Zodletone ciliates either belonged to the classes *Spirotrichea* or *Colpodea* or formed a novel lineage within the ciliates that is designated candidate ciliate class *Zeuk* (Fig. 4A)

Jakoba, Diplomonadida,* and *Cercozoa. Zodletone *Jakoba* clones were closely related to *Jakoba incarcerata*, isolated from intertidal sediments in Quibray Bay, Australia (Fig. 4B). Two *Diplomonadida* clones were detected from the Zodletone source, and mat samples and were only 91 to 93% similar to their closest relative, the free-living amitochondrial flagellate *Hexamita inflata* (Fig. 4B). These *Diplomonadida* clones were the only sequences encountered in this study that belonged to one of the

Figure 4. (A) Distance dendrogram based on the 18S sequences of *Alveolata* OTUs encountered in Zodletone source, mat, and crust clone libraries. The tree was obtained under a Tamura-Nei substitution model, with a variable-site gamma distribution parameter at 0.4022. *Hexamita inflata* (L07836) was used as the outgroup. (B) Distance dendrogram based on the 18S sequences of *Cercozoa*, *Diplomonadida*, and *Jakoba* encountered in Zodletone source, mat, and crust clone libraries. The tree was obtained under a Tamura-Nei substitution model, with a variable-site gamma distribution parameter at 0.5402. *Escherichia coli* strain K-12 16S rRNA gene was used as an outgroup. Bootstrap values (in percentages) are based on 1,000 replicates and are shown for branches with more than 50% bootstrap support. Numbers in parentheses represent the frequencies of occurrence of a specific OTU in the source, mat, and crust clone libraries, respectively.

(A).

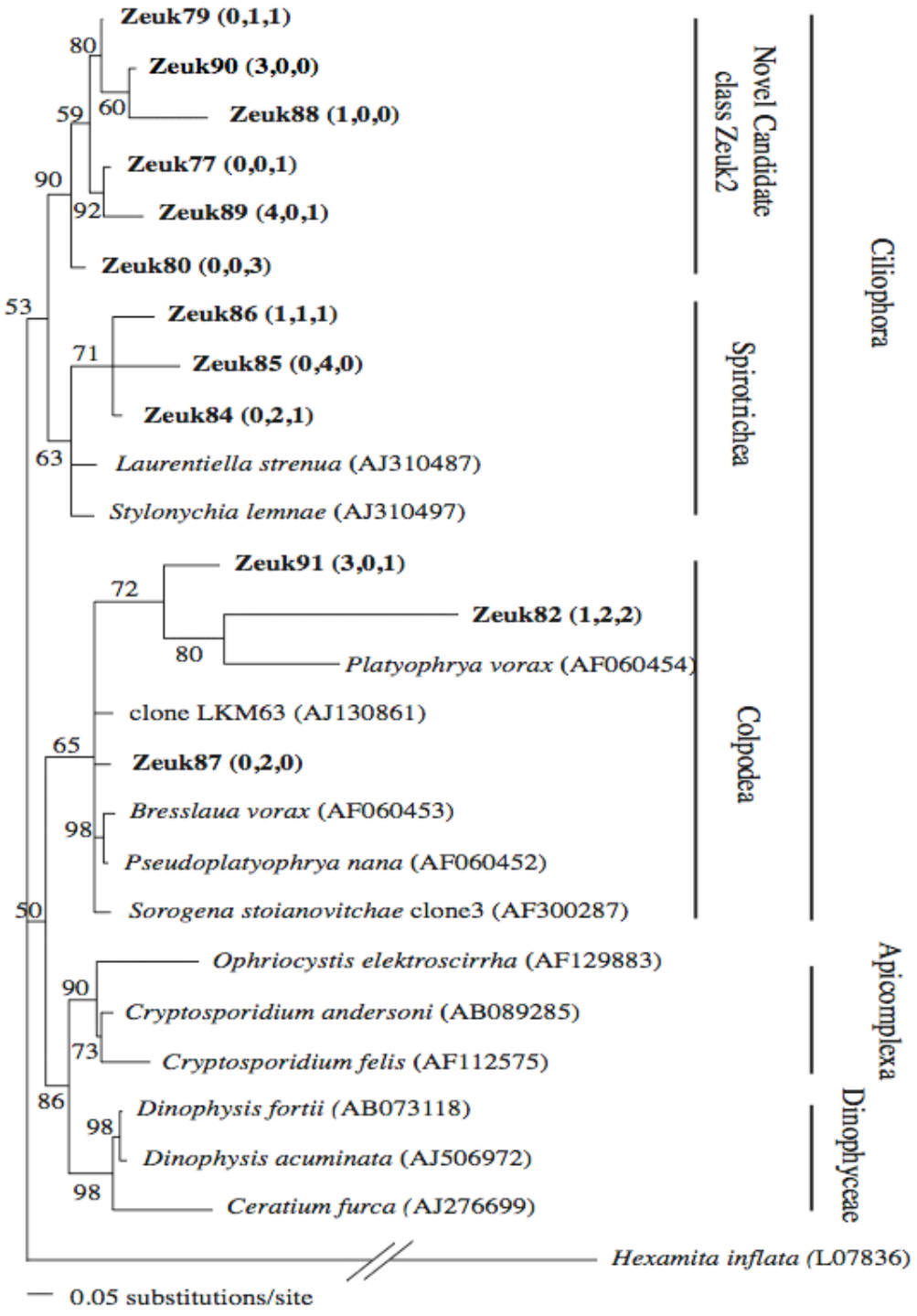
Zeuk79 (0,1,1)
Zeuk90 (3,0,0)
Zeuk88 (1,0,0)
Zeuk77 (0,0,1)
Zeuk89 (4,0,1)
Zeuk80 (0,0,3)
Zeuk86 (1,1,1)
Zeuk85 (0,4,0)
Zeuk84 (0,2,1)
Laurentiella strenua (AJ310487)
Stylonychia lemnae (AJ310497)
Zeuk91 (3,0,1)
Zeuk82 (1,2,2)
Platyophrya vorax (AF060454)
clone LKM63 (AJ130861)
Zeuk87 (0,2,0)
Bresslaua vorax (AF060453)
Pseudoplatyophrya nana (AF060452)
Sorogena stoianovitchae clone3 (AF300287)
Ophriocystis elektroscirrha (AF129883)
Cryptosporidium andersoni (AB089285)
Cryptosporidium felis (AF112575)
Dinophysis fortii (AB073118)
Dinophysis acuminata (AJ506972)
Ceratium furca (AJ276699)
Hexamita inflata (L07836)
0.05 substitutions/site
Novel Candidate class Zeuk2
Spirotrichea
Colpodea
Ciliophora
Apicomplexa
Dinophyceae

(B).

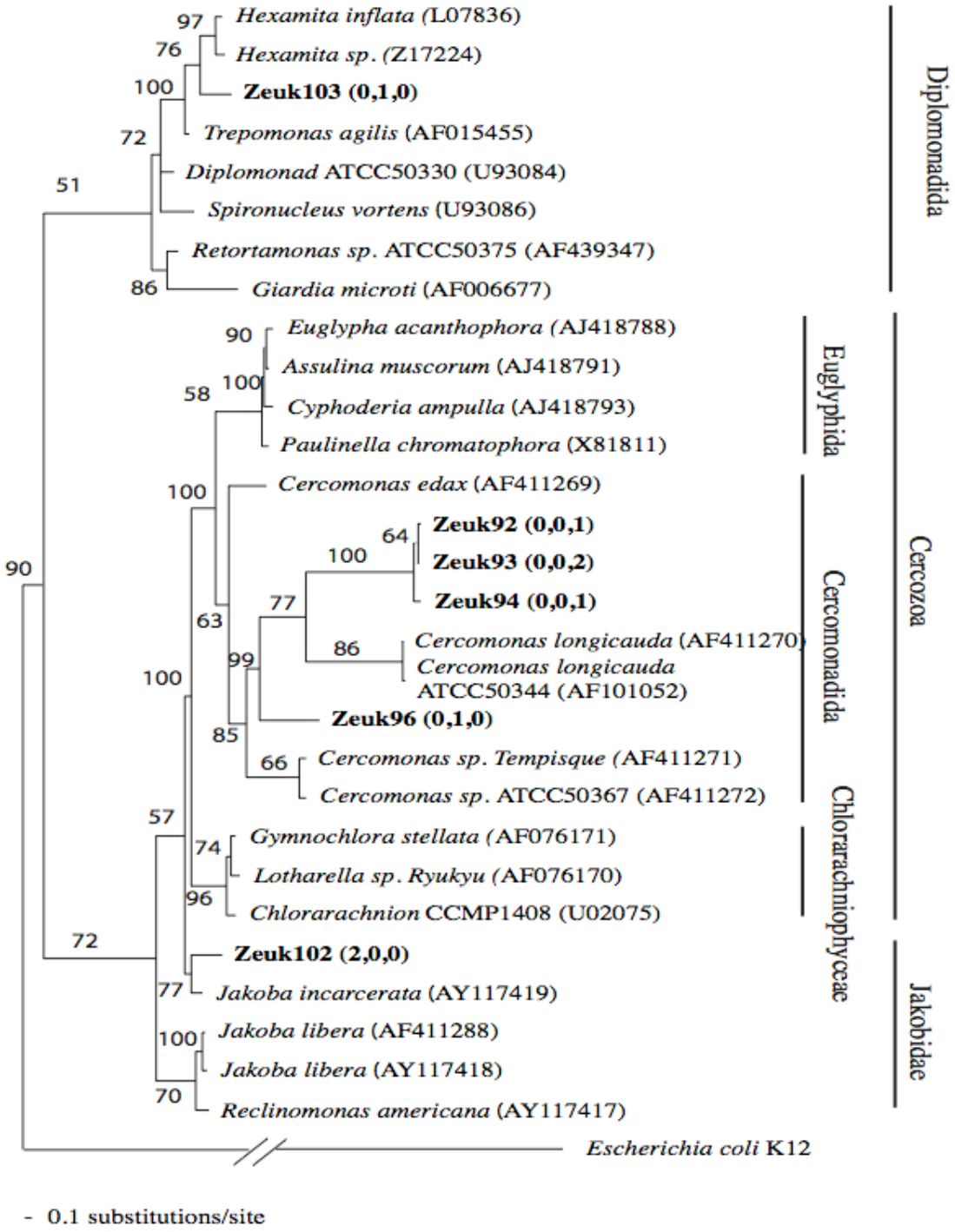
Hexamita inflata (L07836)
Hexamita sp. (Z17224)
Zeuk103 (0,1,0)
Trepomonas agilis (AF015455)
Diplomonad ATCC50330 (U93084)
Spironucleus vortens (U93086)
Retortamonas sp. ATCC50375 (AF439347)
Giardia microti (AF006677)
Euglypha acanthophora (AJ418788)
Assulina muscorum (AJ418791)
Cyphoderia ampulla (AJ418793)
Paulinella chromatophora (X81811)
Cercomonas edax (AF411269)
Zeuk92 (0,0,1)
Zeuk93 (0,0,2)
Zeuk94 (0,0,1)
Cercomonas longicauda (AF411270)
Cercomonas longicauda ATCC50344 (AF101052)
Zeuk96 (0,1,0)
Cercomonas sp. Tempisque (AF411271)
Cercomonas sp. ATCC50367 (AF411272)
Gymnochlora stellata (AF076171)
Lotharella sp. Ryukyu (AF076170)
Chlorarachnion CCMP1408 (U02075)
Zeuk102 (2,0,0)
Jakoba incarcerata (AY117419)
Jakoba libera (AF411288)
Jakoba libera (AY117418)
Reclinomonas americana (AY117417)
Escherichia coli K12
Diplomonadida
Euglyphida
Cercomonadida
Chlorarachniophyceae
Cercozoa
Jakobidae
0.1 substitutions/site

early branching amitochondrial eukaryotic groups. *Cercozoa* clones belonged to the order *Cercomonadida* that has been often encountered in anoxic habitats (5, 10).

Comparison of the Zodletone Spring microeukaryotic community to other anaerobic environments. Samples from an anaerobic sewage digester (ww sequences), a gas-condensate- impacted aquifer (ftlp sequences), and freshwater pond sediments (dp sequences) were used to construct clone libraries, and a total of 210 clones were partially sequenced. The composition of all three libraries is given in Table 1. Interestingly, fungus-affiliated clone sequences represented a significant fraction in all three clone libraries (Fig. 3) (63% in the ww library, 35% of the fl library, and 34% of the dp library). Moreover, clone sequences belonging to the novel fungal LKM group were present in all three environments, suggesting a widespread distribution of this group in anaerobic ecosystems. This group represented 82% of the fungal clones (n = 27) and 28% of the total number of clones (n = 79) in the dp clone library. The remaining fungal clone sequences in the dp clone libraries were members of the phyla *Glomeromycota* and *Chytridiomycota* and the class *Ustilaginomycetes*. Fungal clone sequences from the anaerobic digestor were either saccharomycetous yeasts or members of the fungal LKM group (Fig. 3). Anaerobic aquifer fungal clone sequences were ascomycetous or basidiomycetous yeasts and belonged to the LKM group as well as the orders *Pezizales* and *Ustilaginomycetes* (Fig. 3).

PLFA and sterol analysis. To estimate the relative abundance of eukaryotes in general and fungi in particular in anaerobic environments, we quantified the total, prokaryotic, and eukaryotic PLFA, two fungus-specific PLFAs (18:2w6 and 18:33), and ergosterol in Zodletone Spring as well as in ww, dp, and ftlp samples. Ergosterol, a

Table 1. Phylogenetic affiliation of the microeukaryotic community encountered in wastewater, hydrocarbon-contaminated, and pond sediment clone libraries[a].

Sample	Fungi		Stramenopiles		Alveolates		Green Algae		Metazoa	Higher Plants
	%	Components[b]	%	Components[b]	%	Components[b]	%	Components[b]	%	%
Waste water	63	Saccharomycetales (34) LKM group (3)	0	NA	0	NA	0	NA	37	0
Hydro-carbon contam-inated	35	Saccharomycetales (7) LKM group (1) Pezizomycetes (14) Hymeno-basidiomycetes (2) Ustilagomycetes (1)	13	Labyrinthulida (1) Oomycetes (6) Bacillariophyceae (2)	7	Suessiales (1) Stichotrichia (2) Cyrtophorida (1) Cyrtolophosidida (1)	0	NA	24	22
Duck pond	34	LKM group (22) Chytridomycota (2) Glomeromycetes (1) Ustilagomycetes (2)	24	Labyrinthulida (1) Oomycetes (1) Bacillariophyceae (16) Radiophyceae (1)	25	Armophorida (4) Eimeriida (1) Halteriidae (3) Peniculida (3) Gymnodiniales (1) Euplotida (5) Pleuronematida (3)	14	Volvocales (7) Chlorococcales (2) Chlorosarcinales (1) Prasiolales (1)	4	0

[a] Detailed phylogenetic placement of fungal clones is given in Figure 2.

[b] Number of clones encountered belonging to each phylogenetic group is given in parenthesis. NA, not applicable.

fungus-specific sterol used as an indicator of living fungal biomass (27), was detected in all environments except Zodletone crust samples and ftlp samples (Table 2). However, fungus-specific PLFAs were detected in all samples analyzed, confirming the presence of fungi in all of the anaerobic ecosystems examined. These fungus-specific PLFAs (18:26 and 18:33) represented 4 to 6% of the total PLFAs in the dp, ww, and ftlp samples and represented a significant fraction (between 35% in Zodletone crust samples and 79% in Zodletone source samples) of the total eukaryotic PLFAs in all samples (Table 2). It is interesting to note that among all three Zodletone Spring samples, the highest total eukaryotic PLFA and lowest prokaryotic/eukaryotic ratios were observed in the source sample. Also, the source samples contained more fungus-specific PLFAs (226 pmol/g [dry weight]) than the mat and crust samples (Table 2). The fact that the source has a higher sulfide concentration and lower exposure to light and atmospheric oxygen compared to the mat and crust attests to the ability of eukaryotic groups detected in Zodletone Spring, including *Fungi*, to survive and grow under strict anaerobic, highly reduced conditions.

Discussion

In this study, we surveyed the microeukaryotic community in Zodletone Spring to determine the identity of eukaryotes in this anaerobic, sulfide and sulfur-rich, hydrocarbon-impacted environment. Although this study did not reveal the presence of any novel kingdom level diversity, it suggests the presence of novel lineages within known groups (e.g., novel fungal lineage LKM within the fungi or novel *Zeuk* lineage within the ciliates) and expands the geographical presence of some groups (genus

Table 2. Biomass, ergosterol, and PLFA analysis of sediments from samples examined using 18S rRNA gene analysis in this study[a].

	Total				Ergosterol biomass[b]	Fungi specific PLFA (18:2w6 & 3w3)[b]	
	PLFA biomass[b]	Prokaryotic[b]	Eukaryotic[b]	Prokaryotic /Eukaryotic ratio		Biomass	mol%
Zodletone Source	14755 (3222)	14469 (3135)	286 (86)	52 (4)	0.8 (0.2)	226	<1
Zodletone mat	9246 (3116)	9194 (3095)	52 (20)	177 (11)	0.9 (0.8)	19	<1
Zodletone Crust	11557 (415)	11392 (359)	165 (55)	74 (22)	0 (--)	58	<1
Freshwater pond (dp)	22756 (597)	20722 (718)	2034 (121)	11 (1)	3.3 (1.5)	1315	6
Wastewater (ww)	1198626 (299952)	1137662 (279713)	60964 (20239)	20 (2)	27.6 (1.5)	44726	4
Gas-condensate contaminated sediment (fl)[c]	3053	2882	171	18	0 (--)	143	5

[a] Values are expressed as pmol/g dry weight.

[b] Standard deviation values are given in paranthesis.

[c] Only one sample was analyzed, for all other samples, n=2

Cafeteria, order *Labyrinthulida*, and genus *Jakoba*) previously thought to be restricted to marine habitats.

The presence of ciliates within the anoxic community in Zodletone Spring is not surprising since ciliates have long been known to be inhabitants of anaerobic environments (22). However, several Zodletone clone sequences have low similarity to all GenBank-deposited ciliate 18S rRNA genes and potentially represent a novel uncultured candidate class within the ciliates.

Cafeteria species have been shown to be abundant in a variety of marine habitats. They have been isolated from anaerobic tidal waves (2), pelagic ocean, and hydrothermal vents (2). Here, we show that members of *Cafeteria* spp. are not restricted to marine settings but could also be encountered in other aquatic ecosystems. This conclusion is also true for *Jakoba* spp. and the order *Labyrinthulida*, both of which have previously been detected using culture-dependent and -independent analyses solely in marine environments (17, 39, 43, 51, 61). It is interesting to note that all three previously mentioned groups have been shown to be an integral component of hydrothermal vent ecosystems. Similarly, many clone groups within the prokaryotic community in Zodletone Spring have been observed in hydrothermal vent prokaryotic communities (18, 19, 62). The resemblance between a deep-sea hydrothermal vent and a mesophilic spring is quite unexpected. However, both environments have several geochemical characteristics in common, including the low redox potential, high sulfide content, and high levels of short-chain gaseous alkanes. Therefore, it appears that these previously mentioned factors could play an important role in shaping the microbial communities in both ecosystems.

In Zodletone Spring, samples with sequences suggesting the presence of two different phototrophic groups (within the *Stramenopiles*) were observed: the classes *Chrysophyceae* (golden algae) and *Bacillariophyceae* (diatoms). The fact that almost all *Chrysophyceae* species described so far are oxygenic phototrophs suggests these organisms are introduced into this anaerobic environment with the input of exogenous organic matter (e.g., wood, leaves) to the stream. Alternatively, in the case of the mat and crust, the *Chrysophyceae* might be localized on the uppermost, air-exposed layers and hence directly exposed to atmospheric air and sunlight. These assumptions could also be true with members of the *Bacillariophyceae*, especially since they represent a larger fraction of the clone libraries of the light-exposed microbial mats compared with the less light-exposed source. It should be noted, however, that some of the closest relatives of Zodletone *Chrysophyceae* clone sequences are closely related to the genus *Spumela* (Fig. 2), all of which are obligately phagocytic (33, 37).

Perhaps the most interesting finding of this study is the unexpected abundance and the novel fungal diversity in Zodletone Spring as well as in all other surveyed anaerobic environments (Fig. 1 and 3; Tables 1 and 2). Fungal clones were previously detected and often represented a significant fraction of the 18S rRNA sequences in clone libraries from anaerobic environments (10, 17, 39, 60). Apart from members of the class *Neocallimasticaceae* within the *Chytridiomycota*, no strict anaerobic fungal species has yet been described and fungi have always been thought to play a minor role in ecosystem processes in anaerobic ecosystems (14, 41). Within the various groups encountered in all six clone libraries examined, fermentative metabolism and anaerobic growth abilities are known to exist among yeast species of the order *Saccharomycetales*. It had been shown

that *Candida albicans* and *Saccharomyces cerevisiae* could be grown and maintained under strict anaerobic conditions (16, 58). Also, basidiomycetous yeasts are known to be saprophytes, thriving in high-organic-content environments (20). Although fermentation occurs in only very few of the basidiomycetous yeasts (20), some species had been isolated from seemingly anaerobic environments like subseafloor habitats (45). These fermentative capabilities could explain the presence of these two groups of fungi in Zodletone Spring as well as in other clone libraries. A third group of fungal clones in the libraries is characterized by their close similarity to well known aerobic, wood- and plant-associated fungi e.g., *Ustilago* sp. and *Pezizales*, and their presence is probably a reflection of plant input to the system.

The final group of fungal sequences encountered in Zodletone Spring as well as other environments is the novel fungal lineage LKM (Fig. 3). Since no pure culture representative of this group is yet available, we can only speculate on their metabolic capabilities based on the environments where they have been encountered. A database search revealed the presence of clones belonging to this group in anaerobic brackish sediments and anaerobic freshwater lake sediments (10). This group has also been encountered in soil and lake sediments where no definite information regarding the redox potential is available (65) (GenBank accession numbers AJ506017 and AJ506030), as well as in extremely acidic river sediments (69). However, the fact that several studies using the 18S rRNA gene sequence to study the fungal communities in highly oxic systems, including soil (64), the rhizosphere (57, 66), and freshwater habitats (47), did not detect this group, coupled with their presence in all clone libraries tested in this study as well as several other anaerobic habitats, provides strong evidence for the indigenous

nature of this group and hence the ability to thrive under anaerobic conditions. However, it is important to note that some of the previous studies examining fungal diversity utilizing the large ribosomal subunit (rRNA) as a biomarker have detected several unique yet uncultured fungal lineages (54). Comparing the phylogeny of the novel fungal lineage obtained in this study to that of novel lineages detected in large-subunit rRNA-based studies is not feasible.

PLFA and ergosterol determinations confirmed the presence of fungi in all ecosystems studied. The fact that ergosterol and fungal PLFA levels were highest in anaerobic digester samples is in agreement with the observation that *Fungi* constituted the majority of clone sequences (63%) in ww clone library. Assuming a conversion factor of 5.4 mg ergosterol g1 fungal biomass (35), fungal concentrations were 0.06 to 0.07 mg fungal biomass per gram of sediment in the Zodletone source and mat samples, respectively, 0.24 mg per gram in the pond, and 2.02 mg per gram in sewage digester samples. The lower fungal biomass in Zodletone Spring is in agreement with previous studies showing that ergosterol content decreases considerably with depth-associated change from aerobic to anaerobic redox potential in salt marsh sediments (41). However, fungal biomass values in Zodletone Spring are on average only 2 orders of magnitude less than values obtained in studies examining fungal biomass in aerobic, fungus-rich habitats such as compost (35), fungus-infested sludge (24), leaf litter (26, 59), and biocontaminated building materials (50). Moreover, it has been suggested that ergosterol measurements might underestimate the fungal biomass of yeast cells (50). The fact that several Zodletone clones are closely related to yeast lineages suggests that ergosterol analysis might have underestimated the fungal biomass in Zodletone Spring.

The fact that many of the clones in dp, ftlp, and ww clone libraries are derived from the metazoa and *Viridiplantae* (Table 1), coupled with the unexpected abundance of fungi in these settings and relatively small number of clones sequenced renders this study far from a comprehensive survey of the microeukaryotic community in common anaerobic freshwater settings. Studies examining similar environments using culturing techniques targeting a single group, e.g., ciliates or flagellates, have isolated several microeukaryotes, many of which appear to be numerous but that we failed to detect (5, 21, 22, 29, 48, 49, 56). Nevertheless, the 18S rRNA gene-based study and PLFA analysis collectively suggest that culture-based studies generally underestimate fungal levels in anaerobic ecosystems.

Finally, the lack of novel kingdom level diversity or even clones affiliated with recently described novel kingdoms in all six clone libraries analyzed (a total of 496 clones) is surprising. Previous studies collectively suggest the presence of a large number of yet-undescribed eukaryotic kingdoms (10, 17, 44, 60). However, a recent reanalysis of sequences proposed to represent these kingdoms led the authors to propose only five novel lineages, three of which were detected in more than one study (6). These five lineages may represent new eukaryotic kingdoms; however, additional studies are likely needed to validate them. The view that we may be overestimating the level of eukaryotic diversity at the kingdom level based upon 18S rRNA gene analysis is supported by recent studies which used multiple gene analysis to show that most of the eukaryotic diversity could be grouped into eight supergroups and that many of the lineages previously thought to be early diverging branches of the eukaryotic tree based on the 18S sequence are related to groups belonging to the crown radiation eukaryotes (3, 4).

References

1. **Altschul, S. F., T. L. Madden, A. A. Schaffer, J. Zhang, Z. Zhang, W. Miller, and D. J. Lipman.** 1997. Gapped BLAST and PSI-BLAST: a new generation of protein database search programs. Nucleic Acids Res. **25:**3389-3402.
2. **Atkins, M. S., A. P. Teske, and O. R. Anderson.** 2000. A survey of flagellate diversity at four deep-sea hydrothermal vents in the Eastern Pacific ocean using structural and molecular approaches. J. Eukaryot. Microbiol. **47:**400-411.
3. **Baldauf, S. L.** 2003. The deep roots of eukaryotes. Science **300:**1703-6.
4. **Baldauf, S. L., A. J. Roger, I. Wenk-Siefert, and W. F. Doolittle.** 2000. A kingdom-level phylogeny of eukaryotes based on combined protein data. Science **290:**972-977.
5. **Bernard, C., A. G. Simpson, and D. J. Patterson.** 2000. Some free living flagellates (Protista) from anoxic habitats. Ophelia **52:**113-142.
6. **Berney, C., J. Fahrni, and J. Pawlowski.** 2004. How many novel eukaryotic 'kingdoms'? Pitfalls and limitations of environmental DNA surveys. BMC Biology **2:**1-13.
7. **Bintrim, S. B., T. J. Donohue, J. Handelsman, G. P. Roberts, and R. M. Goodman.** 1997. Molecular phylogeny of Archaea from soil. Proc. Natl. Acad. Sci. U. S. A. **94:**277-282.
8. **Bligh, E. G., and W. J. Deyer.** 1954. A rapid method of total lipid extraction and purification. Canadian journal of biochemistry and physiology **37:**911-917.
9. **Cavalier-Smith, T.** 2004. Only six kingdoms of life. Proceedings of the Royal Society of London, Series B: Biological Sciences **271:**1251-1262.

10. **Dawson, S. C., and N. R. Pace.** 2002. Novel kingdom-level eukaryotic diversity in anoxic environments. Proc. Natl. Acad. Sci. U. S. A. **99:**8324-8329.

11. **DeLong, E. F.** 1992. Archaea in coastal marine environments. Proc. Natl. Acad. Sci. U. S. A. **89:**5685-9.

12. **Diez, B., C. Pedros-Alio, T. L. Marsh, and R. Massana.** 2001. Application of denaturing gradient gel electrophoresis (DGGE) to study the diversity of marine picoeukaryotic assemblages and comparison of DGGE with other molecular techniques. Appl. Environ. Microbiol. **67:**2942-2951.

13. **Diez, B., C. Pedros-Alio, and R. Massana.** 2001. Study of genetic diversity of eukaryotic picoplankton in different oceanic regions by small-subunit rRNA gene cloning and sequencing. Appl. Environ. Microbiol. **67:**2932-2941.

14. **Dighton, J.** 2003. Fungi in ecosystem processes, First edition ed, vol. 17. Marcel Dekker, Inc.,, New York, NY.

15. **Dojka, M. A., P. Hugenholtz, S. K. Haack, and N. R. Pace.** 1998. Microbial diversity in a hydrocarbon- and chlorinated-solvent-contaminated aquifer undergoing intrinsic bioremediation. Appl. Environ. Microbiol. **64:**3869-3877.

16. **Dumitru, R., J. M. Hornby, and K. W. Nickerson.** 2004. Defined anaerobic growth medium for studying *Candida albicans* basic biology and resistance to eight antifungal drugs. Antimicrob. Agents Chemother. **48:**2350-2354.

17. **Edgcomb, V. P., D. T. Kysela, A. Teske, A. de Vera Gomez, and M. L. Sogin.** 2002. Benthic eukaryotic diversity in the Guaymas Basin hydrothermal vent environment. Proc. Natl. Acad. Sci. U. S. A. **99:**7658-7662.

18. **Elshahed, M. S., F. Z. Najar, B. A. Roe, A. Oren, T. A. Dewers, and L. R. Krumholz.** 2004. Survey of archaeal diversity reveals an abundance of halophilic Archaea in a low-salt, sulfide- and sulfur-rich spring. Appl. Environ. Microbiol. **70:**2230-2239.

19. **Elshahed, M. S., J. M. Senko, F. Z. Najar, S. M. Kenton, B. A. Roe, T. A. Dewers, J. R. Spear, and L. R. Krumholz.** 2003. Bacterial diversity and sulfur cycling in a mesophilic sulfide-rich spring. Appl. Environ. Microbiol. **69:**5609-5621.

20. **Fell, J. W., T. Boekhout, A. Fonseca, and J. P. Sampaio.** 2001. Basidiomycetous yeast, p. 3-35. *In* E. G. McLaughlin and P. A. Lemke (ed.), The Mycota: systemics and evolution, First edition ed, vol. VII. Springer-Verlag, Berlin.

21. **Fenchel, T., C. Bernard, G. Esteban, B. J. Finlay, P. J. Hansen, and N. Iversen.** 1995. Microbial diversity and activity in a Danish fjord with anoxic deep water. Ophelia **45:**45-100.

22. **Fenchel, T., and B. J. Finlay.** 1995. Ecology and evolution in anoxic worlds, First edition ed. Oxford university press.

23. **Fenchel, T., and D. J. Patterson.** 1988. *Cafeteria roenbergensis* nov. gen., nov. sp., a heterotrophic microflagellate from marine plankton. Marine Microbial Food Webs **3:**9-19.

24. **Gardner, R. M., G. W. Tindall, S. M. Cline, and K. L. Brown.** 1993. Ergosterol determination in activated sludge and its application as a biochemical marker for monitoring fungal biomass. J. Microbiol. Methods **17:**49-60.

25. **Gast, R. J., M. R. Dennett, and D. A. Caron.** 2004. Characterization of protistan assemblages in the Ross Sea, Antarctica, by denaturing gradient gel electrophoresis. Appl. Environ. Microbiol. **70:**2028-2037.

26. **Gessner, M. O., and E. Chauvet.** 1993. Ergosterol-to-biomass conversion factors for aquatic hyphomycetes. Appl. Environ. Microbiol. **59:**502-507.

27. **Gessner, M. O., and S. Y. Newell.** 1997. Bulk quantitative methods for the examination of eukaryotic organoosmotrophs in plant litter, p. 295-308. *In* C. J. Hrust, G. R. Knudsen, M. J. McInerney, L. D. Stetzenbach, and M. V. Walter (ed.), Mannual of Environmental Microbiology. ASM press, Washington, D. C.

28. **Guckert, J. B., C. P. Antworth, P. D. Nichols, and D. C. White.** 1985. Phospholipid, ester-linked fatty acid profiles as reproducible assays for changes in prokaryotic community structure of estuarine sediments. FEMS Microbiology Ecology **31:**147-58.

29. **Harvey, R. W., N. Mayberry, N. E. Kinner, D. W. Metge, and F. Novarino.** 2002. Effect of growth conditions and staining procedure upon the subsurface transport and attachment behaviors of a groundwater protist. Appl. Environ. Microbiol. **68:**1872-1881.

30. **Huelsenbeck, J. P., and F. Ronquist.** 2001. MrBayes: Bayesian inference of phylogenetic trees. Bioinformatics **17:**754-755.

31. **Hugenholtz, P., and T. Huber.** 2003. Chimeric 16S rDNA sequences of diverse origin are accumulating in the public databases. International Journal of Systematic and Evolutionary Microbiology **54:**289-293.

32. **Humayoun Shaheen, B., N. Bano, and T. Hollibaugh James.** 2003. Depth distribution of microbial diversity in Mono Lake, a meromictic soda lake in California. Appl. Environ. Microbiol. **69:**1030-42.

33. **Johnes, R. I.** 2000. Mixotrophy in planktonic protists: an overview. Freshwater biol. **45:**219-226.

34. **Karpov, S. A.** 2000. Ultrastructure of the aloricate bicosoecid Pseudobodo tremulans with revision of the order Bicosoecida. Protistology **1:**101-109.

35. **Klamer, M., and E. Baath.** 2004. Estimation of conversion factors for fungal biomass determination in compost using ergosterol and PLFA 18:2w6,9. Soil Biol. Biochem. **36:**57-65.

36. **Kopczynski, E. D., M. M. Bateson, and D. M. Ward.** 1994. Recognition of chimeric small-subunit ribosomal DNAs composed of genes from uncultivated microorganisms. Appl. Environ. Microbiol. **60:**746-748.

37. **Kristiansen, J.** 1990. PHylum Chrysophyta. *In* L. Margulis, J. O. Corliss, M. Melkonian, and D. J. Chapman (ed.), Handbook of Protocista. Jones and Bartlett Publishers, Boston, MA.

38. **Lopez-Garcia, P., H. Philippe, F. Gail, and D. Moreira.** 2003. Autochthonous eukaryotic diversity in hydrothermal sediment and experimental microcolonizers at the Mid-Atlantic Ridge. Proc. Natl. Acad. Sci. U. S. A. **100:**697-702.

39. **Lopez-Garcia, P., F. Rodriguez-Valera, C. Pedros-Allo, and D. Moreira.** 2001. Unexpected diversity of small eukaryotes in deep-sea Antarctic plankton. Nature **409:**603-607.

40. **Maidak, B. L., J. R. Cole, T. G. Lilburn, C. T. Parker Jr., P. R. Saxman, R. J. Farris, G. M. Garrity, G. T. Olsen, T. M. Schmidt, and J. M. Tiedje.** 2000. The RDP-II (Ribosomal Databas Project). Nucleic Acids Res. **29:**173-174.

41. **Mansfield, S. D., and F. Barlocher.** 1993. Seasonal variation of fungal biomass in the sediment of a salt marsh in New Brunswick. Microb. Ecol. **26:**37-45.

42. **Martin, A. P.** 2002. Phylogenetic approaches for describing and comparing the diversity of microbial communities. Appl. Environ. Microbiol. **68:**3673-3682.

43. **Moon-van der Staay, S. Y., R. De Wachtert, and D. Vaulot.** 2001. Oceanic 18S rDNA sequences from picoplankton reveal unsuspected eukaryotic diversity. Nature **409:**607-610.

44. **Moreira, D., and P. Lopez-Garcia.** 2002. The molecular ecology of microbial eukaryotes unveils a hidden world. Trends Microbiol. **10:**31-38.

45. **Nagahama, T., M. Hamamoto, T. Nakase, Y. Takaki, and K. Horikoshi.** 2003. *Cryptococcus surugaensis* sp. nov., a novel yeast species from sediment collected on the deep-sea floor of Suruga Bay. International Journal of Systematic and Evolutionary Microbiology **53:**2095-2098.

46. **Nichols, P. D., J. K. Volkman, and R. B. Johns.** 1983. Sterols and fatty acids of the marine unicellular alga, FCRG 51. Phytochemistry **22:**1447-52.

47. **Nikolcheva, L. G., A. M. Cockshutt, and F. Barlocher.** 2002. Determining diversity of freshwater fungi on decaying leaves: Comparison of traditional and molecular approaches. Appl. Environ. Microbiol. **69:**2548-2554.

48. **Novarino, G., A. Warren, H. Butler, G. Lambourne, A. Boxshall, J. Bateman, N. E. Kinner, R. W. Harvey, R. A. Mosse, and B. Teltsch.** 1997. Protistan communities in aquifers: a review. FEMS Microbiol. Rev. **20:**261-275.

49. **Novarino, G., A. Warren, N. E. Kinner, and R. W. Harvey.** 1994. Protists from a sewage-contaminated aquifer on Cape-Cod, Massachusetts. Geomicrobiol. **12:**23-36.

50. **Pasanen, A. L., K. Y. Pietila, P. Pasanen, P. Kalliokoski, and J. Tarhanen.** 1999. Ergosterol content in various fungal species and biocontaminated building materials. Appl. Environ. Microbiol. **65:**138-142.

51. **Porter, D.** 1990. Phylum labyrinthulomycota, p. 388-398. *In* L. Margulis, J. O. Corliss, M. Melkonian, and D. J. Chapman (ed.), Handbook of Protocista, First Edition ed. Jones and Bartlett Publishers, Boston, MA.

52. **Posada, D., and K. A. Crandall.** 1998. MODELTEST: testing the model of DNA substitution. Bioinformatics **14**.

53. **Rappe, M. S., and S. J. Giovannoni.** 2003. The uncultured microbial majority. Annu. Rev. Microbiol. **57:**369-394.

54. **Schadt, C. W., A. P. Martin, D. A. Lipson, and S. K. Schmidt.** 2003. Seasonal dynamics of previously unknown fungal lineages in tundra soils. Science **301:**1359-1361.

55. **Senko, J. M., B. S. Campbell, J. R. Henriksen, M. S. Elshahed, T. A. Dewers, and L. R. Krumholz.** 2004. Barite deposition resulting from phototrophic sulfide-oxidizing bacterial activity. Geochimica et Cosmochimica Acta **68:**773-780.

56. **Sleigh, M.** 1989. Protozoa and other Protists. Edward Arnolds, New York, NY.

57. **Smit, E., P. Leeflang, B. Glandorf, J. D. Van Elsas, and K. Wernars.** 1999. Analysis of fungal diversity in the wheat rhizosphere by sequencing of cloned PCR-amplified genes encoding 18S rRNA and temperature gradient gel electrophoresis. Appl. Environ. Microbiol. **65:**2614-2621.

58. **Sonderegger, M., M. Jeppsson, B. Hahn-Haegerdal, and U. Sauer.** 2004. Molecular basis for anaerobic growth of *Saccharomyces cerevisiae* on xylose, investigated by global gene expression and metabolic flux analysis. Appl. Environ. Microbiol. **70:**2307-2317.

59. **Sridhar, K. R., and F. Barlocher.** 2000. Initial colonization, nutrient supply, and fungal activity on leaves decaying in streams. Appl. Environ. Microbiol. **66:**1114-1119.

60. **Stoeck, T., and S. Epstein.** 2003. Novel eukaryotic lineages inferred from small-subunit rRNA analyses of oxygen-depleted marine environments. Appl. Environ. Microbiol. **69:**2657-2663.

61. **Stoeck, T., G. T. Taylor, and S. S. Epstein.** 2003. Novel eukaryotes from the permanently anoxic Cariaco basin (Caribbean Sea). Appl. Environ. Microbiol. **69:**5656-5663.

62. **Teske, A., K. U. Hinrichs, V. P. Edgcomb, A. V. Gomez, D. T. Kysela, S. P. Sylva, M. L. Sogin, and H. W. Jannasch.** 2002. Microbial diversity of hydrothermal sediments in the Guaymas Basin: evidence for anaerobic methanotrophic communities. Appl. Environ. Microbiol. **68:**1994-2007.

63. **Thompson, J. D., T. J. Gibson, F. Plewniak, F. Jeanmougin, and D. G. Higgins.** 1997. The CLUSTAL X windows interface: flexible strategies for multiple sequence alignment aided by quality analysis tools. Nucleic Acids Res. **25:**4876-4882.

64. **Van Elsas, J. D., G. F. Duarte, A. Keijzer-Wolters, and E. Smit.** 2000. Analysis of fungal-specific PCR of soil DNA followed by denaturing gradient gel eletrophoresis. J. Microbiol. Methods **43:**133-151.

65. **Van Hannen, E. J., W. Mooij, M. P. Van Agterveld, H. J. Gons, and H. J. Laanbroek.** 1999. Detritus-dependent development of the microbial community in an experimental system: qualitative analysis by denaturing gradient gel electrophoresis. Appl. Environ. Microbiol. **65:**2478-2484.

66. **Vandenkoornhuyse, P., L. Baldauf Sandra, C. Leyval, J. Straczek, and J. P. W. Young.** 2002. Extensive fungal diversity in plant roots. Science **295:**2051.

67. **White, D. C., R. J. Bobbie, J. S. Herron, J. D. King, and S. J. Morrison.** 1979. Biochemical measurements of microbial mass and activity from environmental samples. Dep. Biol. Sci.,Florida State Univ.,Tallahassee,FL,USA.

68. **Woese, C. R.** 1987. Bacterial evolution. Microbiol. Rev. **51:**221-71.

69. **Zettler, L. A. A., F. Gomez, E. Zettler, B. K. Keenan, R. Amils, and M. L. Sogin.** 2002. Eukaryotic diversity in Spain's river of Fire. Nature **417:**137.

Supplementary Table 1. Composition and comparative diversity of the source, mat, and crust eukaryotic clone libraries.

Library	Number of Clones sequenced	Number of OTUs	Shannon-Weiner Index	Species Evenness	Percentage Coverage	Average nucleotide diversity (θ)
Source	108	20	2.18	0.73	93	0.22
Mat	95	31	2.88	0.84	83	0.22
Crust	85	31	3.11	0.91	82	0.26

Supplementary Figure 1. Partial tree construction of the full length 18S rRNA OTU fungal sequences from Zodletone spring to detect potential chimeras. Partial sequences were not included in the analysis. Tree (A) was constructed using nucleotide positions 1-865, tree (B) was constructed using nucleotide position 865-1700, and tree (C) was constructed using positions 1-1700. Numbering is based on *Candida albicans* (AJ005123) sequence. *Cafeteria roenbergensis* was used as an outgroup. The distance dendograms were constructed using a Tamura-Nei substitution model, with a proportion of invariable site (I) value of 0.2979 and a variable site gamma distribution shape parameter (G) at 0.5228. Numbers in parentheses represents the frequency of occurrence of a specific OTU in the source, mat, and crust clone libraries, respectively.

(A).

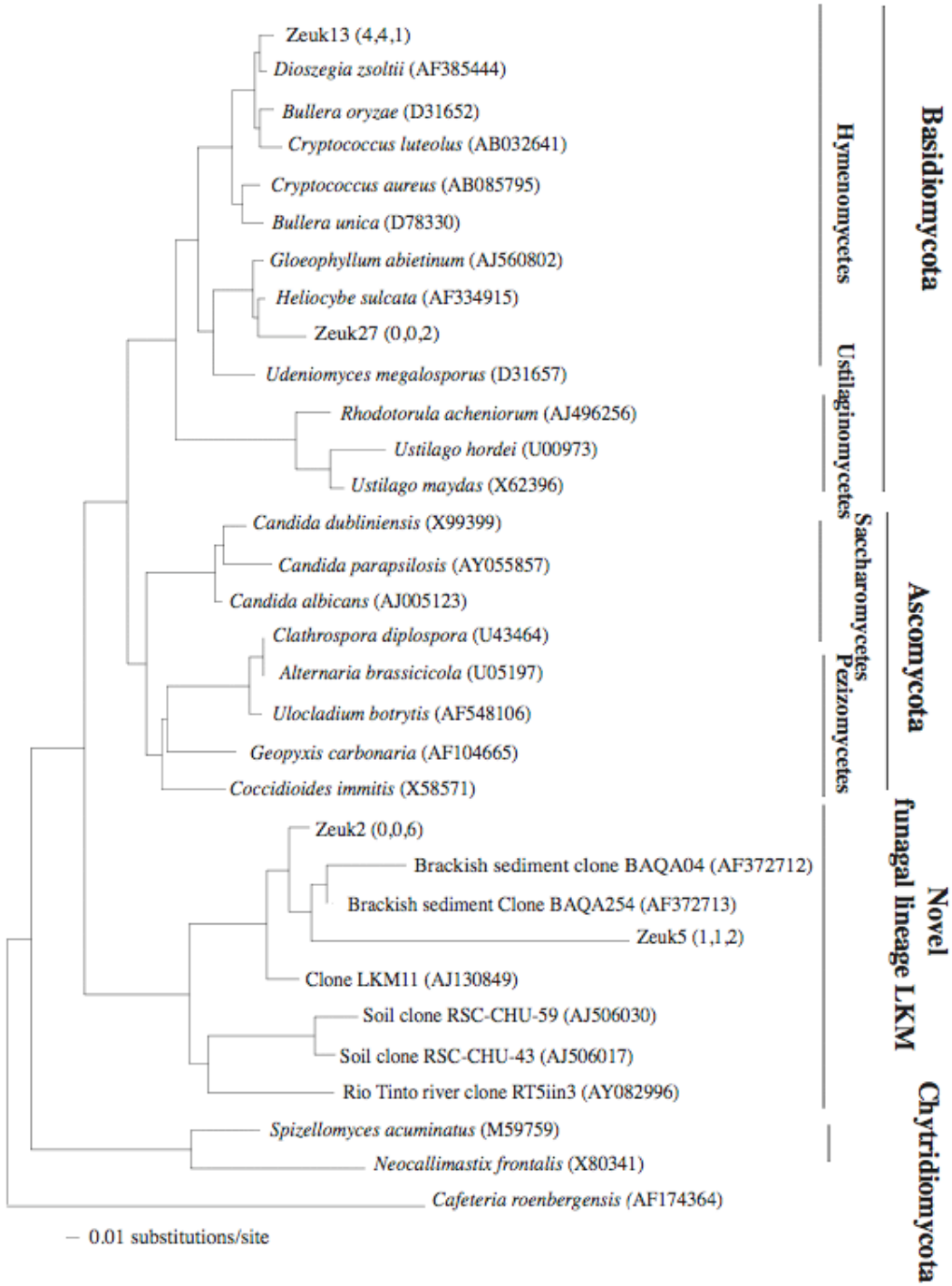
Zeuk13 (4,4,1)
Dioszegia zsoltii (AF385444)
Bullera oryzae (D31652)
Cryptococcus luteolus (AB032641)
Cryptococcus aureus (AB085795)
Bullera unica (D78330)
Gloeophyllum abietinum (AJ560802)
Heliocybe sulcata (AF334915)
Zeuk27 (0,0,2)
Udeniomyces megalosporus (D31657)
Rhodotorula acheniorum (AJ496256)
Ustilago hordei (U00973)
Ustilago maydas (X62396)
Candida dubliniensis (X99399)
Candida parapsilosis (AY055857)
Candida albicans (AJ005123)
Clathrospora diplospora (U43464)
Alternaria brassicicola (U05197)
Ulocladium botrytis (AF548106)
Geopyxis carbonaria (AF104665)
Coccidioides immitis (X58571)
Zeuk2 (0,0,6)
Brackish sediment clone BAQA04 (AF372712)
Brackish sediment Clone BAQA254 (AF372713)
Zeuk5 (1,1,2)
Clone LKM11 (AJ130849)
Soil clone RSC-CHU-59 (AJ506030)
Soil clone RSC-CHU-43 (AJ506017)
Rio Tinto river clone RT5iin3 (AY082996)
Spizellomyces acuminatus (M59759)
Neocallimastix frontalis (X80341)
Cafeteria roenbergensis (AF174364)
0.01 substitutions/site
Hymenomycetes
Ustilaginomycetes
Basidiomycota
Saccharomycetes
Pezizomycetes
Ascomycota
Novel funagal lineage LKM
Chytridiomycota

(B).

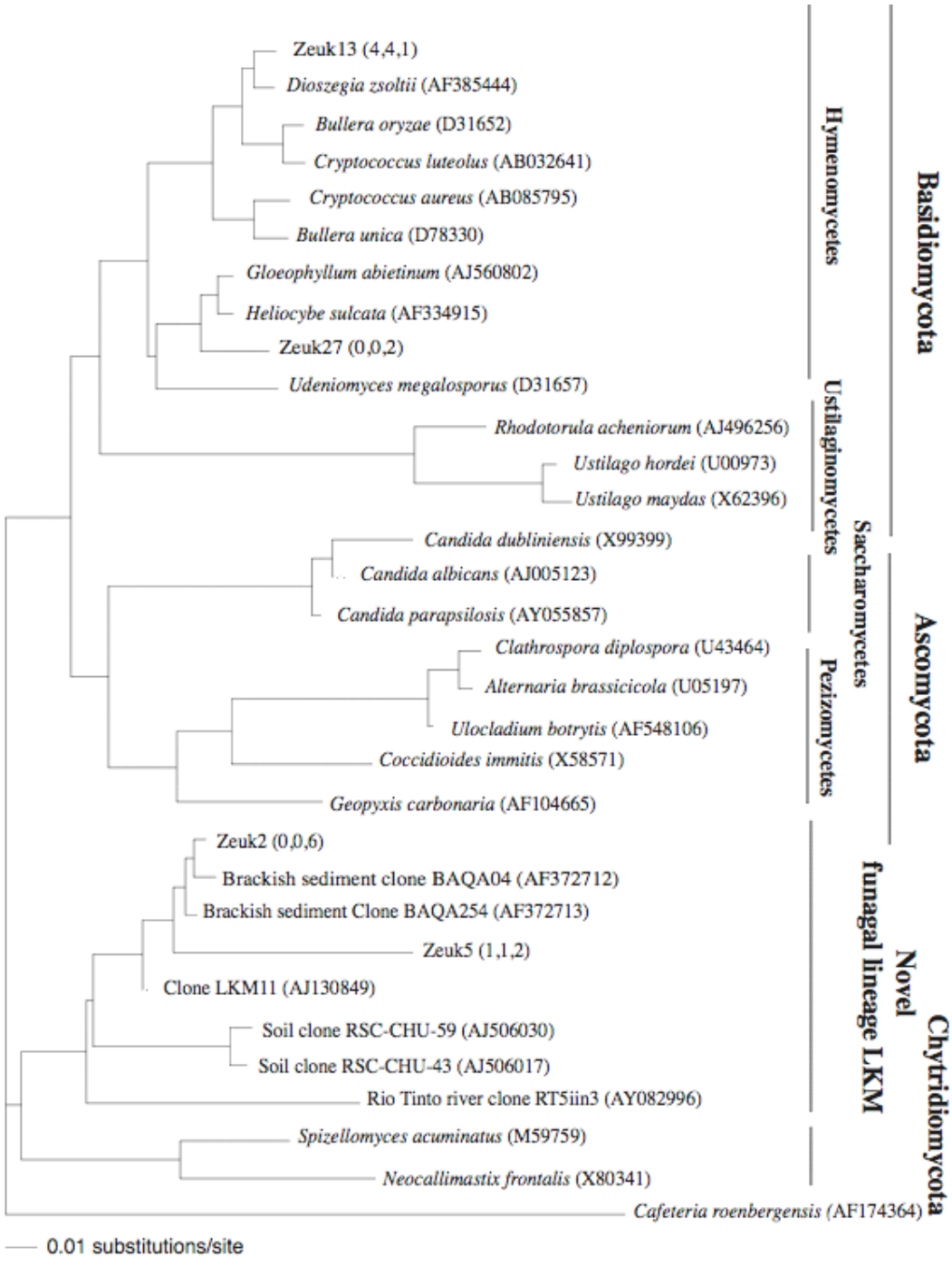
Zeuk13 (4,4,1)
Dioszegia zsoltii (AF385444)
Bullera oryzae (D31652)
Cryptococcus luteolus (AB032641)
Cryptococcus aureus (AB085795)
Bullera unica (D78330)
Gloeophyllum abietinum (AJ560802)
Heliocybe sulcata (AF334915)
Zeuk27 (0,0,2)
Udeniomyces megalosporus (D31657)
Rhodotorula acheniorum (AJ496256)
Ustilago hordei (U00973)
Ustilago maydas (X62396)
Candida dubliniensis (X99399)
Candida albicans (AJ005123)
Candida parapsilosis (AY055857)
Clathrospora diplospora (U43464)
Alternaria brassicicola (U05197)
Ulocladium botrytis (AF548106)
Coccidioides immitis (X58571)
Geopyxis carbonaria (AF104665)
Zeuk2 (0,0,6)
Brackish sediment clone BAQA04 (AF372712)
Brackish sediment Clone BAQA254 (AF372713)
Zeuk5 (1,1,2)
Clone LKM11 (AJ130849)
Soil clone RSC-CHU-59 (AJ506030)
Soil clone RSC-CHU-43 (AJ506017)
Rio Tinto river clone RT5iin3 (AY082996)
Spizellomyces acuminatus (M59759)
Neocallimastix frontalis (X80341)
Cafeteria roenbergensis (AF174364)
0.01 substitutions/site
Hymenomycetes
Ustilaginomycetes
Saccharomycetes
Pezizomycetes
Basidiomycota
Ascomycota
Novel funagal lineage LKM
Chytridiomycota

(C).

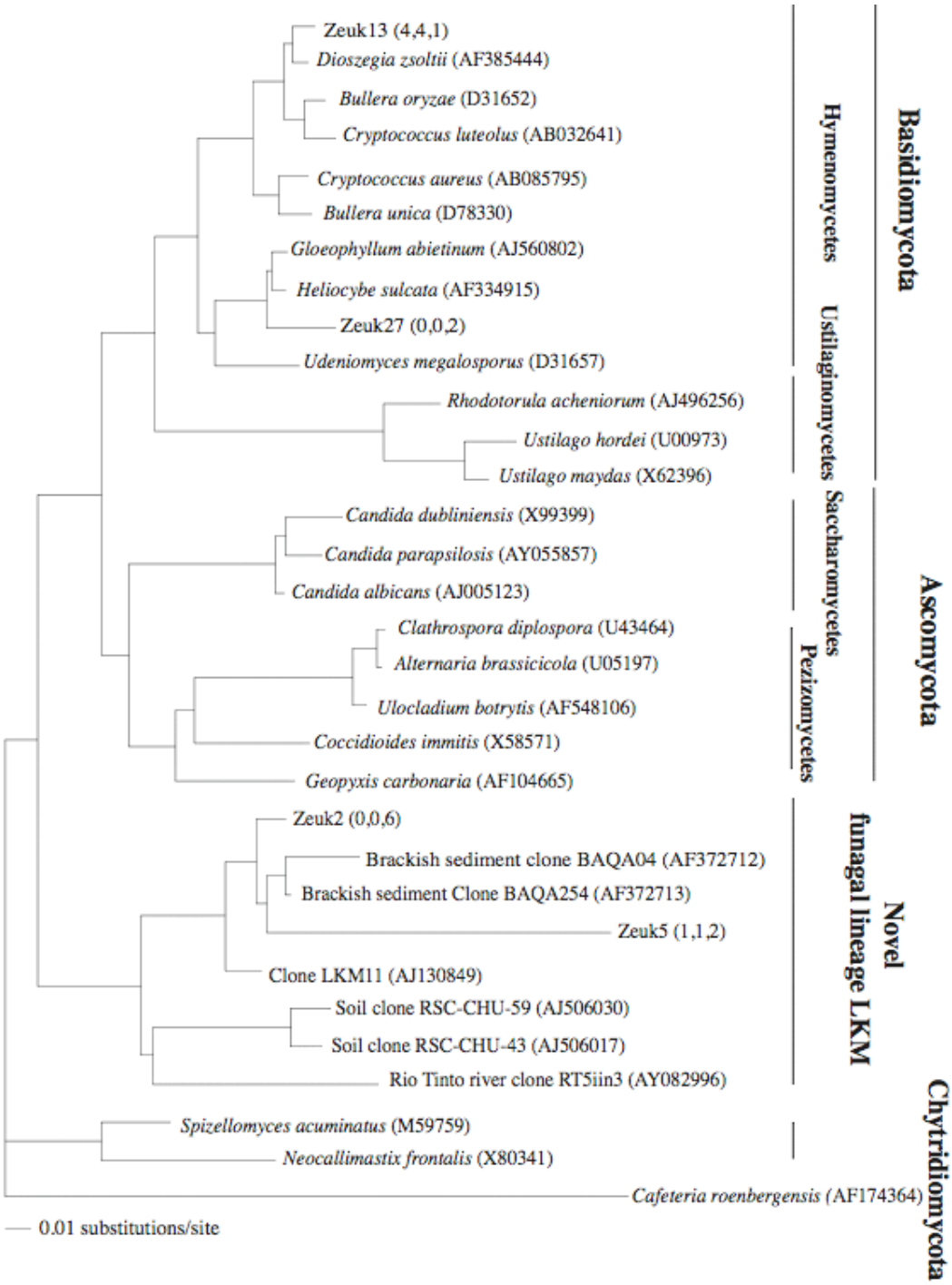
Zeuk13 (4,4,1)
Dioszegia zsoltii (AF385444)
Bullera oryzae (D31652)
Cryptococcus luteolus (AB032641)
Cryptococcus aureus (AB085795)
Bullera unica (D78330)
Gloeophyllum abietinum (AJ560802)
Heliocybe sulcata (AF334915)
Zeuk27 (0,0,2)
Udeniomyces megalosporus (D31657)
Rhodotorula acheniorum (AJ496256)
Ustilago hordei (U00973)
Ustilago maydas (X62396)
Candida dubliniensis (X99399)
Candida parapsilosis (AY055857)
Candida albicans (AJ005123)
Clathrospora diplospora (U43464)
Alternaria brassicicola (U05197)
Ulocladium botrytis (AF548106)
Coccidioides immitis (X58571)
Geopyxis carbonaria (AF104665)
Zeuk2 (0,0,6)
Brackish sediment clone BAQA04 (AF372712)
Brackish sediment Clone BAQA254 (AF372713)
Zeuk5 (1,1,2)
Clone LKM11 (AJ130849)
Soil clone RSC-CHU-59 (AJ506030)
Soil clone RSC-CHU-43 (AJ506017)
Rio Tinto river clone RT5iin3 (AY082996)
Spizellomyces acuminatus (M59759)
Neocallimastix frontalis (X80341)
Cafeteria roenbergensis (AF174364)
0.01 substitutions/site
Hymenomycetes
Ustilaginomycetes
Saccharomycetes
Pezizomycetes
Basidiomycota
Ascomycota
Novel funagal lineage LKM
Chytridiomycota

Supplementary Figure 2. Phylogenetic placement of the 18S rRNA fungal gene sequences encountered in Zodletone source, mat, and crust clone libraries as well as in ww, fl, and dp clone libraries. A). Maximum Parsimony analysis, Conducted using PAUP 4.01b heuristic search option using random stepwise addition of taxa with the TBR branch-swapping algorithm. Bootstrap values (in percent) are based on 1000 replicates and are shown for branches with more than 50% bootstrap support. B). Bayesian analysis conducted using Mr Bayes 4.01 b. The GTR+G model of evolution was used, and the tree shown is a consensus tree of 5000 sampled trees. The posterior probability of each resolved node is included. *Cafeteria roenbergensis* was used as an outgroup. Numbers in parentheses represents the frequency of occurrence of a specific OTU in the source, mat, and crust clone libraries, respectively.

A).

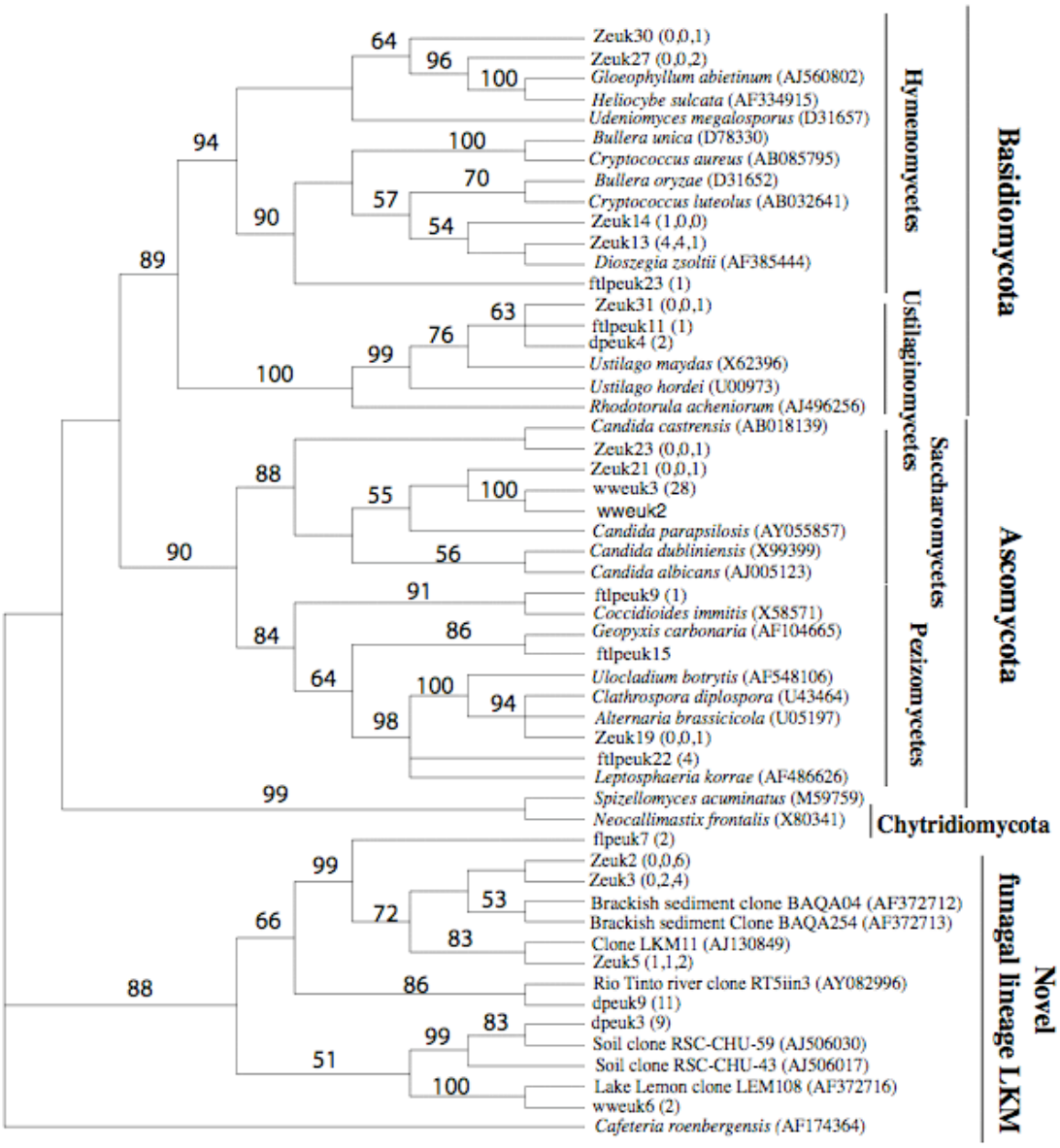
Zeuk30 (0,0,1)
Zeuk27 (0,0,2)
Gloeophyllum abietinum (AJ560802)
Heliocybe sulcata (AF334915)
Udeniomyces megalosporus (D31657)
Bullera unica (D78330)
Cryptococcus aureus (AB085795)
Bullera oryzae (D31652)
Cryptococcus luteolus (AB032641)
Zeuk14 (1,0,0)
Zeuk13 (4,4,1)
Dioszegia zsoltii (AF385444)
ftlpeuk23 (1)
Zeuk31 (0,0,1)
ftlpeuk11 (1)
dpeuk4 (2)
Ustilago maydas (X62396)
Ustilago hordei (U00973)
Rhodotorula acheniorum (AJ496256)
Candida castrensis (AB018139)
Zeuk23 (0,0,1)
Zeuk21 (0,0,1)
wweuk3 (28)
wweuk2
Candida parapsilosis (AY055857)
Candida dubliniensis (X99399)
Candida albicans (AJ005123)
ftlpeuk9 (1)
Coccidioides immitis (X58571)
Geopyxis carbonaria (AF104665)
ftlpeuk15
Ulocladium botrytis (AF548106)
Clathrospora diplospora (U43464)
Alternaria brassicicola (U05197)
Zeuk19 (0,0,1)
ftlpeuk22 (4)
Leptosphaeria korrae (AF486626)
Spizellomyces acuminatus (M59759)
Neocallimastix frontalis (X80341)
flpeuk7 (2)
Zeuk2 (0,0,6)
Zeuk3 (0,2,4)
Brackish sediment clone BAQA04 (AF372712)
Brackish sediment Clone BAQA254 (AF372713)
Clone LKM11 (AJ130849)
Zeuk5 (1,1,2)
Rio Tinto river clone RT5iin3 (AY082996)
dpeuk9 (11)
dpeuk3 (9)
Soil clone RSC-CHU-59 (AJ506030)
Soil clone RSC-CHU-43 (AJ506017)
Lake Lemon clone LEM108 (AF372716)
wweuk6 (2)
Cafeteria roenbergensis (AF174364)
Hymenomycetes
Ustilaginomycetes
Saccharomycetes
Pezizomycetes
Basidiomycota
Ascomycota
Chytridiomycota
Novel fungal lineage LKM

B).

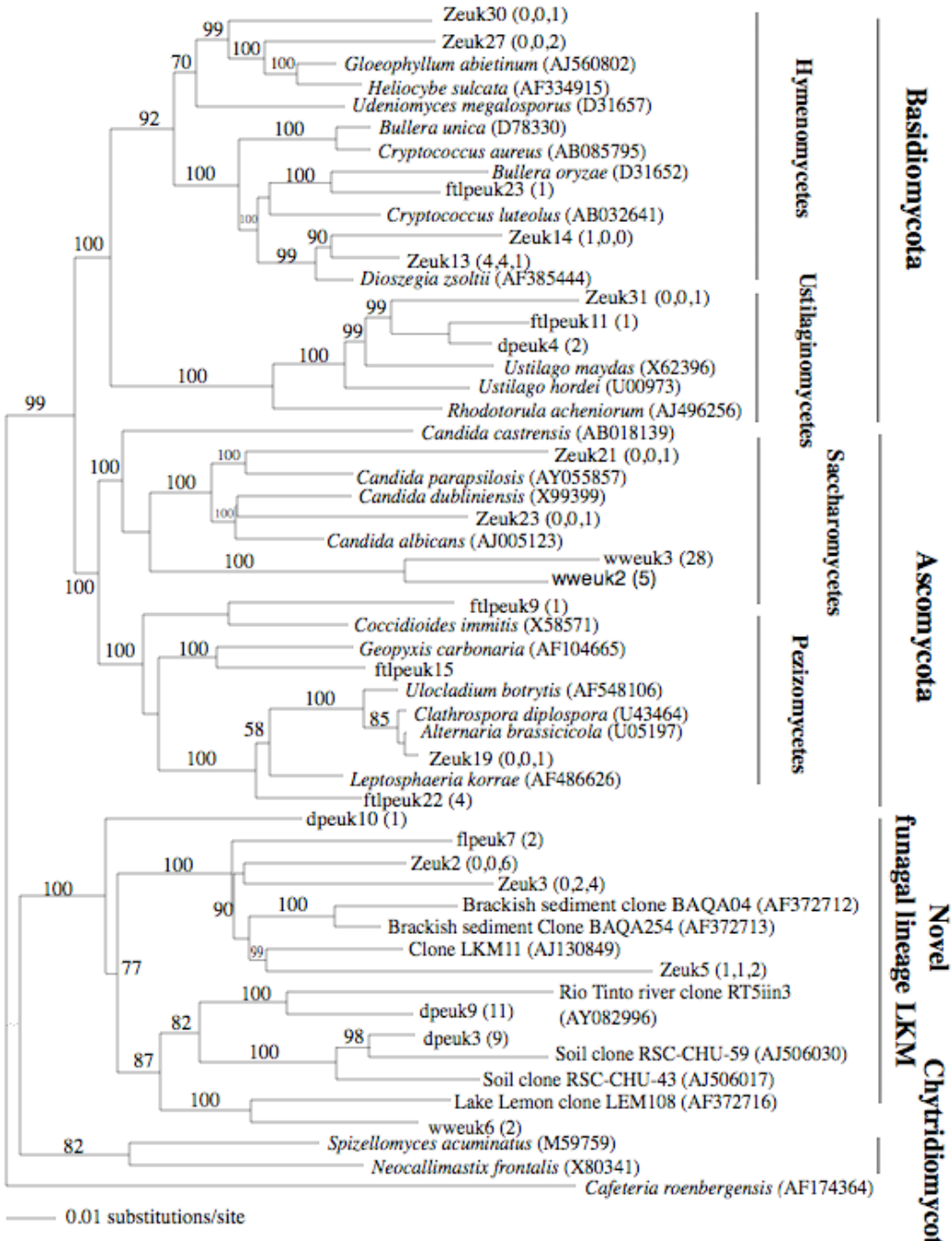
Zeuk30 (0,0,1)
Zeuk27 (0,0,2)
Gloeophyllum abietinum (AJ560802)
Heliocybe sulcata (AF334915)
Udeniomyces megalosporus (D31657)
Bullera unica (D78330)
Cryptococcus aureus (AB085795)
Bullera oryzae (D31652)
ftlpeuk23 (1)
Cryptococcus luteolus (AB032641)
Zeuk14 (1,0,0)
Zeuk13 (4,4,1)
Dioszegia zsoltii (AF385444)
Zeuk31 (0,0,1)
ftlpeuk11 (1)
dpeuk4 (2)
Ustilago maydas (X62396)
Ustilago hordei (U00973)
Rhodotorula acheniorum (AJ496256)
Candida castrensis (AB018139)
Zeuk21 (0,0,1)
Candida parapsilosis (AY055857)
Candida dubliniensis (X99399)
Zeuk23 (0,0,1)
Candida albicans (AJ005123)
wweuk3 (28)
wweuk2 (5)
ftlpeuk9 (1)
Coccidioides immitis (X58571)
Geopyxis carbonaria (AF104665)
ftlpeuk15
Ulocladium botrytis (AF548106)
Clathrospora diplospora (U43464)
Alternaria brassicicola (U05197)
Zeuk19 (0,0,1)
Leptosphaeria korrae (AF486626)
ftlpeuk22 (4)
dpeuk10 (1)
flpeuk7 (2)
Zeuk2 (0,0,6)
Zeuk3 (0,2,4)
Brackish sediment clone BAQA04 (AF372712)
Brackish sediment Clone BAQA254 (AF372713)
Clone LKM11 (AJ130849)
Zeuk5 (1,1,2)
Rio Tinto river clone RT5iin3 (AY082996)
dpeuk9 (11)
dpeuk3 (9)
Soil clone RSC-CHU-59 (AJ506030)
Soil clone RSC-CHU-43 (AJ506017)
Lake Lemon clone LEM108 (AF372716)
wweuk6 (2)
Spizellomyces acuminatus (M59759)
Neocallimastix frontalis (X80341)
Cafeteria roenbergensis (AF174364)
0.01 substitutions/site
Hymenomycetes
Ustilaginomycetes
Saccharomycetes
Pezizomycetes
Basidiomycota
Ascomycota
Novel funagal lineage LKM
Chytridiomycota

Appendix 2

Transmission Electron Microscopic Study on *Desulfovibrio desulfuricans* G20 under Oxygen Stress

Experimental procedures:

G20 culture was incubated overnight at 37°C in a serum tube (Groh et al., 2005). For preparing anaerobic samples, 3 ml of culture was harvested anaerobically with centrifugation at a maximum speed (about 13,200 rpm). For oxygen stressed cells, the stopper was removed from the tube of an early stationary phase G20 culture, the tube was shaked at the speed of 100 rpm in the airfor 24 hours, and then 3 ml of culture was harvested anaerobically by centrifugation. The following sample preparation procedures were modified from the protocol available online (http://ou.edu/research/electron/bmz5364/fix-mbio.html). The cell pellet was washed by centrifugation with a 2% $NaHCO_3$ solution three times in the anaerobic chamber. A glutaraldehyde (GA) (1 ml of 2.5% in 2% $NaHCO_3$ buffer) solution was added to the pellet, mixed and incubated at room temperature for 2 hours. After GA fixation, the cells were washed with 2% $NaHCO_3$ + 5 mM $CaCl_2$ solution twice for 10 minutes each. The cells were then incubated in 2% $NaHCO_3$ + 5 mM $CaCl_2$ solution overnight at 4°C. OsO_4 (1 ml of 2% in 2% $NaHCO_3$ buffer) solution was added to the cell pellet and incubated at room temperature under a fume hood for 1 hour, and the pellet was collected. After OsO_4 fixation, saturated uranyl acetate (pH5.2) was used to stain cells. Samples were then dehydrated by cold ethanol through a gradient of 30%, 50%, 70%, and 95% for 5 to 15 minutes each and then with 100% cold ethanol for 20 minutes. The final dehydration

step was processed twice with room temperature 100% ethanol for 20 minutes. After dehydration, solvent exchange was performed three times on the sample to replace ethanol with propylene oxide, which was the solvent of the Epon 812, for 10 minutes. Before embedding sample in Epon 812, four steps of infiltration were performed as follows: incubating with 1 part of propylene oxide + 1 part of Epon 812 for 15 minutes to 1 hour, with 1 part of propylene oxide + 2 parts of Epon 812 for 15 minutes to 2 hours, with 1 part of propylene oxide + 4 parts of Epon 812 for 15 minutes to 2 hours, then with pure Epon 812 for overnight. Hardeners (DDSA, NMA) were added into fresh prepared Epon 812, mixing thoroughly; accelerator (BDMA) was added, mixing thoroughly; then samples were embedded for 2-4 hours. Samples were incubated at 60 °C for 12 hours to 3 days for polymerization. Thin sections were obtained with an ultramicrotome (Sorvall Porter-Blum MT2) and stained with saturated uranyl acetate (2% aqueous solution) at room temperature for 15 minutes to 1 hour. Lead staining (SATO's lead solution) was also performed at room temperature for 30 seconds to 15 minutes. Dried grids were examined by a transmission electron microscope (Zeiss10A) and images were taken.

Results and Discussion:

Desulfovibrio spp. once were considered as obligate anaerobes, however, in situ studies have found this group of bacteria to occur in the photooxic zone (Risatti et al., 1994; Teske et al., 1998). Although in pure culture conditions, aerobic growth cannot be observed, it was found that some SRB can survive under oxygen stress for as long as 20 days (Holman, 2004). Oxygen stress can induce changes in gene expression and protein production (Fournier et al., 2006); however, it is unknown whether the cell morphology

will also change upon the stress. Electron microscopy is a tool for observing the cell morphology, and it is widely used in eukaryotic studies (Bozzola, 1999). Transmission electron microscopy (TEM) was chosen to visualize the structural changes in oxygen-stressed cells.

TEM images (Figure 1) of G20 under oxic condition showed particles in the periplasmic spaces, which appeared to be from the cell cytosol. This feature is not present in the anoxic sample and has never been observed in other bacterial cells before. A previous study on *D. vulgaris* Hildenborough reported that cellular content decreased when cells were under oxygen stress (Holman, 2004). Our observation may provide the direct evidence that cellular content is lost upon exposure to oxygen.

Figure 1. Transmission electron microscopic images of *D. desulfuricans* G20. (A). TEM image of anaerobic sample from thin section; magnification at 105,000X, scale bar = 200 nm. (B). TEM image of aerobic sample from thin section; magnification at 105,000X, scale bar = 200 nm.

(A).

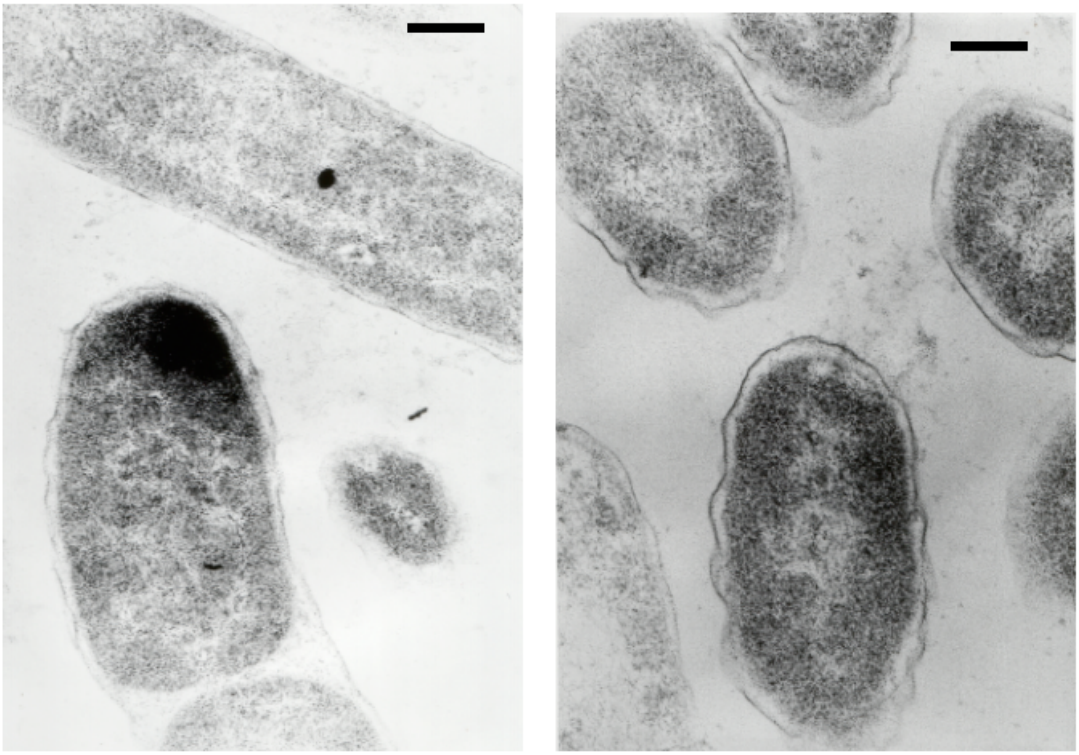

(B).

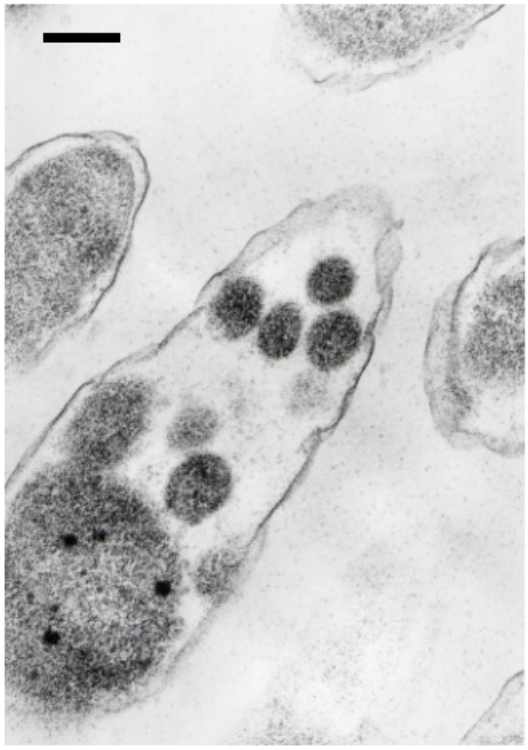

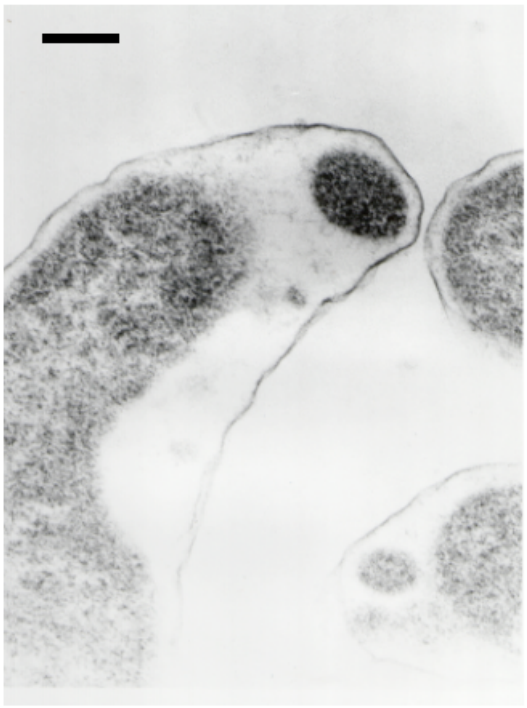

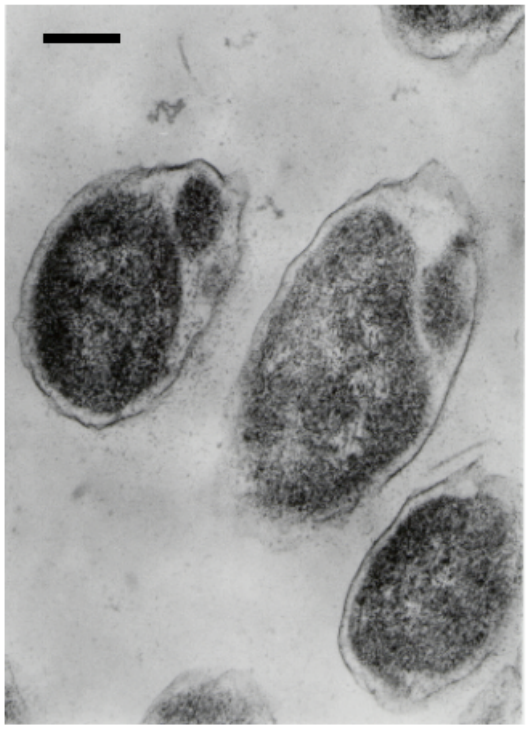

References

Bozzola, J.J.a.R., L. D. (1999) *Electron Microscopy*. Sudbury, Massachusetts: Jones and Bartlett publishers.

Fournier, M., Aubert, C., Dermoun, Z., Durand, M.C., Moinier, D., and Dolla, A. (2006) Response of the anaerobe *Desulfovibrio vulgaris* Hildenborough to oxidative conditions: proteome and transcript analysis. *Biochimie* **88**: 85-94.

Groh, J.L., Luo, Q., Ballard, J.D., and Krumholz, L.R. (2005) A method adapting microarray technology for signature-tagged mutagenesis of *Desulfovibrio desulfuricans* G20 and *Shewanella oneidensis* MR-1 in anaerobic sediment survival experiments. *Appl Environ Microbiol* **71**: 7064-7074.

Holman, H.N., Lin, Z., Hazen, T. C., Joyner, D. (2004) A real-time investigation of *Desulfovibrio vulgaris* response to oxygen stress. *ASM abstract*: 164.

Risatti, J.B., Capman, W.C., and Stahl, D.A. (1994) Community structure of a microbial mat: the phylogenetic dimension. *Proc Natl Acad Sci U S A* **91**: 10173-10177.

Teske, A., Ramsing, N.B., Habicht, K., Fukui, M., Kuver, J., Jorgensen, B.B., and Cohen, Y. (1998) Sulfate-reducing bacteria and their activities in cyanobacterial mats of Solar Lake (Sinai, Egypt). *Appl Environ Microbiol* **64**: 2943-2951.